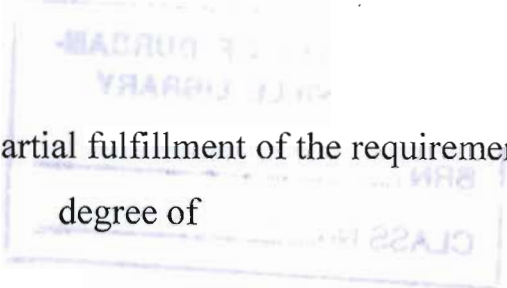# Coriolis effect on the stability of convection in mushy layers during the solidification of binary alloys

by

Saneshan Govender

Dissertation presented in partial fulfillment of the requirements for the

degree of

Doctor of Philosophy Engineering (Mechanical)

In the Faculty of Engineering

University of Durban-Westville

Durban

January 2000

Everything should be made as simple as possible,

but not simpler.

ALBERT EINSTEN

Acknowledgements

The selfless efforts of the following persons is highly appreciated and has facilitated my compiling of this thesis :

Prof. Peter Vadasz, my research supervisor, for his expert guidance, his inspiration and support throughout the project and for believing in me;

Dr. D.M Anderson, University of North Carolina, USA, for consistently replying to my queries regarding his publications;

Prof. M.G. Worster, Cambridge University, for assisting me in locating various authors;

Mrs. Elsabe v/d Merwe, Aerotek, CSIR Library, for her help in locating journal publications;

Mr. Pierre Roussouw, Mattek, CSIR foundry, for his input on the process of directional solidification and the numerous samples exhibiting freckling;

My family, for their support and total belief in me;

My grandfather, for his interest and numerous enquiries about my progress.

The Rock Groups, Jon Bon Jovi, U2, AC/DC, Aerosmith, Queen, Van Halen, Alice Cooper, Metallica, Roxette, Nirvana, REM, Red Hot Chilli Peppers, Guns & Roses and LIVE who provided me with the inspiration and company through those long nights.

Contents

Abstract

We consider the solidification of a binary alloy in a mushy layer subject to Coriolis effects. A near-eutectic approximation and large far-field temperature is employed in order to study the dynamics of the mushy layer in the form of small deviations from the classical case of convection in a horizontal porous layer of homogenous permeability. The linear stability theory is used to investigate analytically the Coriolis effect in a rotating mushy layer for, a diffusion time scale used by Amberg & Homsey (1993) and Anderson & Worster (1996), and for a new diffusion time scale proposed in the current study. As such, it is found that in contrast to the problem of a stationary mushy layer, rotating the mushy layer has a stabilising effect on convection. For the case of the new diffusion time scale proposed by the author, it is established that the viscosity at high rotation rates has a destabilising effect on the onset of stationary convection, ie. the higher the viscosity, the less stable the liquid. Finite amplitude results obtained by using a weak non-linear analysis provide differential equations for the amplitude, corresponding to both stationary and overstable convection. These amplitude equations permit one to identify from the post-transient conditions that the fluid is subject to a pitchfork bifurcation in the stationary case and to a Hopf bifurcation associated with the overstable convection. Heat transfer results were evaluated from the amplitude solution and are presented in terms of the Nusselt number for both stationary and overstable convection. They show that rotation enhances the convective heat transfer in the case of stationary convection and retards convective heat transfer in the oscillatory case, but only for low values of the parameter $\chi_1 = \delta \Pr \phi_0 \vartheta_0$. The parameter $1/\chi_1$ represents the coefficient of the time derivative term in the Darcy equation. For high χ_1 values, the contribution from the time derivative term is small (and may be neglected), whilst for small χ_1 values the time derivative term may be retained.

Nomenclature

Latin Symbols

c	Composition.
Da	Darcy number.
$\hat{e}_g$	Unit vector in the direction of gravity.
$\hat{e}_\omega$	Unit vector in the direction of the rotation.
$\hat{e}_z$	Unit vector in the z-direction.
g^*	Gravitational acceleration $[9.81\ \text{m}/\text{s}^2]$.
H^*	Height of the mushy layer [m].
h_{fs}	Latent heat of fluid [kJ/kg]
k_0	Characteristic permeability $[\text{m}^2]$.
$K^*(\varphi)$	Dimensional permeability function.
L	Length of the mushy layer.
Nu	Nusselt number.
p	Reduced pressure.
q	Specific heat of fluid [kJ/kg].
Pr	Prandtl number.
R	Rescaled mushy layer Rayleigh number.
$Ra_m = \beta^* \Delta c g^* k_0 / (\nu^* V^*)$	Mushy layer Rayleigh number.
s_x	x-component of wavenumber.
s_y	y-component of wavenumber.
s_z	z-component of wavenumber.
R	Modulus of amplitude, corresponding to overstable convection.
St	Stefan number.
t	Time [s].
T	Dimensional temperature [K].
Ta	Taylor number.

u	Horizontal x-component of velocity [m/s].
$\mathbf{U}$	Dimensionless velocity vector.
v	Horizontal y-component of velocity [m/s].
V^*	Velocity of solidifying front [m/s].
w	Vertical component of velocity [m/s]
x	Horizontal length co-ordinate.
X	Slow space scale.
y	Horizontal width co-ordinate.
z	Vertical co-ordinate.

Greek Symbols

α	Scaled wavenumber.
β	Solutal expansion coefficient.
β_T	Thermal expansion coefficient [1/K].
χ_0	$= \Pr \phi_0 \vartheta_0$.
χ	$= \delta^2 \chi_0$.
χ_1	$= \delta \chi_0$.
δ	Dimensionless depth of mushy layer.
ε	Disturbance amplitude.
ϕ	Porosity.
φ	Solid fraction $= 1 - \phi$
Φ	Phase angle corresponding to oscillatory convection.
η_0	Relaxation time corresponding to stationary convection.
η_1	Coefficient of the diffusion term corresponding to stationary convection.
η_2	$= 4 \eta_0$.
κ	Thermal diffusivity of liquid [m^2/s].
λ	$= \overline{S} / \Omega^2 c_S^2$.
μ	Dynamic viscosity of the fluid [Pa-s].

v	Kinematic viscosity $[\text{m}^2/\text{s}]$.
$\Pi(\varphi) = k_0/K^*(\varphi)$	Dimensionless permeability function.
θ	Dimensionless temperature.
ϑ_0	Mobility ratio.
ρ	Fluid density $[\text{kg}/\text{m}^3]$.
Γ	Slope of liquidus line.
σ	Oscillatory frequency $[1/\text{s}]$.
σ_0	Corresponds to the critical frequency for either stationary or overstable convection.
τ	Slow time scale at order ε^2.
τ_0	Slow time scale at order ε.
ω^*	Angular velocity of rotating mushy layer $[\text{rad/s}]$.
Ω	$= 1 + \text{St}/\xi = 1 + \overline{S}/c_S$.
ς	$= K_c/\Omega^2 c_S^2$.
ψ	Stream function.
ξ	Composition ratio.
ξ_{ov}	Linear coefficient corresponding to overstable convection.
ξ_{st}^0	Linear coefficient corresponding to stationary convection.
ξ_{st}	$= 4\xi_{st}^0$

Superscripts

*	Dimensional quantities.
asym	Asymptotical quantities.
oblique	Refers to quantities on the oblique plane containing the streamlines.
$(.)'$	Refers to scaled terms used in the weak non-linear analysis of overstable convection.

Subscripts

00	Refers to quantities at order $\varepsilon^0\delta^0$
01	Refers to quantities at order $\varepsilon^0\delta^1$
1	Refers to quantities at order ε .
2	Refers to quantities at order ε^2 .
3	Refers to quantities at order ε^3
B	Refers to basic flow quantities.
c	Refers to characteristic values.
cr.	Refers to critical values.
E	Refers to eutectic conditions.
h	Refers to homogenous solutions to differential equations.
i1	Refers to quantities at order $\varepsilon^0\delta^1$
i	Refers to oscillatory frequency in Author's scaling.
l/f	Refers to liquid conditions
m	Mush conditions
o	Refers to liquidus conditions.
ov	Refers to overstable conditions.
p	Refers to particular solutions to differential equations.
s	Solid conditions
S	Refers to solidus conditions.
st	Refers to stationary conditions.
∞	Refers to far field conditions.

Over

$-$	Refers to scaled quantities.
$\wedge$	Refers to perturbed quantities
$\sim$	Refers to scaled quantities
$\cdot$	Derivative with respect to time.

1.Introduction

1.1 General

The internal structure of solid alloy depends largely on the history of its solidification from the liquid melt phase. The geometry of the melt region, the rate of solidification, and associated fluid motions in the liquid melt all contribute to the properties of the microstructure of the final product. These properties are all determined by internal processes that occur in response to external conditions such as the shape of the container and the location of the cooled boundaries, degree of cooling, the initial concentration of the liquid melt, and the existence of body forces such as those produced by gravitational, rotational or magnetic forces.

The most commonly analysed case is one where the solidification of the liquid melt occurs in the presence of the gravitational body force. In this case the natural convective flow of the melt can be driven by thermal gradients that are set up by the imposed cooling, or by compositional gradients that are generated when one component of the alloy is preferentially incorporated within the growing solid, or by both thermal and compositional gradients. A detailed description of the solidification process with regards to the phase diagram is provided in Section 1.2. Often during the solidification process, the planar solid-liquid melt interface is highly (morphologically) unstable and takes the form of small dendrite arms occupying a zone of finite thickness, called the mushy layer or mushy zone. These dendrite arms appear as a forest of solid crystals orientated principally along the direction of strongest thermal gradient, with fluid filling the interstitial spaces, see Figure 1. Figure 1 shows a mushy layer of ammonium chloride crystals. The millimetre scale on the top left hand corner shows that the typical spacing between the crystals is very small in comparison with the depth of the mushy layer, which is of the order of 7mm. This dendrite zone can be thought of as performing a function of smearing out the concentration jump over a much larger distance than the planar front in the case of planar solidification.

It must be borne in mind that the dynamics in the mushy layer is governed by the complex interaction between the compositional convection and the solidification process.

6
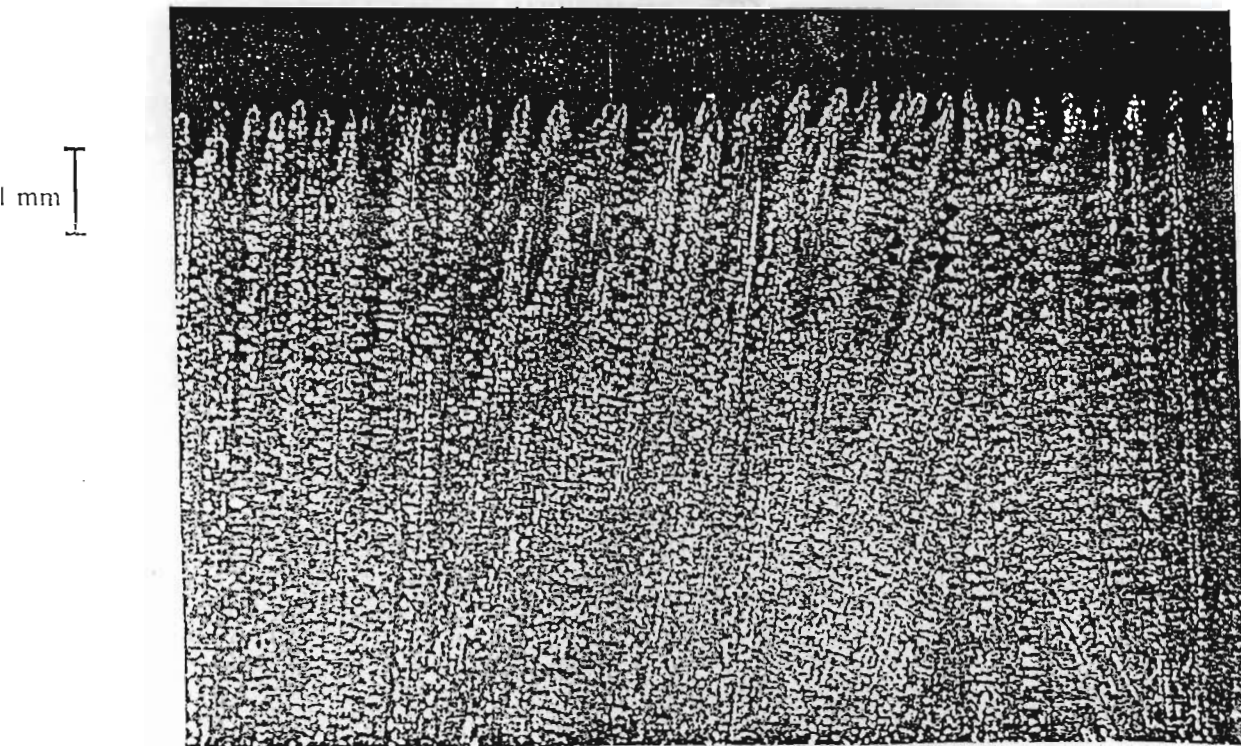
Figure 1: A Mushy layer of ammonium chloride crystals formed by cooling an aqueous solution from below. Courtesy of Worster (1991)

A direct result of compositional convection is the formation of freckles, which are non-uniformities that manifest themselves as vertical channels that are of a composition different from the surrounding solid. In cross section they appear as "spots" and will henceforth be referred to as freckles. In practice, the presence of freckles in the cast alloy compromises the mechanical properties of the component. In the gas turbine blade manufacture industry, where the blade is directionally cast in a "pigtail mould", freckle formation in the cast blades could cause catastrophic failure when the blade is subjected to its harsh operating environment. The need to avoid such failures in practice coupled with the limited understanding of the complex process of solidification has gained considerable international interest among the fluid dynamicists, metallurgists, engineers and applied mathematicians.

The freckles formed in solidified alloys has been compared to the freckles formed in aqueous ammonium chloride salt solutions, and it was concluded that the mechanism for freckle formation was as a result of convection through chimneys in the mushy layer, see Copley et al (1970), Sample & Hellawell (1984) and Sarazin & Hellawell (1988).

Worster (1991) later supplemented this experimental work by providing an analytical solution for the flow and temperature fields in chimneys. In addition Worster (1991) provided a mechanism for the formation of chimneys.

The analogous behaviour that exists between a solidifying metallic alloy and a freezing aqueous salt solution has led to numerous laboratory tests being undertaken, using ammonium salts, to investigate compositional convection and its bearing on freckle formation. Ammonium salts are preferred as a medium for performing laboratory experiments due to its transparency, as far as flow visualisation is concerned, and also due to the fact that it is easy to handle. Such experiments have directed much of the current thought in this field. The solidification process always seems to occur in three phases (see Chen & Chen 1991 and Tait & Jaupart 1992). At the start a uniform layer of dendritic crystals forms at the base of the experimental tank, and buoyant residual fluid, depleted of the ammonium chloride taken up by the crystallised salt, rises convectively to form a layer of double-diffusive fingers. A short time later, a few isolated convective plumes begin to rise to a height much greater than the top layer of double-diffusive fingers. Eventually, a chimney or vent forms beneath each plume, which extends through the crystal pile to the base of the tank. The plume number and strength increases with time, and as a result suppresses the double diffusive mode. This strengthened plume activity decays with time, and the number of chimneys begin to decrease. The experiments revealed that two modes of convection viz. the double-diffusive mode (which emanates from the mush-liquid interface) and the mushy layer mode (as a result of plumes being emitted from chimneys in the mushy layer) exists in a solidifying system.

The experimental investigations led to the development of a mathematical model to describe the flow physics in a solidifying alloy system. Fowler (1985) proposed a model for mushy layer and investigated a limiting case where there was no coupling between the convection and solidification processes. Worster (1992) later performed a stability analysis of the liquid and mushy regions of the binary alloy system and found that the model predicted the two modes of convection mentioned earlier. Up to this point it was assumed that the double diffusive convection provides disturbances that initiate the

that was discovered during the weak non-linear analysis. Anderson & Worster (1996) indicated that although there exists circumstances under which the oscillatory mode is the most critical, it nonetheless gives way to the steady mode for larger values of Rayleigh number. They also pointed out that in practice oscillatory convection may be confined to situations close to the marginal conditions.

The current study utilises the parameter scalings as presented by Anderson & Worster (1996), and includes the effects of rotation. The study is structured as follows : Section 1; the problem geometry is defined, outlining the body forces in the Darcy equation, and a description of the solidification process is provided, whilst the momentum equation for the mushy layer region is rescaled to include the Coriolis body force and a time derivative on the velocity vector, Section 2; a linear stability analysis is performed for the stationary and overstable convection cases adopting Anderson & Worster's (1996) scaling for time, Section 3; a linear stability analysis is performed for the Author's proposed scaling for time, Section 4; A weak non linear analysis of convection as a result of rotational effects is performed for the Author's scaling for time by expansion to higher orders and a complete amplitude equation defining the leading order amplitude is developed for both stationary and oscillatory convection, Section 5; The Nusselt number for both the stationary and oscillatory is developed, Section 6; Graphical plots for the flow, temperature and solid fraction patterns is provided for Anderson & Worster's (1996) scaling for time, Section 7; a conclusion summarising the findings in the thesis is provided.

Solidification of binary alloys are to a large extent governed by the phase diagram which differs for different alloys. The phase diagrams provide relations between composition c^* and temperature T^* at the solid/melt boundaries. A typical phase diagram for a binary alloy system is shown in Figure 3 below.

Figure 3 : Sketch of phase diagram

During the solidification of binary alloys, the liquid melt will always solidify into an extremely fine mixture usually visible under a microscope. The two separate parts of this mixture initially exists as pure metal A and pure metal B as depicted in Figure 3. If we assume that a small amount of pure metal A is solidified, then the remaining liquid melt is left rich in metal B. This causes a slight shift in the composition to the right. To restore the liquid composition to its equilibrium value, metal B will now solidify. Now if too much of metal B solidifies, the liquid melt composition will shift to the left, thereby causing metal A to solidify to restore equilibrium. Therefore, at constant temperature, the

liquid solidifies alternately pure A and pure B, resulting in an extremely fine mixture. An alloy exhibiting this behaviour is referred to as an eutectic alloy.

In freezing aqueous ammonium salt ($NH_4Cl - H_2O$) systems as used in laboratory experiments, the components A and B, in Figure 3, refers to the H_2O and NH_4Cl respectively, see Sarazin & Hellawell (1988).

The composition, referred to above, may be thought of as the weight percentage of each component A and B in the alloy. The liquidus line $T_L(c^*)$ relates the composition of the liquid in the porous mush to the temperature. The mushy layer is taken to be in thermo-dynamic equilibrium and the relationship between T^* and c^* is given by the following linear liquidus relation of the form

$$T^* = T_L(c^*) = T_E + \Gamma(c^* - c_E),\qquad (1.1)$$

where Γ is the gradient of the liquidus line at c_0, see Figure 3. Note that the relation given in Eqn.(1.1) is valid for the range $T_E < T^* < T_\infty$. For temperatures above the melting point of the alloy ie. for $T^* > T_\infty$, no solid is formed regardless of the composition c^*. When the temperature falls below the eutectic temperature, T_E, all remaining liquid, which by that time has a composition c_E, solidifies immediately. Note that the two solidus curves are assumed to be vertical, ie. the gradient of the solidus lines are infinitely large. Noting that the segregation/partition coefficient is the ratio of the liquidus to solidus line slopes, we may infer that in our case the segregation coefficient is zero. The density in the liquid is a much stronger function of composition (c^*) than it is of temperature (T^*), as shown in Figure 3. Adopting the Boussinesq approximation and using the result given in Eqn.(1.1), we define a linear relation between the density ρ_l and the composition c^* to be of the form,

$$\rho_1^* = \rho_o^*(c_o)\left[1 - \beta_T^*\left(T^* - T_E\right) + \beta^*\left(c^* - c_E\right)\right] = \rho_o(c_o)\left(1 + \left[\left(\beta^*/\Gamma\right) - \alpha^*\right]\left(T^* - T_E\right)\right), \qquad (1.2)$$

where Γ is the slope of the liquidus curve. The effective expansion coefficient $\left[\left(\beta^*/\Gamma\right) - \beta_T^*\right]$, may become positive and lead to buoyancy driven convection when solutal effects dominate. Note that typically $\beta^* > \Gamma\beta_T^*$ (and β^* is positive) due to the fact that density is largely a function of composition than it is of temperature, see vertical solidus lines in Figure 3. This provides the explanation as to why a melt whose composition is less than the eutectic composition c_E releases more dense fluid, while a melt whose composition exceeds c_E releases less dense fluid when the fluid is cooled and solidified. In the problem presented in Figure 2, the initial composition c_o is taken to be greater than the eutectic composition c_E.

Many authors have proposed formulations for the governing equations in the mushy layer, see Chiarelli & Worster (1995) and Brattkus & Davies (1988). The formulation presented here follows closely that of Anderson & Worster (1996). Not far (at distances $L^* << g^*/\omega^{*2}$) from the axis of rotation it may be assumed that the gravitational buoyancy to be greater than the centrifugal buoyancy. For this reason the centrifugal effect may be neglected thus limiting the effect of rotation to the Coriolis acceleration . The centrifugal effects are taken to be constant and absorbed into the reduced pressure term. The Darcy equation is extended only to include the time derivative and the Coriolis terms, while the Boussinesq approximation is applied to account for the effects of the density variations. Subject to these conditions the following dimensionless set of governing equations for the continuity, energy, solute balance and Darcy equation extended to include Coriolis effects is obtained :

$$\nabla \cdot \mathbf{U} = 0 \qquad\qquad (1.3)$$

$$\left(\frac{\partial}{\partial t} - \frac{\partial}{\partial z}\right)\left(\theta - St\,\varphi\right) + \mathbf{U} \cdot \nabla\theta = \nabla^2\theta \qquad\qquad (1.4)$$

$$\left(\frac{\partial}{\partial t} - \frac{\partial}{\partial z} \right) \left[(1 - \varphi)\theta + \xi\varphi \right] + \mathbf{U} \cdot \nabla\theta = 0 \tag{1.5}$$

$$\frac{1}{\chi_o} \frac{\partial \mathbf{U}}{\partial t} + \Pi(\varphi)\mathbf{U} = -\nabla p + Ra_m \theta \, \hat{\mathbf{e}}_g - Ta^{1/2} \, \hat{\mathbf{e}}_\omega \times \mathbf{U}. \tag{1.6}$$

In the system (1.3-1.6), φ refers to the solid fraction, $\mathbf{U}$ refers to the filtration velocity in the mush, whilst θ refers to the temperature. Note that the non-dimensional form of the liquidus relation ($c = \theta$) has been used to replace the solute concentration by the non-dimensional temperature, Eqn.(1.8) below. This is inferred from the simplified phase diagram given in Figure 3. Eqns. (1.3-1.6) were rendered dimensionless by using V^* (the advance velocity of the melt/mush interface) for the velocity scale, $l_\kappa = \kappa^*/V^*$ (the thermal diffusion length scale) for length, and $\kappa^*/(V^*)^2$ for the time scale, where κ^* is the thermal diffusivity of the liquid. The pressure scale is $\kappa^*\mu^*/k_0$ where μ^* is the dynamic viscosity of the liquid and k_0 is a characteristic permeability of the mush defined as

$$\Pi(\varphi) = \frac{k_0}{K^*}. \tag{1.7}$$

The non-dimensional temperature for the mush (or equivalently the composition) is given by

$$\theta = \frac{T^* - T_L(c_o)}{T_L(c_o) - T_E} = \frac{c^* - c_o}{c_o - c_E} = c. \tag{1.8}$$

Refer *Appendix A* provides a detailed non-dimensionalisation analysis for (1.3-1.8).

The dimensionless parameters that emanate as a result of the non-dimensionalisation of the governing equations are the Stefan number St, the concentration ratio ξ, the mushy layer Rayleigh number Ra_m, the Taylor number Ta and a parameter χ_o which represents

the coefficient of the time derivative in the Darcy equation. These dimensionless parameters may be presented as follows:

$$St = \frac{h_{fs}}{q_S\left(T_L(c_0) - T_E\right)} = \frac{h_{fs}}{q_S \Delta T}, \tag{1.9}$$

$$\xi = \frac{c_s' - c_E}{c_o - c_E}, \tag{1.10}$$

$$Ra_m = \frac{\beta^* \Delta c \, g^* k_0}{\nu^* V^*}, \tag{1.11}$$

$$Ta = \left[\frac{2\omega^* k_0}{\nu^* \phi_0}\right]^2, \tag{1.12}$$

$$\chi_o = \phi_0 \, Pr \, \vartheta_o, \tag{1.13}$$

where h_{fs} is the latent heat, q_S is the specific heat, c_s' is the solid composition, c_E is the eutectic composition, g^* is the gravitational acceleration, ω^* is the angular velocity of rotation, and ν^* is the kinematic viscosity of the liquid. The Stefan number gives an indication of the latent heat relative to the heat content, or internal energy. The composition ratio ξ relates the difference in characteristic compositions of the liquid and solid phases with the compositional variation of the liquid within the mushy layer. In Eqn.(1.13) $Pr = \nu^*/\kappa^*$ is the Prandtl number, $\vartheta_o = l_\kappa^2/k_0$ is the mobility ratio which is typically very large ($\vartheta_o \approx O(10^5 \to 10^6)$, see Worster (1992)) and can be thought of as the square of the ratio of the thermal length scale (on which the mushy layer height depends) to the average spacing between the dendrites within the mushy layer.

The boundary conditions applicable to the system (1.3- 1.6) are given by

$$\theta = -1, \quad w = 0 \qquad \text{at} \quad z = 0$$
$$\theta = 0, \quad w = 0, \quad \varphi = 0 \quad \text{at} \quad z = \delta. \tag{1.14}$$

The parameter $\delta = H^*/(\kappa^*/V^*)$ is the dimensionless depth of the layer, or growth Peclet number that will play a major role in the scaling of the governing equations later on. For all intents and purposes the growth Peclet number simply denotes the ratio between the actual height of the domain H^* and the length scale $l_\kappa = \kappa^*/V^*$, which has been used in the non-dimensionalization.

We follow Anderson & Worster(1996) in reducing the model asymptotically. We assume that the mushy layer is thin so that $\delta \ll 1$. Chen et al (1994) found that $V^* = 1.5 \times 10^{-4} \text{cm/s}$ as the mush height reached $H^* = 1\text{cm}$. Using a thermal diffusivity of $\kappa^* = 1.58 \times 10^{-3} \text{cm}^2/\text{s}$, yields $\delta = 0.095$, which satisfies the requirement $\delta \ll 1$. Worster (1991) showed, by analysing the exact solution for a non-convecting mushy layer that as $\theta_\infty = T_\infty/\Delta T \to \infty$ (where $\theta_\infty \gg 1$), the mush thickness is given by $\delta \approx \ln(1 + 1/\theta_\infty) \approx 1/\theta_\infty$. Physically this implies that the dimensionless mushy layer thickness can be associated with the inverse of the non-dimensional far field temperature. We also consider the case when the initial composition of the liquid is close to the eutectic composition ($c_0 \approx c_E$) thus resulting in a large value for ξ (see Eqn.(1.10)) which may be defined as,

$$\xi = \frac{c_S}{\delta}, \tag{1.15}$$

where c_S is O(1) as $\delta \to 0$. This approximation ($\delta \to 0, \xi \to \infty$) corresponds to the near-eutectic approximation used by Fowler (1985). This limit allows for the *leading order* system describing the mushy layer to be expressed as a mushy layer of constant permeability by usage of the permeability definition $\Pi(\varphi) = 1 + O(\varphi)$ where φ is $O(\varepsilon, \delta)$. The effects of permeability variations will then be introduced at a later stage as

18

perturbations to the system. We follow Anderson & Worster (1996) and assume that the Stefan number is large by expressing it as,

$$St = \frac{\overline{S}}{\delta},$$

(1.16)

where $\overline{S} = O(1)$ as $\delta \to 0$. This is different from the Amberg & Homsey (1993) who assumed a Stefan number of the form $St = O(1)$.

2. Case One : Time scale used by Anderson & Worster (1996)

2.1 Rescaled Equations

We proceed to rescale space and time and also introduce a new effective Rayleigh number based on the mushy layer thickness δ as follows,

$$x\hat{e}_x + y\hat{e}_y + z\hat{e}_z = \delta(\overline{x}\hat{e}_x + \overline{y}\hat{e}_y + \overline{z}\hat{e}_z), \quad t = \delta^2\overline{t}, \quad R^2 = \delta Ra_m. \tag{2.1a-c}$$

The scaling adopted for the dependent variables in Eqn.(2.1) is consistent with that used by Anderson & Worster (1996). The time scale represented here is associated with the diffusion time across the mushy layer. Next, we introduce the following scalings as used in the non-linear analysis of Anderson & Worster (1996):

$$\mathbf{U} = \frac{R}{\delta}\overline{\mathbf{U}}, \quad p = R\overline{p}. \tag{2.2a-b}$$

These scalings are applied to the system (1.3-1.6) and result in the following governing set of equations:

$$\overline{\nabla}\cdot\overline{\mathbf{U}} = 0 \tag{2.3}$$

$$\left(\frac{\partial}{\partial\overline{t}} - \delta\frac{\partial}{\partial\overline{z}}\right)\left(\theta - \frac{\overline{S}}{\delta}\varphi\right) + R\overline{\mathbf{U}}\cdot\overline{\nabla}\theta = \overline{\nabla}^2\theta \tag{2.4}$$

$$\left(\frac{\partial}{\partial\overline{t}} - \delta\frac{\partial}{\partial\overline{z}}\right)\left[(1-\varphi)\theta + \frac{c_S}{\delta}\varphi\right] + R\overline{\mathbf{U}}\cdot\overline{\nabla}\theta = 0 \tag{2.5}$$

$$\frac{1}{\chi}\frac{\partial\overline{\mathbf{U}}}{\partial t'} + \Pi(\varphi)\overline{\mathbf{U}} = -\overline{\nabla}\overline{p} - R\theta\,\hat{\mathbf{e}}_z - Ta^{1/2}\,\hat{\mathbf{e}}_z\times\overline{\mathbf{U}} \tag{2.6}$$

where $\chi = \delta^2\chi_o$. Using the earlier definition for the thermal length scale, δ, and χ_o, the expression for χ may be transformed to the following form:

$$\chi = \frac{\phi_0 \, \mathrm{Pr}}{\mathrm{Da}}, \tag{2.7}$$

where Pr is the fluid Prandtl number, ϕ_0 is the porosity and Da is the Darcy number defined as $\mathrm{Da} = k_0/(H^*)^2$. The Darcy number ($\mathrm{Da} = k_0/(H^*)^2$) is very similar to the mobility ratio ($\vartheta_0 = l_\kappa^2 / k_0$), the only difference that being that it is the inverse of the mobility ratio with the mushy layer height H^* being replaced by the thermal length scale l_κ, as observed from their respective definitions. Vadasz (1998) was the first to point out the definition of the parameter χ in his paper on flows in porous media. In porous media theory the value of χ is usually quite big and allows to neglect the time derivative term, hence usually it is neglected. In the current case the parameter χ would be retained based on the following arguments: the Prandtl number (Pr) in systems undergoing solidification ranges from $\mathrm{Pr} = 10^{-3}$ (for metallic alloys) to $\mathrm{Pr} = 10$ (for aqueous solutions). Vadasz (1998) suggested that $\mathrm{Da} = 10^{-4}$, $\phi_0 = 0.1$, and $\mathrm{Pr} = 10^{-3}$ are typical values for a mushy layer. Using Vadasz's (1998) suggested values for the mushy layer yields $\chi = 1$. Furthermore the mobility ratio may be recovered from the calculated value of χ and a growth Peclet number (δ) using the relation $\chi = \delta^2 \chi_0$. Using the values of Prandtl number (Pr), porosity (ϕ_0), together with the calculated value of χ yields a mobility ratio of $\vartheta_0 = 1 \times 10^6$. This value of mobility ratio is in total agreement with the value range suggested by Worster (1991). In the present study we retain the time derivative term in the equation in order to allow for the possibility of oscillatory convection and will observe how the value of χ affects the various parameters in the system. A full derivation of the system (2.3-2.6) as well as the derivation of Eqn.(2.7) is provided in *Appendix B*.

2.2 Basic Flow Solution

There is a basic steady state ($\partial\theta_B/\partial\bar{t} = \partial\varphi_B/\partial\bar{t} = 0$) represented by subscript 'B', which is horizontally uniform ($\partial\theta_B/\partial\bar{x} = \partial\varphi_B/\partial\bar{x} = 0$, $\partial\theta_B/\partial\bar{y} = \partial\varphi_B/\partial\bar{y} = 0$), corresponds to zero flow ($\mathbf{U}_B = 0$) and satisfies the following system of equations :

$$-\delta \frac{d}{d\bar{z}}\left[\theta_B - \frac{\overline{S}}{\delta}\varphi_B\right] = \frac{d^2\theta_B}{d\bar{z}^2} \tag{2.8}$$

$$-\delta \frac{d}{d\bar{z}}\left[(1-\varphi_B)\theta_B + \frac{c_S}{\delta}\varphi_B\right] = 0 \tag{2.9}$$

$$-\frac{d\bar{p}_B}{d\bar{z}} - R\theta_B = 0 \tag{2.10a}$$

$$\frac{d\bar{p}_B}{d\bar{x}} = \frac{d\bar{p}_B}{d\bar{y}} = 0. \tag{2.10b}$$

It is interesting to note that Eqns.(2.8-2.10) resemble Anderson & Worster's (1996) system exactly. Eqns.(2.8 – 2.10) are subject to the boundary conditions

$$\theta_B = -1 \qquad \text{at} \qquad \bar{z} = 0 \tag{2.11}$$

$$\theta_B = 0, \qquad \varphi_B = 0, \qquad \text{at} \qquad \bar{z} = 1. \tag{2.12}$$

Using an expansion in δ (where $\delta \ll 1$) to express the basic state solution as follows:

$$\theta_B(\bar{z}) = \theta_{B0}(\bar{z}) + \delta\theta_{B1}(\bar{z}) + \delta^2\theta_{B2}(\bar{z}) + O(\delta^3) \tag{2.13}$$

$$\varphi_B(\bar{z}) = \varphi_{B0}(\bar{z}) + \delta\varphi_{B1}(\bar{z}) + \delta^2\varphi_{B2}(\bar{z}) + O(\delta^3). \tag{2.14}$$

Substituting expansions (2.13 – 2.14) in the system (2.8 – 2.10) and solving for the functions of $\bar{z}$ to the different orders in δ yields the following result:

$$\theta_B(\bar{z}) = (\bar{z} - 1) + \delta\left[-\frac{\Omega}{2}(\bar{z}^2 - \bar{z}) \right] +$$

$$\delta^2\left[\frac{\Omega^2}{2}\left(\frac{1}{3}\bar{z}^3 - \frac{1}{2}\bar{z}^2\right) - \frac{\bar{S}}{c_S^2}\left(\frac{1}{3}\bar{z}^3 - \bar{z}^2\right) + \frac{1}{3}\left(\frac{2\bar{S}}{c_S^2} + \frac{1}{4}\Omega^2\right)\bar{z} \right] \quad (2.15)$$

$$\varphi_B(\bar{z}) = -\delta\frac{(\bar{z} - 1)}{c_S} + \delta^2\left[\frac{-(\bar{z} - 1)^2}{c_S^2} + \frac{\Omega}{2c_S}(\bar{z}^2 - \bar{z}) \right], \quad (2.16)$$

where $\Omega = 1 + \bar{S}/c_S = 1 + St/\xi$. The parameter Ω can assume values greater than unity, ie. $\Omega > 1$. For $\Omega = 1$, we note that the Stefan number becomes zero. This is unphysical as the Stefan number St used in the current study is non zero. In the current study we ensure that Ω is always greater than unity. Recall that the assumption that $\xi \cong O(1/\delta)$ leads to a small basic state solid fraction. A detailed derivation of the basic state solution is presented in *Appendix C*. It is interesting to note that in the limit $\delta \to 0$ we find that $\varphi_B \to 0$ thereby corresponding to convection in a non-porous medium.

The scaling in the Stefan number leads to a basic solution that is slightly different to that found by Amberg & Homsey (1993), see Eqns.(2.9a) and (2.9b) in their paper.

Note that the governing partial differential system (2.3 – 2.6) forms a three dimensional non-linear coupled system . To provide a non-trivial solution to the system it is convenient to apply the *curl* operator ($\nabla \times$) on Eqn.(2.6) and obtain an equation which includes the vorticity, defined as $\omega = \nabla \times \bar{U}$, in the form

$$\frac{1}{\chi}\frac{\partial\omega}{\partial\bar{t}} + \Pi(\varphi)\omega + \frac{d\Pi}{d\bar{z}}\left[\bar{u}\hat{e}_y - \bar{v}\hat{e}_x\right] - Ta^{1/2}\frac{\partial\bar{U}}{\partial\bar{z}} = -R\left[\frac{\partial\theta}{\partial\bar{y}}\hat{e}_x - \frac{\partial\theta}{\partial\bar{x}}\hat{e}_y\right] \quad (2.17)$$

It can be noticed that the vertical component of Eqn.(2.17) is independent of temperature and may be given as,

$$\left[\frac{\partial}{\chi \partial \bar{t}} + \Pi(\varphi) \right] \omega_z = Ta^{1/2} \, \partial \bar{w}/\partial \bar{z} \tag{2.18}$$

where ω_z is the vertical component of vorticity. Then, applying the *curl* operator ($\nabla \times$) again on Eqn.(2.17) and using the property of $\bar{U}$ being solenoidal, which comes out as a result of Eqn.(2.3) , and considering only the z-component of the result yields the following equation,

$$\left[\frac{1}{\chi} \frac{\partial}{\partial \bar{t}} + \Pi(\varphi) \right] \nabla^2 \bar{w} + \frac{d\Pi}{d\bar{z}} \frac{\partial \bar{w}}{\partial \bar{z}} + R\nabla_H^2 \theta + Ta^{1/2} \frac{\partial \omega_z}{\partial \bar{z}} = 0, \tag{2.19}$$

where the horizontal Laplacian operator is defined in the form $\nabla_H^2 = \partial^2/\partial \bar{x}^2 + \partial^2/\partial \bar{y}^2$.

2.3 Linear Stability Analysis

The stability of the basic solution (2.15 –2.16) is examined by determining the growth and decay of infinitesimal disturbances around this solution. We introduce normal-mode perturbations to the basic state solution as follows:

$$\theta = \theta_B + \varepsilon \hat{\theta}(\bar{z}) e^{\sigma \bar{t}} e^{i(s_x \bar{x} + s_y \bar{y})} + c.c \tag{2.20}$$

$$\varphi = \varphi_B + \varepsilon \hat{\varphi}(\bar{z}) e^{\sigma \bar{t}} e^{i(s_x \bar{x} + s_y \bar{y})} + c.c \tag{2.21}$$

$$\bar{U} = 0 + \varepsilon \hat{\bar{U}}(\bar{z}) e^{\sigma \bar{t}} e^{i(s_x \bar{x} + s_y \bar{y})} + c.c \tag{2.22}$$

where σ is the growth rate, s_x and s_y are the horizontal wave numbers of the perturbation and c.c represents the complex conjugate. By substituting the normal-mode

expansions (2.20-2.22) in Eqns.(2.3–2.5) and Eqns.(2.18-2.19) yields the following linearised heat and solute balance equations and Darcy equation to order ε,

$$[\sigma - \delta D]\left[\hat{\theta} - \frac{\overline{S}}{\delta}\hat{\varphi}\right] + R\hat{\overline{w}}D\theta_B = \left(D^2 - s^2\right)\hat{\theta} \qquad (2.23)$$

$$[\sigma - \delta D]\left[(1 - \varphi_B)\hat{\theta} - \theta_B\hat{\varphi} + \frac{c_S}{\delta}\hat{\varphi}\right] + R\hat{\overline{w}}D\theta_B = 0 \qquad (2.24)$$

$$\left[\frac{\sigma}{\chi} + \Pi(\varphi)\right]^2\left(D^2 - s^2\right)\hat{\overline{w}} + \left[\frac{\sigma}{\chi} + \Pi(\varphi)\right]\left[D\Pi(\varphi).D\hat{\overline{w}} - Rs^2\hat{\theta}\right] + TaD^2\hat{\overline{w}} = 0, \qquad (2.25)$$

where $D = d/d\overline{z}$ and $\sigma = \sigma_r + i\sigma_i$. A detailed derivation of Eqns.(2.18-2.19) and the system (2.23-2.25) is given in *Appendix D*. The system is solved subject to the following boundary conditions:

$$\hat{\theta} = 0, \quad \hat{\overline{w}} = 0 \qquad : \quad \overline{z} = 0$$
$$\hat{\theta} = 0, \quad \hat{\overline{w}} = 0, \quad \hat{\varphi} = 0 \quad : \quad \overline{z} = 1. \qquad (2.26)$$

We assume longitudinal roll solutions for $\overline{y} \ll 1$ ($y \ll \delta$). We are interested in the solution to these equations for $\delta \ll 1$, so we follow Anderson & Worster (1996) an expand the dependent variables in powers of δ as follows,

$$\sigma = \sigma_{00} + \delta\sigma_{01} \qquad (2.27)$$

$$R = R_{00} + \delta R_{01} \qquad (2.28)$$

$$\hat{\theta} = \theta_{00} + \delta\theta_{01} \qquad (2.29)$$

$$\hat{\varphi} = \varphi_{00} + \delta\varphi_{01} \qquad (2.30)$$

$$\hat{\overline{w}} = w_{00} + \delta w_{01}. \tag{2.31}$$

Note that owing to the fact that the basic state solid fraction is small, the permeability function $\Pi(\varphi)$ is expanded in a Taylor series following Anderson & Worster (1996) as follows,

$$\Pi(\varphi) = 1 + \delta \varphi_{B1} K_1. \tag{2.32}$$

From Eqn.(2.16) $\varphi_{B1} = -(\overline{z} - 1)/c_S$, where the constant K_1 characterises the linear variation of the permeability with the local solid fraction and must be positive in order to ensure that the permeability decreases with increasing solid fraction. It can also be noted from Eqn.(2.32) that at the leading order the permeability is constant. We proceed with the expansion in powers of δ and find from the solute balance equation, Eqn.(2.24), that there exists an $O(1/\delta)$ problem which may be expressed as,

$$\sigma_{00} c_S \varphi_{00} = 0, \tag{2.33}$$

where $\sigma_{00} = \sigma_{r0} + \sigma_{i0}$. Eqn.(2.33) is solved by taking $\sigma_{r0} = \sigma_{i0} = 0$, ie. $\sigma_{00} = 0$. Note that to order $O(\delta^0)$ we find that

$$\left(D^2 - s^2\right)\theta_{00} - \Omega R_{00} w_{00} = 0 \tag{2.34}$$

$$c_S\left(\sigma_{r1} + i\sigma_{i1} - D\right)\varphi_{00} + R_{00} w_{00} = 0 \tag{2.35}$$

$$\left(D^2 - s^2\right)w_{00} - R_{00} s^2 \theta_{00} + TaD^2 w_{00} = 0, \tag{2.36}$$

subject to the boundary conditions

$$\begin{aligned}
\theta_{00} &= 0, \quad w_{00} = 0 && : \quad \overline{z} = 0 \\
\theta_{00} &= 0, \quad w_{00} = 0, \quad \varphi_{00} = 0 && : \quad \overline{z} = 1.
\end{aligned} \tag{2.37}$$

26

where $\Omega = 1 + \overline{S}/c_S$. See *Appendix E* for the derivation of the equations to order $O(\delta^0)$. The solution to order $O(\delta^0)$ may be presented as,

$$\theta_{00} = -A_{00} \sin(\pi\overline{z}) \tag{2.38}$$

$$w_{00} = B_{00} \sin(\pi\overline{z}) \tag{2.39}$$

$$\varphi_{00} = -C_{00}\left[e^{(\sigma_{rl}+\sigma_{il})(\overline{z}-1)} + \cos(\pi\overline{z}) + \frac{(\sigma_{rl}+\sigma_{il})}{\pi}\sin(\pi\overline{z}) \right] \tag{2.40}$$

$$R_{00}^2 = \frac{(\pi^2 + s^2)(\pi^2 + s^2 + \pi^2 Ta)}{\Omega s^2} \tag{2.41}$$

where the coefficients in Eqn.(2.39) and Eqn.(2.40) are given as

$$B_{00} = \frac{(\pi^2 + s^2)}{\Omega R_{00}} A_{00} \tag{2.42}$$

$$C_{00} = \frac{\pi(\pi^2 + s^2)}{\Omega c_S\left[\pi^2 + \left(\sigma_{rl} + i\sigma_{il}\right)^2\right]} A_{00}. \tag{2.43}$$

A detailed derivation of Eqns.(2.38-2.43) is provided in *Appendix F*. We note from Eqn.(2.40) that σ_{rl} and σ_{il} yet to be determined (where $\sigma_{01} = \sigma_{rl} + i\sigma_{il}$). In order to evaluate these terms we need to continue our expansion to order $O(\delta)$. At order $O(\delta)$ the modified heat balance equation and the Darcy equation is given as,

$$\left(D^2 - s^2\right)\theta_{01} - \Omega R_{00} w_{01} = \left[\left(\sigma_{rl} + i\sigma_{il}\right) - D\right]\left[\Omega\theta_{00} - \frac{\overline{S}}{c_S}\theta_{B0}\varphi_{00}\right] +$$

$$\Omega R_{00} w_{00} D\theta_{B1} + \Omega R_{01} w_{00} \tag{2.44}$$

27

$$\left(D^2 - s^2\right)w_{01} - s^2 R_{00}\theta_{01} + TaD^2 w_{01} = -2\left[\frac{\left(\sigma_{r1} + i\sigma_{i1}\right)}{\chi} + K_1\varphi_{B1}\right]\left(D^2 - s^2\right)w_{00} -$$

$$K_1 D\varphi_{B1}Dw_{00} + s^2 R_{01}\theta_{00} + s^2 R_{00}\theta_{00}\left[\frac{\left(\sigma_{r1} + i\sigma_{i1}\right)}{\chi} + K_1\varphi_{B1}\right]. \qquad (2.45)$$

A detailed derivation of Eqns.(2.44-2.45) is provided in *Appendix G*. The existence of solutions to Eqns.(2.44-2.45) requires that a solvability condition be satisfied. The determination of the solvability condition involves decoupling Eqns.(2.44) and (2.45) to obtain a single non-homogenous partial differential equation for θ_{01}. Multiplying the resulting partial differential equation for θ_{01} by θ_{00} (Eqn.(2.38)) and integrating over the region $\bar{z} \in [0,1]$, and using the boundary conditions $\theta_{01}(0) = \theta_{01}(1) = 0$, $w_{01}(0) = w_{01}(1) = 0$ and $d^2 w_{01}(0)/d\bar{z}^2 = P_1$, $d^2 w_{01}(1)/d\bar{z}^2 = P_2$, which is obtained from Eqn.(2.45), to give the solvability condition that must be satisfied as,

$$\frac{(\pi^2 + s^2)^2(\pi^2 + s^2 - \pi^2 Ta)}{(\pi^2 + s^2 + \pi^2 Ta)}\left[\frac{1}{4}\frac{K_1}{c_S} + \frac{\left(\sigma_{r1} + i\sigma_{i1}\right)}{2\chi}\right] - \left(\pi^2 + s^2\right)^2\frac{R_{01}}{R_{00}} + \left(\pi^2 + s^2\right)\frac{\Omega}{2}\left(\sigma_{r1} + i\sigma_{i1}\right) +$$

$$\frac{\bar{S}}{\Omega c_S^2}\left(\pi^2 + s^2\right)^2\left[\frac{1}{4} + \frac{\left(\sigma_{r1} + i\sigma_{i1}\right)}{2\left[\pi^2 + \left(\sigma_{r1} + i\sigma_{i1}\right)^2\right]} + \frac{\pi^2\left(1 + e^{-\left(\sigma_{r1} + i\sigma_{i1}\right)}\right)}{\left[\pi^2 + \left(\sigma_{r1} + i\sigma_{i1}\right)^2\right]^2}\right] = 0. \qquad (2.46)$$

Note that the quantities P_1 and P_2 are scalar quantities that represent the second derivative of the vertical component of the velocity, w_{01}, at the lower and upper boundary of the domain. Refer to *Appendix H* for a detailed derivation of the solvability condition. The real and imaginary parts of the characteristic equation, Eqn.(2.46), represents two conditions relating R_{01}, σ_{r1}, and σ_{i1}. In the following section we proceed to search for solutions to Eqn.(2.46) in order to determine the linear stability properties of the mushy layer.

2.4 Stationary Convection

For stationary convection σ_{rl} and σ_{il} in Eqn.(2.46) are real and for marginal stability $\sigma_{rl} = 0$, therefore the corresponding Rayleigh number correction R_{01} associated with stationary convection is obtained by substituting $\sigma_{il} = 0$ in Eqn.(2.46) and is presented in the form,

$$\frac{R_{01c,st}}{R_{00}} = \frac{(\pi^2 + s^2 - \pi^2 Ta)}{(\pi^2 + s^2 + \pi^2 Ta)} \frac{1}{4} \frac{K_l}{c_S} + \frac{\overline{S}}{\Omega c_S^2}\left[\frac{1}{4} + \frac{2}{\pi^2}\right]. \tag{2.47}$$

Rescaling the wavenumber in the form $\alpha = s^2/\pi^2$, setting $\lambda = \overline{S}/(\Omega\, c_S)^2$ and applying to Eqn.(2.47) yields,

$$\frac{R_{01c,st}}{R_{00}} = \frac{(1+\alpha - Ta)}{(1+\alpha + Ta)} \frac{1}{4} \frac{K_l}{c_S} + \Omega\lambda\left[\frac{1}{4} + \frac{2}{\pi^2}\right]. \tag{2.48}$$

Rescaling Eqn.(2.41) using the above scaling parameters yields,

$$R_{00}^2 = \frac{\pi^2}{\Omega} \frac{(\alpha + 1)(\alpha + 1 + Ta)}{\alpha} . \tag{2.49}$$

The parameter $\lambda = \overline{S}/(\Omega\, c_S)^2$ refers to a ratio between the Stefan number and the composition ratio. The parameter $\Omega = 1 + \overline{S}/c_S$ may assume values greater than unity, as mentioned earlier. If we select $\Omega = 2$ say, then $\overline{S}/c_S = 1$. Noting that the composition ratio c_S can assume values ranging from $c_S = 0.25$ (for molten alloys) to about $c_S = 4$ (for aqueous salt solutions) we may infer that the parameter λ can assume values ranging from $\lambda = 0.0625$ to $\lambda = 1$ across the band of composition ratios at $\Omega = 2$.

Noting that $R = R_{00} + \delta R_{01}$ yields characteristic Rayleigh number values associated with stationary convection which may be presented as

$$R_{c,st} = \pi \sqrt{\frac{(\alpha + 1)(\alpha + 1 + Ta)}{\Omega \alpha}} \left[1 + \delta \left(\frac{(\alpha + 1 - Ta)}{(\alpha + 1 + Ta)} \frac{1}{4} \frac{K_1}{c_S} + \Omega \lambda \left(\frac{1}{4} + \frac{2}{\pi^2} \right) \right) \right] \qquad (2.50)$$

where the subscript $(.)_{st}$ stands for identifying stationary convection. Note that as $Ta \rightarrow 0$ Eqn.(2.50) collapses to the exact Rayleigh number definition as proposed by Anderson & Worster (1996) and is presented using the current scaling as,

$$R_{c,st} = \pi (\alpha + 1) \sqrt{\frac{1}{\Omega \alpha}} \left[1 + \delta \left(\frac{1}{4} \frac{K_1}{c_S} + \Omega \lambda \left(\frac{1}{4} + \frac{2}{\pi^2} \right) \right) \right] . \qquad (2.51)$$

The form of the equation, given by Eqn.(2.50), however presents the case when the effects of rotation is included and it is this case that is our current area of interest. Graphical representation of the characteristic curves for Ta=0, Ta=5, Ta=10,Ta=20, Ta=50 and Ta=100 for different λ values following Eqn.(2.50). It can be observed from Figures 4 to 9 that as the Taylor number is increased from Ta=0 (non-rotating case) to Ta=100, there is a corresponding increase in the critical Rayleigh and wave numbers respectively. Another interesting feature that can be noted is that as the Rayleigh number becomes larger the curves begin to flatten out or reach an asymptotical limit. The onset of this asymptote occurred for wavenumber values (s/π) greater than unity, ie for larger wavenumbers. This feature is most evident at Ta=50 and Ta=100. Incidentally this feature persists for values of Taylor number greater than Ta=100.

Figure 4 : Characteristic Rayleigh number curves at Ta=0 for different values of λ

Figure 5 : Characteristic Rayleigh number curves at Ta=5 for different values of λ
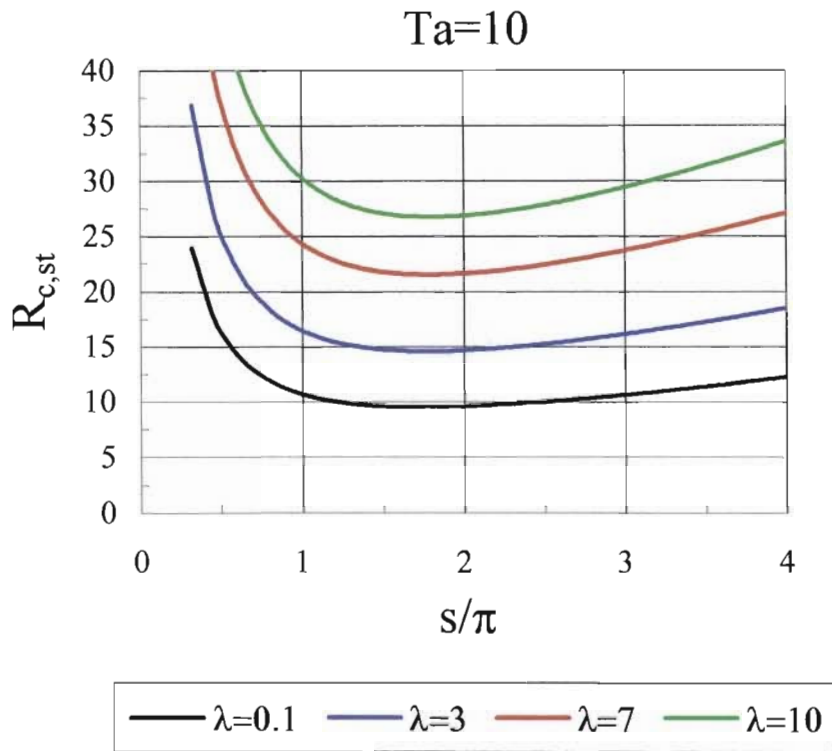
Figure 6 : Characteristic Rayleigh number curves at Ta=10 for different values of λ

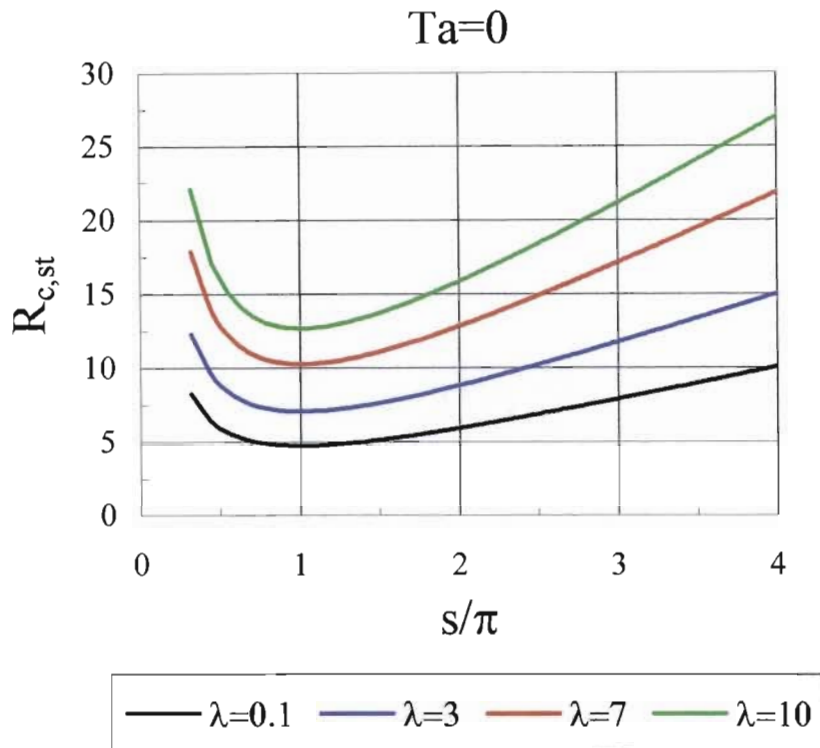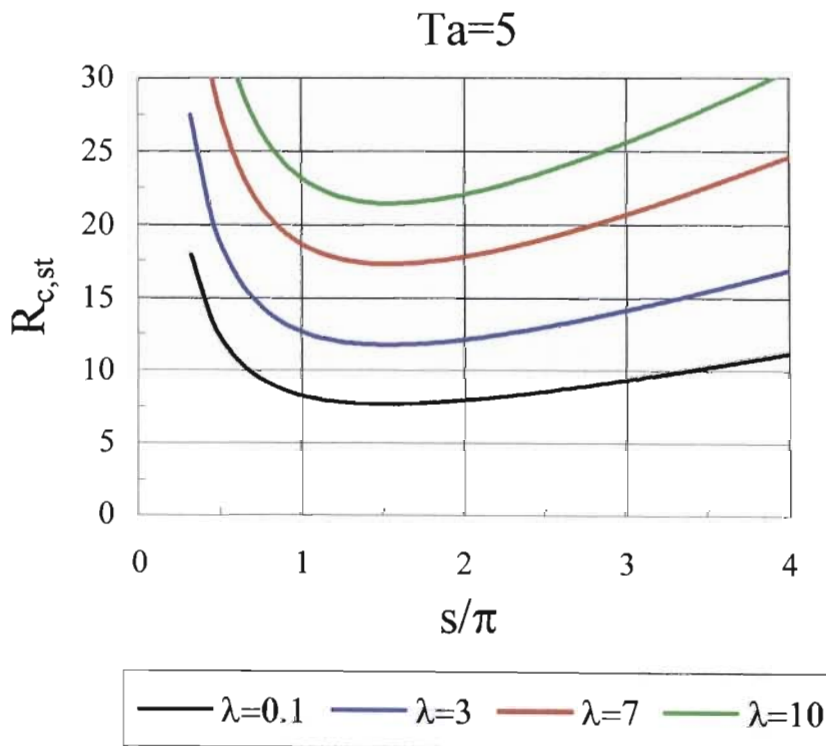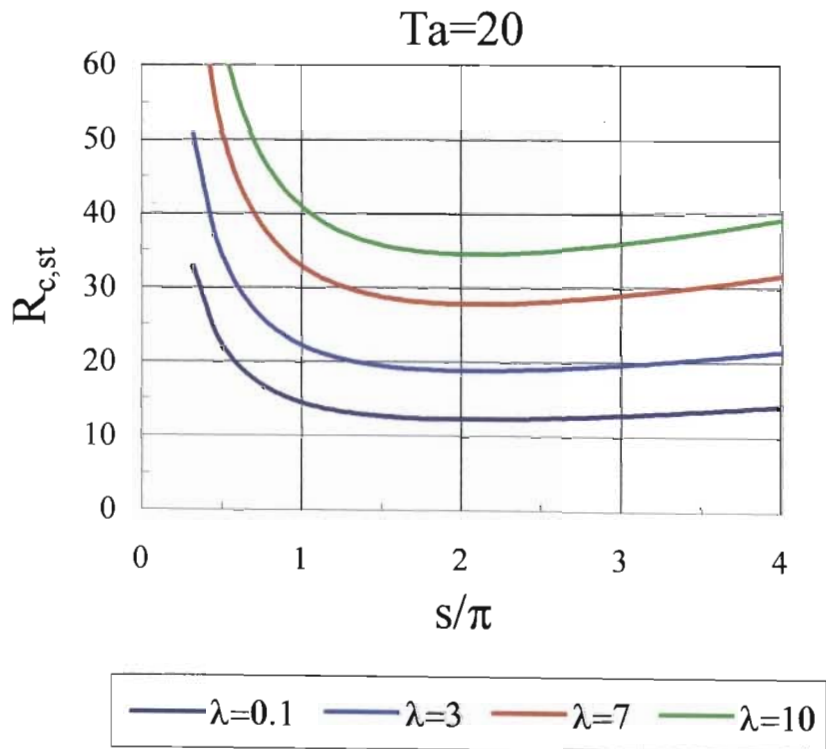Figure 7 : Characteristic Rayleigh number curves at Ta=20 for different values of λ
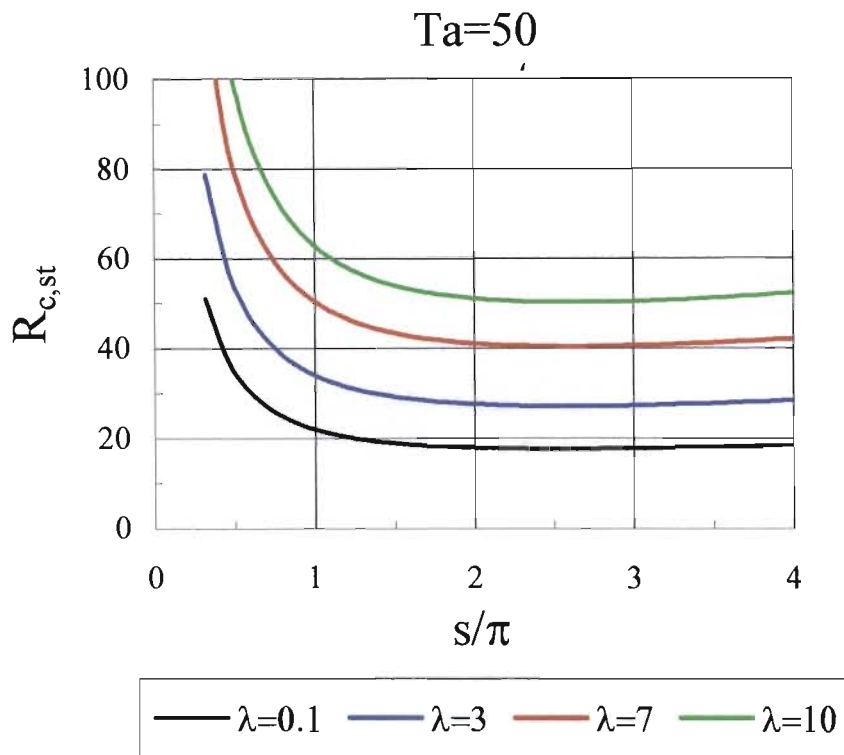
Figure 8 : Characteristic Rayleigh number curves at Ta=50 for different values of λ
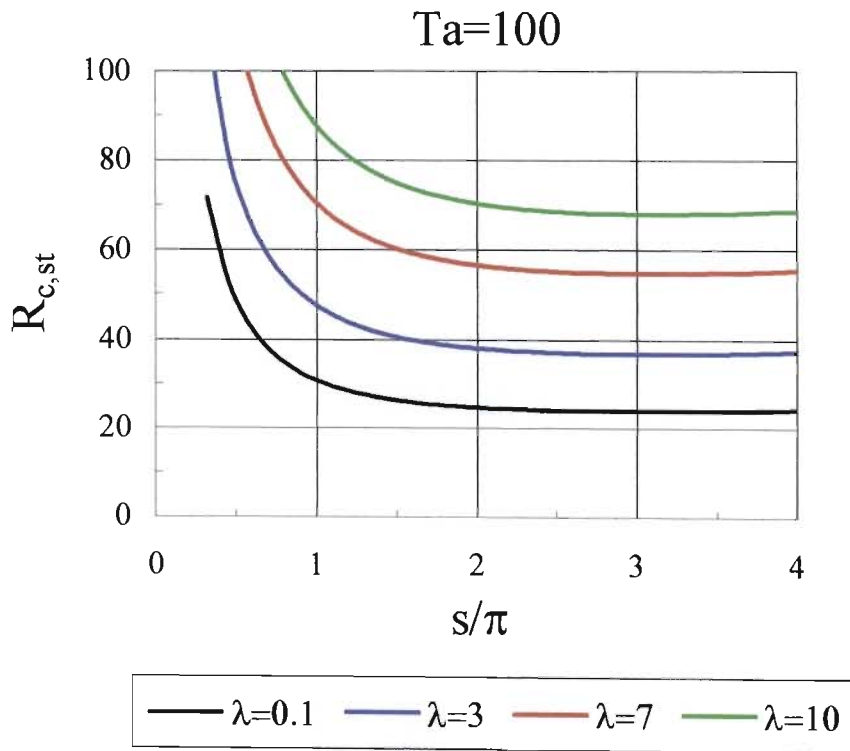
Figure 9 : Characteristic Rayleigh number curves at Ta=100 for different values of λ

For high values of Taylor number Eqn.(2.50) may be approximated as,

$$\lim_{Ta \to \infty} R_{c,st} = \left(\pi \sqrt{\frac{Ta}{\Omega}} \right) \sqrt{1 + \frac{1}{\alpha}} \left[1 + \delta \left(-\frac{1}{4} \frac{K_1}{c_S} + \Omega \lambda \left(\frac{2}{\pi^2} + \frac{1}{4} \right) \right) \right]. \tag{2.52}$$

Refer to *Appendix I* for the derivation of Eqn.(2.50) and Eqn.(2.52). Now it can be very clearly seen from Eqn.(2.52) that for large values of wavenumber, α, we approach a critical value for the asymptote at high Taylor numbers,

$$R_{cr,st}^{(asym)} = \left(\pi \sqrt{\frac{Ta}{\Omega}} \right) \left[1 + \delta \left(-\frac{1}{4} \frac{K_1}{c_S} + \Omega \lambda \left(\frac{2}{\pi^2} + \frac{1}{4} \right) \right) \right] \tag{2.53}$$

for appreciably large values of wavenumber, where $R_{c,st}^{(asym)}$ represents the asymptotical value of Rayleigh number. For all intents and purposes this represents the minimum point for any given value of Taylor number and λ value. The critical Rayleigh and wavenumbers are obtained by minimising $R_{c,st}$ in Eqn.(2.50) with respect to α, a process which produces a cubic algebraic equation for $\alpha_{cr,st}$ in the form,

$$\left[4 + \delta \left(\frac{K_1}{c_S} + 4\eta_s \right) \right] \alpha^3 + \left[4(1 + Ta) + \delta \left(\frac{K_1}{c_S}(1 + 3Ta) + 4\eta_s(1 + Ta) \right) \right] \alpha^2 +$$

$$\left[-4(1 + Ta) - \delta \left(\frac{K_1}{c_S}(1 - 3Ta) + 4\eta_s(1 + Ta) \right) \right] \alpha +$$

$$\left[-4(1 + Ta)^2 - \delta \left(\frac{K_1}{c_S}(1 - Ta^2) + 4\eta_s(1 + Ta)^2 \right) \right] = 0, \tag{2.54a}$$

where $\eta_s = \Omega \lambda \left(1/4 + 2/\pi^2 \right)$. It is interesting to note that for very small values of δ, ie. as $\delta \to 0$, Eqn.(2.54a) reduces to,

$$\alpha^3 + (1 + Ta) \alpha^2 - (1 + Ta)\alpha - (1 + Ta)^2 = 0, \tag{2.54b}$$

34

which is applicable to flow in a non-porous medium. Another point worthy of note is that at very low Taylor numbers, ie. $Ta \rightarrow 0$, Eqn.(2.54a) reduces to,

$$\alpha^3 + \alpha^2 - \alpha - 1 = 0.$$
(2.54c)

The only real and positive solution to Eqn.(2.54c) is $\alpha = 1$. This corresponds to the critical wavenumber evaluated by Anderson & Worster (1996) in their study of a non-rotating (Ta=0) mushy layer. It can be noted that this critical value of wavenumber is independent of the parameter λ. The solution to Eqn.(2.54a) was obtained numerically showing that only one real and positive root, associated with the various selected parameter values, existed. *Appendix J* provides a derivation of Eqn.(2.54a). A solution to Eqn.(2.54a) is presented for $\delta = 0.2$, $K_l/c_S = 1.0$, and $\Omega = 2$ in Figures 10 and 11.

Figure 10 provides a plot of the critical wavenumber as a function of the Taylor number for different values of the parameter λ. It can be observed from Figure 10 that for any selected value of Taylor number there is very little variation in the critical wavenumber across the parameter range λ. However the critical wavenumber increases with increasing Taylor number for a selected λ curve. The locus of the critical Rayleigh number values as a function of the Taylor number is shown in Figure 11. It can be seen that increasing the value of the parameter λ causes the gradient of the curves to increase across the Taylor number range. If we set say $\overline{S}/c_S = 1$ so that $\Omega = 2$, this implies that $\lambda = \overline{S}/(\Omega c_S)^2 = 1/(4c_S) = 1/(4\delta\xi)$, where the value for δ is fixed. It can be seen that materials with high composition ratios ξ (typically aqueous ammonium chloride) result in low values for the parameter λ, whilst those with low values of composition ratio ξ (typically liquid metals) result in relatively higher values of the parameter λ. Therefore for a particular setting of Taylor number it can be observed from Figure 10 that the onset of the stationary mode of convection for liquid metals occurs at a higher value of critical wavenumber in comparison to the lower value observed for the aqueous salts.
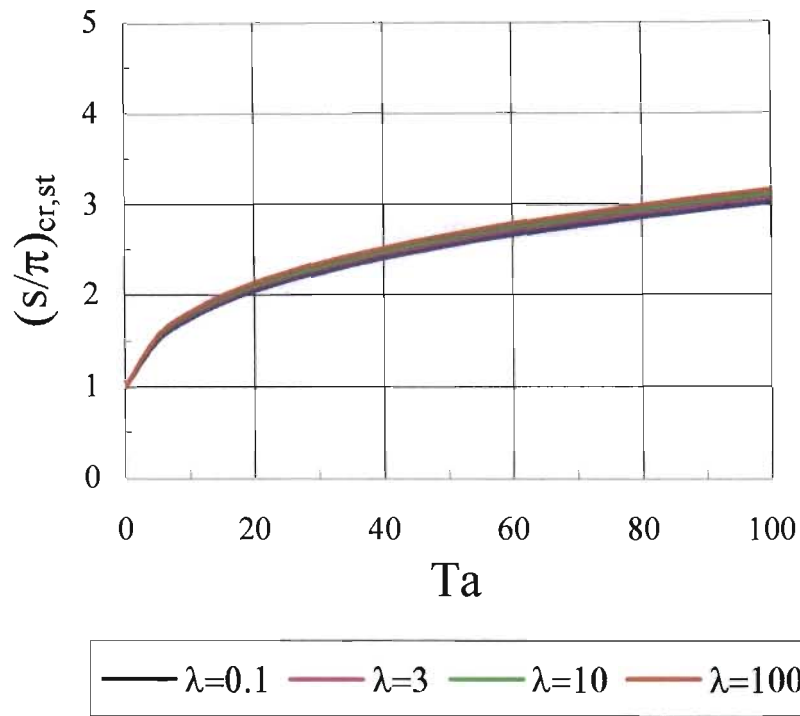
Figure 10 : Critical wavenumber $(s/\pi)_{cr,st}$ versus Ta
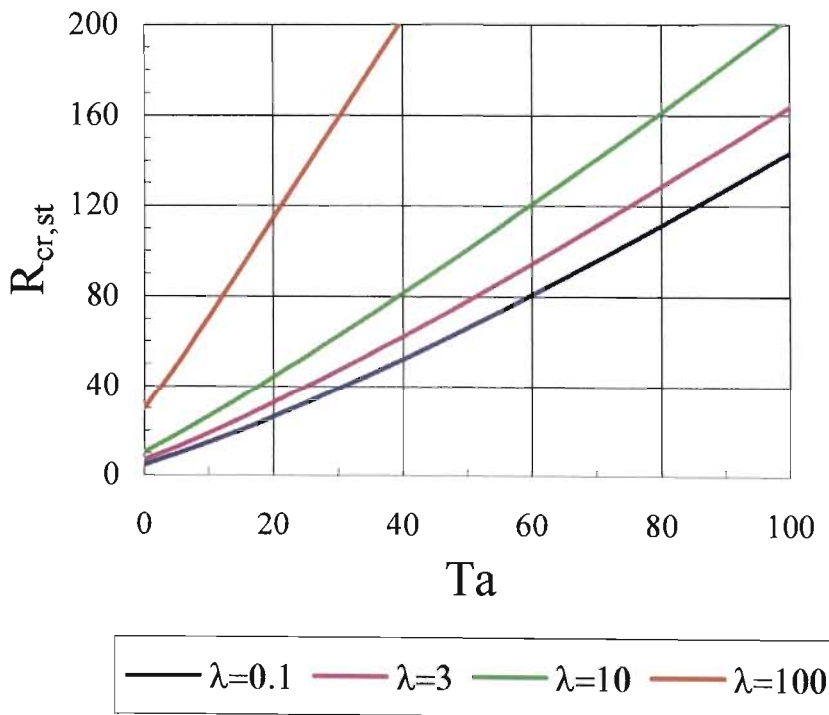
Figure 11 : Critical Rayleigh number ($R_{cr,st}$) versus Ta

$$\sigma_{i1}\left(1+\lambda\pi^2(\alpha+1)\left[\frac{1}{(\pi^2-\sigma_{i1}^2)}-\frac{2\pi^2}{(\pi^2-\sigma_{i1}^2)^2}\frac{\sin(\sigma_{i1})}{\sigma_{i1}}\right]\right)=0,\qquad(2.63)$$

which is of a form that was solved for by Anderson & Worster (1996).

It can be noted from Eqn.(2.60) and Eqn.(2.61) that the frequency σ_{i1} couples these two equations, and it is for this reason that they need to be solved simultaneously using a numerical technique. It was decided upon to express Eqn.(2.61) in a manner such that α is made the subject of the formula as follows,

$$\alpha_{1,2}=\frac{-a_2\pm\sqrt{a_2^2-4a_1a_3}}{2a_1},\qquad(2.64)$$

where the coefficients of Eqn.(2.64) are given by,

$$a_1=\frac{1}{\Omega\gamma}+\lambda\pi^2\left[\frac{1}{(\pi^2-\sigma_{i1}^2)}-\frac{2\pi^2}{(\pi^2-\sigma_{i1}^2)^2}\frac{\sin\sigma_{i1}}{\sigma_{i1}}\right]\qquad(2.65)$$

$$a_2=(2-\mathrm{Ta})\frac{1}{\Omega\gamma}+\lambda\pi^2(2+\mathrm{Ta})\left[\frac{1}{(\pi^2-\sigma_{i1}^2)}-\frac{2\pi^2}{(\pi^2-\sigma_{i1}^2)^2}\frac{\sin\sigma_{i1}}{\sigma_{i1}}\right]+1\qquad(2.66)$$

$$a_3=(1-\mathrm{Ta})\frac{1}{\Omega\gamma}+\left(\lambda\pi^2\left[\frac{1}{(\pi^2-\sigma_{i1}^2)}-\frac{2\pi^2}{(\pi^2-\sigma_{i1}^2)^2}\frac{\sin\sigma_{i1}}{\sigma_{i1}}\right]+1\right)(1+\mathrm{Ta}).\qquad(2.67)$$

It can be observed that Eqn.(2.64) is a function of the frequency and the mentioned scaled parameters. Note that Eqn.(2.64) yields two solutions to the wavenumber, given by α_1 and α_2 respectively, note the subscripts in Eqn.(2.64). Now we may proceed to generate characteristic values for the wavenumber α for varying σ_{i1} values at different parameter values (ie. Ta, λ, and γ etc.). Note that the wavenumber can only assume values greater

than or equal to zero, hence it satisfies the inequality, $\alpha_{1,2} \geq 0$. Eqn.(2.64) produces two real values for the wavenumber, which then produces two corresponding characteristic values for the Rayleigh number, given by $R_{c,ov} = R_{00} + \delta R_{01,ov}$. Note that R_{00} is as given by Eqn.(2.49). The Rayleigh number curve producing the smaller critical Rayleigh number value is then selected. Note that the characteristic values for the Rayleigh number is given by,

$$R_{c,ov} = \pi \sqrt{\frac{(\alpha + 1)(\alpha + 1 + Ta)}{\Omega \alpha}} \left[1 + \delta \left(\frac{(\alpha + 1 - Ta)}{(\alpha + 1 + Ta)} \frac{1}{4} \frac{K_1}{c_S} + \Omega \lambda \left[\frac{1}{4} + \frac{\pi^2}{(\pi^2 - \sigma_{i1}^2)^2} \left(1 + \cos \sigma_{i1} \right) \right] \right) \right]$$

$$(2.68)$$

Refer to *Appendix M* for the derivation of Eqn.(2.64) and Eqns.(2.65-2.67). A graphical representation of the characteristic curves for Ta=3 is presented below for the indicated parameter settings. To illustrate the results in the following figures we have chosen to show the case where $\overline{S} = c_S$ so that $\Omega = 2$. Further we have fixed $\delta = 0.2$ and $K_1/c_S = 1$.

Figures 12a-12d also depicts the characteristic curve corresponding to stationary convection ($\sigma_{i1} = 0$). It can be noted that at $\lambda = 0.4$, Figure 12a, the curve denoted by $\chi = 2$ seems to intersect the stationary curve ($\sigma_{i1} = 0$) close to the minimum of the stationary curve. The intersection point with the stationary curve denotes the transition to stationary convection. However, the curve denoted by $\chi = 10$ and $\chi = 50$ never intersects the stationary curve. The curve denoted by $\chi = 10$ ends at the point $s/\pi \approx 1.29$. The region beyond the endpoints of the curves for $\chi = 2$, $\chi = 10$, and $\chi = 50$ indicates the absence of real positive solutions there. As the value of λ is increased from $\lambda = 0.4$ to $\lambda = 5.0$, we see that the transition point to stationary convection moves towards the right as observed from Figures 12b and 12d until it becomes detached from the stationary curve at $\lambda = 5.0$ in Figure 12d for the selected range of χ values. Physically the graphs

Ta=3
λ=0.4

(a)

Ta=3
λ=0.6
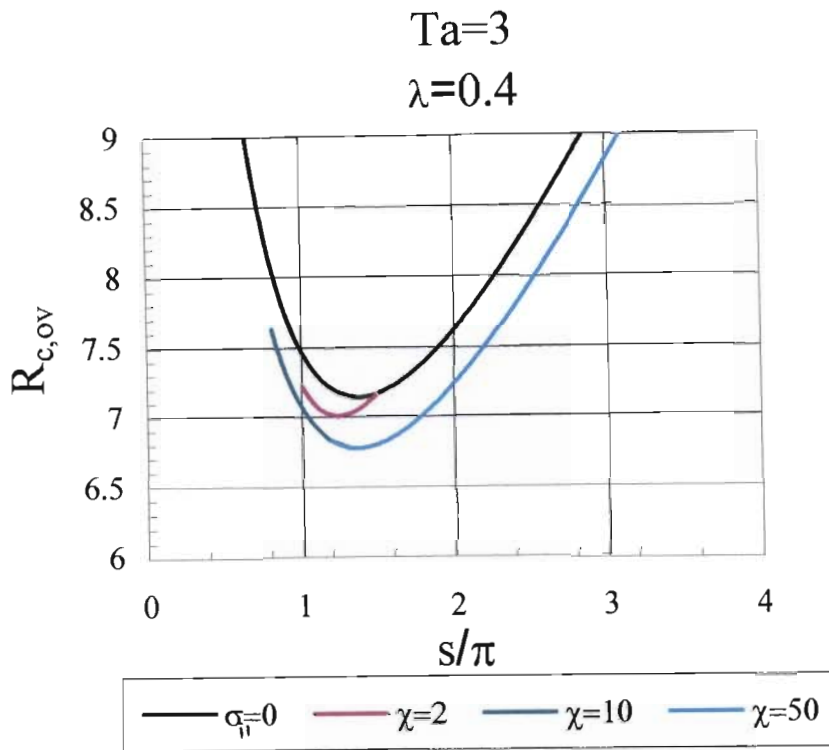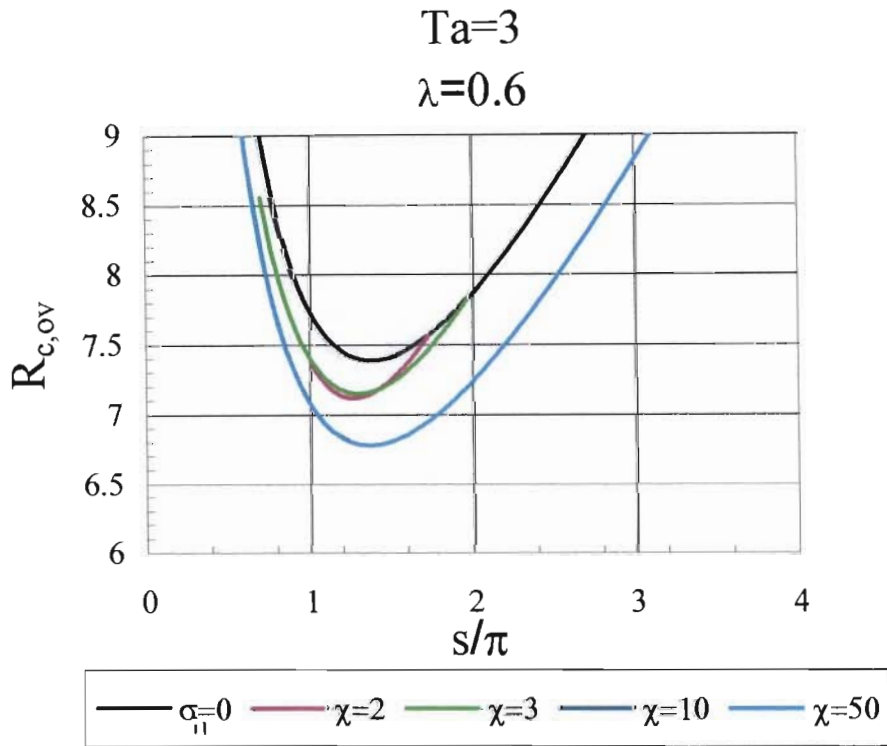
(b)

Figure 12 : Characteristic curves for Rayleigh number for selected values of χ , at, (a) $\lambda = 0.4$ (b) $\lambda = 0.6$

Figure 12: Characteristic curves for Rayleigh number for selected values of χ, at (c) $\lambda = 1.0$ (d) $\lambda = 5.0$

imply that as the value of λ increases for a particular setting of Taylor number , the possibility of stationary convection diminishes and oscillatory convection exists over the entire bandwidth of wavenumbers. It was found that the lowest oscillatory convection threshold point exists for high χ values. In Figures 12a-12d, it can be noted that increasing the λ value for $\chi = 50$ served to decrease slightly the critical value at which the onset of oscillatory convection results. The characteristic curves corresponding to Ta=5 are presented below in Figures 13a to 13d for $\Omega = 2$, $\delta = 0.2$ and $K_1/c_S = 1$.

It can be observed that a similar behaviour as that reported for Ta=3 occurs at Ta=5. The only difference is that at a higher Taylor number of Ta=5 and for at $\lambda = 0.1 - 1.0$, the transition to stationary convection has moved further to the right of the minimum point on the characteristic curve denoting stationary convection ($\sigma_{i1} = 0$) for low values of the parameter χ . This is very clearly seen in on comparing Figures 12a-c to Figures 13a-c. Again, it can be noted that at $\lambda = 5.0$, Figure 13d, there is no transition to stationary convection for the entire range of at χ values. The interesting point to note is that at Ta=5 the critical values for the Rayleigh number have increased in value and the absolute difference between the stationary curve and the oscillatory curves for the different values of χ has diminished. Again, the region beyond the endpoints of the curves for χ indicates the absence of real positive solutions there.

Ta=5

λ=0.4

(a)

Ta=5

λ=0.6

(b)

Figure 13 : Characteristic curves for Rayleigh number for selected values of χ , at, (a) λ = 0.4 (b) λ = 0.6

44

Ta=5

λ=1.0

(c)

Ta=5

λ=5.0
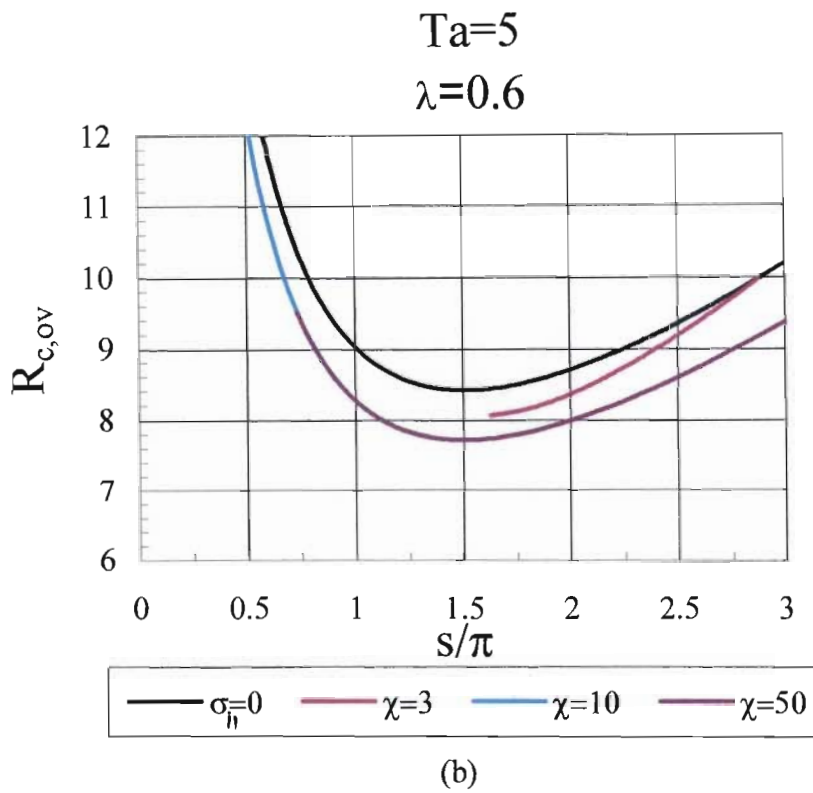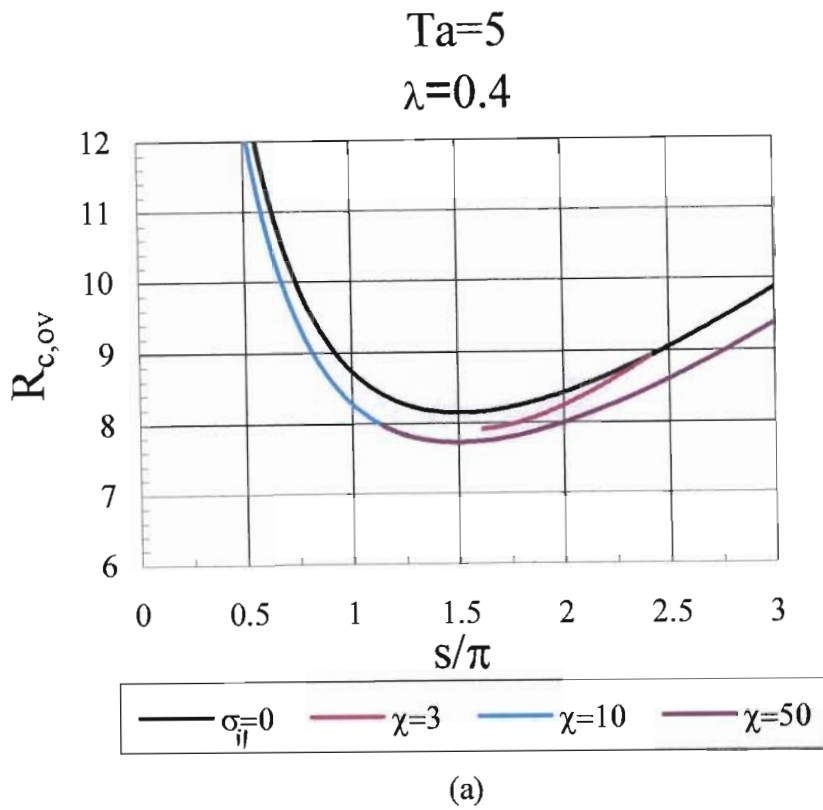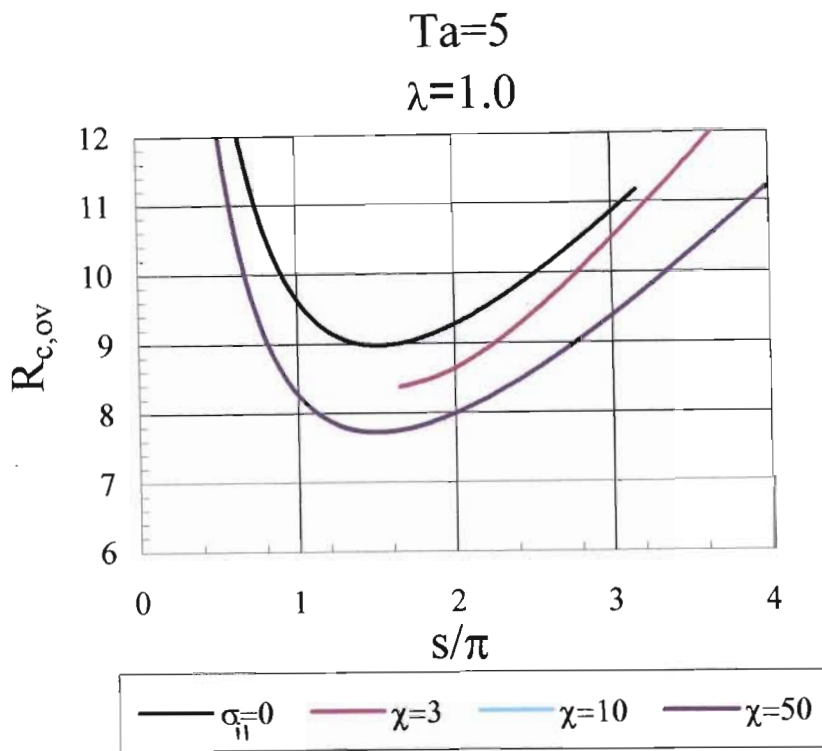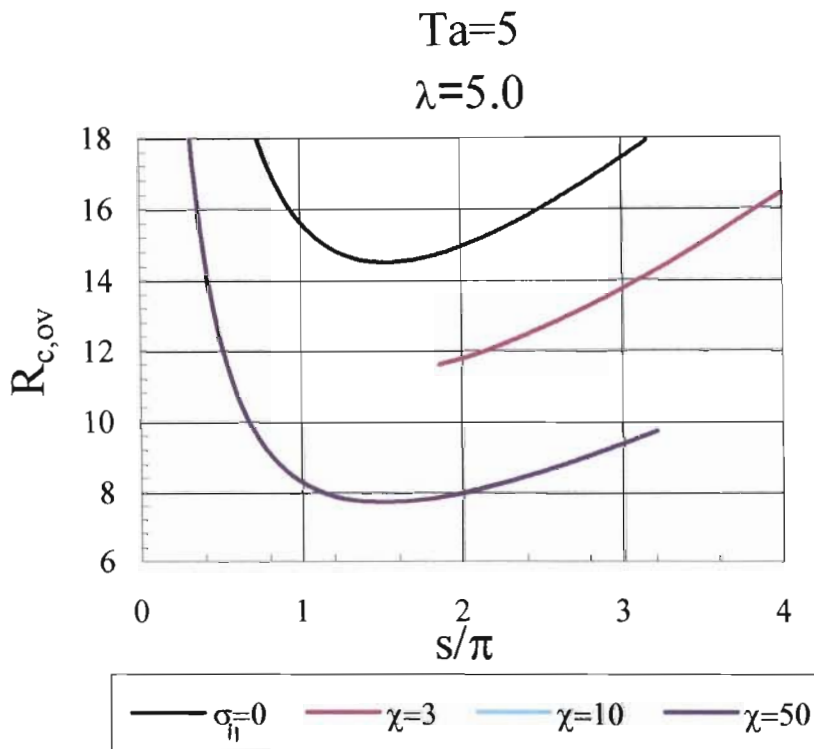
(d)

Figure 13 : Characteristic curves for Rayleigh number for selected values of χ , at, (c) λ = 1.0 (d) λ = 5.0

We present yet another set of curves for Ta=6 in Figures 14a to 14d for $\Omega = 2$, $\delta = 0.2$ and $K_1/c_S = 1$. As the Taylor number is increased beyond Ta=6, it becomes clear that for $\lambda \leq 1.0$ the stationary mode becomes the more dangerous mode, ie. the critical Rayleigh number for the onset of oscillatory convection becomes greater than the critical Rayleigh number for the stationary mode. It can be seen that for $\lambda \leq 1.0$ increasing the Taylor number renders the stationary mode most unstable. Though not presented, it was confirmed that for $\lambda \leq 5.0$, increasing the Taylor number considerably, to say Ta=1000, causes the stationary mode to become most unstable. This point may be inferred from Figures 12d-14d for increasing Taylor numbers. It can be very clearly observed from Figure 12d and Figure 13d that increasing the Taylor number from Ta=3 to Ta=6 has moved the curves for the different χ values closer to the stationary convection curve ($\sigma_{i1} = 0$).
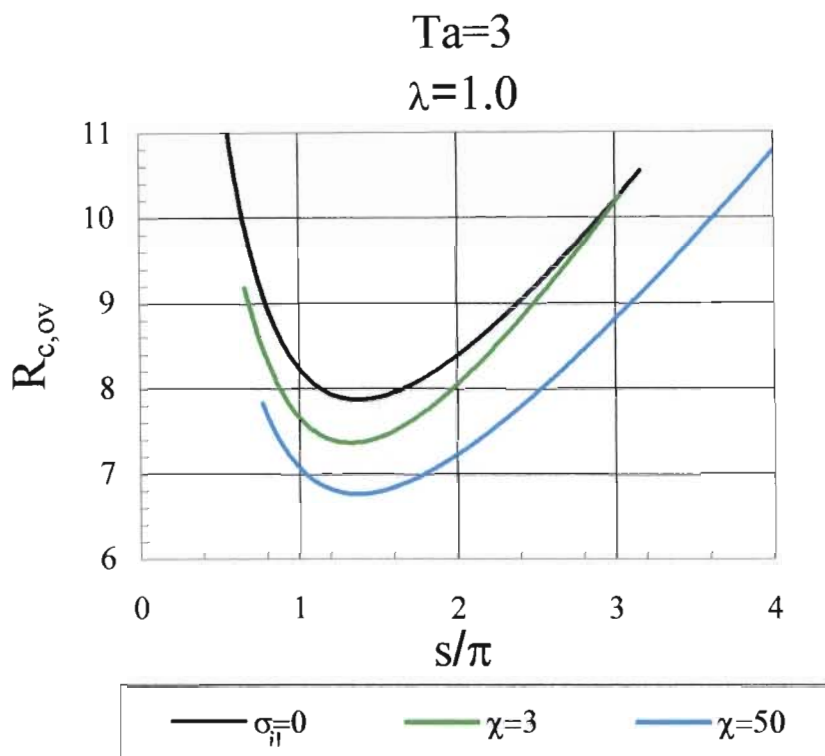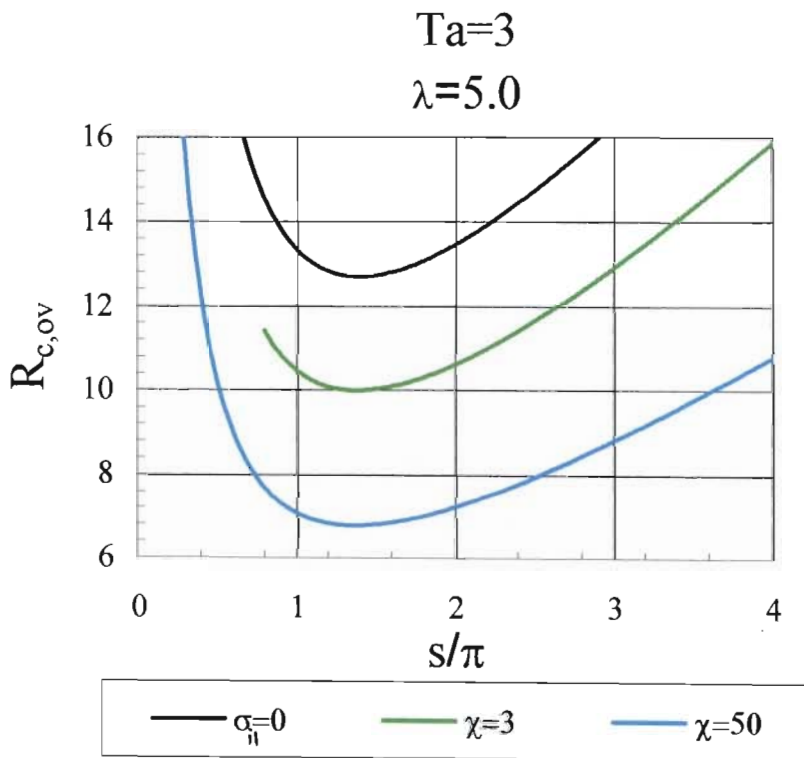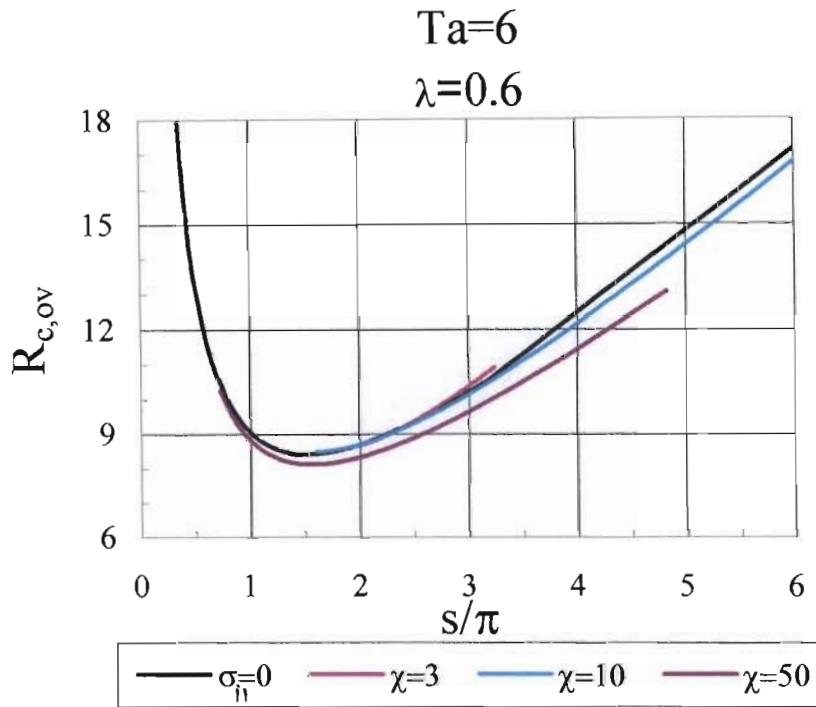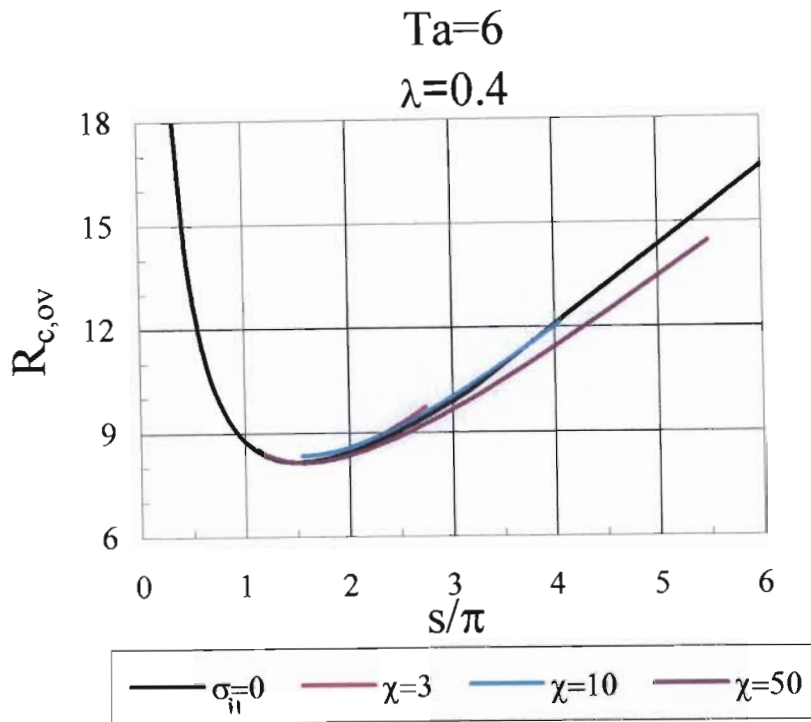
Figure 14 : Characteristic curves for Rayleigh number for selected values of χ, at, (a) $\lambda = 0.4$ (b) $\lambda = 0.6$
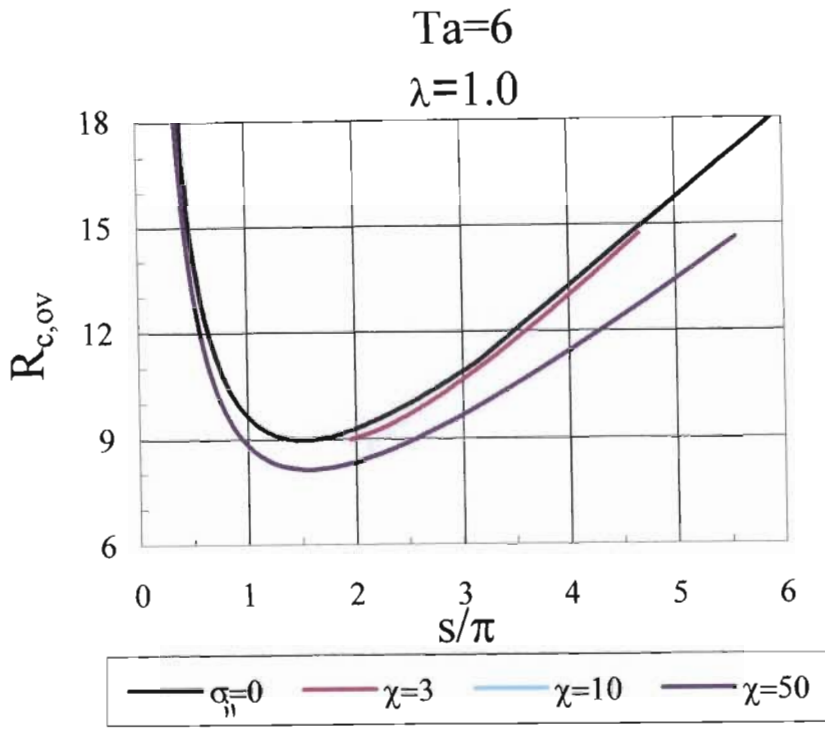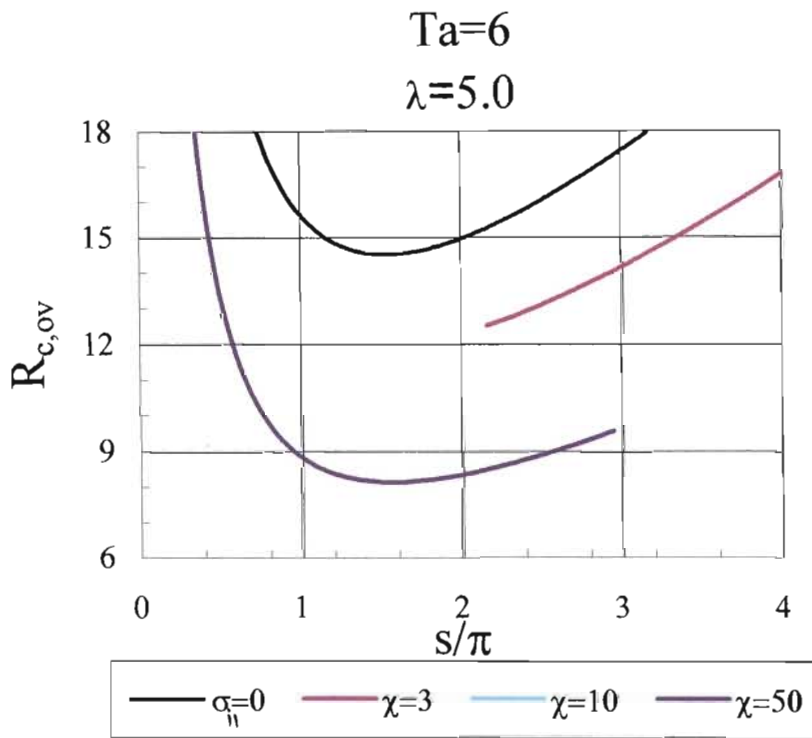
Figure 14 : Characteristic curves for Rayleigh number for selected values of χ , at, (c) $\lambda = 1.0$ (d) $\lambda = 5.0$

Figures 15 to 18 denotes the non-zero solutions to Eqn.(2.61) as a function of the wavenumber s/π for different values of λ. These results are presented at Ta=3 for different values of χ for $\Omega = 2$, $\delta = 0.2$ and $K_1/c_s = 1$. It can be noted from Figures 15 to 18 that as the value of χ is increased from $\chi = 2$ to $\chi \to \infty$ the curves tend to approach the form of the curves presented by Anderson & Worster (1996) at high values of χ. At $\chi = 2$ we note that the curves presented in Figure 15 for the different values of λ collapses to an asymptote denoted by a value of wavenumber on the x-axis. It can be seen that increasing the value of the parameter λ causes the curves to move towards this asymptote. However, for large values of the parameter λ, say $\lambda = 5.0$, it can be observed from Figure 15 that the asymptote is reached only at very high values of the oscillatory frequency (σ_{i1}). At $\chi = 5$, approximately, there is a transition from the curves depicted in Figure 15 to that of a form similar to Anderson & Worster (1996). Increasing the value of χ to $\chi = 50$, we note that the resulting set of curves presented in Figure 17 resembles the form of the curves presented by Anderson and Worster (1996). The curves presented in Figure 18 for $\chi \to \infty$ bears a strong resemblance to Anderson & Worster's (1996) curves. It can be seen in Figure 18 that at $\lambda = 1$ the oscillatory mode attaches to the stationary mode at zero wavenumber (infinite Rayleigh number) and therefore exists for all wavenumbers s.

Ta=3
χ=2

Figure 15 : σ_{i1} versus s/π for Ta=3 χ = 2

Ta=3
χ=5

Figure 16 : σ_{i1} versus s/π for Ta=3 and χ = 5

Ta=3

χ=50

Figure 17 : σ_{i1} versus s/π for Ta=3 and χ = 50

Ta=3

χ → ∞

Figure 18 : σ_{i1} versus s/π for Ta=3 and χ → ∞
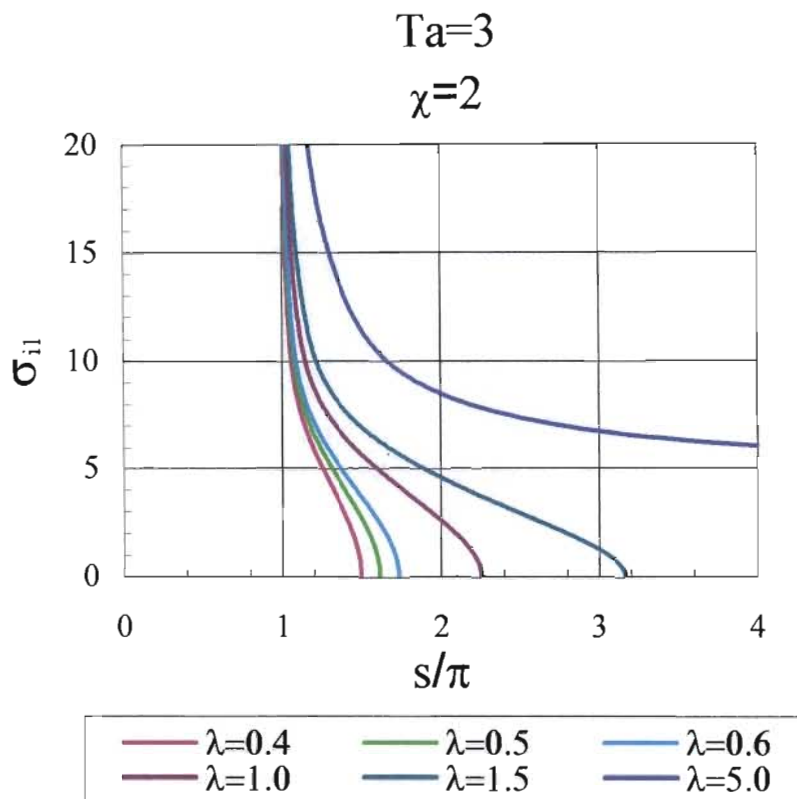
Figures 19 to 22 presents results at Ta=50 for different values of χ for $\Omega = 2$, $\delta = 0.2$ and $K_1/c_S = 1$. It can be noted that the asymptote for the curves for different values of λ at $\chi = 2$ has moved to the right but the basic form of the curves resembles Figure 15. It may be inferred that the asymptote is a strong function of the Taylor number, a point that will be elucidated on at a later stage. The point at which the curves showed transition to the form of the curves presented by Anderson & Worster (1996) was found to occur at $\chi = 9$ and is presented in Figure 20. We also observe that increasing the Taylor number has increased the value of χ at which the curves begin to resemble Anderson & Worster's set of curves. We note from Figure 21 that only oscillatory convection is possible for $\lambda > 1.0$ and is always the most unstable mode. This point is also evident in Figure 17. The curves presented in Figure 12 for $\chi \to \infty$ bears a strong resemblance to Anderson & Worster's (1996) curves. It can be seen again in Figure 22 that at $\lambda = 1$ the oscillatory mode attaches to the stationary mode at zero wavenumber (infinite Rayleigh number) and therefore exists for all wavenumbers s.
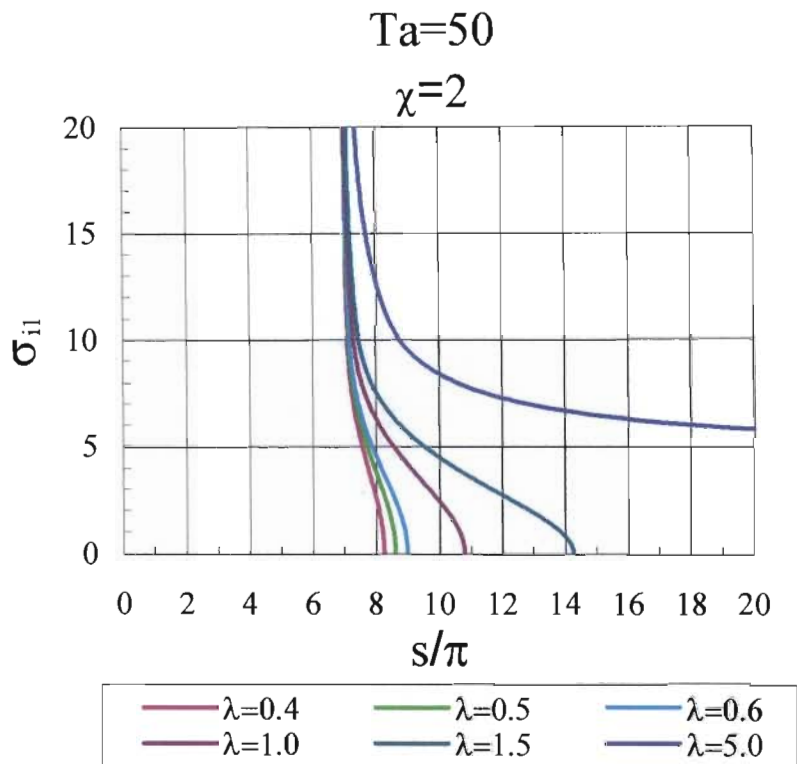
Figure 19 : σ_{i1} versus s/π for Ta=50 and $\chi = 2$
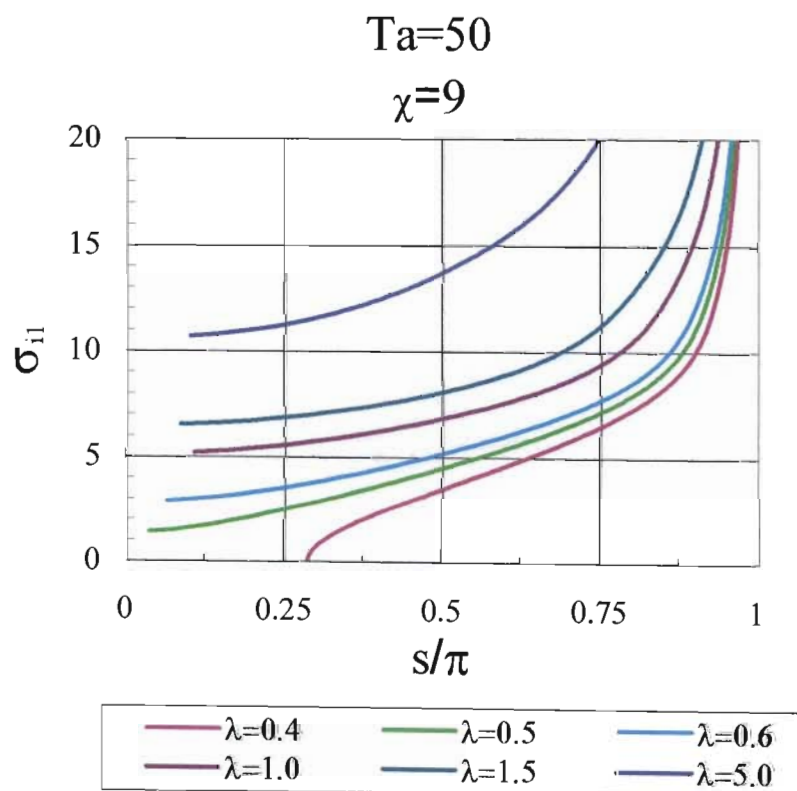
Figure 20 : σ_{i1} versus s/π for Ta=50 and $\chi = 9$
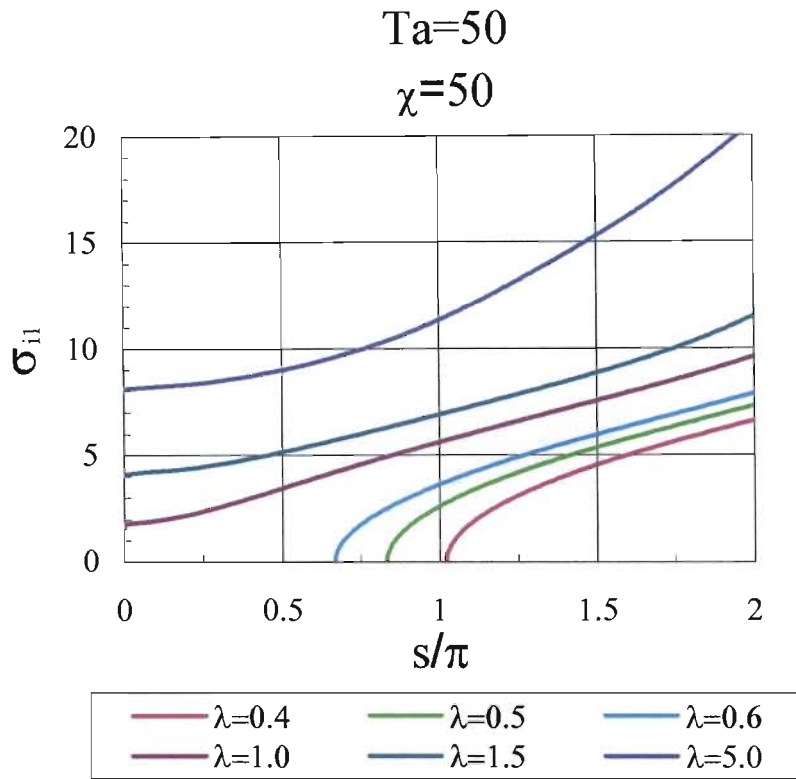
Ta=50
χ=50

Figure 21 : σ_{i1} versus s/π for Ta=50 and $\chi = 50$
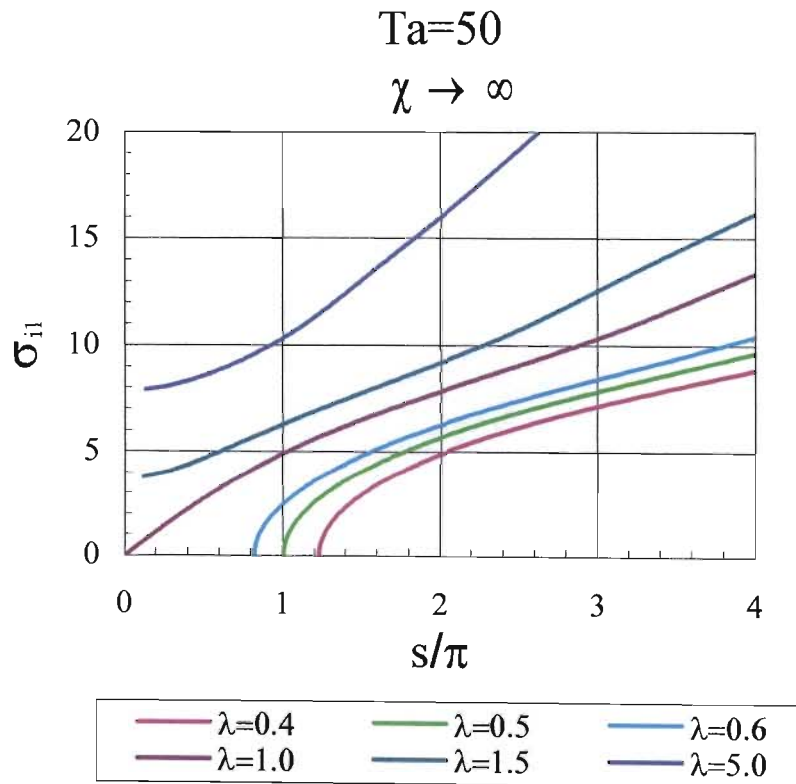
Ta=50
χ → ∞

Figure 22 : σ_{i1} versus s/π for Ta=50 and $\chi \to \infty$

The asymptote discovered at low values of χ will be explained in further detail by examining the behaviour of Eqn.(2.61) a bit more closely. It was noted that this behaviour occurred for high values of σ_{i1} and low values of the parameter $\gamma = \chi/\pi^2$. Firstly multiplying Eqn.(2.61) by γ yields,

$$\frac{1}{\Omega}\frac{(\alpha+1)(\alpha+1-\mathrm{Ta})}{(\alpha+1+\mathrm{Ta})} + \gamma + \gamma\lambda\pi^2(\alpha+1)\left[\frac{1}{(\pi^2-\sigma_{i1}^2)} - \frac{2\pi^2}{(\pi^2-\sigma_{i1}^2)^2}\frac{\sin(\sigma_{i1})}{\sigma_{i1}}\right] = 0. \qquad (2.69)$$

Applying the limit $\lim_{\gamma\to 0}(\cdot)$ to Eqn.(2.69) as follows,

$$\lim_{\gamma\to 0}\left\{\frac{1}{\Omega}\frac{(\alpha+1)(\alpha+1-\mathrm{Ta})}{(\alpha+1+\mathrm{Ta})} + \gamma + \gamma\lambda\pi^2(\alpha+1)\left[\frac{1}{(\pi^2-\sigma_{i1}^2)} - \frac{2\pi^2}{(\pi^2-\sigma_{i1}^2)^2}\frac{\sin(\sigma_{i1})}{\sigma_{i1}}\right]\right\} = 0,$$

$$(2.70)$$

yields the following result for the location of the asymptote,

$$\alpha = \left(s/\pi\right)^2 = \mathrm{Ta} - 1. \qquad (2.71)$$

Eqn.(2.71) shows that the location of the asymptote is independent of the parameter λ. We may demonstrate that at Ta=3, the location of the asymptote given by Eqn.(2.71) is $s/\pi = \sqrt{2} \approx 1.14$ and corresponds to the value noted in Figure 15. Similarly for Ta=50, the asymptote is found to be $s/\pi = 7$, which corresponds exactly to the value noted in Figure 19. It can be noted from Figures 15 and 19 that the curves corresponding to the different values of λ reaches the asymptote calculated using Eqn.(2.71) at high σ_{i1} values only. The corresponding asymptotical Rayleigh number at high values of σ_{i1} may be inferred from Eqn.(2.60) by applying the limit $\lim_{\sigma_{i1}\to\infty}(\cdot)$ and is given as,

$$R_{asym,ov} = \pi\sqrt{\frac{(\alpha+1)(\alpha+1+\mathrm{Ta})}{\Omega\alpha}}\left[1 + \delta\left(\frac{(\alpha+1-\mathrm{Ta})}{(\alpha+1+\mathrm{Ta})}\frac{1}{4}\frac{K_1}{c_s} + \frac{\Omega\lambda}{4}\right)\right]. \qquad (2.72)$$

It must be borne in mind that the asymptotical wavenumber found in Eqn.(2.71) and the asymptotical Rayleigh number given in Eqn.(2.72) indicates the critical values for the onset of convection at low settings of the parameter χ. Refer to *Appendix N* for a derivation of Eqns. (2.71-2.72).

The comparative behaviour of the critical Rayleigh number between the stationary mode (black curve) and the oscillatory mode (blue curve) is presented in Figure 23 to 26. Also indicated in Figures 23 to 26 is the frequency σ_{i1} (red curve) along the oscillatory branch with only the positive root shown. We have noted that the oscillatory mode depends on the presence of the parameter λ. To illustrate the results we have chosen to show the case where $\overline{S} = c_S$ so that $\Omega = 2$. We have also fixed $\delta = 0.2$ and taken $K_1/c_S = 1$. The results will be presented for Ta=3, Ta=20, Ta=50, and Ta=100. For each of these Taylor numbers we will allow the parameter χ to assume the values, $\chi = 2$, $\chi = 10$, $\chi = 50$ and $\chi \to \infty$. It can be observed from Figure 23a that stationary mode is the most unstable mode for $\lambda \leq 0.125$, whilst the oscillatory mode the most unstable $\lambda > 0.125$. The transition to oscillatory convection occurs at $\lambda \cong 0.125$. In figure 23b however, it is noted that the oscillatory mode remains the most unstable mode for the entire bandwidth of λ values. In Figure 23c, $\chi = 50$, it is noted that the stationary mode again becomes the most unstable mode at low λ values and the most unstable mode at higher λ values. It can be noted that the absolute difference between the two modes is extremely small for high λ values, ie. the curves for the stationary and oscillatory modes practically overlap. The point at which the transition to oscillatory convection occurs is $\lambda \cong 0.375$. At very high χ values as depicted in Figure 23d that the result is similar to that in Figure 23a. the transition to oscillatory convection occurs at $\lambda \cong 0.498$.
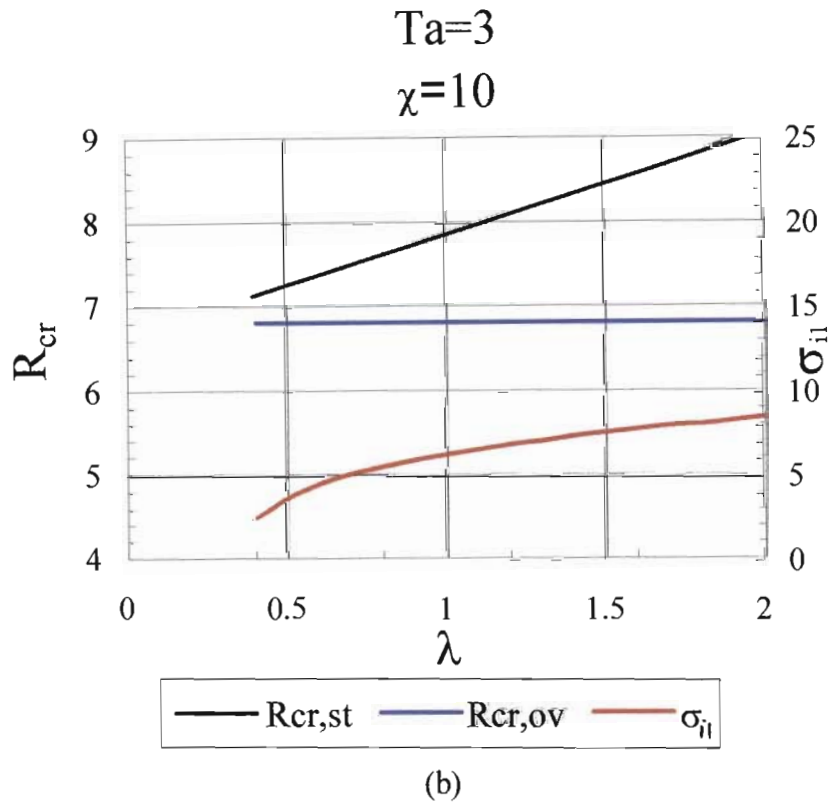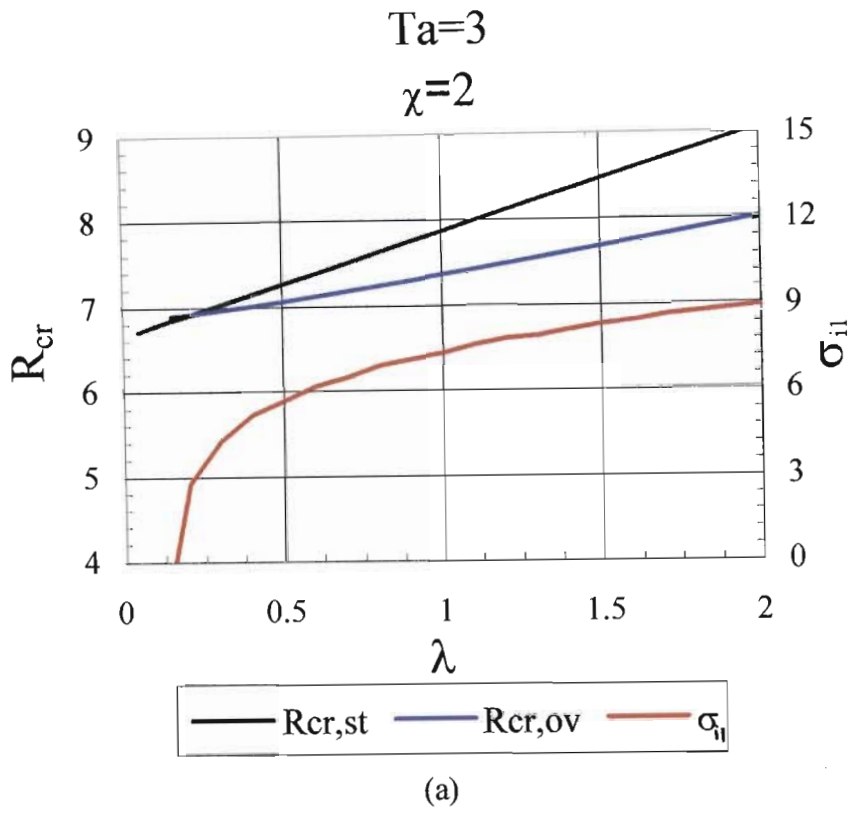
Figure 23 : Critical Rayleigh number R_{cr} versus λ at Ta=3 for (a) $\chi = 2$ and (b) $\chi = 10$.
Stationary mode (black curve), oscillatory mode (blue curve) and frequency σ_{il} (red curve)
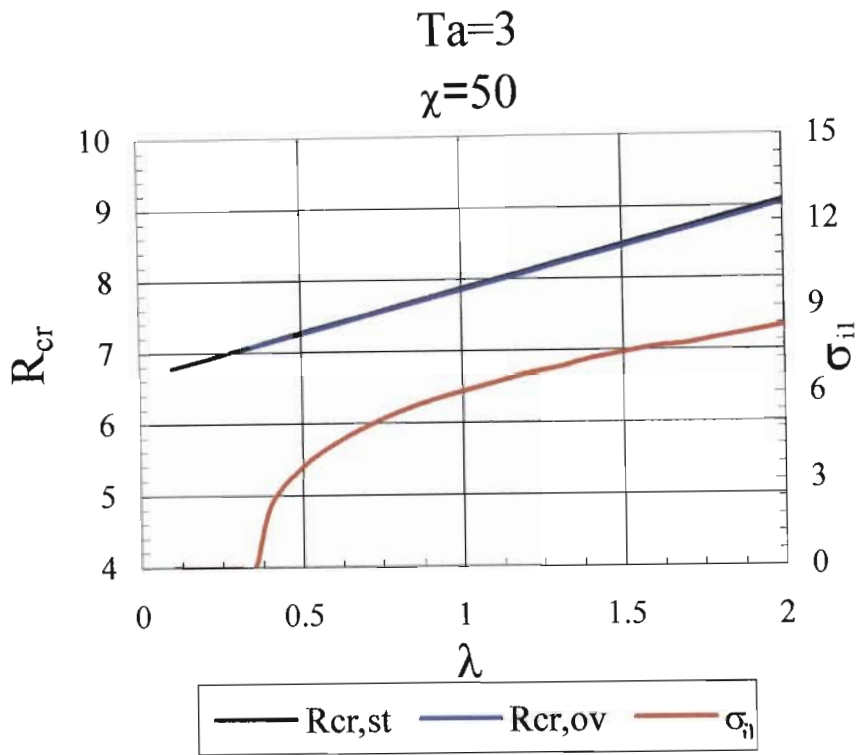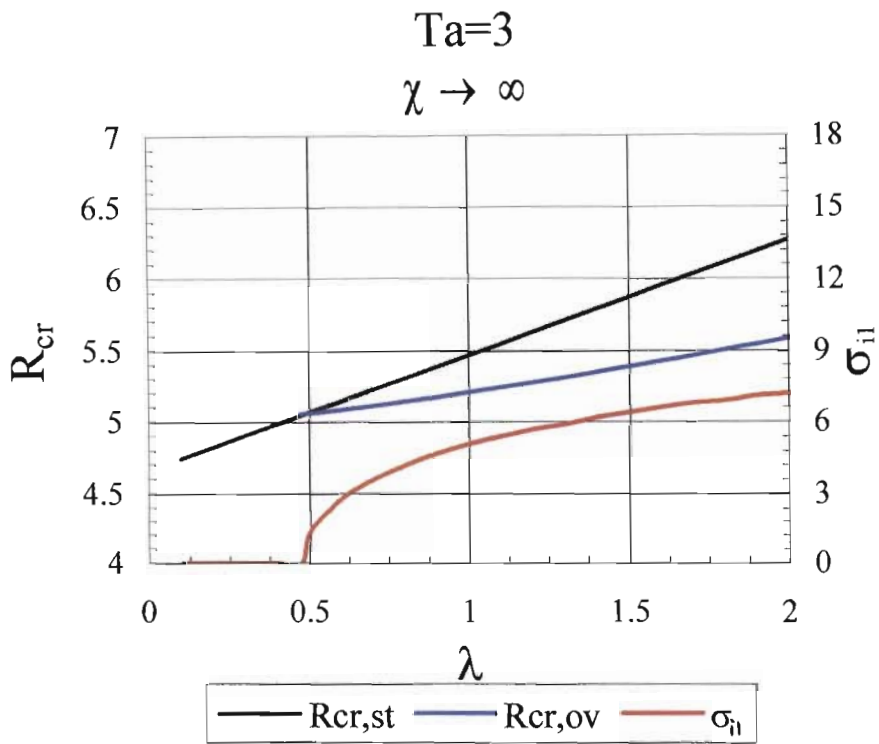
Figure 23 : Critical Rayleigh number R_{cr} versus λ at Ta=3 for (c) $\chi = 50$ and (d) $\chi \to \infty$.
Stationary mode (black curve), oscillatory mode (blue curve) and frequency σ_{i1} (red curve)

To further investigate the effects of Taylor number on these curves we present results to Ta=20 in Figure 24. From Figure 24a, $\chi = 2$, it can be noted that an increase in the Taylor number caused the onset of an asymptote (as discussed above). The stationary mode is the most unstable mode for the entire λ domain. Figure 24b provides an interesting result, in that increasing the Taylor number has caused the stationary mode to now become the most unstable mode. It can be observed from Figure 24c that increasing the Taylor number has caused stationary mode to become the most unstable for low λ values and the oscillatory mode to become the most unstable for high λ values. The transition to oscillatory convection occurs at $\lambda \cong 0.1$. From Figure 24d it can be noted that increasing the Taylor number has only caused the exchange of stability point to move to $\lambda \cong 0.125$. The stationary mode still is the most unstable at low λ values and the oscillatory mode is still the most unstable at high λ values.

Figure 24 : Critical Rayleigh number R_{cr} versus λ at Ta=20 for (a) $\chi = 2$ and (b) $\chi = 10$. Stationary mode (black curve), oscillatory mode (blue curve) and frequency σ_{i1} (red curve)

Figure 24 : Critical Rayleigh number R_{cr} versus λ at Ta=20 for (c) $\chi = 50$ and (d) $\chi \to \infty$. Stationary mode (black curve), oscillatory mode (blue curve) and frequency σ_{i1} (red curve)

We now present results for Ta=50 in Figure 25. It can be very clearly seen from Figures 25a and 25b that increasing the Taylor number for the lower χ values causes the stationary mode to become unstable. Figures 25c and 25d show that for the higher χ values the oscillatory modes remain most unstable. This is in agreement with the observations made from the characteristic Rayleigh number curves. In Figure 25d, the exchange of stability occurs at $\lambda \cong 0.125$.
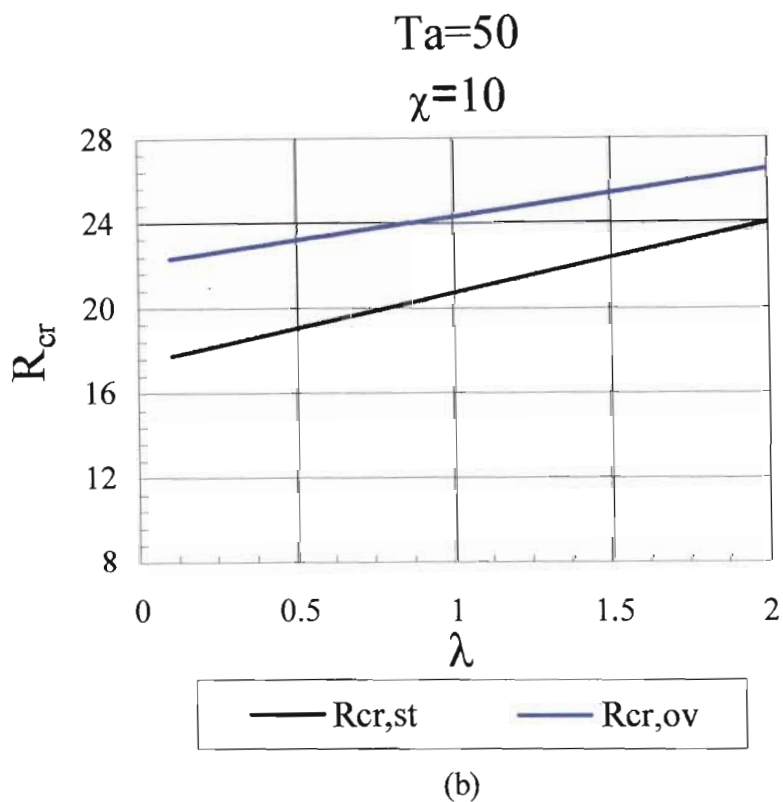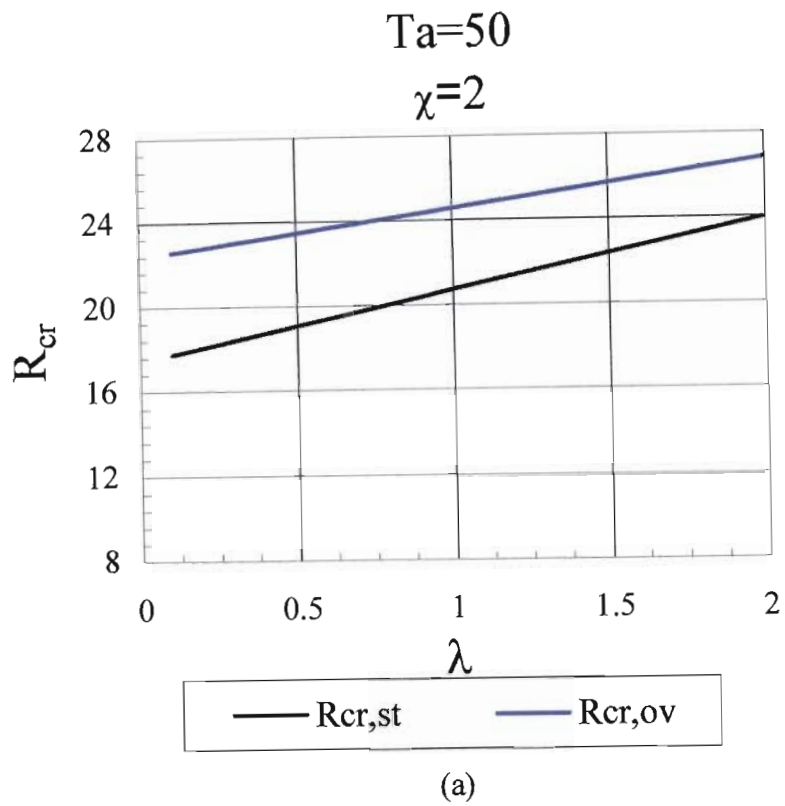
Ta=50

χ=2

(a)

Ta=50

χ=10

(b)

Figure 25 : Critical Rayleigh number R_{cr} versus λ at Ta=50 for (a) $\chi = 2$ and (b) $\chi = 10$. Stationary mode (black curve), oscillatory mode (blue curve) and frequency σ_{i1} (red curve)
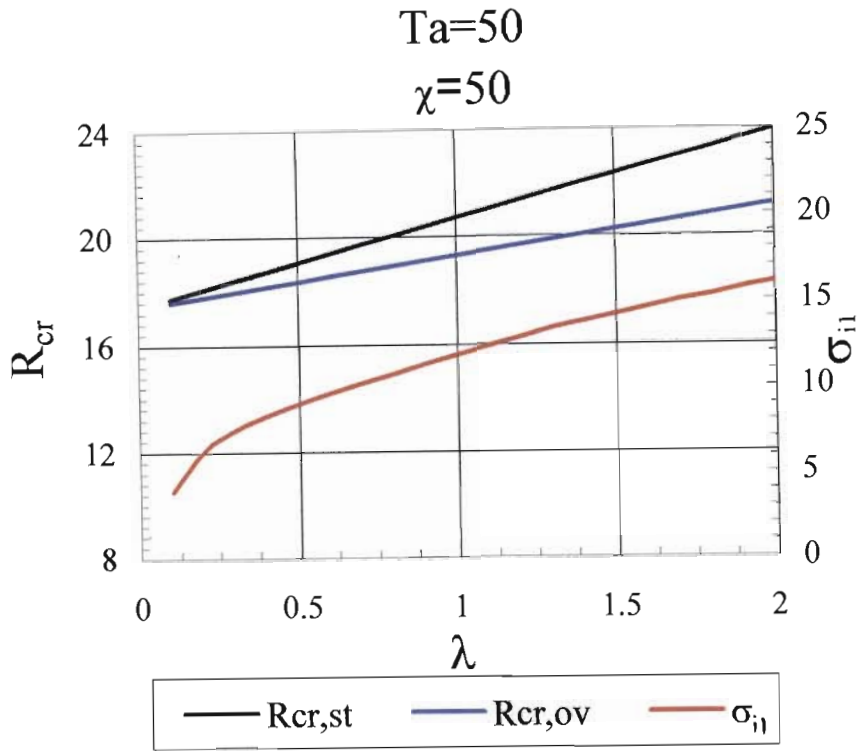
(c)
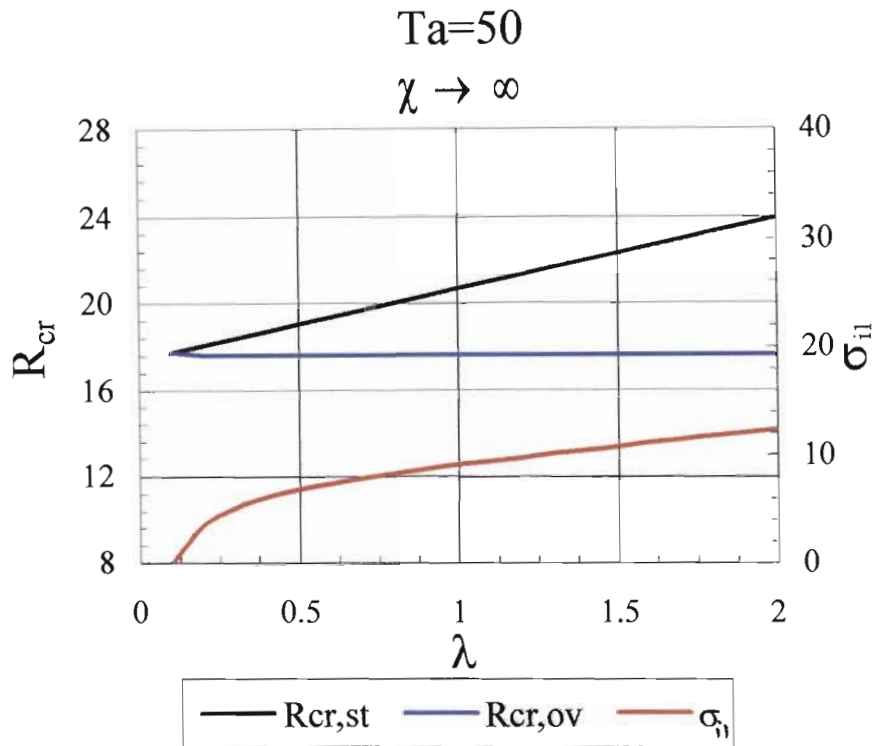
(d)

Figure 25 : Critical Rayleigh number R_{cr} versus λ at Ta=50 for (c) $\chi = 50$ and (d) $\chi \rightarrow \infty$. Stationary mode (black curve), oscillatory mode (blue curve) and frequency σ_{i1} (red curve)

We now proceed to present the final graph set at Ta=100 in Figure 26. It can be very clearly seen from Figures 26a and 26 b that for small values of χ the stationary mode becomes the most unstable for increasing Taylor numbers. Comparing Figures 25c and 26c we note that the absolute difference between the stationary and oscillatory curves has diminished. Although the oscillatory mode is still the most unstable mode, further increases in the Taylor causes the stationary mode to become the most unstable mode, as pointed out earlier. At very high χ values, the oscillatory mode still remains the most unstable mode as observed from Figures 26c-d.

Figures 23 to 26 show that either the stationary or the oscillatory mode of convection can be the most unstable depending on the value of λ for each setting of Taylor number and χ.

Ta=100

χ=2

(a)

Ta=100

χ=10

(b)

Figure 26 : Critical Rayleigh number R_{cr} versus λ at Ta=50 for (a) $\chi = 2$ and (b) $\chi = 10$. Stationary mode (black curve), oscillatory mode (blue curve) and frequency σ_{i1} (red curve)

Ta=100
χ=50

(c)

Ta=100
χ → ∞

(d)

Figure 26 : Critical Rayleigh number R_{cr} versus λ at Ta=100 for (c) $\chi = 50$ (d) $\chi \to \infty$. Stationary mode (black curve), oscillatory mode (blue curve) and frequency σ_{i1} (red curve)

We now compare the results of the current case involving rotation with that of Anderson & Worster (1995), who neglected rotational effects. In order to compare our results with Anderson & Worster (1995) we need to apply the limit $\chi \to \infty$ and consider the problem at different values of Taylor number. Note that $\chi \to \infty$ and Ta=0 represents the problem solved by Anderson & Worster. This was presented earlier in Eqn.(2.62) and Eqn(2.63). Figure 27a and 27b shows the variation of the critical Rayleigh numbers for the stationary and oscillatory cases as a function of λ for $\chi \to \infty$ for varying Taylor numbers. Note that in Figures 27a and 27b the curve denoted by Ta=0 represents the result of Anderson & Worster (1995). It can be very clearly seen in Figures 27a and 27b that as the Taylor number is increased the critical Rayleigh number curves for both the stationary and oscillatory case lies above the case when Ta=0. This implies that increasing the Taylor number has a stabilising effect on the convection in the mushy layer as the onset of convection in the presence of rotation is delayed.

It can also be noted from Figure 27c that increasing the Taylor number at high values of χ causes the oscillatory mode to become the most unstable mode. It can also be noted from Figure 27c that stationary convection can only occur below $\lambda \cong 0.48$. For increasing Taylor numbers the λ values for transition to oscillatory convection decreases, thus oscillatory convection occurs over a larger band of λ values. At Ta=100 it can be seen that no stationary convection is possible. In summary it can be seen that at high χ values, increasing the Taylor number results in the oscillatory mode becoming the most unstable mode. This feature is clearly observed in Figures 23d to 26d as well.

In the interest of identifying ways in which instabilities in the mushy layer can be avoided in practice, we investigate the dependence of the critical Rayleigh number and the frequency σ_{i1} on each of the experimental control parameters St, ξ, δ as a function of χ and Ta.
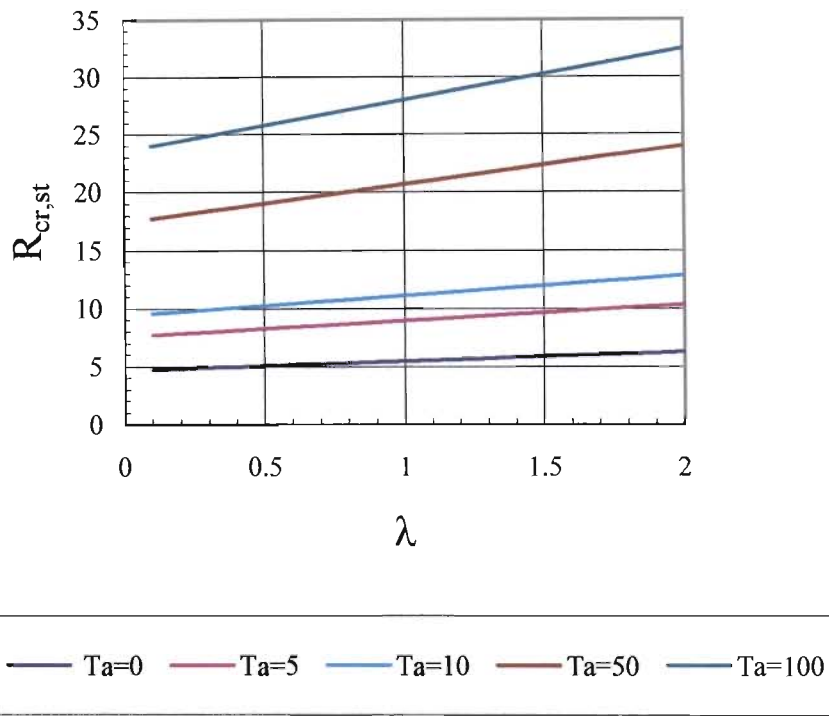
(a)
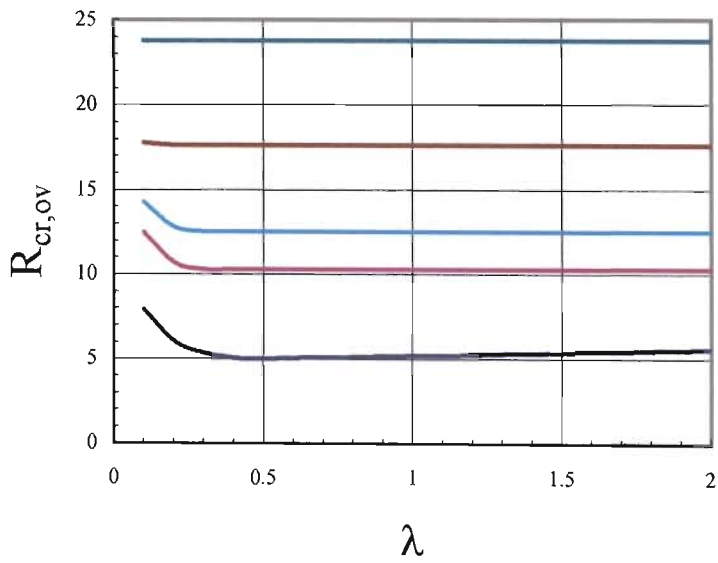
(b)

Figure 27 : Locus of critical Rayleigh numbers as a function of λ for (a) Stationary convection (b) Oscillatory Convection .
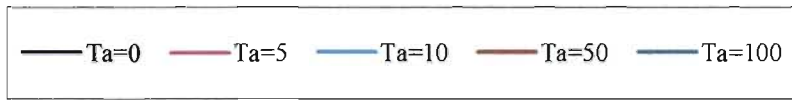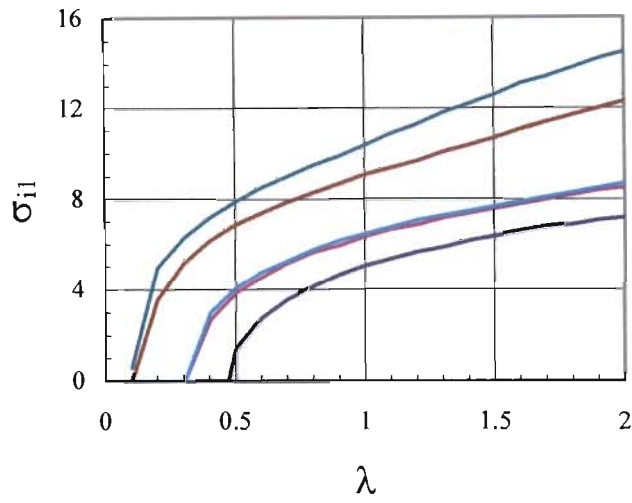
(c)

Figure 27 : Frequency σ_{i1} versus λ

2.6 Parametric Dependencies

Figures 28a to 28d shows the critical Rayleigh number curves for the stationary and oscillatory modes as well as the frequency σ_{i1} for a variation in the Stefan number St for increasing Taylor number. The other parameters are fixed as $\delta = 0.1$, $\xi = 3$, $K_1 = 3$, and

$\chi = 1$. Note that only the positive root of the frequency is shown. We note from Figure 28a that at low Stefan numbers and Taylor number the stationary mode is the most unstable mode. In Figure 28a for low Taylor numbers (Ta=3) the transition to oscillatory convection occurs at about $St \cong 0.9$ (ie. the oscillatory mode becomes the most unstable mode). Note that as the Taylor number is increased the stationary mode becomes the most unstable mode over the entire range of Stefan numbers, as observed from Figures 28b-d.
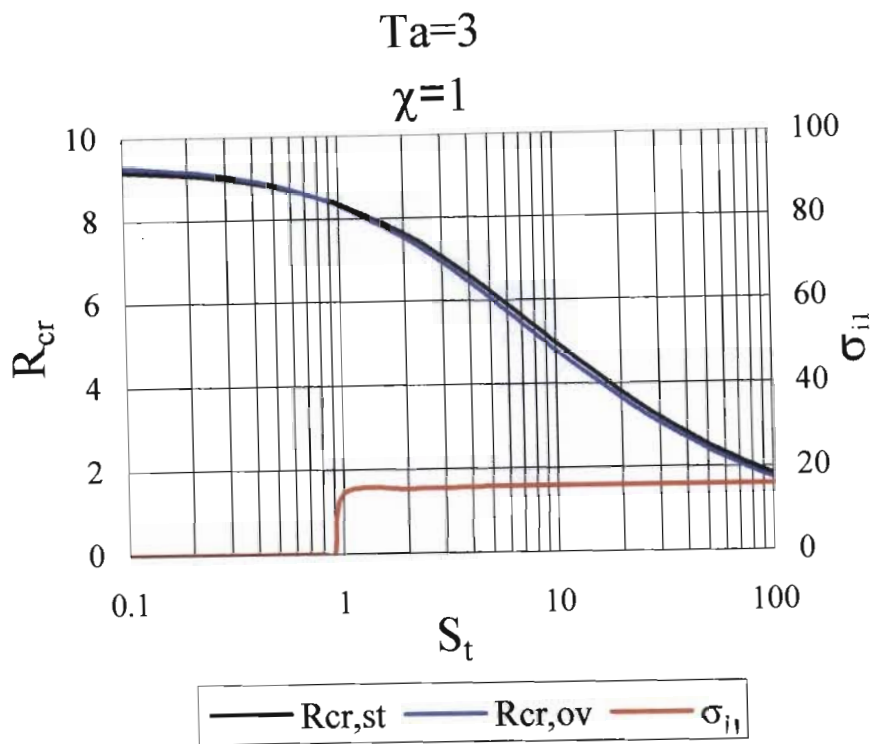
(a)
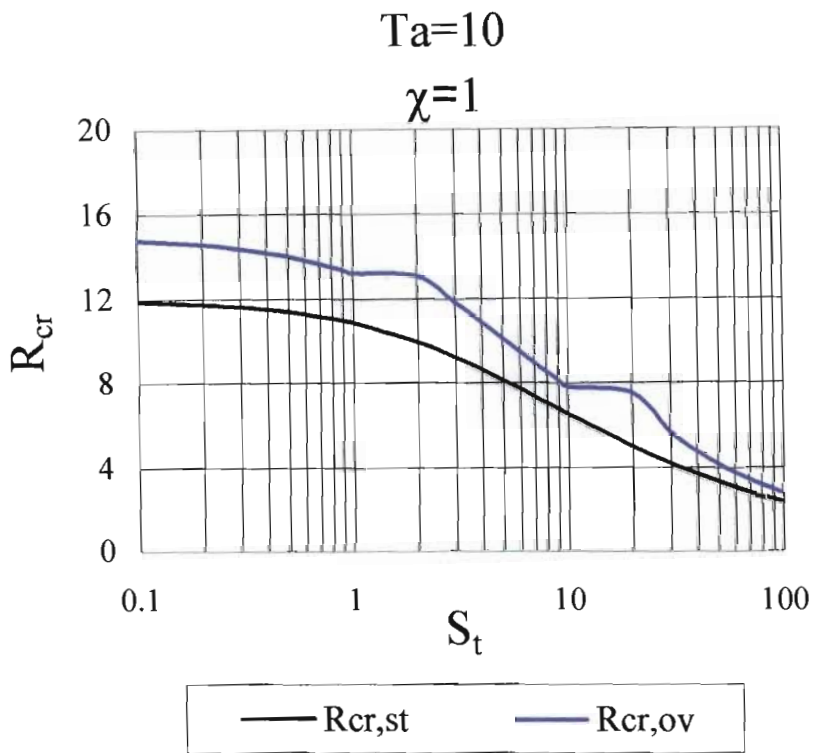
(b)

Figure 28 : Critical Rayleigh number R_{cr} versus St at $\chi = 1$ for (a) Ta=3 and (b) Ta=10. Stationary mode (black curve), oscillatory mode (blue curve) and frequency σ_{i1} (red curve)

Ta=50

$\chi=1$

(c)

Ta=100

$\chi=1$

(d)
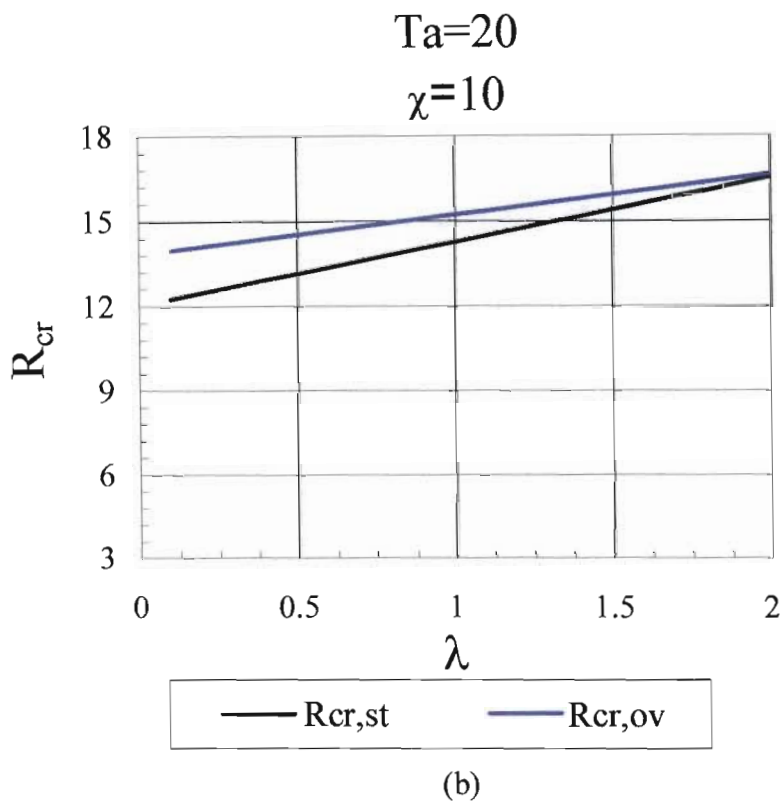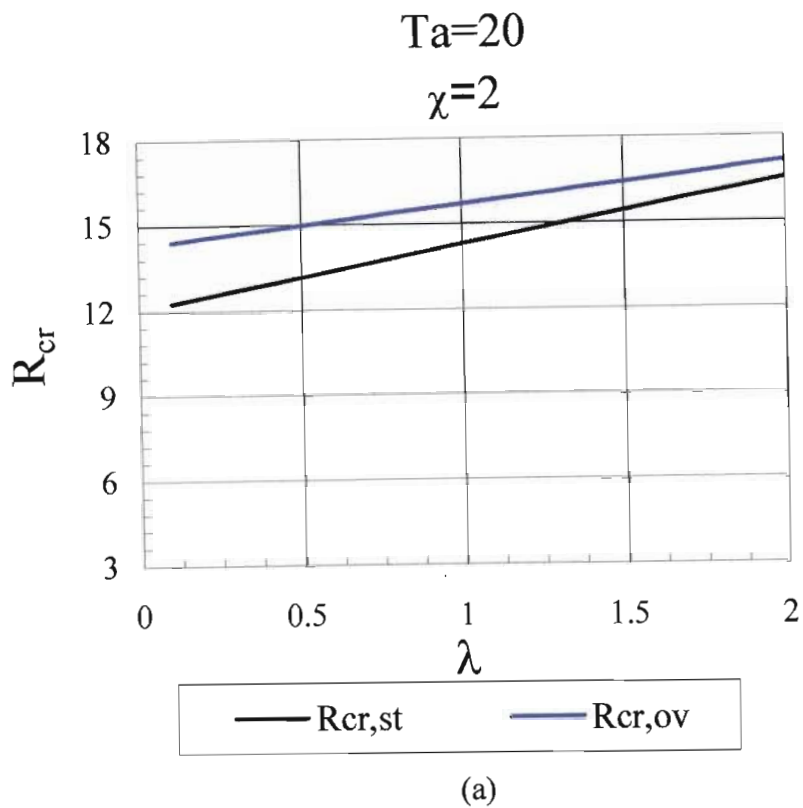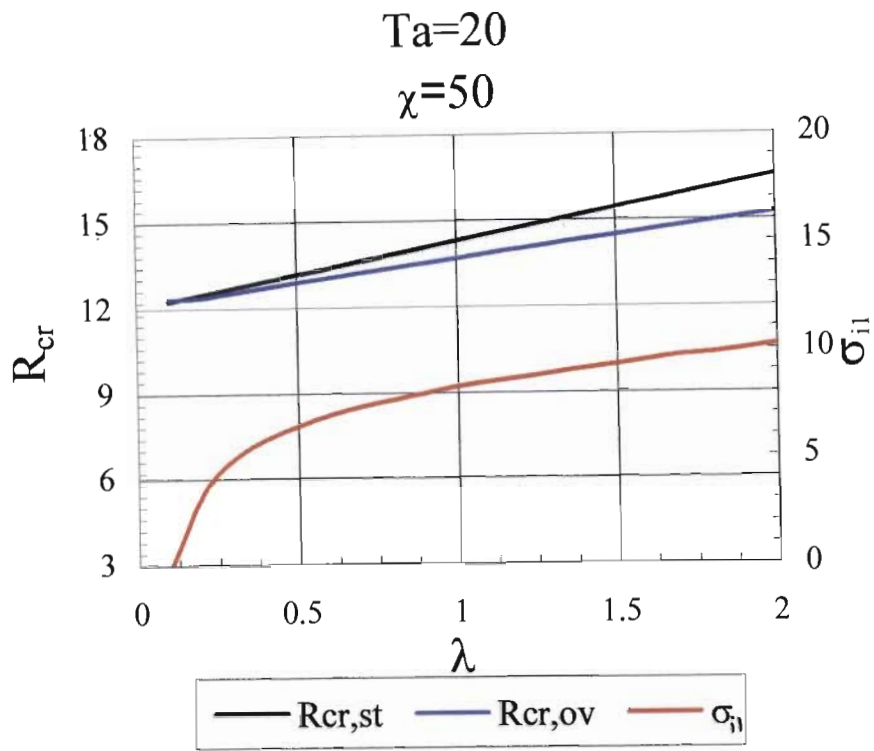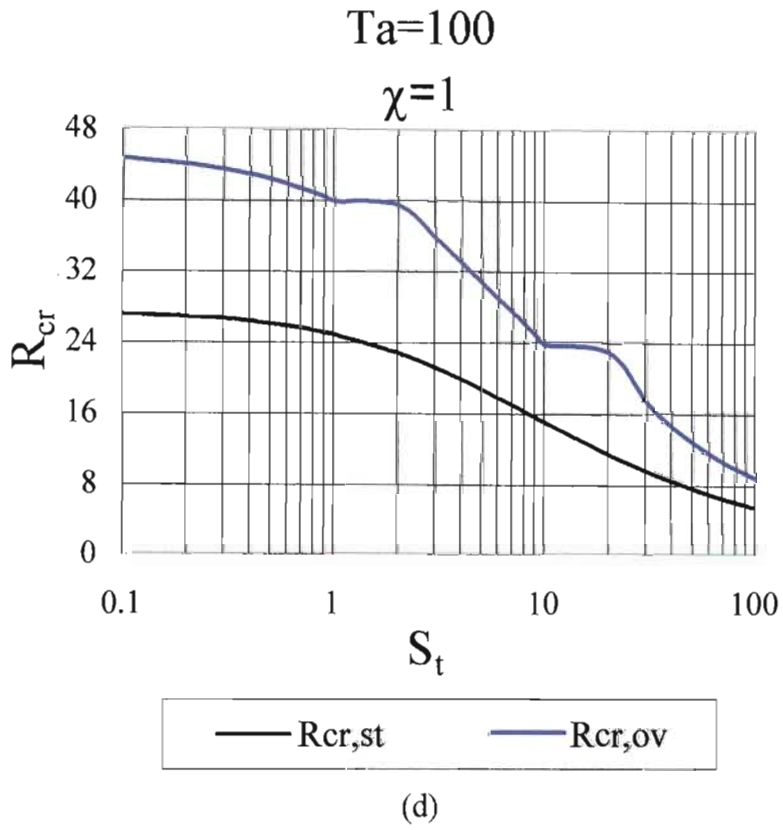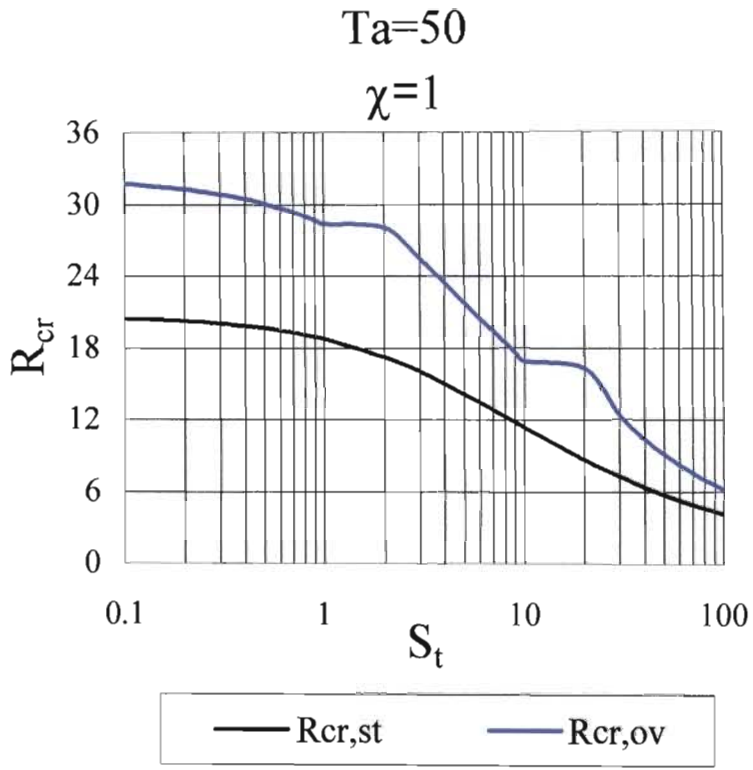
Figure 28 : Critical Rayleigh number R_{cr} versus St at $\chi = 1$ for (c) Ta=50 and (d) Ta=100. Stationary mode (black curve), oscillatory mode (blue curve) and frequency σ_{i1} (red curve)

Figures 29a to 29d shows the critical Rayleigh number curves for the stationary and oscillatory modes as well as the frequency σ_{i_1} for a variation in the compositional ratio ξ for increasing Taylor number. The other parameters are fixed as $\delta = 0.1$, $\xi = 3$, $K_1 = 3$, and St=5. It may be observed from Figure 29a that at low composition ratios (ξ) the stationary mode is the most unstable. The oscillatory mode is most unstable for the higher composition ratios with transition to oscillatory convection occurring at $\xi \cong 6$. As the Taylor number from is increased from Ta=3 to Ta=100, the stationary mode becomes the most unstable mode across the range of selected ξ values, as can be observed from Figures 29b to 29d.
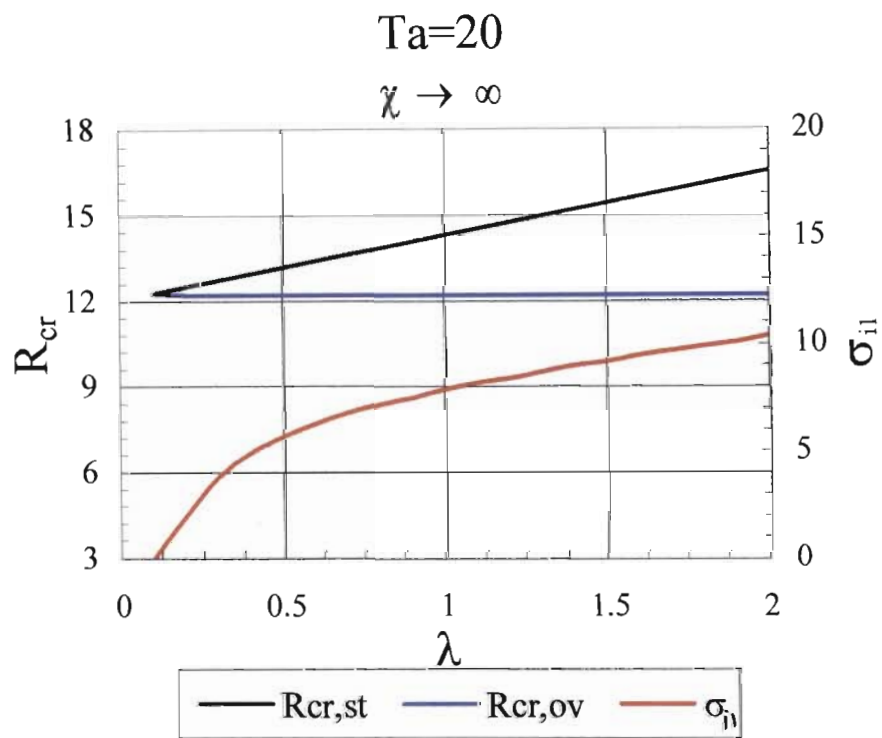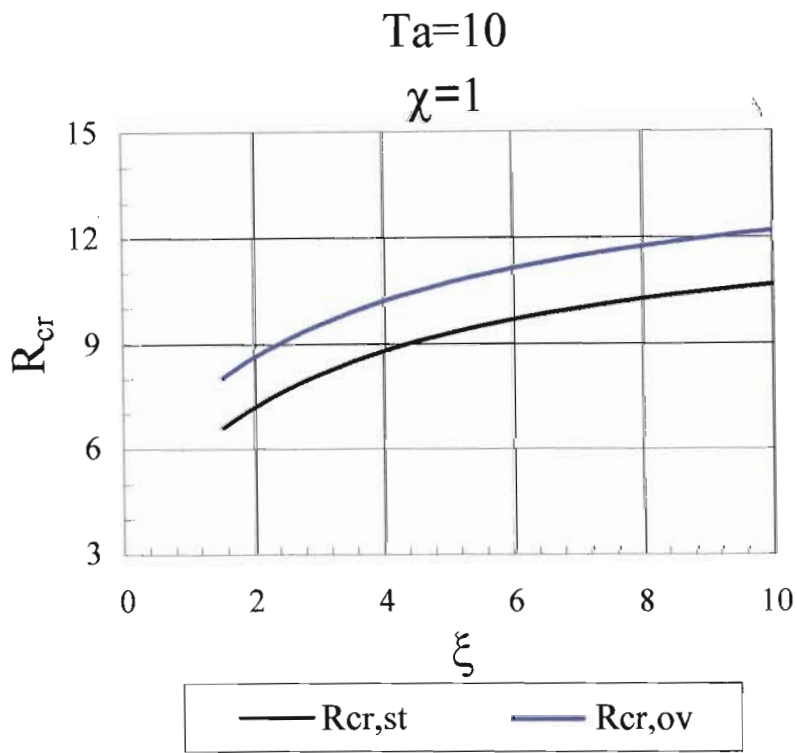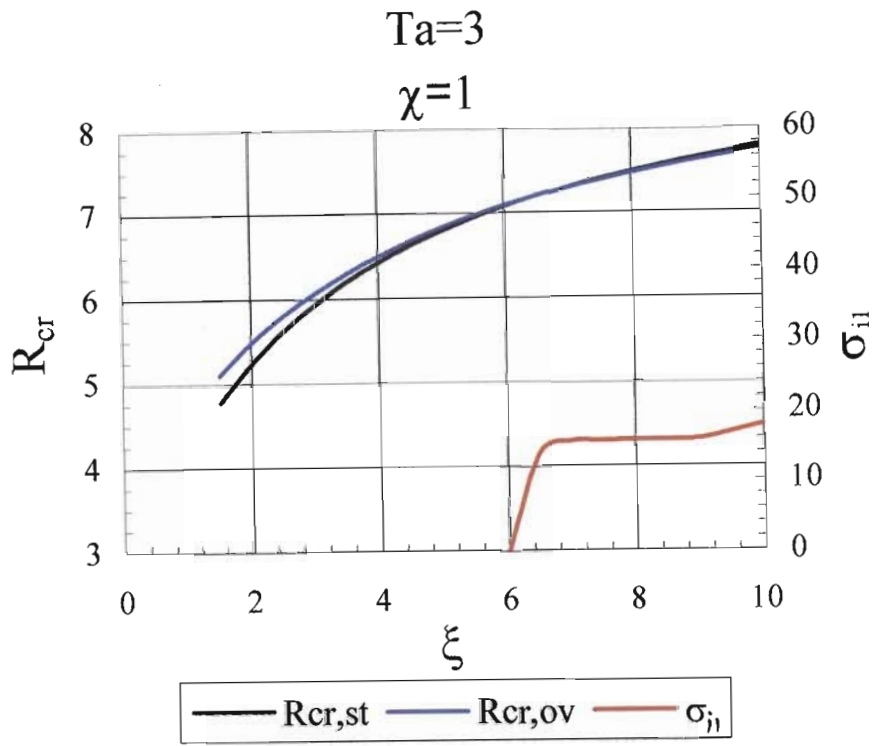
Figure 29 : Critical Rayleigh number R_{cr} versus ξ at $\chi = 1$ for (a) Ta=3 and (b) Ta=10. Stationary mode (black curve), oscillatory mode (blue curve) and frequency σ_{i1} (red curve)
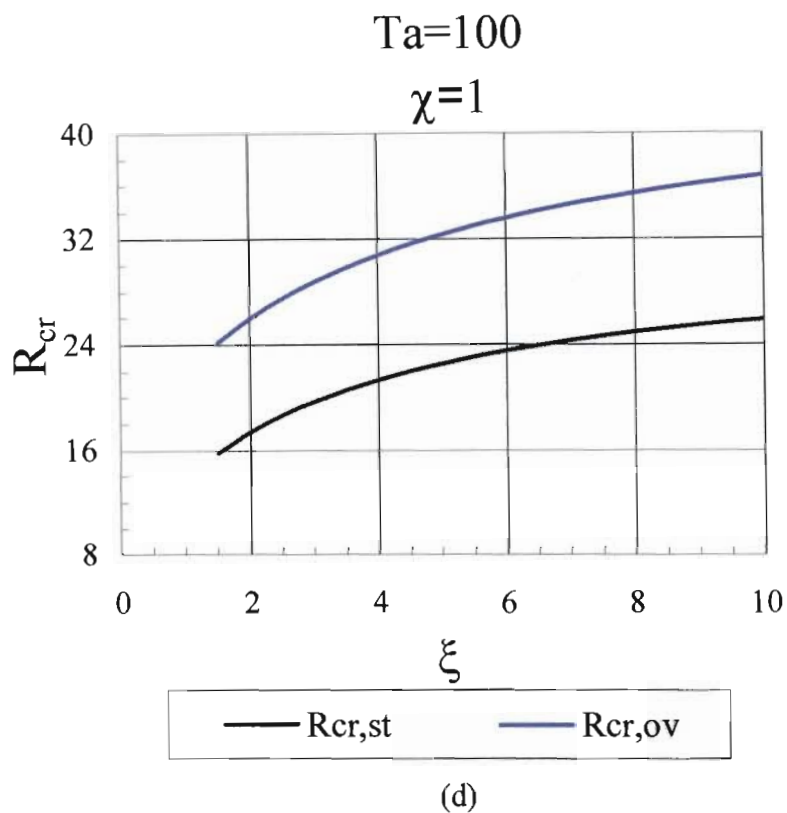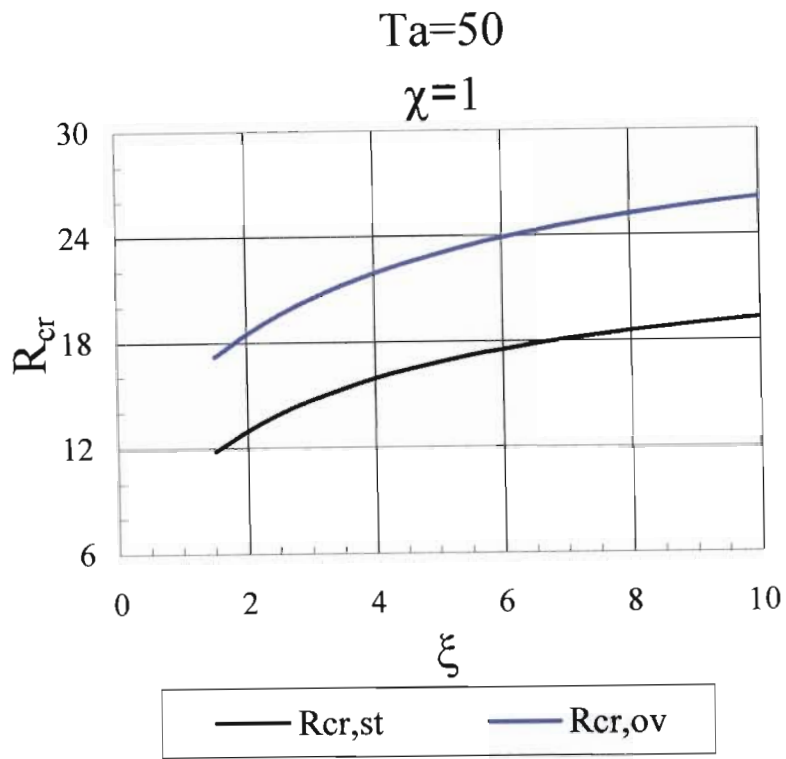
Figure 29 : Critical Rayleigh number R_{cr} versus ξ at $\chi = 1$ for (c) Ta=50 and (d) Ta=100. Stationary mode (black curve), oscillatory mode (blue curve) and frequency σ_{i1} (red curve)

Figures 30a to 30d shows the critical Rayleigh number curves for the stationary and oscillatory modes as well as the frequency σ_{i1} for a variation in the mushy layer depth δ for increasing Taylor number. The other parameters are fixed as $\chi = 1$, $\xi = 3$, $K_1 = 3$, and St=5.

It can be observed from Figures 30a to 30d that the curves for the oscillatory mode adopts a flat shape over the appropriate δ range. The stationary mode remains the most stable mode over a wider range of δ values at lower Taylor number settings, as can be seen from Figure 30a. As the Taylor number is increased, this bandwidth of these δ values over which the stationary mode is stable becomes smaller as can be observed in Figures 30b to 30d. This point may be illustrated by considering the transition points. The transition to stationary convection occurs at $\delta \cong 0.112$ for Ta=3, at $\delta \cong 0.0625$ for Ta=10, at $\delta \cong 0.025$ for Ta=50 and at $\delta \cong 0.024$ for Ta=100. By increasing the Taylor number at small values of χ the stationary mode becomes the most unstable mode for larger δ values.
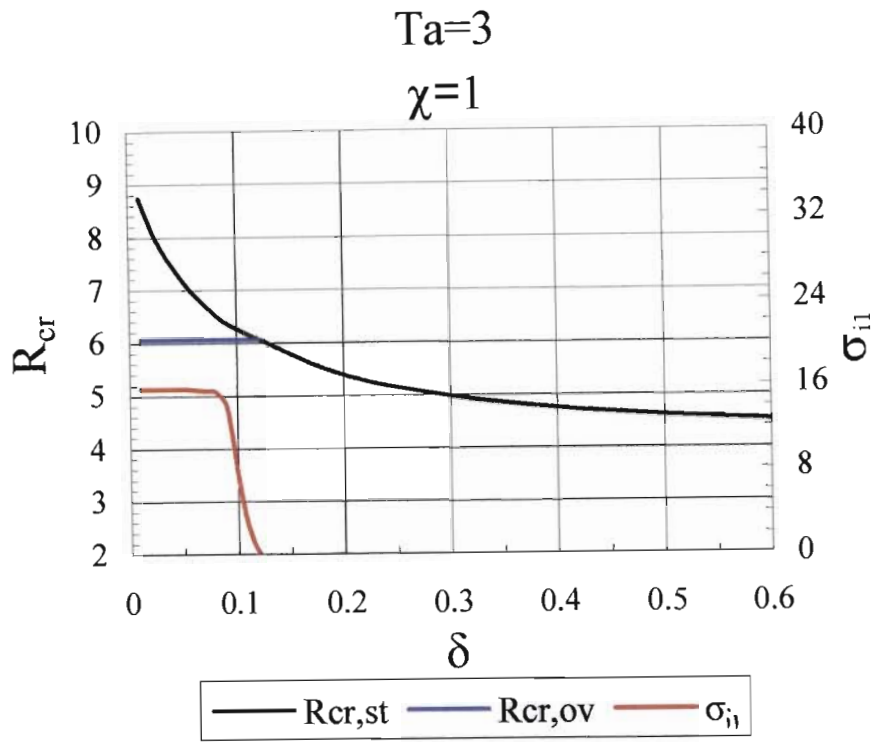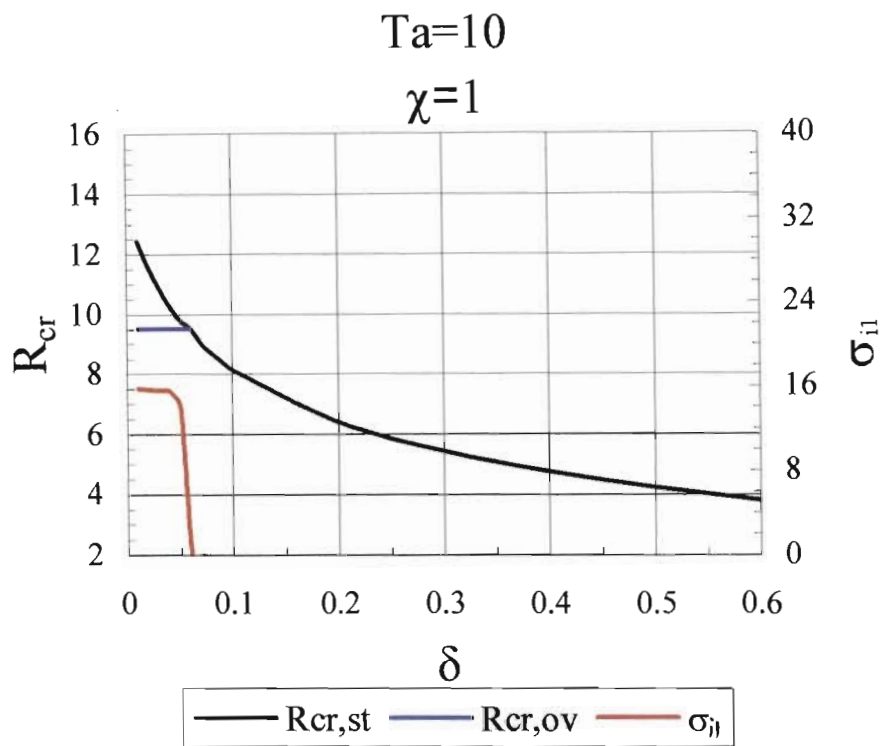
Figure 30 : Critical Rayleigh number R_{cr} versus δ at $\chi = 1$ for (a) Ta=3 (b) Ta=10. Stationary mode (black curve), oscillatory mode (blue curve) and frequency σ_{i1} (red curve)
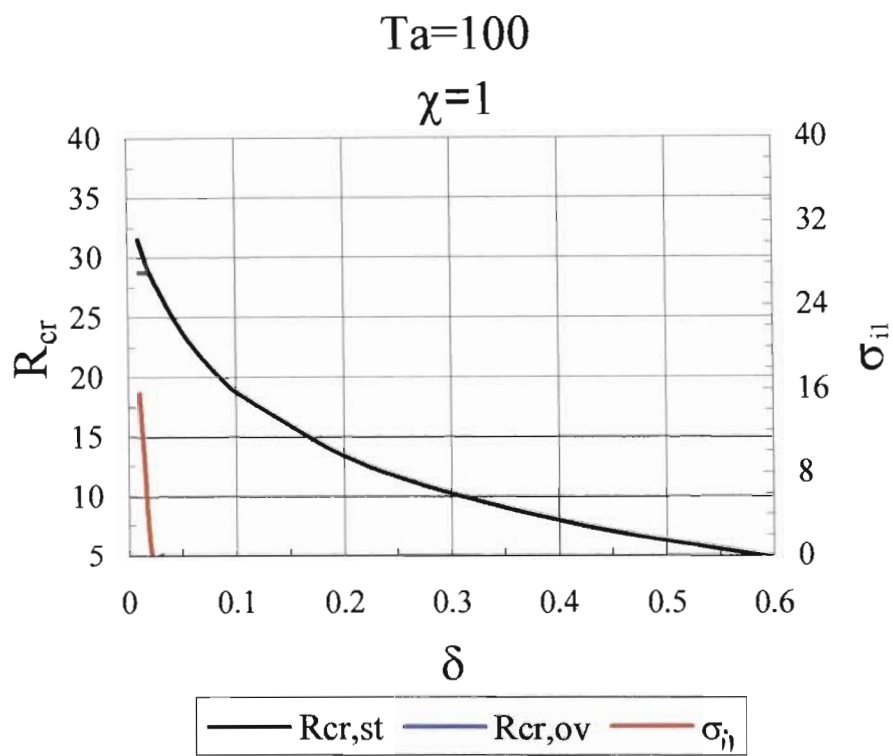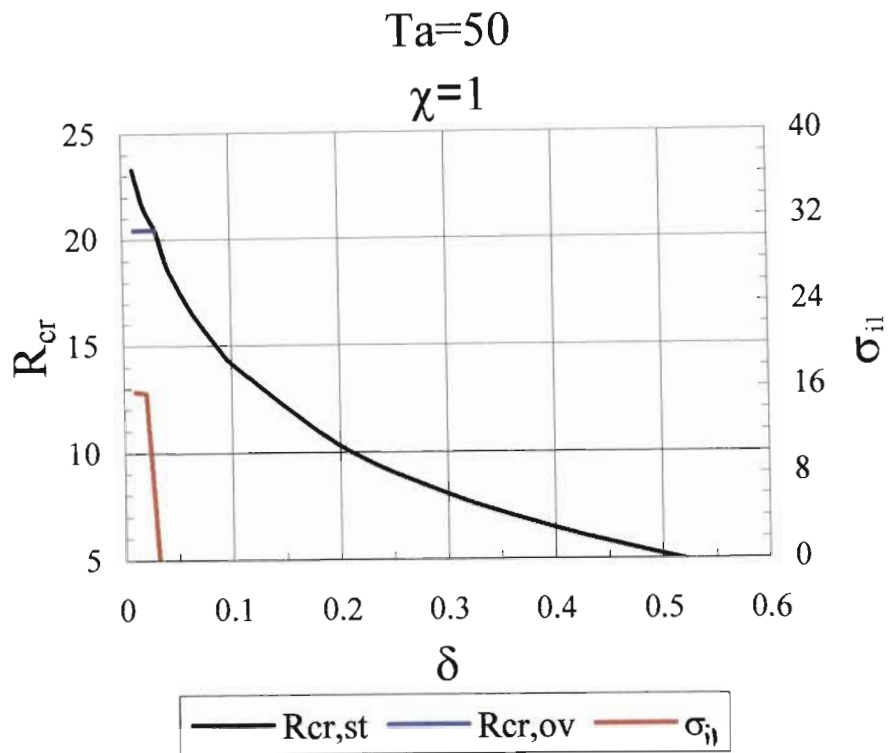
Figure 30 : Critical Rayleigh number R_{cr} versus δ at $\chi = 1$ for (c) Ta=50 and (d) Ta=100. Stationary mode (black curve), oscillatory mode (blue curve) and frequency σ_{i1} (red curve)

Figures 31a to 31d shows the critical Rayleigh number curves for the stationary and oscillatory modes as well as the frequency σ_{it} for a variation in the Taylor number Ta for increasing χ values. The other parameters are fixed as $\delta = 0.1$, $\xi = 3$, $K_1 = 3$, and St=5.

The value of λ was approximated to be about 0.8 for the case presented in Figures 31a to 31d. It can be observed from Figures 31a-b that the oscillatory mode is the most unstable mode for the lower range of Taylor numbers. The transition to stationary convection occurs at approximately $Ta \cong 4$. In figure 31c it can be noted that the stationary mode is now most unstable for Taylor numbers $Ta \geq 4$. The oscillatory mode however is the most unstable for Taylor numbers $Ta < 4$. A similar behaviour is noted from Figure 31d, the only difference being that the band of Taylor numbers within which oscillatory convection is most unstable lies between $Ta \cong 3$ and $Ta \cong 5$. The endpoints refer to the points of transition to stationary convection. Outside this band stationary convection is the most unstable.
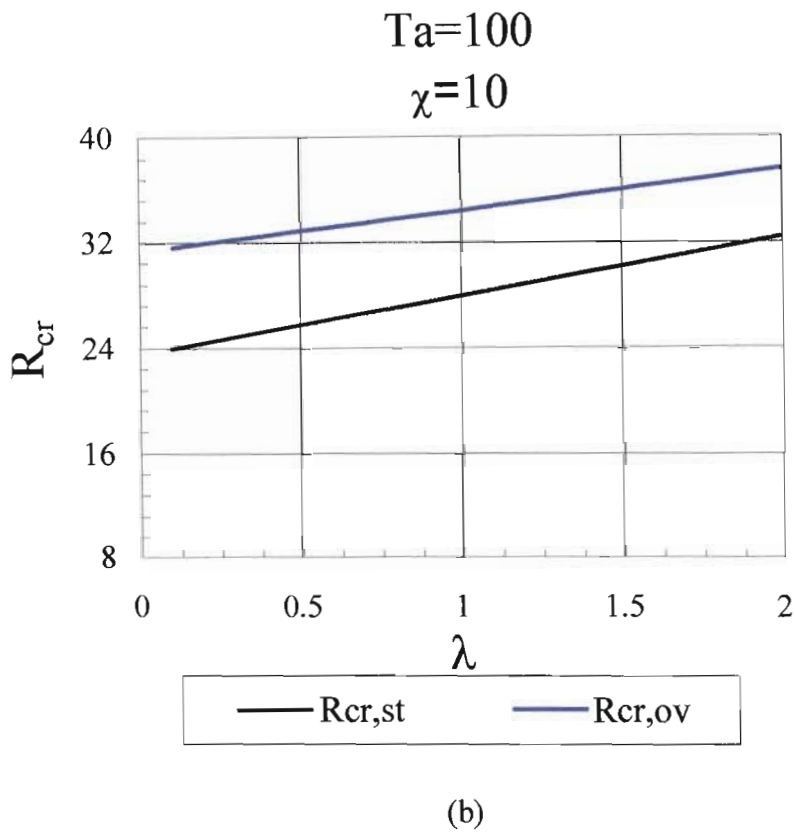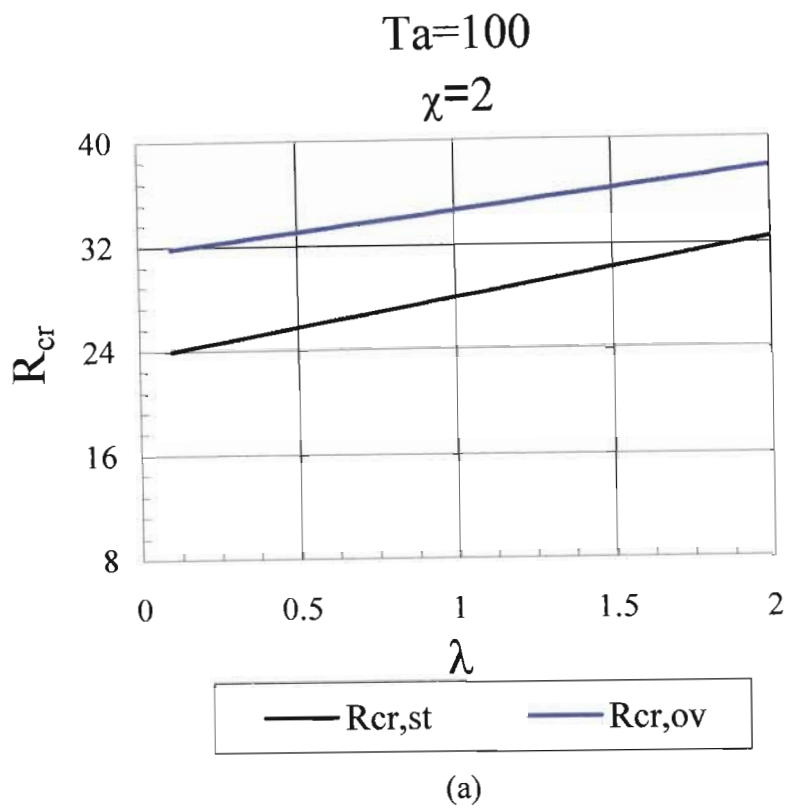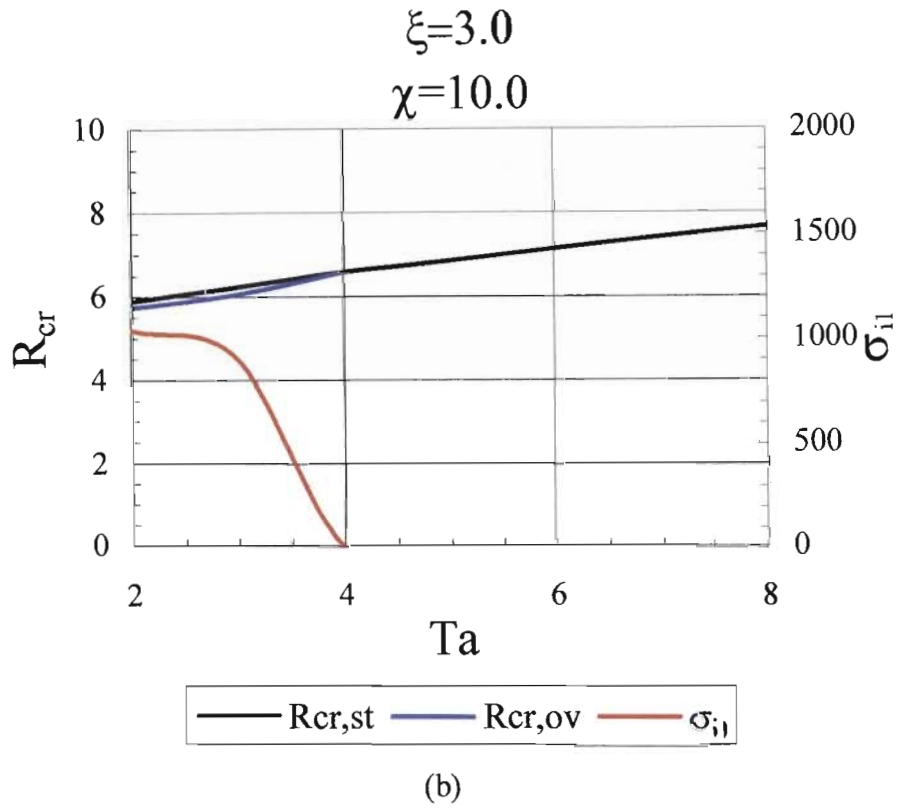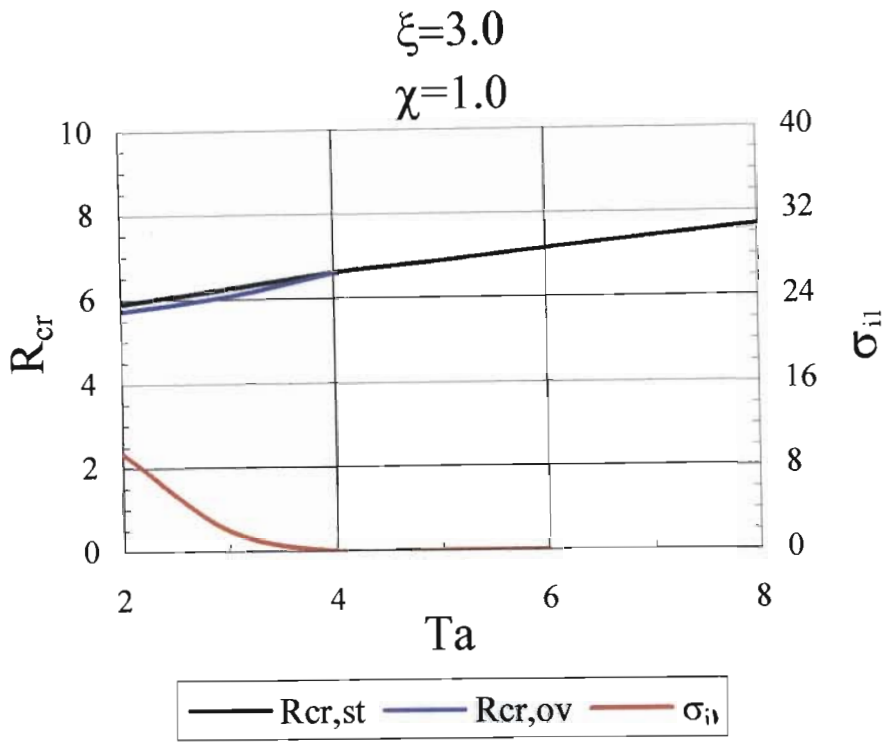
Figure 31 : Critical Rayleigh number R_{cr} versus Ta at $\xi = 3$ for (a) $\chi = 1$ and (b) $\chi = 10$. Stationary mode (black curve), oscillatory mode (blue curve) and frequency σ_{i1} (red curve)
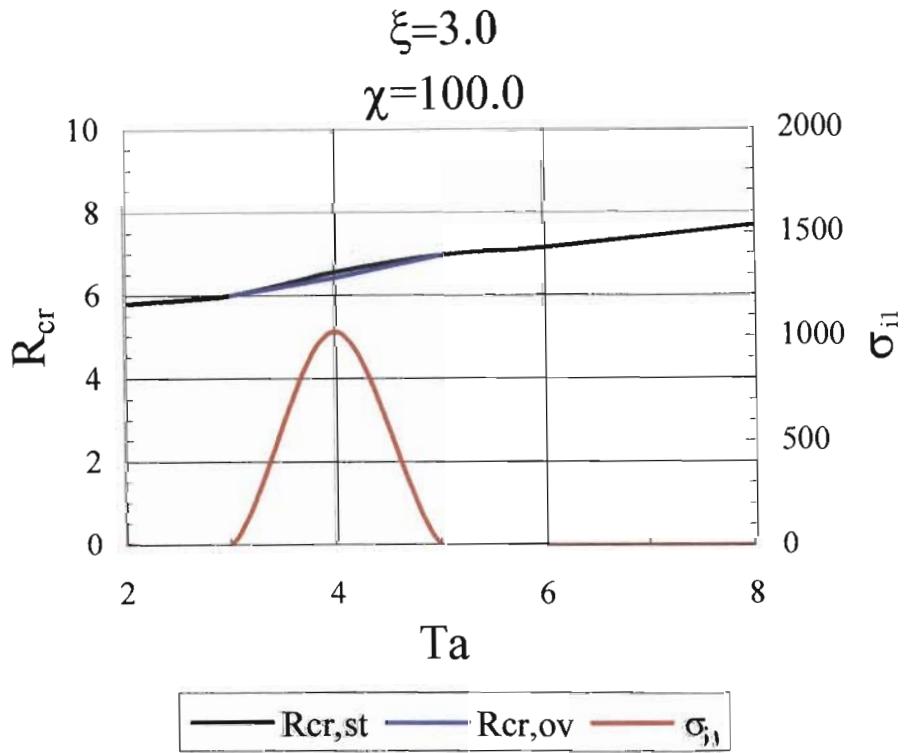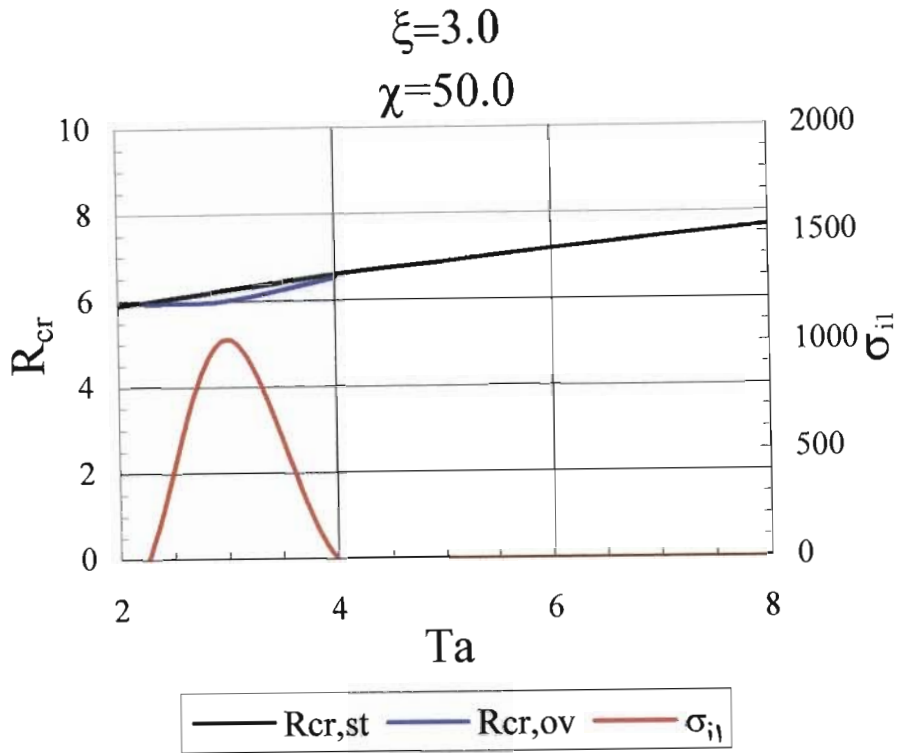
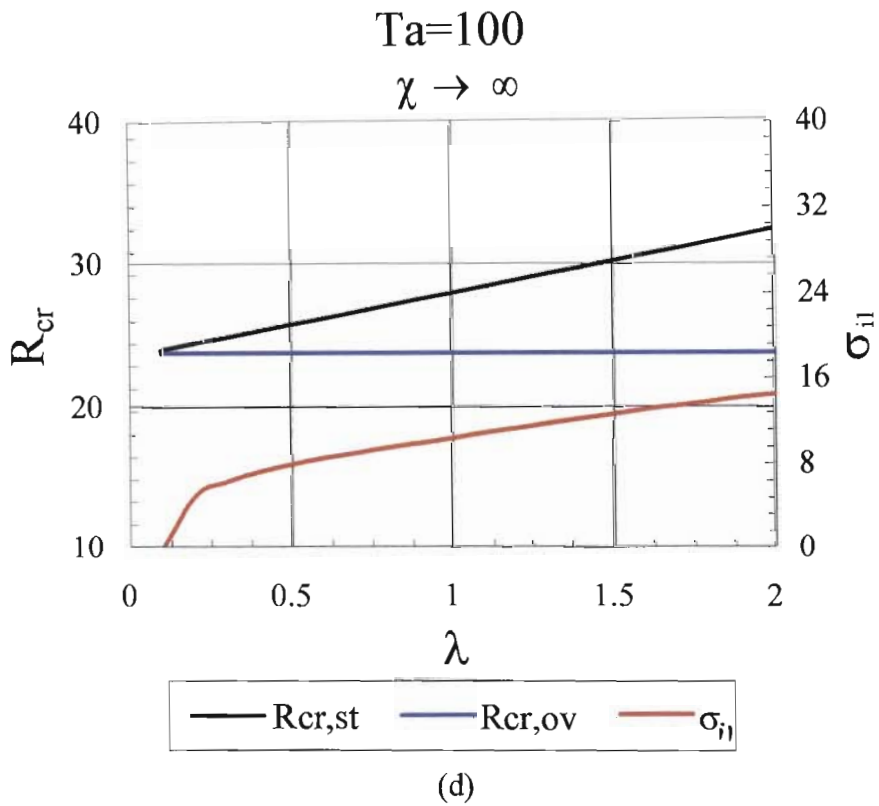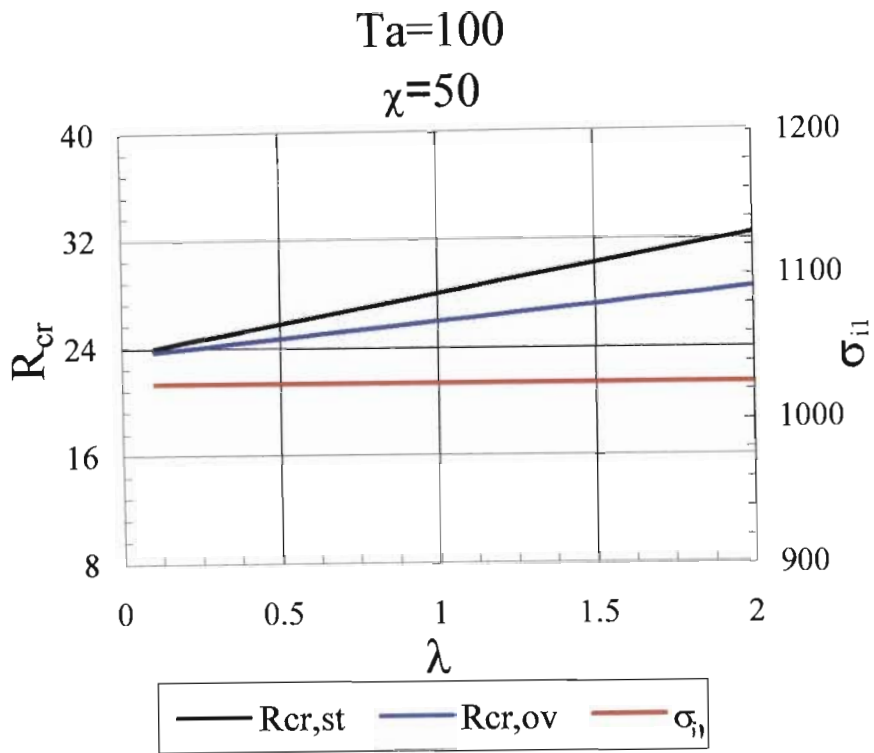Figure 31 : Critical Rayleigh number R_{cr} versus Ta at $\xi = 3$ for (c) $\chi = 50$ and (d) $\chi = 100$. Stationary mode (black curve), oscillatory mode (blue curve) and frequency σ_{i1} (red curve)

2.7 Eigenfunctions for Oscillatory Case

To describe the oscillatory instability we shall develop and present the eigenfunctions for the temperature, solid fraction and the stream function. We combine the basic-state solution and the leading order solution defined by the given normal mode expansion, Eqns.(2.20-2.22). Using the solutions given by Eqns.(2.38-2.41) we may proceed to present the solutions to the eigenfunctions for θ, φ, and ψ defined in Eqns.(2.20-2.22).

Note that in evaluating the eigenfunctions we let $s_y = 0$ so that $s^2 = s_x^2$. The solution to the temperature field is given as;

$$\theta = \theta_B - 2(\varepsilon A_{00}) \sin(\pi \bar{z}) \cos\left[s\bar{x} + \delta\sigma_{i1}\bar{t}\right]. \tag{2.73}$$

The eigenfunction for the stream function is given as,

$$\psi = -2(\varepsilon A_{00}) \frac{(\pi^2 + s^2)}{\Omega R_{00} s} \sin(\pi \bar{z}) \sin\left[s\bar{x} + \delta\sigma_{i1}\bar{t}\right]. \tag{2.74}$$

Finally, the solution for the solid fraction is given as,

$$\varphi = \varphi_B - 2(\varepsilon A_{00}) \frac{\pi(\pi^2 + s^2)}{\Omega c_s (\pi^2 - \sigma_{i1}^2)} \left\{ \left(\cos(\pi\bar{z}) + \cos\left[\sigma_{i1}(\bar{z}-1)\right]\right) \cdot \cos\left[s\bar{x} + \delta\sigma_{i1}\bar{t}\right] - \right.$$

$$\left. \left(\sigma_{i1}/\pi \cdot \sin(\pi\bar{z}) + \sin\left[\sigma_{i1}(\bar{z}-1)\right]\right) \cdot \sin\left[s\bar{x} + \delta\sigma_{i1}\bar{t}\right] \right\}. \tag{2.75}$$

Note that θ_B and φ_B have been previously evaluated and are given by Eqns.(2.15-2.16). Note that the system (2.73-2.75) contains a parameter εA_{00} which represents the amplitude. Note that ε is understood to be a small parameter as required by linear theory.

A detailed derivation of the system (2.73-2.75) is provided in *Appendix K*. Graphical plots will be provided in Section 6.

3. Case Two : Time scale proposed by Author
3.1 Rescaled Equations

In this part of the study we propose a new scaling in time as compared to that proposed by Anderson & Worster (1996). The scaling on the other dependent variables are as presented by Anderson & Worster (1996). For clarity, the scaling on all the dependent variables will be outlined. We use the same space and Rayleigh number scaling as Anderson & Worster (1996) which is given as,

$$x\hat{e}_x + y\hat{e}_y + z\hat{e}_z = \delta(\overline{x}\hat{e}_x + \overline{y}\hat{e}_y + \overline{z}\hat{e}_z), \quad R^2 = \delta Ra_m. \tag{3.1a-b}$$

We now introduce the following scales on the velocity vector and the pressure terms,

$$U = \frac{R}{\delta}\overline{U}, \quad p = R\overline{p}. \tag{3.2a-b}$$

The author used the following scaling on time which is of the form,

$$t = \delta\overline{t}, \tag{3.3a}$$

(instead of $t = \delta^2\overline{t}$ proposed by Anderson & Worster (1996)) and represents the diffusion time scale across the mushy layer. We note that our time scaling ($t = \delta\overline{t}$) represents a relatively shorter time scale when compared to Anderson & Worster's (1996) time scaling ($t = \delta^2\overline{t}$). We propose to absorb the parameter χ_1 in the scaling for time and propose the following scaling for time,

$$t' = \chi_1\overline{t} \tag{3.3b}$$

These scalings are applied to the system (2.3-2.6), which results in the following scaled set of governing equations,

$$\nabla \cdot \overline{U} = 0, \tag{3.4}$$

$$\delta \left(\chi_1 \frac{\partial}{\partial t'} - \frac{\partial}{\partial \overline{z}} \right) \left(\theta - \frac{\overline{S}}{\delta} \varphi \right) + R\overline{U} \cdot \overline{\nabla} \theta = \overline{\nabla}^2 \theta , \tag{3.5}$$

$$\delta \left(\chi_1 \frac{\partial}{\partial t'} - \frac{\partial}{\partial \overline{z}} \right) \left[(1 - \varphi) \theta + \frac{c_S}{\delta} \varphi \right] + R\overline{U} \cdot \overline{\nabla} \theta = 0 , \tag{3.6}$$

$$\frac{\partial \overline{U}}{\partial t'} + \Pi(\varphi) \overline{U} = -\overline{\nabla} \overline{p} - R\theta \hat{e}_z - Ta^{1/2} \hat{e}_z \times \overline{U} \tag{3.7}$$

where $\chi_1 = \delta \chi_0$. Recall that δ is the growth Peclet number, and parameter χ_0 is defined as,

$$\chi_0 = Pr \phi_0 \vartheta_0 , \tag{3.8}$$

where ϑ_0 is the mobility ratio, Pr is the Prandtl number and ϕ_0 is a characteristic value for the porosity, all of which have been defined earlier in Section 2. Vadasz (1998) suggested that for solidifying binary alloys, $Pr = 10^{-3}$, and $\phi_0 = 0.1$ represent typical values in metallic systems. Obviously, in aqueous systems, the Prandtl number will be considerably higher. In addition Worster (1992) suggested that mobility ratios have values that lie within the range $\vartheta_0 \in [10^5, 10^6]$. Selecting $\delta = 0.1$, $Pr = 10^{-3}$, $\phi_0 = 0.1$, and $\vartheta_0 = 10^5$ yields $\chi_1 = 1$, implying that there exists combinations of the mentioned parameters for which χ_1 is of the order unity thus allowing the time derivative to be of significance in the system (3.4-3.7). A full derivation of the system (3.4-3.7) is provided in *Appendix O*.

3.2 Basic Flow Solution

There is a basic steady state ($\partial\theta_B/\partial\bar{t} = \partial\varphi_B/\partial\bar{t} = 0$) represented by subscript 'B', which is horizontally uniform ($\partial\theta_B/\partial\bar{x} = \partial\varphi_B/\partial\bar{x} = 0$, $\partial\theta_B/\partial\bar{y} = \partial\varphi_B/\partial\bar{y} = 0$), corresponds to zero flow ($\mathbf{U}_B = 0$) and satisfies the following system of equations :

$$-\delta\frac{d}{d\bar{z}}\left[\theta_B - \frac{\bar{S}}{\delta}\varphi_B\right] = \frac{d^2\theta_B}{d\bar{z}^2} \tag{3.9}$$

$$-\delta\frac{d}{d\bar{z}}\left[(1-\varphi_B)\theta_B + \frac{c_S}{\delta}\varphi_B\right] = 0 \tag{3.10}$$

$$-\frac{d\bar{p}_B}{d\bar{z}} - R\theta_B = 0. \tag{3.11}$$

Eqns.(3.9-3.11) corresponds exactly with that given by the system (2.8-2.10) found earlier using Anderson & Worster's (1996) scaling. The system (3.9-3.11) is subject to the boundary conditions,

$$\theta_B = -1 \qquad \text{at} \qquad \bar{z} = 0 \tag{3.12a}$$

$$\theta_B = 0 \qquad \text{at} \qquad \bar{z} = 1. \tag{3.12b}$$

As before the solution to this systems is given as,

$$\theta_B(\bar{z}) = (\bar{z}-1) + \delta\left[-\frac{\Omega}{2}(\bar{z}^2 - \bar{z})\right] +$$

$$\delta^2\left[\frac{\Omega^2}{2}\left(\frac{1}{3}\bar{z}^3 - \frac{1}{2}\bar{z}^2\right) - \frac{\bar{S}}{c_S^2}\left(\frac{1}{3}\bar{z}^3 - \bar{z}^2\right) + \frac{1}{3}\left(\frac{2\bar{S}}{c_S^2} + \frac{1}{4}\Omega^2\right)\bar{z}\right] \tag{3.13}$$

$$\varphi_B = -\delta \frac{(\bar{z}-1)}{c_S} + \delta^2 \left[-\frac{(\bar{z}-1)^2}{c_S^2} + \frac{\Omega}{2c_S}(\bar{z}^2 - \bar{z}) \right],$$
(3.14)

where $\Omega = 1 + \bar{S}/c_S$. This corresponds exactly to the solution given in Eqns.(2.14-2.15). A detailed derivation is provided in *Appendix C*. Applying twice the curl operator $(\nabla \times)$ on Eqn.(3.7) and considering only the vertical component of this results yields the following form,

$$\left[\frac{\partial}{\partial t'} + \Pi(\varphi) \right] \nabla^2 \bar{w} + \frac{d\Pi}{d\bar{z}} \frac{\partial \bar{w}}{\partial \bar{z}} + R\nabla_H^2 \theta + Ta^{1/2} \frac{\partial \omega_z}{\partial \bar{z}} = 0,$$
(3.15)

where the horizontal Laplacian operator is defined in the form $\nabla_H^2 = \partial^2/\partial \bar{x}^2 + \partial^2/\partial \bar{y}^2$ and the component of vertical vorticity is given as,

$$\left[\frac{\partial}{\partial t'} + \Pi(\varphi) \right] \omega_z = Ta^{1/2} \partial \bar{w}/\partial \bar{z}.$$
(3.16)

Refer to *Appendix D* for a detailed derivation of Eqns.(3.15-3.16).

3.3 Linear Stability Analysis

The stability of the system (3.4-3.7) is examined by determining the growth and decay of infinitesimal disturbances to the steady solution. We introduce normal-mode perturbations of the following form to order ε,

$$\theta = \theta_B + \varepsilon\theta_1 = \theta_B + \varepsilon\hat{\theta}(\bar{z})e^{\sigma t'}e^{i(s_x\bar{x}+s_y\bar{y})} + c.c$$
(3.17)

$$\varphi = \varphi_B + \varepsilon\varphi_1 = \varphi_B + \varepsilon\hat{\varphi}(\bar{z})e^{\sigma t'}e^{i(s_x\bar{x}+s_y\bar{y})} + c.c$$
(3.18)

$$\bar{U} = \varepsilon\bar{U}_1 = 0 + \varepsilon\hat{\bar{U}}(\bar{z})e^{\sigma t'}e^{i(s_x\bar{x}+s_y\bar{y})} + c.c,$$
(3.19)

where σ is the growth rate, s_x and s_y are the horizontal wave numbers of the perturbation and (c.c) stands for the complex conjugate. Apply the normal-mode (3.17-3.19) to the (3.5-3.7) and in Eqns.(3.15-3.16) yields the following heat balance, solute balance and Darcy equation to order $\varepsilon\,\delta$,

$$\delta\left(\chi_i\sigma - D\right)\left[\hat{\theta} - \frac{\overline{S}}{\delta}\hat{\varphi}\right] + R\widehat{\overline{w}}D\theta_B = (D^2 - s^2)\hat{\theta} \tag{3.20}$$

$$\delta\left(\chi_i\sigma - D\right)\left[(1 - \varphi_B)\hat{\theta} - \theta_B\hat{\varphi} + \frac{c_S}{\delta}\hat{\varphi}\right] + R\widehat{\overline{w}}D\theta_B = 0 \tag{3.21}$$

$$\left[\sigma + \Pi(\varphi)\right]^2(D^2 - s^2)\widehat{\overline{w}} + \left[\sigma + \Pi(\varphi)\right]\left[D\Pi(\varphi).D\widehat{\overline{w}} - Rs^2\hat{\theta}\right] + TaD^2\widehat{\overline{w}} = 0. \tag{3.22}$$

The system above is solved subject to the following boundary conditions,

$$\hat{\theta} = 0, \quad \widehat{\overline{w}} = 0 \qquad\qquad \text{at} \qquad \overline{z} = 0 \tag{3.23a}$$

$$\hat{\theta} = 0, \quad \widehat{\overline{w}} = 0, \quad \hat{\varphi} = 0 \qquad\qquad \text{at} \qquad \overline{z} = 1. \tag{3.23b}$$

A detailed derivation of the system (3.20-3.22) is given in *Appendix P*.

In the system (3.20-3.23) $D = d/d\overline{z}$ and $\sigma = \sigma_r + i\sigma_i$. Note also that φ_B and θ_B represents the basic state solution for the temperature distribution given by Eqn.(3.13-3.14) and $\Pi(\varphi)$ is the permeability function as a function of the solid fraction φ. Since the basic state solid fraction is small and the perturbations to the solid fraction will also be small, we follow a form similar Amberg and Homsey (1993) and propose a truncated form of the function $\Pi(\varphi)$ in a Taylor series expansion for $\varphi \ll 1$.

$$\Pi(\varphi) = 1 + K_c\varphi^2 + O(\varphi^3) \tag{3.24}$$

89

It can be seen from Eqn.(3.24) that the effects of permeability are only introduced at $O(\varphi^2)$. We shall not specify a form for the permeability at this stage but we require that $K_c > 0$ so that the permeability decreases with increasing solid fraction. Note that the solid fraction may be written in terms of the basic solution and the pertubation as follows,

$$\varphi = \delta \overline{\varphi}_B + \varepsilon \varphi_1, \tag{3.25}$$

where $\varphi_B = \delta \overline{\varphi}_B$ and $\varphi_1 = \hat{\varphi}(\overline{z})e^{\sigma t'}e^{i(s_x \overline{x} + s_y \overline{y})}$. This implies that the permeability function may be represented as $\Pi(\varphi) = \Pi(\delta \overline{\varphi}_B + \varepsilon \varphi_1)$. Since we only consider the order $O(\delta^0)$ problem for the current study, the permeability function becomes $\Pi(\varphi) = \Pi(\varepsilon \varphi_1)$. Applying this result to Eqn.(3.24) and using the expansion given in Eqn.(3.25) yields to $O(\varepsilon^2)$ the following form of the permeability function as used in the current study,

$$\Pi(\varepsilon \varphi_1) = 1 + \varepsilon^2 K_c \varphi_1^2 + O(\varepsilon^3). \tag{3.26}$$

It should be borne in mind that φ_1 represents the solution to the solid fraction at order $O(\varepsilon)$. It can be seen that to $O(\varepsilon^0)$ the permeability is 1, ie. the mushy layer is homogenous medium at the zeroth order. Refer to *Appendix Q* for the derivation of Eqn.(3.26).

Consider the system (3.20-3.22) to order $O(\varepsilon \delta^0)$

$$(D^2 - s^2)\hat{\theta} - \Omega R\hat{\overline{w}} = 0 \tag{3.27}$$

$$(\chi_1 \sigma - D)c_S \hat{\varphi} + R\hat{\overline{w}} = 0 \tag{3.28}$$

$$[\sigma + 1]^2 (D^2 - s^2)\hat{\overline{w}} - (\sigma + 1)Rs^2\hat{\theta} + TaD^2\hat{\overline{w}} = 0. \tag{3.29}$$

Refer to *Appendix R* for a detailed derivation of Eqns.(3.27-3.29). The solution to the system (3.27-3.29) is given as,

$$\hat{\theta} = -B_1 \sin(\pi \bar{z}) \qquad (3.30)$$

$$\hat{\bar{w}} = N_1 \sin(\pi \bar{z}) \qquad (3.31)$$

$$\hat{\varphi} = -C_1 \left[e^{\pi^2 \gamma \sigma (\bar{z}-1)} + \sigma \pi \gamma \sin(\pi \bar{z}) + \cos(\pi \bar{z}) \right], \qquad (3.32)$$

where the coefficients B_1 and C_1 are given by,

$$N_1 = \frac{(1+\alpha)}{\Omega \bar{R}} B_1 \qquad (3.33)$$

$$C_1 = \frac{\pi(1+\alpha)}{\Omega c_S (1+\pi^2 \gamma^2 \sigma^2)} B_1. \qquad (3.34)$$

In addition the characteristic Rayleigh number is given as,

$$\bar{R}^2 = \frac{(1+\alpha)}{\Omega \alpha \pi^2 (\sigma+1)} \left[(\sigma+1)^2 (1+\alpha) + \mathrm{Ta} \right]. \qquad (3.35)$$

The scaling $\alpha = s^2 / \pi^2$, $\gamma = \chi_1 / \pi^2$ and $\bar{R} = R/\pi^2$ has been applied to Eqns.(3.30-3.35). A detailed derivation of Eqns.(3.30-3.35) is given in *Appendix S*. It is interesting to note that as $\sigma \to 0$ and $\mathrm{Ta} \to 0$, Eqn.(3.35) collapses to,

$$\bar{R}^2 = \frac{(1+\alpha)^2}{\Omega \alpha \pi^2}, \qquad (3.36)$$

91

which resembles the form of the Rayleigh number definition obtained by Anderson & Worster (1996) in the author's notation. We now proceed to analyse the above results for both stationary and oscillatory convection as separate analyses.

3.4 Stationary Convection

For stationary convection σ in Eqn.(3.35) is real and for marginal stability, $\sigma = 0$, therefore the corresponding characteristic values of Rayleigh number associated with stationary convection are obtained by setting $\sigma = 0$ in Eqn.(3.35). This operation then yields characteristic values of the form,

$$\overline{R}^2_{c,st} = \frac{(1+\alpha)^2}{\Omega \alpha \pi^2} + \frac{(1+\alpha)}{\Omega \alpha \pi^2} Ta . \tag{3.37}$$

The first term in Eqn.(3.37) represents the characteristic Rayleigh number for convection in the absence of rotation, whilst the second term introduces the contribution of rotation. Minimising $\overline{R}_{st,c}$ with respect to α yields the critical wave number and Rayleigh number for stationary convection,

$$\alpha_{cr,st} = \sqrt{Ta + 1} \tag{3.38}$$

$$\overline{R}_{cr,st} = \frac{1}{\pi \sqrt{\Omega}} \left(1 + \sqrt{Ta + 1}\right). \tag{3.39}$$

Refer to *Appendix T* for a derivation of the critical values given in Eqns.(3.38-3.39). Note that the critical conditions proposed in Eqns.(3.38-3.39) closely resembles the form defined by Vadasz (1998). By using the stability conditions in Eqns.(3.38-3.39) we can establish the limit as $Ta \to \infty$ in the form,

$$Ta \to \infty : \begin{cases} \overline{R}_{cr,st} \to \left[1 + O(Ta^{1/2})\right]/\pi\Omega \\ \\ \alpha_{cr,st} \to Ta^{1/2} \end{cases}$$

(3.40)

Then using the definition of the Rayleigh number and of $\overline{\beta} = \beta^*(c_0 - c_E)$, we can express the critical compositional difference over the porous layer as follows,

$$\overline{\beta}_{cr,st} = \frac{4\pi^2(\omega^*)^2 k_0 \kappa^*}{g^* H^* \phi_0^2 (1 + St/\xi)} \frac{1}{\nu^*} \qquad \text{for} \qquad Ta \to \infty .$$

(3.41)

Eqn.(3.41) shows that the critical composition difference for a fast rotating mushy layer depends on the inverse power of viscosity. For the case $Ta \to 0$, the critical composition difference is given as ,

$$\overline{\beta}_{cr,st} = \frac{4\pi^2 \kappa^*}{g^* H^* (1 + St/\xi) k_0} \nu^* \qquad \text{for} \qquad Ta \to 0 .$$

(3.42)

The result shown in Eqn.(3.42) for a non-rotating mushy layer shows that the critical composition difference is in contrast to the result shown in Eqn.(3.41). Eqn.(3.41) implies that at high rotational speeds ($Ta \gg 1$) increasing the fluid viscosity has a destabilising effect. This is because the as the difference $\overline{\beta}_{cr} = \beta^*(c_0 - c_E)$ is made smaller, the corresponding critical Rayleigh number for the onset of convection is also made smaller, hence convection threshold point is lowered with increasing the fluid's viscosity. On the other hand, for the case with no rotation, Eqn.(3.42), increasing the fluid's viscosity has a stabilising effect since the convection threshold point occurs at a much higher Rayleigh number. Refer to *Appendix U* for the derivation of the critical composition differences.

With the stability results evaluated, we may now proceed to present the complete eigenfunction solutions. For three dimensional flow patterns corresponding to convection rolls whose axes are parallel to the y direction, the variation of the variables in the y-

direction vanishes, which allows the existence of a stream function, ψ, to satisfy identically the continuity equation (3.4). Note that despite the existence of a stream function, the flow is still three dimensional and in general the component of filtration velocity in the y direction does not vanish. Setting $s_y = 0$ and $s^2 = s_x^2$, which upon substitution in the solution for θ_1 (Eqn.(3.17)) and accounting for the symmetry conditions at the axis of rotation yields for stationary convection,

$$\theta_1 = -2B_1 \cos(s\bar{x})\sin(\pi\bar{z}).$$

(3.43)

Using Eqn.(3.32) and substituting in Eqn.(3.18) yields the solution for the solid fraction φ_1,

$$\varphi_1 = -2C_1\left[1 + \cos(\pi\bar{z})\right]\cos(s\bar{x})$$

(3.44)

Using Eqn.(3.31) and substituting in Eqn.(3.19) yields the solution for the vertical component of the filtration velocity $\overline{w}_1$,

$$\overline{w}_1 = 2N_1 \cos(s\bar{x})\sin(\pi\bar{z}).$$

(3.45)

Now using Eqn.(3.45) and the vertical component of the vorticity given by

$$\omega_z = Ta^{1/2}\frac{\partial\overline{w}_1}{\partial\bar{z}},$$

(3.46)

yields the y component of the velocity,

$$\overline{v}_1 = 2Ta^{1/2}\frac{N_1}{\alpha^{1/2}}\sin(s\bar{x})\cos(\pi\bar{z}).$$

(3.47)

using the following form of the continuity equation,

$$\frac{\partial \bar{u}_1}{\partial \bar{x}} = -\frac{\partial \bar{w}_1}{\partial \bar{z}} \tag{3.48}$$

and the vertical component of the velocity, Eqn.(3.45) yields the x-component of the velocity,

$$\bar{u}_1 = -2\frac{N_1}{\alpha^{1/2}}\sin(s\bar{x})\cos(\pi\bar{z}). \tag{3.49}$$

Note that the coefficients N_1 and C_1 used above are as given in Eqns.(3.33-3.34). The amplitude A_1 will be determined later when a weak non-linear analysis is performed.

The solution presented in Eqn.(3.47) and Eqn.(3.49) describes the convection cells which are tilted in the y-direction, forming an angle $\tan^{-1}(\bar{v}_1/\bar{u}_1)$ with respect to the x-axis. On this tilted plane there is no velocity component normal to the plane, hence this is regarded as the plane oblique plane containing the streamlines. From Eqn.(3.47) and Eqn.(3.49) one can evaluate the ratio between the horizontal components of the filtration velocity in the form,

$$\frac{\bar{v}_1}{\bar{u}_1} = -Ta^{1/2}. \tag{3.50}$$

This result corresponds identically with that found by Vadasz (1998). Using the relation given in Eqn.(3.50) and the critical value of the wave number, given by Eqn.(3.38), allows us to describe the wave number in the oblique plane containing the streamlines in the form,

$$s_{st,cr}^{oblique} = s_{st,cr}\cos(\tan^{-1}(\bar{v}_1/\bar{u}_1)) = \frac{\pi}{(Ta+1)^{1/4}}. \tag{3.51}$$

Eqn.(3.51) implies that the wavelength of the roll measured in the plane containing the streamlines is a function of the Taylor number, thus implying that it is dependent on rotation.

A detailed derivation of the leading order solutions given in Eqns.(3.43-3.45), Eqn.(3.47), Eqn.(3.49) and Eqn.(3.51) is provided in *Appendix V*.

3.5 Overstable Convection

For overstable convection we allow for the possibility of oscillatory motion and therefore σ is represented in the form $\sigma = \sigma_r + i\sigma_i$. At the marginal stability state $\sigma_r = 0$ leaving only the imaginary part in the equation. Substituting $\sigma = i\sigma_i$ into Eqn.(3.35) and imposing the condition $\sigma_i^2 > 0$, which is the requirement for σ_i to be real in order to get overstability possible at all, yields two algebraic equations by letting the real and imaginary part of Eqn.(3.35) to vanish separately. This provides the solution for the characteristic values of Rayleigh number and the frequency σ_i of the oscillations at marginal stability, in the form,

$$\overline{R}^2_{c,ov} = \frac{2}{\pi^2 \alpha \Omega}(\alpha + 1)^2 \tag{3.52}$$

$$\sigma_i^2 = \frac{Ta}{\alpha + 1} - 1, \tag{3.53}$$

where the subscript $(.)_{,ov}$ stands for identifying the overstable convection. *Appendix W* provides a detailed derivation of the characteristic Eqns.(3.52-3.53). An interesting point to note is that the frequency σ_i^2 given in Eqn.(3.53) is identical to Vadasz's (1998) results for the case when $\gamma \to 0$. Vadasz (1998) stated that the case $\gamma \to 0$ depicted the lower bound for the overstable characteristic curves. It can be observed from Eqn.(3.53) that when there is no rotation (Ta=0) then oscillatory convection is impossible since $\sigma_i^2 < 0$. Minimising $R_{c,ov}$ with respect to α yields the critical wave number and Rayleigh number which is of the form,

$$\alpha_{cr,ov} = 1 \qquad\qquad\qquad\qquad (3.54)$$

$$\overline{R}_{cr,ov} = \frac{2}{\pi}\sqrt{\frac{2}{\Omega}} \qquad\qquad\qquad\qquad (3.55)$$

$$\sigma^2_{i,cr} = \frac{Ta}{2} - 1. \qquad\qquad\qquad\qquad (3.56)$$

Refer to *Appendix X* for a detailed derivation of the critical values in Eqns.(3.54-3.56). It can be observed from Eqn.(3.56) that the Taylor number limit should be $Ta \geq 2$ in order for the frequency to be real for $\alpha_{cr,ov} = 1$. This is however not sufficient in order to have the instability setting in as overstable convection. For this to occur one must require the overstable critical Rayleigh number to be less than the corresponding stationary critical Rayleigh number, ie. $\overline{R}_{cr,ov} \leq \overline{R}_{cr,st}$. This condition implies that $Ta \geq 4\left(2 - \sqrt{2}\right)$.

Graphical representation of the characteristic curves is provided in Figure 32 for different values of Taylor number. It can be observed from Figure 32 that the oscillatory mode becomes the most unstable mode with increasing Taylor number. In the case of no rotation (Ta=0) the stationary mode is the most unstable mode. The frequency σ_i as a function of the wavenumber is shown in Figure 33a. Note that the points at which the curves for each of the Taylor number values intersects the x-axis represents the points at which stationary convection sets in. Figure 33b shows the variation of the critical frequency as a function of the Taylor number. It can be observed that the critical frequency increases proportionally with increasing Taylor number.

The complete eigenfunctions for the oscillatory case will be developed and presented in the following section when the weak non-linear analysis of overstable convection is undertaken.
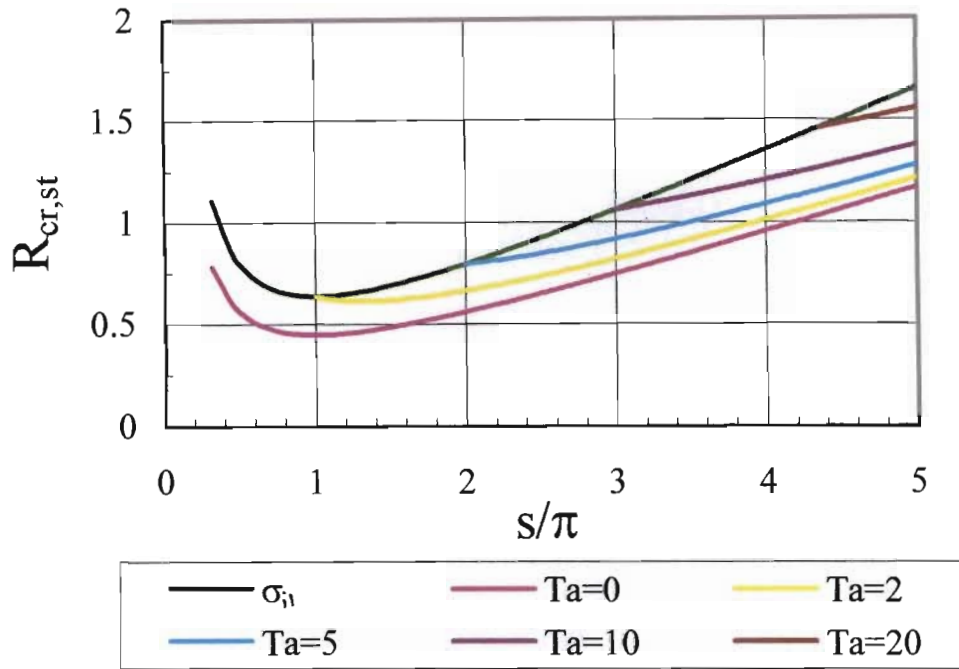
Figure 32 : The characteristic curves representing the marginal stability limit with respect to overstable convection for various Taylor number values.
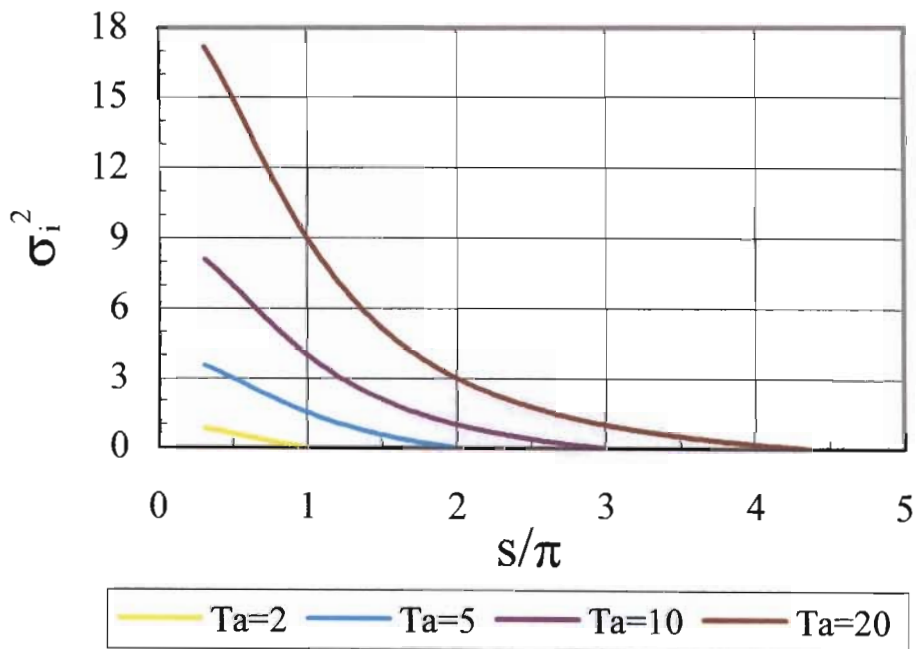
Figure 33a : The variation characteristic values of frequency associated with overstable convection for different values of Taylor number.
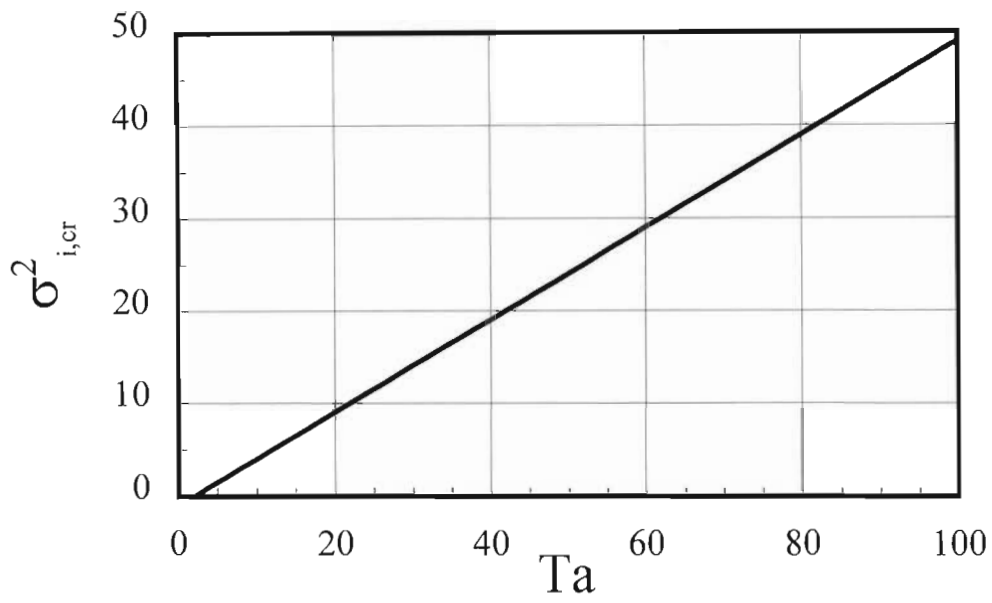
Figure 33 b : The variation critical values of frequency associated with overstable convection as a function Ta.

4. Weak Non-linear Analysis of Author scaling

For the weak non-linear analysis it is convenient to use the definition of the stream function in the form $\bar{u} = \partial\psi/\partial\bar{z}$; $\bar{w} = -\partial\psi/\partial\bar{x}$, and present Eqns.(3.5-3.6) and Eqns.(3.15-3.16) in terms of the stream function, temperature and solid fraction, following resolution of the coupling between the components of Eqn.(3.15), as follows,

$$\delta\left(\chi_1\frac{\partial}{\partial t'} - \frac{\partial}{\partial\bar{z}}\right)\left[\theta - \frac{\overline{S}}{\delta}\varphi\right] + R\frac{\partial\psi}{\partial\bar{z}}\frac{\partial\theta}{\partial\bar{x}} - R\frac{\partial\psi}{\partial\bar{x}}\frac{\partial\theta}{\partial\bar{z}} = \nabla^2\theta \tag{4.1}$$

$$\delta\left(\chi_1\frac{\partial}{\partial t'} - \frac{\partial}{\partial\bar{z}}\right)\left[(1-\varphi)\theta + \frac{c_S}{\delta}\varphi\right] + R\frac{\partial\psi}{\partial\bar{z}}\frac{\partial\theta}{\partial\bar{x}} - R\frac{\partial\psi}{\partial\bar{x}}\frac{\partial\theta}{\partial\bar{z}} = 0 \tag{4.2}$$

$$\left[\frac{\partial}{\partial t'} + \Pi(\varphi)\right]^2\nabla^2\psi + \left[\frac{\partial}{\partial t'} + \Pi(\varphi)\right]\left(\frac{\partial\psi}{\partial\bar{z}}\frac{\partial\Pi}{\partial\bar{z}} - R\frac{\partial\theta}{\partial\bar{x}}\right) + Ta\frac{\partial^2\psi}{\partial\bar{z}^2} + Ta^{1/2}\bar{v}\frac{\partial\Pi}{\partial\bar{z}} = 0, \tag{4.3}$$

where $t' = \chi_1\bar{t}$. Refer to *Appendix Y* for a detailed derivation of the stream function representation illustrated in Eqns.(4.1-4.3). Note that the definition of the Laplacian operator is given as $\nabla^2 = \partial^2/\partial\bar{x}^2 + \partial^2/\partial\bar{z}^2$. The point of the weak non-linear analysis is to provide quantitative results regarding the amplitude of convection and the heat flux for both the stationary and overstable cases. The existence of the codimension-2 point (CTP) which exists at the point of intersection of the stationary and overstable solutions is expected but not investigated in the current analysis. To investigate the solution in the vicinity of the codimension-2 point requires a further expansion, over and above the one that we use here. This expansion would then yield a differential equation for the amplitude which is second order in time.

4.1 Expansions around Stationary Solutions

The system (4.1-4.3) presented above contains a small parameter δ, which represents the mushy layer thickness. It was pointed out at the linear stability level that in the current study we are only interested in solutions to order $O(\delta^0)$. The system (4.1-4.3) may be presented to order $O(\delta^0)$ as follows,

$$-\overline{S}\left(\chi_1\frac{\partial}{\partial t'} - \frac{\partial}{\partial \overline{z}}\right)\varphi + R\frac{\partial \psi}{\partial \overline{z}}\frac{\partial \theta}{\partial \overline{x}} - R\frac{\partial \psi}{\partial \overline{x}}\frac{\partial \theta}{\partial \overline{z}} = \nabla^2\theta \tag{4.4}$$

$$c_s\left(\chi_1\frac{\partial}{\partial t'} - \frac{\partial}{\partial \overline{z}}\right)\varphi + R\frac{\partial \psi}{\partial \overline{z}}\frac{\partial \theta}{\partial \overline{x}} - R\frac{\partial \psi}{\partial \overline{x}}\frac{\partial \theta}{\partial \overline{z}} = 0 \tag{4.5}$$

$$\left[\frac{\partial}{\partial t'} + \Pi(\varphi)\right]^3\nabla^2\psi + \left[\frac{\partial}{\partial t'} + \Pi(\varphi)\right]^2\left(\frac{\partial \psi}{\partial \overline{z}}\frac{\partial \Pi}{\partial \overline{z}} - R\frac{\partial \theta}{\partial \overline{x}}\right) + Ta\left[\frac{\partial}{\partial t'} + \Pi(\varphi)\right]\frac{\partial^2\psi}{\partial \overline{z}^2} - Ta\frac{\partial \psi}{\partial \overline{z}}\frac{\partial \Pi}{\partial \overline{z}} = 0 \tag{4.6}$$

The stream function, temperature and solid fraction may be expanded in terms of a small parameter ε, which is defined as,

$$\varepsilon = \left[\frac{R}{R_{cr}} - 1\right]^{1/2}, \tag{4.7}$$

following Newell & Whitehead (1969) and Segel (1969), in the form,

$$[\psi,\theta,\varphi] = [\psi_B,\theta_B,\varphi_B] + \varepsilon[\psi_1,\theta_1,\varphi_1] + \varepsilon^2[\psi_2,\theta_2,\varphi_2] + \varepsilon^3[\psi_3,\theta_3,\varphi_3] + O(\varepsilon^4), \tag{4.8}$$

where the basic motionless solution to order $O(\delta^0)$ is given as,

$$\theta_B = \overline{z} - 1, \qquad \varphi_B = 0, \qquad \psi_B = 0. \tag{4.9}$$

By using the definition for ε given in Eqn.(4.7), the Rayleigh number may be expanded as $R = R_{cr}(1+\varepsilon^2)$. The permeability function, referred to in the system (4.4-4.6) was defined at the linear stability level to order $O(\delta^0)$ as,

$$\Pi(\varepsilon\hat{\varphi}) = 1 + \varepsilon^2 K_c \varphi_1^2 + O(\varepsilon^3),$$
(4.10)

where φ_1 represents the solid fraction solution to order $O(\varepsilon)$. In addition we allow time variations only at the slow time scale $\tau = \varepsilon^2 t'$ in order to prevent exponential growth and reaching finite values for the amplitude at the steady state. Slow space scales are also introduced, in the form $X = \varepsilon\overline{x}$, following Newell & Whitehead (1969) and Segel (1969), in order to include a continuous finite band of horizontal modes. Substituting the expansions (4.7), (4.8) and (4.10) as well as the slow time and space scales just defined into the system (4.4-4.6) and equating like powers of ε produces a hierarchy of linear partial differential equations to each order. Refer to *Appendix Z* for the derivation of the system of equations to the different orders in ε.

At the leading order the $O(\varepsilon)$ equations are very similar to the equations solved at the linear stability level, ie

$$\overline{S}\frac{\partial\varphi_1}{\partial\overline{z}} - R_{cr}\frac{\partial\psi_1}{\partial\overline{x}} - \nabla^2\theta_1 = 0$$
(4.11)

$$-c_s\frac{\partial\varphi_1}{\partial\overline{z}} - R_{cr}\frac{\partial\psi_1}{\partial\overline{x}} = 0$$
(4.12)

$$\nabla^2\psi_1 - R_{cr}\frac{\partial\theta_1}{\partial\overline{x}} + Ta\frac{\partial^2\psi_1}{\partial\overline{z}^2} = 0.$$
(4.13)

The solution at this order is given by the eigenvalues of the stationary convection which are of the form,

$$\psi_1 = \left[A_1 e^{is\overline{x}} + A_1^* e^{-is\overline{x}} \right] \sin(\pi \overline{z}) \tag{4.14}$$

$$\theta_1 = \left[B_1 e^{is\overline{x}} + B_1^* e^{-is\overline{x}} \right] \sin(\pi \overline{z}) \tag{4.15}$$

$$\varphi_1 = \left[C_1 e^{is\overline{x}} + C_1^* e^{-is\overline{x}} \right] \left[1 + \cos(\pi \overline{z}) \right], \tag{4.16}$$

where $(.)^*$ stands for identifying complex conjugate terms and the amplitudes $A_1(\tau, X)$, $A_1^*(\tau, X)$, $B_1(\tau, X)$, $B_1^*(\tau, X)$, $C_1(\tau, X)$ and $C_1^*(\tau, X)$ are allowed to vary over the slow time and space scales. The relationship between the amplitudes is obtained by substituting Eqns.(4.14-4.16) in the system (4.11-4.13) and is found to be,

$$B_1 = i \frac{\Omega R_{cr} \alpha^{1/2}}{\pi (1+\alpha)} A_1, \qquad B_1^* = -i \frac{\Omega R_{cr} \alpha^{1/2}}{\pi (1+\alpha)} A_1^*, \tag{4.17}$$

and,

$$C_1 = i \frac{R_{cr} \alpha^{1/2}}{c_S} A_1, \qquad C_1^* = -i \frac{R_{cr} \alpha^{1/2}}{c_S} A_1^*. \tag{4.18}$$

The solution to Eqns.(4.11-4.13) and the relationships between the coefficients presented in Eqns.(4.17-4.18) are derived in *Appendix AA*. The amplitudes A_1 and A_1^* remain undetermined at this stage, and will be determined from a solvability condition of the order $O(\varepsilon^3)$ equations at order ε^3.

At order ε^2 the $O(\varepsilon^2)$ equations are presented in the form,

$$\overline{S} \frac{\partial \varphi_2}{\partial \overline{z}} - R_{cr} \frac{\partial \psi_2}{\partial \overline{x}} - \nabla^2 \theta_2 = R_{cr} \frac{\partial \psi_1}{\partial X} + 2 \frac{\partial^2 \theta_1}{\partial \overline{x} \partial \overline{z}} - R_{cr} \left[\frac{\partial \psi_1}{\partial \overline{z}} \frac{\partial \theta_1}{\partial \overline{x}} - \frac{\partial \psi_1}{\partial \overline{x}} \frac{\partial \theta_1}{\partial \overline{z}} \right] \tag{4.19}$$

$$c_S \frac{\partial \varphi_2}{\partial \overline{z}} + R_{cr} \frac{\partial \psi_2}{\partial \overline{x}} = -R_{cr} \frac{\partial \psi_1}{\partial X} + R_{cr} \left[\frac{\partial \psi_1}{\partial \overline{z}} \frac{\partial \theta_1}{\partial \overline{x}} - \frac{\partial \psi_1}{\partial \overline{x}} \frac{\partial \theta_1}{\partial \overline{z}} \right] \tag{4.20}$$

103

$$\nabla^2 \psi_2 - R_{cr} \frac{\partial \theta_2}{\partial \overline{x}} + Ta \frac{\partial^2 \psi_2}{\partial \overline{z}^2} = R_{cr} \frac{\partial \theta_1}{\partial X} - 2 \frac{\partial^2 \psi_1}{\partial \overline{x} \partial X}, \tag{4.21}$$

where the right hand side of Eqns.(4.19-4.21) represents the non-homogenous part consisting of terms that include known solutions evaluated at the leading order ε. These non-homogenous terms forces a particular solution in addition to the solution of the homogenous operator. De-coupling the equations and working out the particular solutions yields the following complete solution to this order,

$$\psi_2 = \left[A_2 e^{is\overline{x}} + A_2^* e^{-is\overline{x}} \right] \sin(\pi \overline{z}) \tag{4.22}$$

$$\theta_2 = \left[B_2 e^{is\overline{x}} + B_2^* e^{-is\overline{x}} \right] \sin(\pi \overline{z}) + \frac{\alpha \Omega^2 R_{cr}^2}{2\pi (\alpha + 1)} A_1 A_1^* \sin(2\pi \overline{z}) \tag{4.23}$$

$$\varphi_2 = \left[C_2 e^{is\overline{x}} + C_2^* e^{-is\overline{x}} \right]\left[1 + \cos(\pi \overline{z}) \right] + \frac{\alpha \Omega R_{cr}^2}{c_s (\alpha + 1)} A_1 A_1^* \left[\cos(2\pi \overline{z}) - 1 \right] +$$

$$\frac{R_{cr}}{\pi c_s} \left[\frac{\partial A_1}{\partial X} e^{is\overline{x}} + \frac{\partial A_1^*}{\partial X} e^{-is\overline{x}} \right] \left(1 + \cos(\pi \overline{z}) \right), \tag{4.24}$$

where the relationship between the amplitudes B_2 and A_2 and C_2 and A_2 is identical to that presented in Eqns.(4.17) and (4.18). A complete derivation of the solutions given in (4.22-4.24) is presented in *Appendix AB*.

The equations at order $O(\varepsilon^3)$ are presented in the form

$$\overline{S} \frac{\partial \varphi_3}{\partial \overline{z}} - R_{cr} \frac{\partial \psi_3}{\partial \overline{x}} - \nabla^2 \theta_3 = \overline{S} \frac{\partial \varphi_1}{\partial \tau} + R_{cr} \frac{\partial \psi_1}{\partial \overline{x}} + R_{cr} \frac{\partial \psi_2}{\partial X} + 2 \frac{\partial^2 \theta_2}{\partial \overline{x} \partial \overline{z}} -$$

$$R_{cr}\left[\left\{\frac{\partial\psi_1}{\partial\overline{z}}\frac{\partial\theta_2}{\partial\overline{x}} - \frac{\partial\psi_1}{\partial\overline{x}}\frac{\partial\theta_2}{\partial\overline{z}}\right\} + \left\{\frac{\partial\psi_2}{\partial\overline{z}}\frac{\partial\theta_1}{\partial\overline{x}} - \frac{\partial\psi_2}{\partial\overline{x}}\frac{\partial\theta_1}{\partial\overline{z}}\right\} + \left\{\frac{\partial\psi_1}{\partial\overline{z}}\frac{\partial\theta_1}{\partial X} - \frac{\partial\psi_1}{\partial X}\frac{\partial\theta_1}{\partial\overline{z}}\right\} + \frac{\partial^2\theta_1}{\partial X^2}\right]$$

$$(4.25)$$

$$-c_S\frac{\partial\varphi_3}{\partial\overline{z}} - R_{cr}\frac{\partial\psi_3}{\partial\overline{x}} = -c_S\frac{\partial\varphi_1}{\partial\tau} + R_{cr}\frac{\partial\psi_1}{\partial\overline{x}} + R_{cr}\frac{\partial\psi_2}{\partial X} -$$

$$R_{cr}\left[\left\{\frac{\partial\psi_1}{\partial\overline{z}}\frac{\partial\theta_2}{\partial\overline{x}} - \frac{\partial\psi_1}{\partial\overline{x}}\frac{\partial\theta_2}{\partial\overline{z}}\right\} + \left\{\frac{\partial\psi_2}{\partial\overline{z}}\frac{\partial\theta_1}{\partial\overline{x}} - \frac{\partial\psi_2}{\partial\overline{x}}\frac{\partial\theta_1}{\partial\overline{z}}\right\} + \left\{\frac{\partial\psi_1}{\partial\overline{z}}\frac{\partial\theta_1}{\partial X} - \frac{\partial\psi_1}{\partial X}\frac{\partial\theta_1}{\partial\overline{z}}\right\}\right] \qquad (4.26)$$

$$\nabla^2\psi_3 - R_{cr}\frac{\partial\theta_3}{\partial\overline{x}} + Ta\frac{\partial^2\psi_3}{\partial\overline{z}^2} = -2K_c\varphi_1^2\nabla^2\psi_1 - 2\frac{\partial}{\partial\tau}\nabla^2\psi_1 - 2\frac{\partial^2\psi_2}{\partial\overline{x}\partial X} + K_cTa\frac{\partial\varphi_1^2}{\partial\overline{z}}\frac{\partial^2\psi_1}{\partial\overline{z}} -$$

$$K_c\frac{\partial\varphi_1^2}{\partial\overline{z}}\frac{\partial\psi_1}{\partial\overline{z}} + R_{cr}\frac{\partial\theta_1}{\partial\overline{x}} + K_c\varphi_1^2R_{cr}\frac{\partial\theta_1}{\partial\overline{x}} + R_{cr}\frac{\partial}{\partial\overline{x}}\frac{\partial\theta_1}{\partial\tau} + R_{cr}\frac{\partial\theta_2}{\partial X} - \frac{\partial^2\psi_1}{\partial X^2}.$$

$$(4.27)$$

The right hand side of Eqns.(4.25-4.27) consists of known solutions evaluated at orders ε and ε^2 and the differential operator of the system (4.25-4.27) is identical to the operator of the equations at order ε. Since equations (4.25-4.27) at order ε^3 are non-homogenous versions of the equations at order ε, a solvability condition for the for the equations at order ε^3 must be satisfied. This constrains the amplitude of the solution at order ε and enables its determination. The solvability condition is obtained by decoupling Eqns.(4.25-4.27) to yield a single partial differential equation for ψ_3 with a corresponding forcing function which is represented in the following form,

$$\nabla^2(\nabla^2\psi_3) + \Omega R_{cr}^2\frac{\partial^2\psi_3}{\partial\overline{x}^2} + Ta\frac{\partial^2}{\partial\overline{z}^2}\nabla^2\psi_3 = \nabla^2RHS(4.27) +$$

$$R_{cr}\frac{\partial}{\partial\overline{x}}\left\{\Omega R_{cr}\left[\left\{\frac{\partial\psi_1}{\partial\overline{z}}\frac{\partial\theta_2}{\partial\overline{x}} - \frac{\partial\psi_1}{\partial\overline{x}}\frac{\partial\theta_2}{\partial\overline{z}}\right\} + \left\{\frac{\partial\psi_2}{\partial\overline{z}}\frac{\partial\theta_1}{\partial\overline{x}} - \frac{\partial\psi_2}{\partial\overline{x}}\frac{\partial\theta_1}{\partial\overline{z}}\right\} + \left\{\frac{\partial\psi_1}{\partial\overline{z}}\frac{\partial\theta_1}{\partial X} - \frac{\partial\psi_1}{\partial X}\frac{\partial\theta_1}{\partial\overline{z}}\right\}\right]\right\} -$$

105

$$\Omega R_{cr} \frac{\partial \psi_1}{\partial \bar{x}} - \Omega R_{cr} \frac{\partial \psi_2}{\partial X} - 2 \frac{\partial^2 \theta_2}{\partial \bar{x} \partial X} - \frac{\partial^2 \theta_1}{\partial X^2} \Bigg\} , \qquad (4.28)$$

where $\nabla^2 RHS(4.27)$ refers to the Laplacian operator $\nabla^2 = \partial^2/\partial \bar{x}^2 + \partial^2/\partial \bar{z}^2$ being applied to the forcing function on the right hand side of Eqn.(4.27). By multiplying Eqn.(4.28) by complex conjugate ($\overline{\psi}_1$) of the stream function, which has the form,

$$\overline{\psi}_1 = A_1^* e^{-is\bar{x}} \sin(\pi \bar{z}) , \qquad (4.29)$$

integrating over, $\bar{x} \in [0, L]$ and $\bar{z} \in [0,1]$, and noting that $\psi_3(\bar{x},0) = \psi_3(\bar{x},1) = 0$, $\psi_3(0,\bar{z}) = \psi_3(L,\bar{z}) = 0$ at the boundaries, yields the following differential equation for the complex $O(\varepsilon)$ amplitude,

$$\eta_0 \frac{\partial A}{\partial \bar{t}} + \eta_1 \frac{\partial^2 A}{\partial \bar{x}^2} = \left[\xi_{st}^0 - AA^* \right] A . \qquad (4.30)$$

The process of decoupling the equation at $O(\varepsilon^3)$ as well as the derivation of the amplitude equation (4.30) is outlined in *Appendix AC*. Note in Eqn.(4.30) that $A = \varepsilon A_1$ and $A^* = \varepsilon A_1^*$ whilst the original time and space scales defined as $\bar{t} = t'/\chi_1$ and $X = \varepsilon \bar{x}$ are re-introduced as illustrated in Eqn.(4.30). The following notation was introduced,

$$\eta_0 = \frac{2\left[Ta - (\alpha + 1) \right]}{\pi^4 \Omega \gamma (\alpha + 1 + Ta) \left[\dfrac{K_c}{2\Omega^2 c_S^2} (\alpha + 1)\left\{ 7Ta - (5\alpha + 7) \right\} - (\alpha + 1 + Ta) \right]} \qquad (4.31)$$

$$\eta_1 = \frac{2\left[Ta + 2(\alpha + 1) \right]}{\pi^4 \Omega (\alpha + 1)(\alpha + 1 + Ta) \left[\dfrac{K_c}{2\Omega^2 c_S^2} (\alpha + 1)\left\{ 7Ta - (5\alpha + 7) \right\} - (\alpha + 1 + Ta) \right]} \qquad (4.32)$$

$$\xi_{st}^0 = \cfrac{4}{\pi^2\Omega\left[\cfrac{K_e}{2\Omega^2 c_S^2}(\alpha+1)\{5\alpha+7-7Ta\}+(\alpha+1+Ta)\right]}\left[\cfrac{R}{R_{cr,st}}-1\right].$$ (4.33)

The coefficients referred to in Eqns.(4.31-4.33) are derived in detail in *Appendix AC*. It can be noted from amplitude differential equation, Eqn.(4.30) , that the presence of space scales results in the appearance of the diffusion term. With the imposition of the symmetry conditions at the axis of rotation ($\overline{x} = 0$) leads to the amplitude relation, $A_1 = -A_1^*$, thereby resulting in the $O(\epsilon)$ taking the form,

$$\psi_1 = F_1 \sin(s\overline{x})\sin(\pi\overline{z}) ,$$ (4.34)

where $F_1 = i2A_1$. This result satisfies the equations and all boundary conditions. A phase angle is not involved, and a solution without slow space scales is possible. The diffusion term is then negated from Eqn.(4.30), which then transforms to an ordinary differential equation for the real amplitude D_1,

$$\eta_2 \frac{\partial F}{\partial \overline{t}} = \left[\xi_{st} - F^2\right]F ,$$ (4.35)

where $F = \epsilon F_1$, $\xi_{st} = 4\xi_{st}^0$, and $\eta_2 = 4\eta_0$. Equation (4.35) yields the following solutions at steady state,

$$F = \begin{cases} 0 & \forall\ R < R_{cr,st} \\ \\ \pm\xi_{st}^{1/2} & \forall\ R \geq R_{cr,st} \end{cases}$$ (4.36)

The steady amplitude solution, Eqn.(4.36) shows that a pitchfork bifurcation occurs at the critical value of the Rayleigh number associated with stationary convection. The current study will focus only on the case when the relaxation time η_2 is positive. The results for

the case when the relaxation time is negative will be presented nonetheless. Figures 34a-34d shows the amplitude trend for varying Taylor number and χ_1 values for different values of the parameter $\varsigma = K_c / (\Omega c_S)^2$. If we set $K_c = c_S$, and $\overline{S} = c_S$ so that $\Omega = 2$ then we may present the parameter ς as $\varsigma = 1/(4c_S)$. It is very interesting to note that the parameter λ defined in Section 2 may be expressed for the above parameter settings as,

$\lambda = \overline{S}/(\Omega c_S)^2 = 1/(4c_S) = \varsigma$. This is deemed to be an important result as it connects the two different scalings used in Section 2 and Section 3. As pointed out earlier the parameter c_S may assume values ranging from $c_S = 0.125$ (for liquid metals) to $c_S = 4.0$ (for aqueous salts). This implies that ς may assume values ranging from $\varsigma = 0.0625$ to about $\varsigma = 2.0$.

It can be observed from Figure 34a-d that over that increasing the value of the parameter χ_1 serves to damp the relaxation time η_2. It is also very interesting to note that that Ta=3 represents a transition point in the sign of the relaxation time η_2. It can be observed from Figures 34a- 34d that at the lower values of ς (say $\varsigma = 0.1$), the relaxation time assumes a negative sign over a larger range of Taylor numbers before becoming positive again at a Taylor number of approximately Ta $\cong 30$. At a larger value of ς (say $\varsigma = 1$) it can be noted very clearly from Figure 34 that the relaxation time sign is negative over a very small range of Taylor numbers. It was found that to higher Taylor numbers the curves presented in Figure 34 become asymptotical with respect to the x-axis. It is seen that increasing the Taylor number considerably tends to damp out the relaxation time. Figure 35 shows the variation of the parameter ξ_{st}/ε^2 with the Taylor number for different parameter settings for ς.

It can be noted from Figure 35 that a low values of the parameter ς (say $\varsigma = 0.1$), the sign of the linear amplitude coefficient remains positive over a larger range of Taylor numbers. Increasing the value of ς causes the range of Taylor number values over which the linear amplitude is positive, to become smaller. It was found that once the curve for a particular value of ς changes sign, it remains negative for increasing Taylor numbers and

becomes asymptotical with respect to the x-axis. Another feature apparent from Figure 35 is that the Taylor number for which the curves change sign decreases as the value of the parameter ζ is increased.
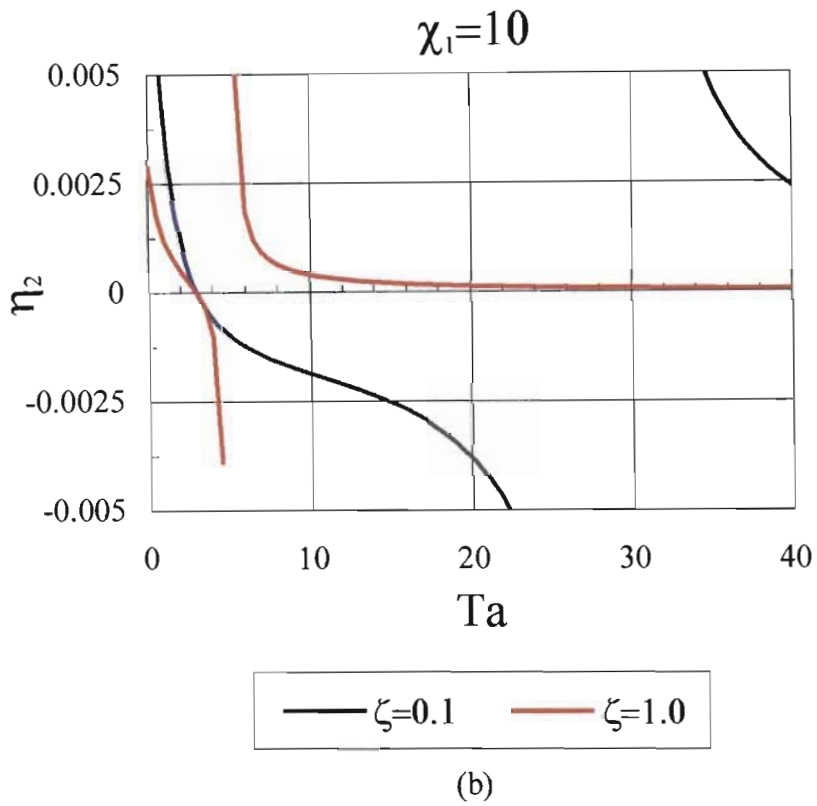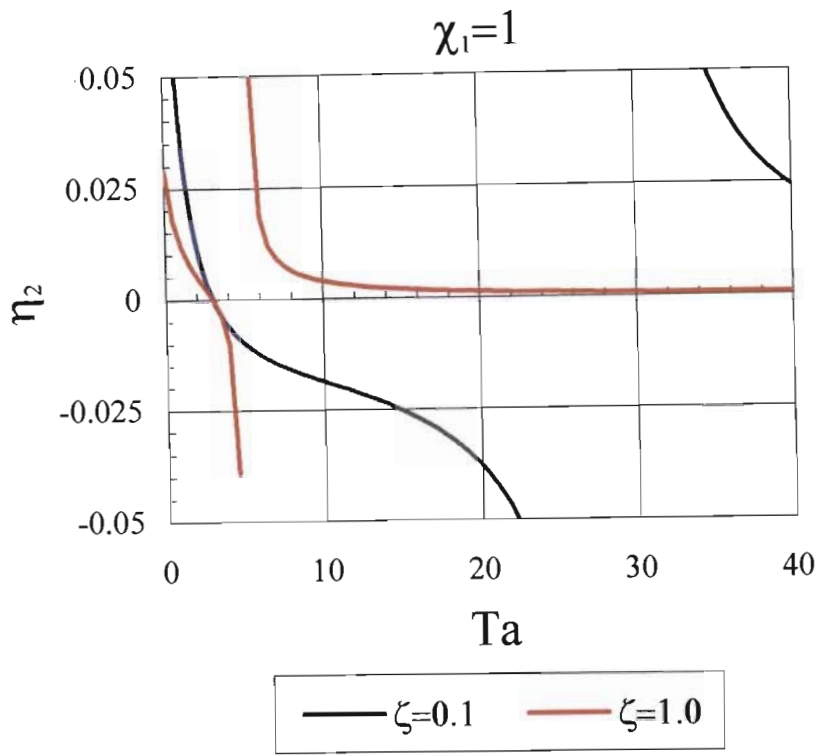
Figure 34 : Relaxation time η_2 versus the Taylor number for various ξ values for different settings in the parameter χ_1 for (a) $\chi_1 = 1$ and (b) $\chi_1 = 10$
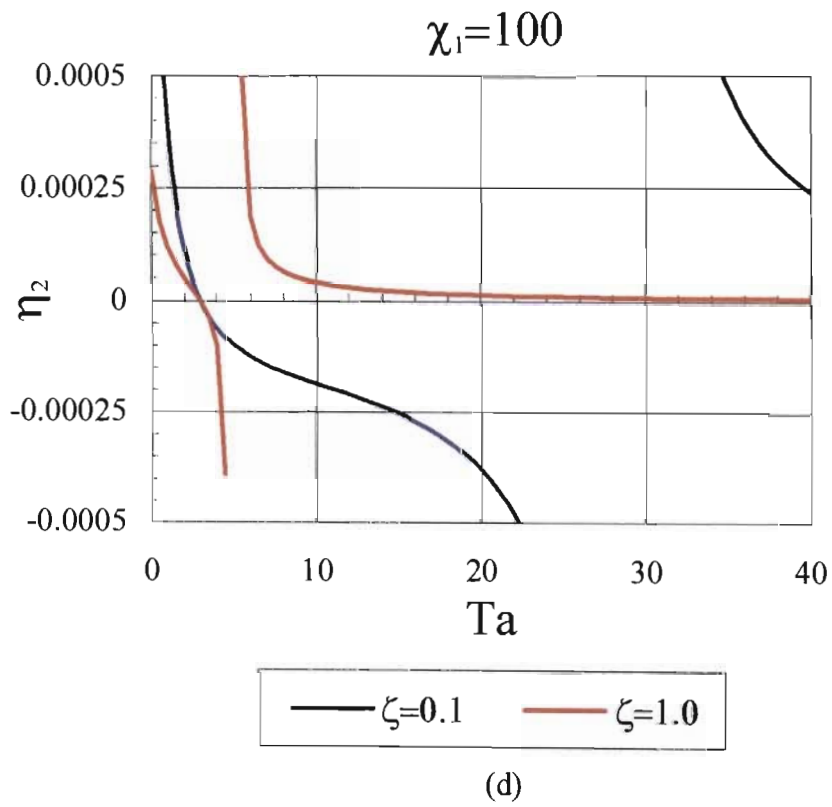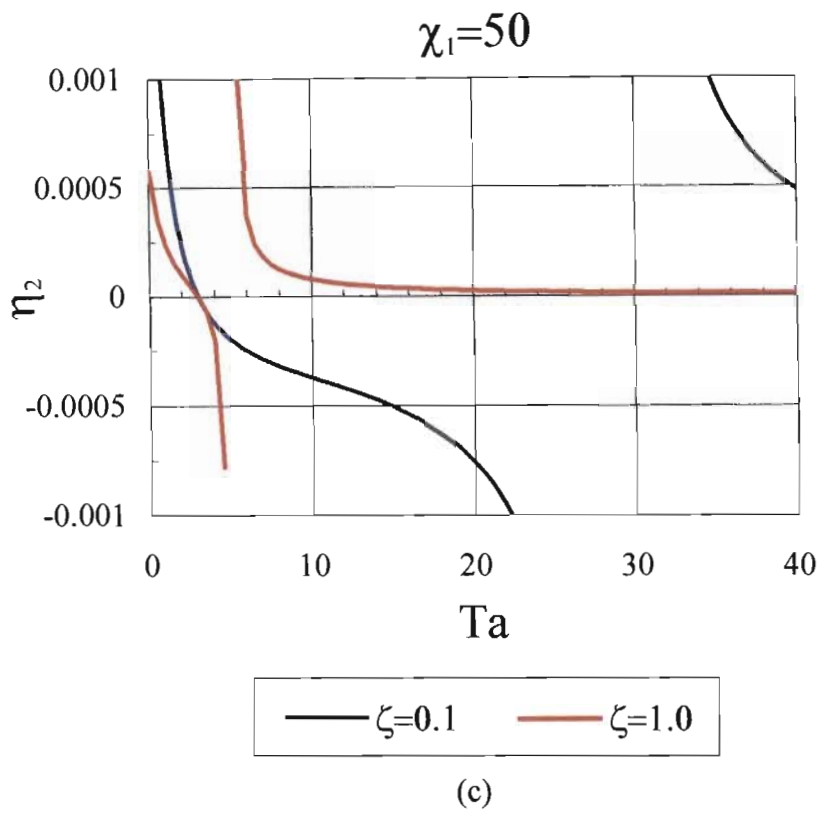
Figure 34 : Relaxation time η_2 versus the Taylor number for various ξ values for different settings in the parameter χ_1 for (c) $\chi_1 = 50$ and (d) $\chi_1 = 100$
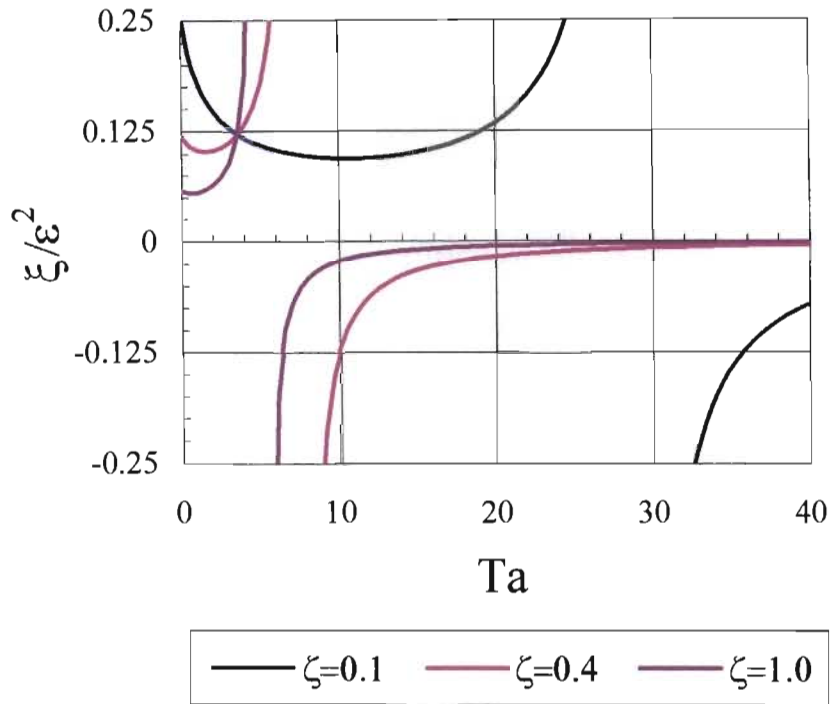
Figure 35 : Variation of the linear amplitude coefficient ξ_{st} with Taylor number for different values of the parameter ζ.

4.2 Expansions around Overstable Solutions

Eqns.(4.4-4.6) are still applicable for the weak non-linear analysis of the overstable convection in the mushy layer. Expansion (4.8) is still valid with the only difference being that we refer to the corresponding critical values consistent with overstable convection. Note that permeability definition as stated in Eqn.(4.10) is applicable for the case of overstable convection. In addition we also introduce the slow time scales $\tau = \varepsilon^2 t'$ and $\tau_0 = \varepsilon t'$, but allow the short time scale t' to be present in order to represent the amplitude fluctuations. We further rescale the short time scale in the form $\tilde{t} = \sigma_0 t'$ where the notation $\sigma_0 = \sigma_{i,cr}$ was used. Substituting these into the Eqns.(4.4-4.6) yield at the leading order the following system of equations,

$$\overline{S}\left(\chi_1\sigma_0\frac{\partial}{\partial\tilde{t}} - \frac{\partial}{\partial\overline{z}}\right)\varphi_1 + R_{cr}\frac{\partial\psi_1}{\partial\overline{x}} + \nabla^2\theta_1 = 0 \tag{4.37}$$

$$c_s\left(\chi_1\sigma_0\frac{\partial}{\partial\tilde{t}} - \frac{\partial}{\partial\overline{z}}\right)\varphi_1 - R_{cr}\frac{\partial\psi_1}{\partial\overline{x}} = 0 \tag{4.38}$$

$$\left(\sigma_0\frac{\partial}{\partial\tilde{t}} + 1\right)^2\nabla^2\psi_1 - R_{cr}\left(\sigma_0\frac{\partial}{\partial\tilde{t}} + 1\right)\frac{\partial\theta_1}{\partial\overline{x}} + Ta\frac{\partial^2\psi_1}{\partial\overline{z}^2} = 0. \tag{4.39}$$

Refer to *Appendix AD* for a detailed derivation of the system (4.37-4.39) and the governing systems to the different orders in ε. The general solution for the stream function ψ_1 may be presented as,

$$\psi_1 = \left[A_1e^{i(s\overline{x}+\tilde{t})} + B_1e^{i(s\overline{x}-\tilde{t})} + A_1^*e^{-i(s\overline{x}+\tilde{t})} + B_1^*e^{-i(s\overline{x}-\tilde{t})}\right]\sin(\pi\overline{z}), \tag{4.40}$$

where the amplitudes $A_1(\tau_0,\tau,X)$ and $B_1(\tau_0,\tau,X)$ describe the modulations of the waves on the slow time ($\tau_0 = \varepsilon t'$, $\tau = \varepsilon^2 t'$) and space ($X = \varepsilon\overline{x}$) scales for a Hopf bifurcation. The concept of Hopf Bifurcation phenomena is well documented in Iooss & Joseph (1980) and Drazin & Reid (1981). The special cases of a pure left travelling wave

($B_1 = 0$) or a pure right travelling wave ($A_1 = 0$) and of standing waves ($A_1 = \pm B_1$ or $A_1 = \pm B_1^*$) can be recovered from Eqn.(4.40). By imposing the symmetry boundary conditions at the axis of rotation, $\psi_1 = 0$ at, yields upon substitution in Eqn.(4.40) the following relations between the amplitudes,

$$B_1^* = -A_1 \qquad \text{and} \qquad B_1 = -A_1^*. \tag{4.41}$$

This result shows very clearly that the boundary condition at the axis of rotation results in a special case of standing waves thus eliminating travelling waves. The implications are that we may eliminate slow space scales from the system of governing equations using an argument similar to that presented in the case of stationary convection. Furthermore the absence of the slow space scales negates the diffusion term in the amplitude equation. Using the amplitude relations given in Eqn.(4.41) the solution for the stream function, temperature and solid fraction at the leading order may be expressed as,

$$\psi_1 = 2i\left[A_1 e^{i\tilde{t}} + A_1^* e^{-i\tilde{t}}\right]\sin(s\overline{x})\sin(\pi\overline{z}) \tag{4.42}$$

$$\theta_1 = 2\left[C_1 e^{i\tilde{t}} + C_1^* e^{-i\tilde{t}}\right]\cos(s\overline{x})\sin(\pi\overline{z}) \tag{4.43}$$

$$\varphi_1 = \left[D_1\left\{e^{i\pi^2\gamma\sigma_0(\overline{z}-1)} + i\pi\gamma\sigma_0\sin(\pi\overline{z}) + \cos(\pi\overline{z})\right\}e^{i\tilde{t}} + \right.$$

$$\left. D_1^*\left\{e^{-i\pi^2\gamma\sigma_0(\overline{z}-1)} - i\pi\gamma\sigma_0\sin(\pi\overline{z}) + \cos(\pi\overline{z})\right\}e^{-i\tilde{t}}\right]\cos(s\overline{x}). \tag{4.44}$$

The relationships between the coefficients in the system (4.42-4.44) is as follows,

$$C_1 = i\frac{\alpha^{1/2}\Omega R_{cr}}{\pi(1+\alpha)}A_1, \qquad C_1^* = i\frac{\alpha^{1/2}\Omega R_{cr}}{\pi(1+\alpha)}A_1^* \tag{4.45}$$

and,

$$D_1 = i\frac{2\alpha^{1/2}R_{cr}}{c_S\left(1 - \pi^2\gamma^2\sigma_0^2\right)}A_1, \qquad\qquad D_1^* = i\frac{2\alpha^{1/2}R_{cr}}{c_S\left(1 - \pi^2\gamma^2\sigma_0^2\right)}A_1^*. \qquad (4.46)$$

Refer to *Appendix AE* for a derivation of the solutions in Eqns.(4.42-4.44) and the relationships between the coefficients presented in Eqns.(4.45-4.46).

The system of governing equations to order ε^2,

$$\overline{S}\left(\chi_1\sigma_0\frac{\partial}{\partial\tilde{t}} - \frac{\partial}{\partial\overline{z}}\right)\varphi_2 + R_{cr}\frac{\partial\psi_2}{\partial\overline{x}} + \nabla^2\theta_2 = -\overline{S}\chi_1\frac{\partial\varphi_1}{\partial\tau_0} + R_{cr}\left[\frac{\partial\psi_1}{\partial\overline{z}}\frac{\partial\theta_1}{\partial\overline{x}} - \frac{\partial\psi_1}{\partial\overline{x}}\frac{\partial\psi_1}{\partial\overline{z}}\right] \qquad (4.47)$$

$$c_S\left(\chi_1\sigma_0\frac{\partial}{\partial\tilde{t}} - \frac{\partial}{\partial\overline{z}}\right)\varphi_2 - R_{cr}\frac{\partial\psi_2}{\partial\overline{x}} = -\chi_1 c_S\frac{\partial\varphi_1}{\partial\tau_0} - R_{cr}\left[\frac{\partial\psi_1}{\partial\overline{z}}\frac{\partial\theta_1}{\partial\overline{x}} - \frac{\partial\psi_1}{\partial\overline{x}}\frac{\partial\theta_1}{\partial\overline{z}}\right] \qquad (4.48)$$

$$\left(\sigma_0\frac{\partial}{\partial\tilde{t}} + 1\right)^2\nabla^2\psi_2 - R_{cr}\left(\sigma_0\frac{\partial}{\partial\tilde{t}} + 1\right)\frac{\partial\theta_2}{\partial\overline{x}} + Ta\frac{\partial^2\psi_2}{\partial\overline{z}^2} = -2\frac{\partial}{\partial\tau_0}\left(\sigma_0\frac{\partial}{\partial\tilde{t}} + 1\right)\nabla^2\psi_1 + R_{cr}\frac{\partial}{\partial\tau_0}\frac{\partial\theta_1}{\partial\overline{x}}$$
$$(4.49)$$

Refer to *Appendix AD* for a derivation of the system (4.47-4.49). The solution to the system (4.47-4.49) is obtained by superimposing the homogenous solution and the particular solutions arising from the non-homogenous terms on the right hand side of Eqns.(4.47-4.49), which incidentally are known from the solutions obtained at order ε. The homogenous operator in Eqns.(4.47-4.49) is exactly the same as that for the governing system at order ε, hence the homogenous solution at order ε^2 will resemble the order ε solution somewhat and the stream function and temperature solution may be presented as,

$$\psi_{2,h} = 2i\left[A_2 e^{i\tilde{\tau}} + A_2^* e^{-i\tilde{\tau}}\right]\sin(s\overline{x})\sin(\pi\overline{z}) \qquad (4.50)$$

$$\theta_{2,h} = 2\left[C_2 e^{i\tilde{\tau}} + C_2^* e^{-i\tilde{\tau}}\right]\cos(s\overline{x})\sin(\pi\overline{z}) \qquad (4.51)$$

115

The relationships between the coefficients are exactly the same as those given for A_1 and C_1 are as given in Eqns.(4.45-4.45). When evaluating the right hand side of Eqns.(4.47-4.49) in order to evaluate the particular solutions, it is observed that the these non-homogenous terms will produces particular solutions of the form $\tilde{t}\sin(\tilde{t})\sin(s\bar{x})\sin(\pi\bar{z})$ or $\tilde{t}\cos(\tilde{t})\sin(s\bar{x})\sin(\pi\bar{z})$ which are secular terms in solution, ie. they have a condition of resonance unless $\partial A_1/\partial\tau_0 = 0$. To avoid resonance we obtain particular solutions by setting $\partial A_1/\partial\tau_0 = 0$. The particular solution for the stream function vanishes, ie $\psi_{2,p} = 0$, and the particular solution for the temperature and solid fraction may be given as,

$$\theta_{2,p} = \left[b_2 + b_1 e^{2i\tilde{t}} + b_1^* e^{-2i\tilde{t}}\right]\sin(2\pi\bar{z}) \tag{4.52}$$

where the coefficients b_2, b_1 and b_1^* are related to the amplitude at order ε as follows,

$$b_2 = \frac{\alpha\Omega^2 R_{cr}^2}{\pi(\alpha+1)} A_1 A_1^* \tag{4.53}$$

$$b_1 = \frac{\alpha\Omega^2 R_{cr}^2}{2\pi(\alpha+1)} A_1^2 \tag{4.54}$$

$$b_1^* = \frac{\alpha\Omega^2 R_{cr}^2}{2\pi(\alpha+1)} A_1^{*2}. \tag{4.55}$$

The complete solution at this order is therefore $\psi_2 = \psi_{2,h}$ and $\theta_2 = \theta_{2,h} + \theta_{2,p}$. The complete solution for the solid fraction at this order is given as,

$$\varphi_2 = \left[D_2 \left\{ e^{i\pi^2\gamma\sigma_0(\bar{z}-1)} + i\pi\gamma\sigma_0 \sin(\pi\bar{z}) + \cos(\pi\bar{z}) \right\} e^{i\bar{t}} + \right.$$

$$\left. D_2^* \left\{ e^{-i\pi^2\gamma\sigma_0(\bar{z}-1)} - i\pi\gamma\sigma_0 \sin(\pi\bar{z}) + \cos(\pi\bar{z}) \right\} e^{-i\bar{t}} \right] \cos(s\bar{x}) -$$

$$\left[F_2 \left\{ -e^{2i\pi^2\gamma\sigma_0(\bar{z}-1)} + i\pi\gamma\sigma_0 \sin(2\pi\bar{z}) + \cos(2\pi\bar{z}) \right\} e^{2i\bar{t}} + \right.$$

$$\left. F_2^* \left\{ -e^{-2i\pi^2\gamma\sigma_0(\bar{z}-1)} - i\pi\gamma\sigma_0 \sin(2\pi\bar{z}) + \cos(2\pi\bar{z}) \right\} e^{-2i\bar{t}} \right] \cos(s\bar{x}) +$$

$$G\left[\cos(2\pi\bar{z}) - 1 \right],$$

$$(4.56)$$

where the amplitude relations for D_2 and D_2^* are exactly the same as that presented in Eqn.(4.46). The amplitude relations for F_2, F_2^* and G are given as,

$$F_2 = \frac{\alpha\Omega R_{cr}^2}{(\alpha + 1)(1 - \pi^2\sigma_0^2\gamma^2)} A_1^2 \qquad (4.57)$$

$$F_2^* = \frac{\alpha\Omega R_{cr}^2}{(\alpha + 1)(1 - \pi^2\sigma_0^2\gamma^2)} A_1^{*2} \qquad (4.58)$$

$$G = \frac{2\alpha\Omega R_{cr}^2}{(\alpha + 1)} A_1 A_1^*. \qquad (4.59)$$

Refer to *Appendix AF* for the derivation of the stream function, temperature and solid fraction eigenfunctions and their associated coefficients.

The governing equations to order ε^3 was decoupled to provide a single equation for the stream function in the form,

$$\left(\sigma_0 \frac{\partial}{\partial \tilde{t}} + 1\right)^2 \nabla^4 \psi_3 + \Omega R_{cr}^2 \left(\sigma_0 \frac{\partial}{\partial \tilde{t}} + 1\right) \frac{\partial^2 \psi_3}{\partial \overline{x}^2} + Ta \frac{\partial^2}{\partial \overline{z}^2} \nabla^2 \psi_3 =$$

$$R_{cr}\left(\sigma_0 \frac{\partial}{\partial \tilde{t}} + 1\right) \frac{\partial}{\partial \overline{x}} RHS1 + \nabla^2 RHS2, \qquad (4.60)$$

where RHS1 and RHS2 are the non-homogenous terms defined as,

$$RHS1 = \Omega R_{cr}\left\{\left[\frac{\partial \psi_1}{\partial \overline{z}} \frac{\partial \theta_2}{\partial \overline{x}} - \frac{\partial \psi_1}{\partial \overline{x}} \frac{\partial \psi_2}{\partial \overline{z}}\right] + \left[\frac{\partial \psi_2}{\partial \overline{z}} \frac{\partial \theta_1}{\partial \overline{x}} - \frac{\partial \psi_2}{\partial \overline{x}} \frac{\partial \psi_1}{\partial \overline{z}}\right] - \frac{\partial \psi_1}{\partial \overline{x}}\right\} \qquad (4.61)$$

$$RHS2 = -2\left(\sigma_0 \frac{\partial}{\partial \tilde{t}} + 1\right)\left(K_c \varphi_1^2 + \frac{\partial}{\partial \tau}\right) \nabla^2 \psi_1 - 2 \frac{\partial}{\partial \tau_0}\left(\sigma_0 \frac{\partial}{\partial \tilde{t}} + 1\right) \nabla^2 \psi_2 -$$

$$K_c\left(\sigma_0 \frac{\partial}{\partial \tilde{t}} + 1\right) \frac{\partial \varphi_1^2}{\partial \overline{z}} \frac{\partial \psi_1}{\partial \overline{z}} + R_{cr}\left(\sigma_0 \frac{\partial}{\partial \tilde{t}} + 1\right) \frac{\partial \theta_1}{\partial \overline{z}} - K_c Ta^{1/2} v_1 \frac{\partial \varphi_1^2}{\partial \overline{z}} +$$

$$R_{cr} K_c \varphi_1^2 \frac{\partial \theta_1}{\partial \overline{x}} + R_{cr} \frac{\partial}{\partial \tau} \frac{\partial \theta_1}{\partial \overline{x}} + R_{cr} \frac{\partial}{\partial \tau_0} \frac{\partial \theta_1}{\partial \overline{x}}, \qquad (4.62)$$

where RHS1 and RHS2 stands to identify the right hand side terms which have been evaluated from previously known solutions at orders ε and ε^2. Refer to *Appendix AD* for the derivation of the system of equations to order ε^3 and the decoupled form stream function partial differential equation given by Eqn.(4.60). The algebra associated with the solutions at this order are extremely tedious so solutions to order will not be established at this order. However the right hand side of Eqn.(4.62) contains terms that are secular and thus cause resonance. In order to make the partial differential equation at order ε^3, given by Eqn.(6.60), *solvable* we need to establish a solvability condition. We proceed by multiplying Eqn.(4.60) by the complex conjugate solution of the stream function at order ε,

118

$$\psi_1 = i2A_1^* e^{-i\tilde{t}} \sin(s\overline{x}) \sin(\pi\overline{z}) \tag{4.63}$$

and integrating over the length, $\overline{x} \in [0,L]$ and height, $\overline{z} \in [0,1]$, of the mushy, using the boundary conditions $\psi_3(0,\overline{z}) = \psi_3(L,\overline{z}) = \psi_3(\overline{x},0) = \psi_3(\overline{x},L) = 0$. The resulting expression, after performing the mentioned operation, is representative of the relation that needs to be satisfied in order to render Eqn.(4.60) solvable. The resulting solvability condition may be expressed as,

$$\frac{dA}{d\overline{t}} = h_{21} \left[\xi_{ov} - h_{32} A^* A \right] A . \tag{4.64}$$

Eqn.(4.64) represents an ordinary differential equation for the unknown complex amplitude of the convection at order ε. Refer to *Appendix AG* for a complete derivation of the solvability condition. A scaling of the form $A = \varepsilon A_1$ and $A^* = \varepsilon A_1^*$ has been used on the amplitude in Eqn.(4.64). The original time scale of the form $\overline{t} = \tilde{t}/\chi_1$ has also been reintroduced in Eqn.(4.64) and the following notation has been adopted,

$$\xi_{ov} = \varepsilon^2 = \left[\frac{R}{R_{cr,ov}} - 1 \right], \quad h_{21} = h_{21}^0 + im_{21}, \quad h_{32} = h_{32}^0 + im_{32}, \tag{4.65}$$

while the definition of h_{21}^0, m_{21}, h_{32}^0 and m_{32} is given as

$$h_{21}^0 = \frac{2\pi^2\gamma}{(\alpha+1)^3} \tag{4.66}$$

$$m_{21} = -\frac{2\pi^2\gamma}{\sigma_0(\alpha+1)^3} \tag{4.67}$$

$$h_{32}^0 = \frac{1}{2}\pi^2(\alpha+1)(2+\Omega) - j_1\left[(1+\sigma_0^2)h_{r0} + 2\sigma_0 h_{i0}\right] - j_2\left[(1+\sigma_0^2)h_{r1} + 2\sigma_0 h_{i1}\right], \tag{4.68}$$

$$m_{32} = -j_1\left[\left(1+\sigma_0^2\right)h_{i0} - 2\sigma_0 h_{r0}\right] - j_2\left[\left(1+\sigma_0^2\right)h_{i1} - 2\sigma_0 h_{r1}\right], \tag{4.69}$$

where

$$h_{r0} = -\frac{1}{8}\sigma_0\pi^2(7\alpha+1)\left[\frac{1}{8}\left(11+3\pi^2\gamma^2\sigma_0^2\right) - \frac{22\gamma\sigma_0}{q^0 g^0}\sin(\pi^2\gamma\sigma_0) + \frac{1}{4\pi^2\gamma\sigma_0 q^0}\sin(2\pi^2\gamma\sigma_0)\right] -$$

$$\frac{1}{8}\pi^2(7\alpha+1)\left[\frac{6\gamma\sigma_0 p^0}{q^0 g^0} - \frac{f^0}{4\pi^2\gamma\sigma_0 q^0}\sin(\pi^2\gamma\sigma_0) + \frac{1}{4\pi^2\gamma\sigma_0 q^0}\sin(2\pi^2\gamma\sigma_0)\right] \tag{4.69a}$$

$$h_{i0} = -\frac{1}{8}\sigma_0\pi^2(7\alpha+1)\left[\frac{6\gamma\sigma_0 p^0}{q^0 g^0} - \frac{f^0}{4\pi^2\gamma\sigma_0 q^0}\sin(\pi^2\gamma\sigma_0) + \frac{1}{4\pi^2\gamma\sigma_0 q^0}\sin(2\pi^2\gamma\sigma_0)\right] +$$

$$\frac{1}{8}\pi^2(7\alpha+1)\left[\frac{1}{8}\left(11+3\pi^2\gamma^2\sigma_0^2\right) - \frac{22\gamma\sigma_0}{q^0 g^0}\sin(\pi^2\gamma\sigma_0) + \frac{1}{4\pi^2\gamma\sigma_0 q^0}\sin(2\pi^2\gamma\sigma_0)\right] \tag{4.69b}$$

$$h_{r1} = \frac{1}{8}\pi^3(7\alpha+1)\left(1-\sigma_0^2 - Ta\right)\left[-\frac{4\gamma\sigma_0\left(5+\pi^2\gamma^2\sigma_0^2\right)}{\pi^2 q^0 g^0}\sin(\pi^2\gamma\sigma_0) - \frac{4\gamma\sigma_0}{g^0}\sin(\pi^2\gamma\sigma_0) +\right.$$

$$\frac{1}{4}\left(3-\pi^2\gamma^2\sigma_0^2\right) - \frac{\gamma\sigma_0}{2q^0}\sin(2\pi^2\gamma\sigma_0 0\right] + \frac{\pi^3\gamma\sigma_0}{2}\left(1-\sigma_0^2 - Ta\right)p^0\sin(\pi^2\gamma\sigma_0) -$$

$$\frac{\sigma_0\pi^3}{4}(7\alpha+1)\left[-\frac{4\gamma\sigma_0\left(5+\pi^2\gamma^2\sigma_0^2\right)}{q^0 g^0}p^0 + \frac{4\gamma\sigma_0}{g^0}p^0 + \frac{\gamma\sigma_0}{2q^0}f^0\right] -$$

$$\pi^3\gamma\sigma_0^2 p^0\cos(\pi^2\gamma\sigma_0), \tag{4.69c}$$

$$h_{i1} = \frac{\pi^3}{8}\left(1 - \sigma_0^2 - Ta\right)(7\alpha + 1)\left[-\frac{4\gamma\sigma_0\left(5 + \pi^2\gamma^2\sigma_0^2\right)}{q^0 g^0}p^0 + \frac{4\gamma\sigma_0}{g^0}p^0 + \frac{\gamma\sigma_0}{2q^0}f^0\right] -$$

$$\frac{\pi^3\gamma\sigma_0}{2}p^0\left(1 - \sigma_0^2 - Ta\right)\cos(\pi^2\gamma\sigma_0) +$$

$$\frac{1}{4}\pi^3(7\alpha + 1)\sigma_0\left[-\frac{4\gamma\sigma_0\left(5 + \pi^2\gamma^2\sigma_0^2\right)}{\pi^2 q^0 g^0}\sin(\pi^2\gamma\sigma_0) - \frac{4\gamma\sigma_0}{g^0}\sin(\pi^2\gamma\sigma_0) +\right.$$

$$\left.\frac{1}{4}\left(3 - \pi^2\gamma^2\sigma_0^2\right) - \frac{\gamma\sigma_0}{2q^0}\sin(2\pi^2\gamma\sigma_0 0\right] + \pi^3\gamma\sigma_0^2 p^0 \sin(\pi^2\gamma\sigma_0). \qquad (4.69d)$$

Note that in Eqns.4.68 and Eqns.4.69(a-d) the parameters j_1 and j_2 is defined as,

$$j_1 = \frac{16(\alpha + 1)\varsigma\Omega\sigma_0}{(\sigma_0^2 + 1)^2(1 - \pi^2\gamma^2\sigma_0^2)^2}, \qquad j_2 = \frac{8\varsigma\Omega}{\pi(\sigma_0^2 + 1)^2(1 - \pi^2\gamma^2\sigma_0^2)}. \qquad (4.70)$$

In addition p^0, s^0, q^0 and g^0 are defined as,

$$p^0 = 1 + \cos(\pi^2\gamma\sigma_0), \qquad g^0 = \left(9 - \pi^2\gamma^2\sigma_0^2\right)$$

$$q^0 = \left(1 - \pi^2\gamma^2\sigma_0^2\right), \qquad f^0 = 1 - \cos(2\pi^2\gamma\sigma_0). \qquad (4.71)$$

Refer to *Appendix AG* for a derivation of the coefficients in Eqns.(4.66-4.69).

It is convenient to represent Eqn.(4.64) for the complex amplitude as a system of two equations for the absolute value of the amplitude ($r = |A|$) and its phase angle (Φ) in the form

$$A = re^{i\Phi}; \qquad A^* = re^{-i\Phi} \qquad (4.72)$$

with $AA^* = r^2$ and

$$h_{12}^0 \frac{dr}{d\bar{t}} = \left[\xi_{ov} - h_{42}^0 r^2 \right] r \qquad (4.73)$$

$$\frac{d\Phi}{d\bar{t}} = m_{21} \xi_{ov} - m_{42} r^2 \ , \qquad (4.74)$$

where ,

$$h_{31}^0 = h_{32}^0 h_{21}^0 - m_{32} m_{21} ; \quad m_{42} = h_{32}^0 m_{21} + h_{21}^0 m_{32} ; \quad h_{42}^0 = h_{31}^0 / h_{21}^0 . \qquad (4.75)$$

Refer to *Appendix AH* for the derivation of Eqns.(4.74-4.75). The sign of the coefficient of the non-linear term, ie. h_{42}^0 indicates whether the bifurcation is forward or inverse. When $h_{42}^0 > 0$ the bifurcation is forward while a negative value of h_{42}^0 suggests an inverse bifurcation. The point where h_{42}^0 changes sign is known as the (non-equilibrium) tricritical point. Figures 36a-36d shows the variation of the coefficient of the non linear term, h_{42}^0, as a function of the Taylor number for different values of the parameter $\xi = K_c / (\Omega c_S)^2$. If we set $K_c = c_S$, and $\overline{S} = c_S$ so that $\Omega = 2$ then we may present the parameter ξ as $\xi = 1/(4c_S)$. It is very interesting to note that the parameter λ defined in Section 2 may be expressed for the above parameter settings as, $\lambda = \overline{S} / (\Omega c_S)^2 = 1/(4c_S) = \xi$. As pointed out earlier the parameter c_S may assume values ranging from $c_S = 0.125$ (for liquid metals) to $c_S = 4.0$ (for aqueous salts). This implies that ξ may assume values ranging from $\xi = 0.0625$ to about $\xi = 2.0$.

Figures 36a-d shows the variation of the non-linear coefficient as a function of χ_1 for various Taylor number values and ξ values. The linear stability results are insufficient to stipulate a maximum value for χ_1 consistent with overstable convection. For this reason we are not able to pin point the domain of χ_1 values for which overstable convection is possible. The points of intersection with the horizontal x-axis are referred to as the tricritical points. It can be observed from Figures 36a to 36d that there exists two tricritical points for the low ξ values and Taylor number values (see curve corresponding

to Ta=10 in Figures 36a-b) and at least three tricritical points for the higher ξ values and higher Taylor number values (see curve corresponding to Ta=100 in Figures 36c-d).

However as the value for ξ increases for the higher Taylor number settings, the number of tricritical points decreases correspondingly, a trend that is in contrast to the lower Taylor number case. It must be borne in mind that the relaxation time h_{12}^0 is always positive in the parameter domain considered.
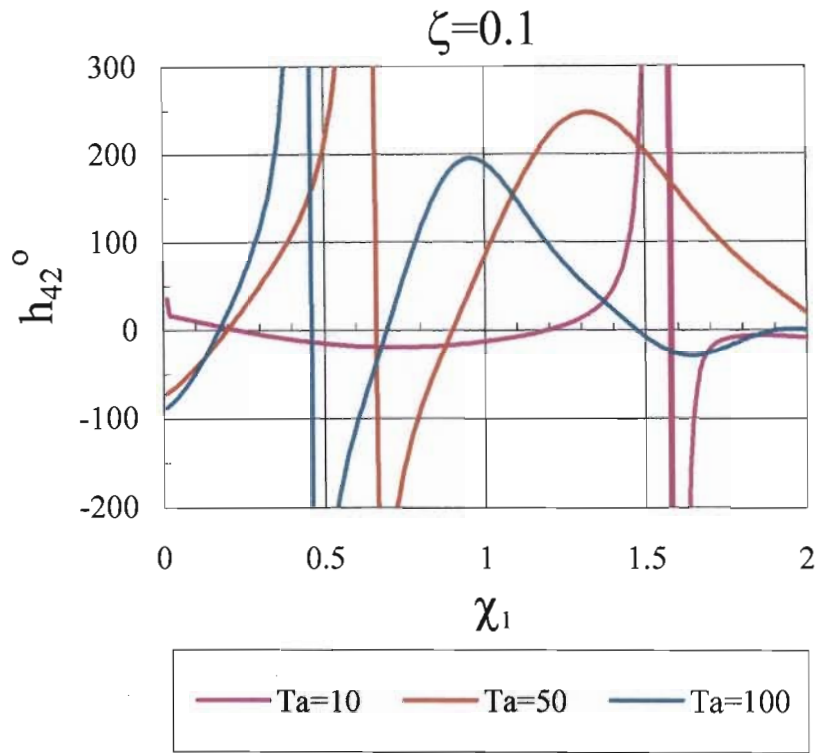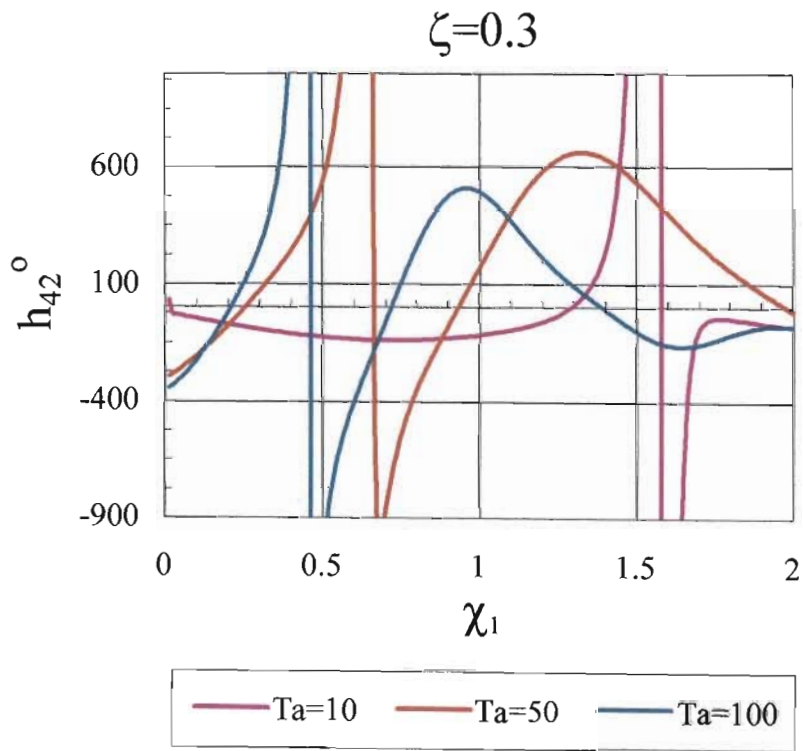
Figure 36 : Finite amplitude results for overstable convection : Variation of the non linear coefficient, h_{42}^{0} as a function of χ_1 (a) $\zeta = 0.1$ and (b) $\zeta = 0.3$ for selected settings of Taylor number.
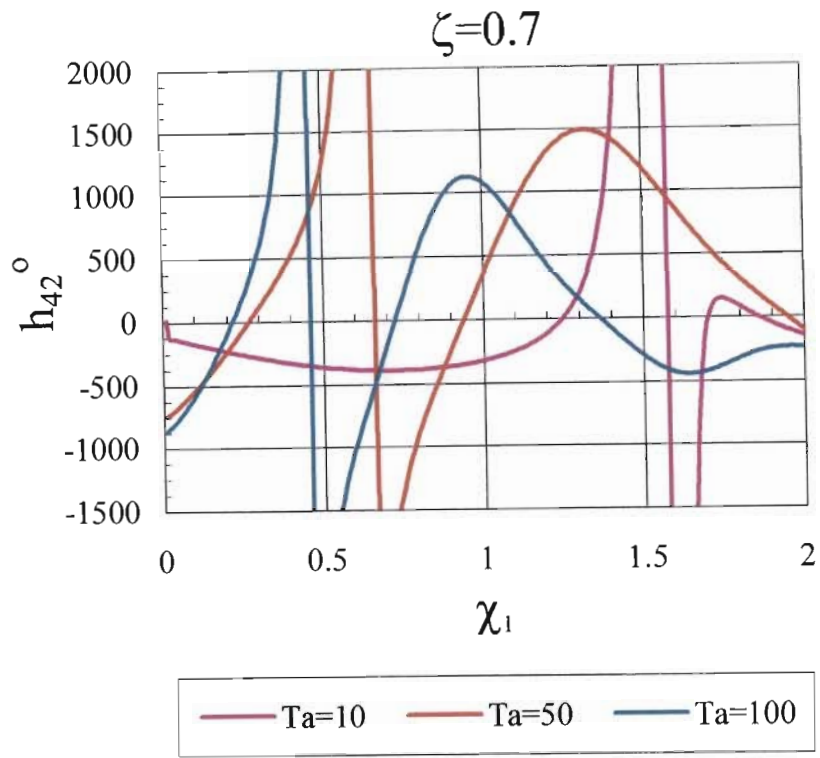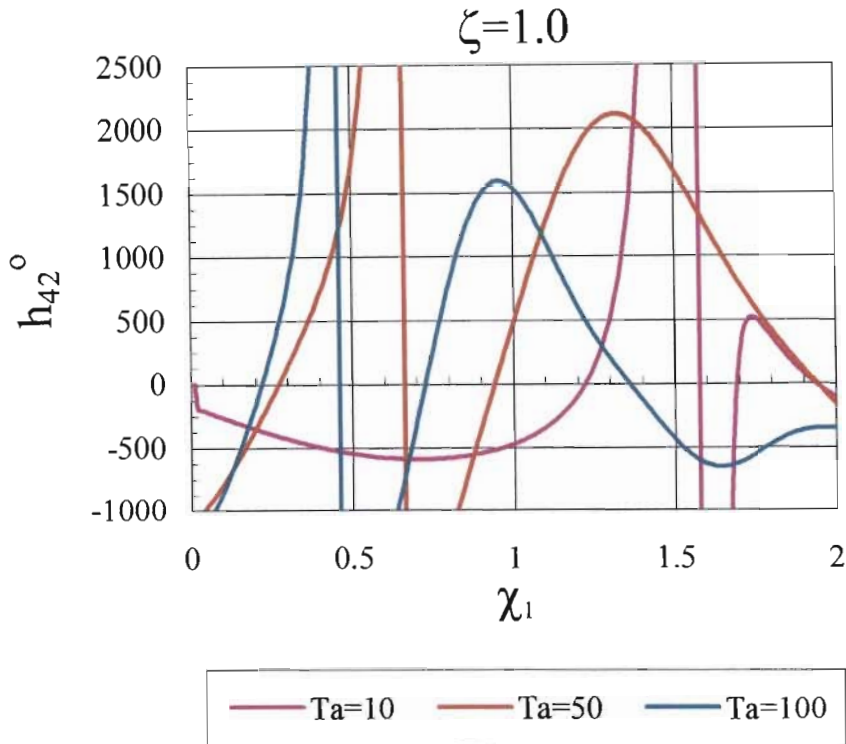
Figure 36 : Finite amplitude results for overstable convection : Variation of the non linear coefficient, h_{42}^0 as a function of χ_1 (c) $\zeta = 0.7$ and (d) $\zeta = 1.0$ for selected settings of Taylor number.

Eqn.(4.73) yields at the post-transient state $r^2 = h_{24}^0 \xi_{ov}$ for supercritical values of R, where $h_{24}^0 = 1/h_{42}^0$, hence providing the solution for r in the form,

$$r = \begin{cases} 0 & \forall \quad R < R_{cr,ov} \\ \\ \pm\left[h_{24}^0 \xi_{ov} \right]^{1/2} & \forall \quad R \geq R_{cr,ov} \end{cases} \qquad (4.76)$$

With solution of r being defined at the post-transient state, the post-transient amplitude solution may be defined as,

$$A = r e^{i\Phi i} = \pm\left(h_{24}^0 \xi_{ov} \right)^{1/2} e^{i\Phi i}, \qquad (4.77)$$

where the non linear frequency correction $\dot{\Phi}$ is obtained by substituting the solution for r^2 in Eqn.(4.74) which may be presented as,

$$\dot{\Phi} = \frac{d\Phi}{dt} = \left(m_{21} - m_{31} h_{24}^0 \right) \xi_{ov}. \qquad (4.78)$$

The post-transient values of $|A|$ as presented in Eqn.(4.76) were evaluated in terms of $\log_{10}\left[|A|/\varepsilon \right]$ and are presented graphically in Figures 37a to 37d. It can be observed from Figures 37a to 37d that the solutions diverge in the vicinity of the CTP points

.

The bucket shaped curves for some of the Taylor number settings attributed to the presence of two co-dimension two (CTP) points very close to each other. The curves presented in Figures 37a to 37d nonetheless give a very clear indication that the points of divergence indicate that the CTP point is close by. At these points of divergence, ie. in the CTP neighbourhood, a different expansion is needed to investigate the solution there, as the divergence of the amplitude violates the assumptions made regarding the amplitude expansion.
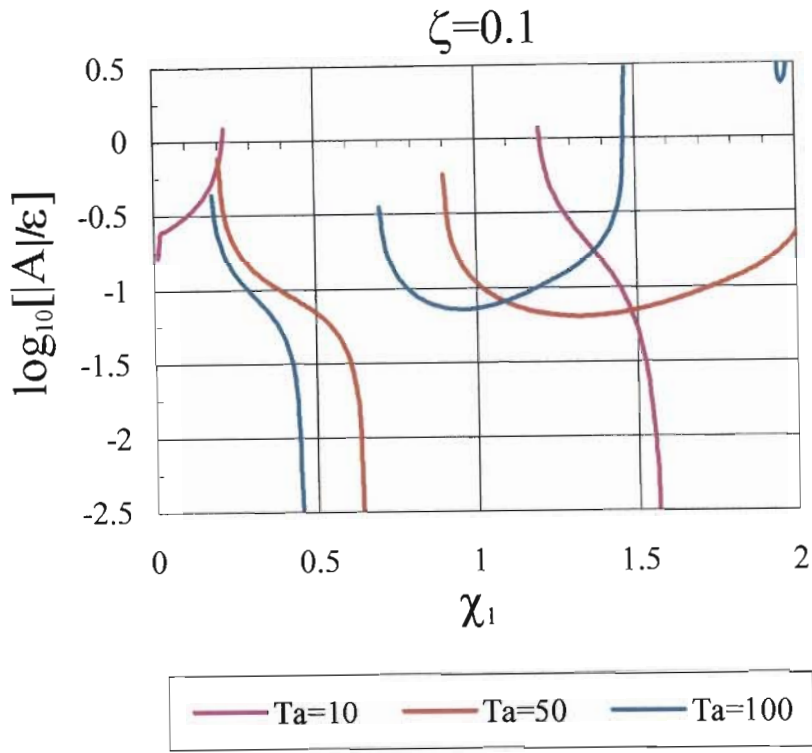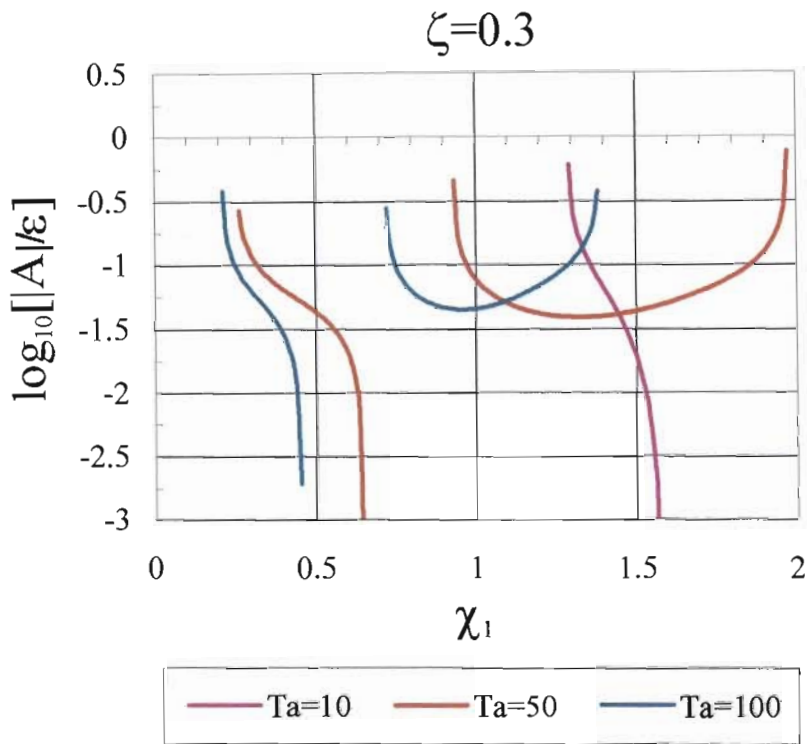
Figure 37 : Finite amplitude results for overstable convection : Post -transient amplitude as a function of χ_1 for different values of Taylor number for (a) $\xi = 0.1$ and (b) $\xi = 0.3$.

Figure 37 : Finite amplitude results for overstable convection : Post -transient   amplitude as a function of χ_1 for different values of Taylor number for (c) $\zeta = 0.7$ and (d) $\zeta = 1.0$.

128
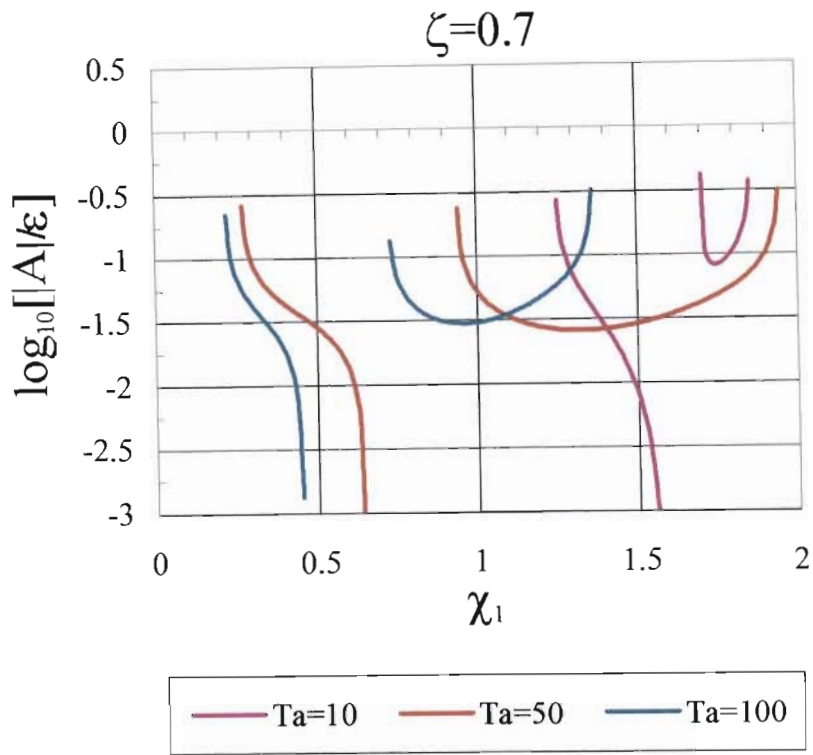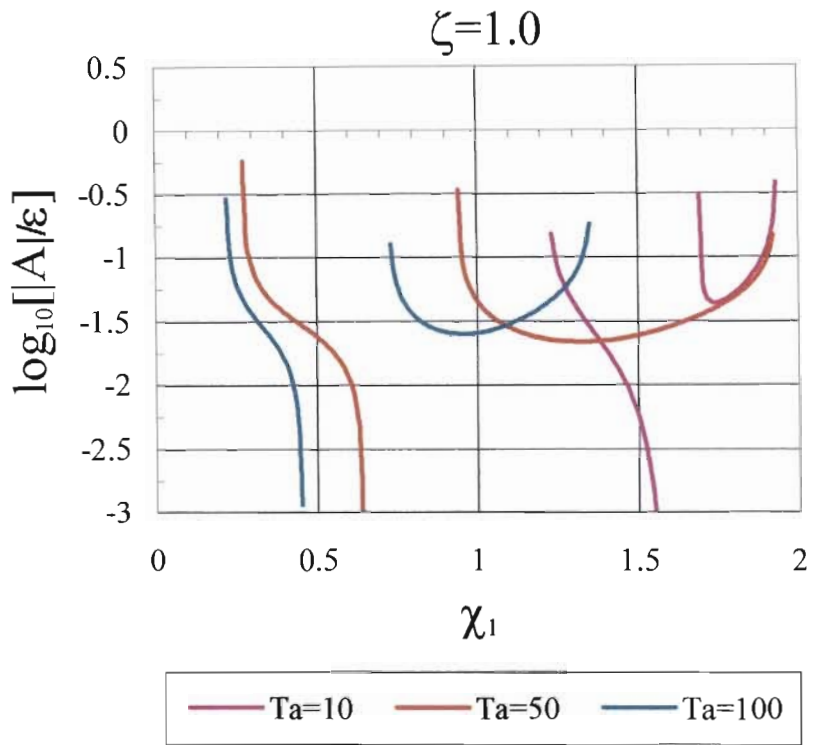
The post-transient values for the non-linear frequency correction were evaluated using Eqn.(4.78) in terms of $\log_{10}\left[\dot{\Phi}/\xi_{ov}\right]$ and are presented in Figures 38a to 38d as a function of χ_1 for various Taylor number values over a range of ξ values. It can be observed from Figures 38a to 38d that the nonlinear frequency correction diverges in the vicinity of the CTP points. The behaviour observed in Figures 38a to 38d are is very similar to the that presented in Figures 37a to 37d. A very clear feature presented by Figures 38a to 38d is that for low Taylor numbers (Ta=10), the CTP points move to the left as the value of ξ is increased. Increasing the value of ξ for higher Taylor numbers (say Ta=100) reduces the number of solutions for the midrange χ_1 values. The same argument applies to the intermediate Taylor numbers, a feature that is quite apparent in Figures 38a to 38d.

$\zeta = 0.1$

(a)

$\zeta = 0.3$

(b)

Figure 38 : Finite amplitude results for overstable convection : Post -transient non linear frequency correction as a function of χ_1 for different values of Taylor number for (a) $\xi = 0.1$ and (b) $\xi = 0.3$

130

$\zeta = 0.7$

(c)

$\zeta = 1.0$

(d)
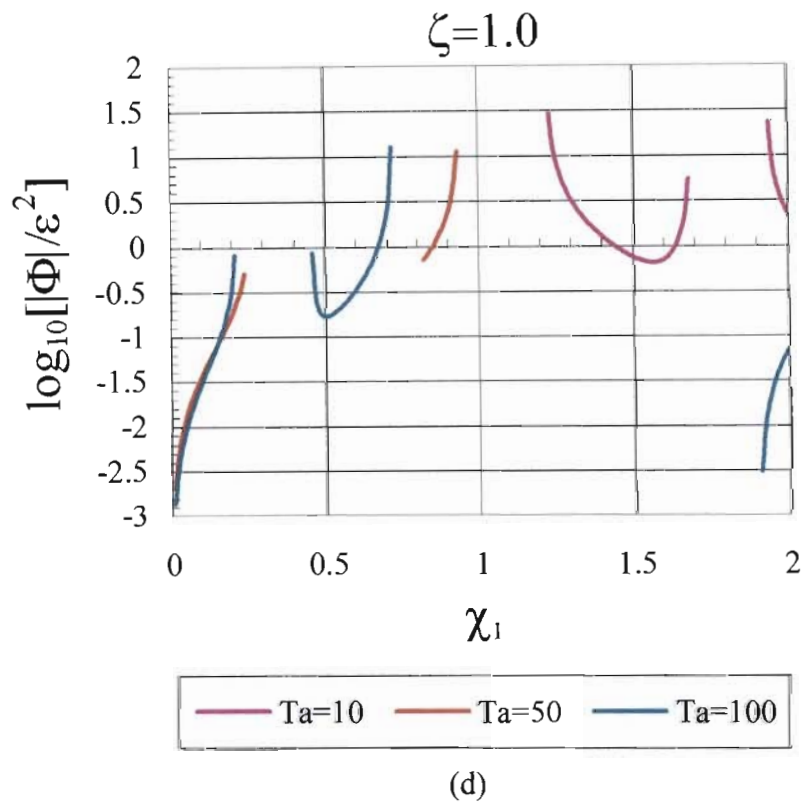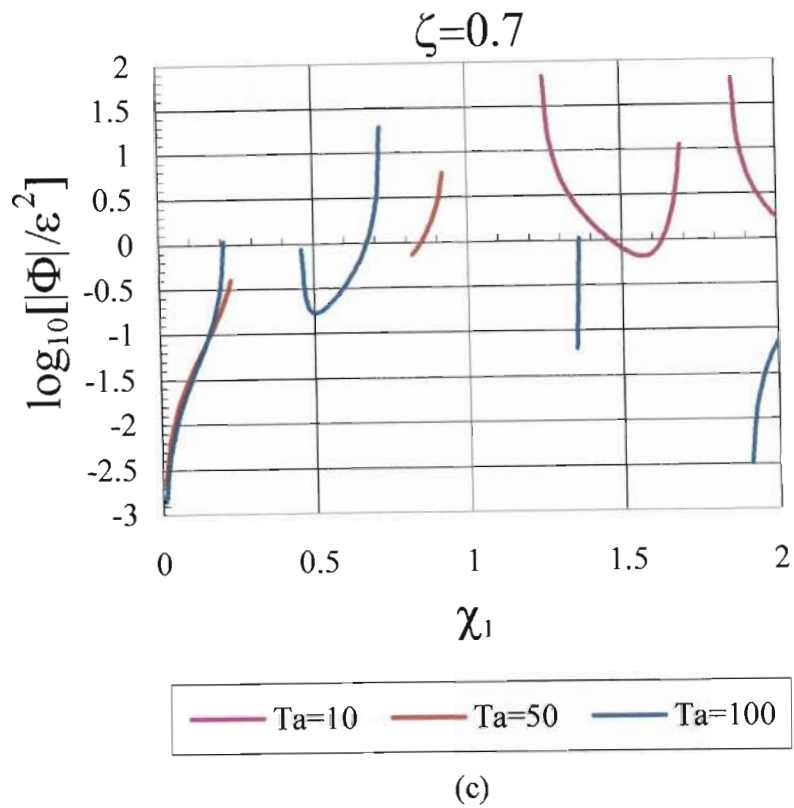
Figure 38 : Finite amplitude results for overstable convection : Post -transient non linear frequency correction as a function of χ_1 for different values of Taylor number for (c) $\zeta = 0.7$ and (d) $\zeta = 1.0$.

5. Heat Flux and Nusselt number : Author's Scaling

This part of the study will be allocated to determining the heat flux in terms of the Nusselt number for both the stationary and overstable convection by making use of the of the previously evaluated amplitude results.

5.1 Nusselt number for Stationary convection

The mean Nusselt number may be defined as,

$$\overline{Nu}_{st} = \frac{1}{L} \int_0^L \left[-\overline{w}\theta + \partial\theta/\partial\overline{z} \right] d\overline{x}, \tag{5.1}$$

where L is the length of the domain and may well be taken as the cell wavelength. Using the fact that,

$$\frac{\partial}{\partial\overline{z}} \int_0^L \left[-\overline{w}\theta + \partial\theta/\partial\overline{z} \right] d\overline{x} = 0, \tag{5.2}$$

implies that the Nusselt number is not a function of $\overline{z}$ and may therefore be evaluated for convenience at $\overline{z} = 0$ where $\overline{w} = 0$. Using the solutions for θ at the different orders and using the result just evaluated above allows the Nusselt number definition given in Eqn.(5.1) to be represented as,

$$\overline{Nu}_{st} = \frac{1}{L} \int_0^L \left[d\theta_B/d\overline{z} \big|_{\overline{z}=0} + \varepsilon \, d\theta_1/d\overline{z} \big|_{\overline{z}=0} + \varepsilon^2 d\theta_2/d\overline{z} \big|_{\overline{z}=0} + O(\varepsilon^3) \right] d\overline{x}. \tag{5.3}$$

Substituting the solutions to the different orders in θ and evaluating the integral given in Eqn.(5.3) yields the following Nusselt number definition for the case of stationary convection,

$$\overline{\text{Nu}}_{\text{st}} = 1 + \frac{4\alpha(\alpha + 1)\left[R/R_{\text{cr,st}} - 1\right]}{\pi^4\left[\dfrac{1}{2}\varsigma(\alpha + 1)(5\alpha + 7 - 7\text{Ta}) + (\alpha + 1 + \text{Ta})\right]} + O(\varepsilon^3) \qquad \forall\ R \geq R_{\text{cr,st}} . \quad (5.4)$$

Note that the slow space scales have been eliminated from Eqn.(5.4) using the arguments as presented in Section 4.1. Refer to *Appendix AI* for the derivation of the Nusselt number for stationary convection. It can be observed from Eqn.(5.4) that $\overline{\text{Nu}}_{\text{st}} = 1$ $\forall\ R < R_{\text{cr,st}}$, indicating that the convection heat transfer branches off from the conductive heat transfer line at the critical value of Rayleigh number. The variation of the Nusselt number as a function of the Taylor number was evaluated for different values of ς and is presented in Figure 39 in terms of $\log_{10}\left[\left(\overline{\text{Nu}}_{\text{st}} - 1\right)/\varepsilon^2\right]$.
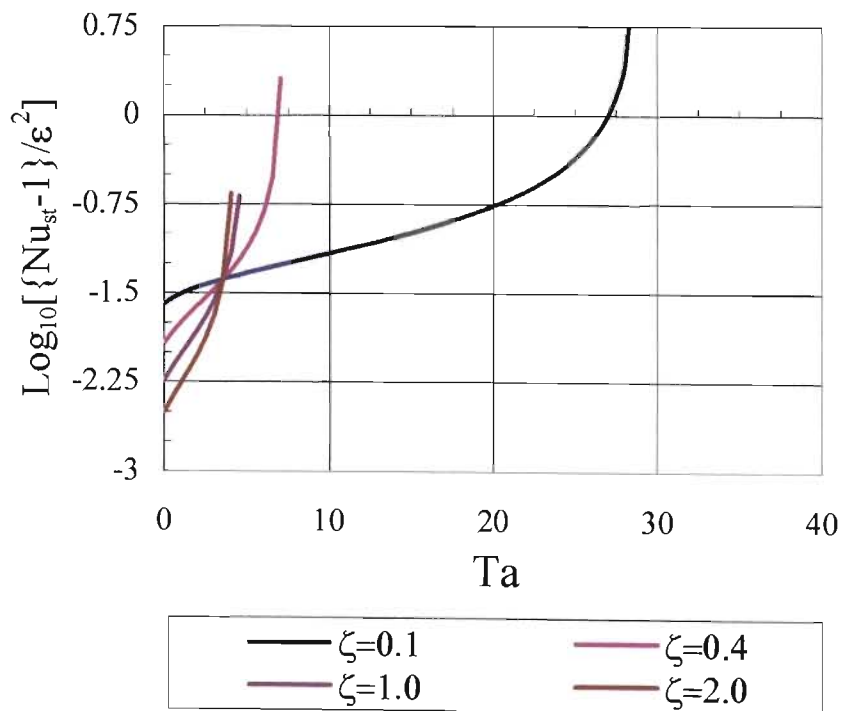
Figure 39 : Heat transfer results for stationary convection : post-transient Nusselt numbers as a function of Taylor number for different values of ς.

We may observe that the for a constant value of ς, increasing the Taylor number , increases the values the heat flux value, thus implying that rotation enhances heat transfer

as far as stationary convection is concerned. We may now proceed to develop the Nusselt number for oscillatory convection.

5.2 Nusselt number for Overstable convection

The heat flux corresponding to overstable convection may be evaluated as for stationary convection, the only difference being that here a time average over one cycle is performed. The pertinent form of the equation at $\bar{z} = 0$ may be given as,

$$\overline{Nu}_{ov} = \frac{1}{2\pi L} \int_0^{2\pi} \int_0^L \left[d\theta_B / d\bar{z} \big|_{\bar{z}=0} + \varepsilon \, d\theta_1 / d\bar{z} \big|_{\bar{z}=0} + \varepsilon^2 d\theta_2 / d\bar{z} \big|_{\bar{z}=0} + O(\varepsilon^3) \right] d\bar{x} d\bar{t} . \qquad (5.5)$$

The mean Nusselt number presented in Eqn.(5.5) has the meaning of being averaged in space as well as in time. To order ε^2 this yields for the post transient state,

$$\overline{Nu}_{ov} = 1 + \frac{4(\alpha + 1)\Omega h_{24}^0}{\pi^2} \left[R / R_{cr,st} - 1 \right] + O(\varepsilon^3) \qquad \forall \ R \geq R_{cr,ov} . \qquad (5.6)$$

Note that $h_{24}^0 = 1/h_{42}^0$ and h_{42}^0 is defined in Eqn.(4.75). Refer to *Appendix AI* for the derivation of Eqn.(5.6). Figures 40a to 40d shows the variation of the Nusselt number as a function of χ_1 for different Taylor numbers and selected ξ values, in terms of $\log_{10}\left[\left(\overline{Nu}_{ov} - 1 \right) / \varepsilon^2 \right]$. It can be noted from Figures 40a to 40d that the Nusselt number solutions diverge in the presence of the CTP points. In general it can be observed from Figures 40a to 40 d that increasing the parameter value for ξ results in a decrease in the Nusselt number, for all the Taylor numbers, thereby causing a retardation in the heat transfer. For a fixed ξ value, increasing the Taylor number (from Ta=50 to Ta=100) causes the Nusselt number to decrease for low χ_1 (say $\chi_1 \leq 1.1$) values whilst a notable increase is heat transfer is observed for high χ_1 values(say $\chi_1 > 1.1$).

$\zeta=0.1$

(a)

$\zeta=0.3$
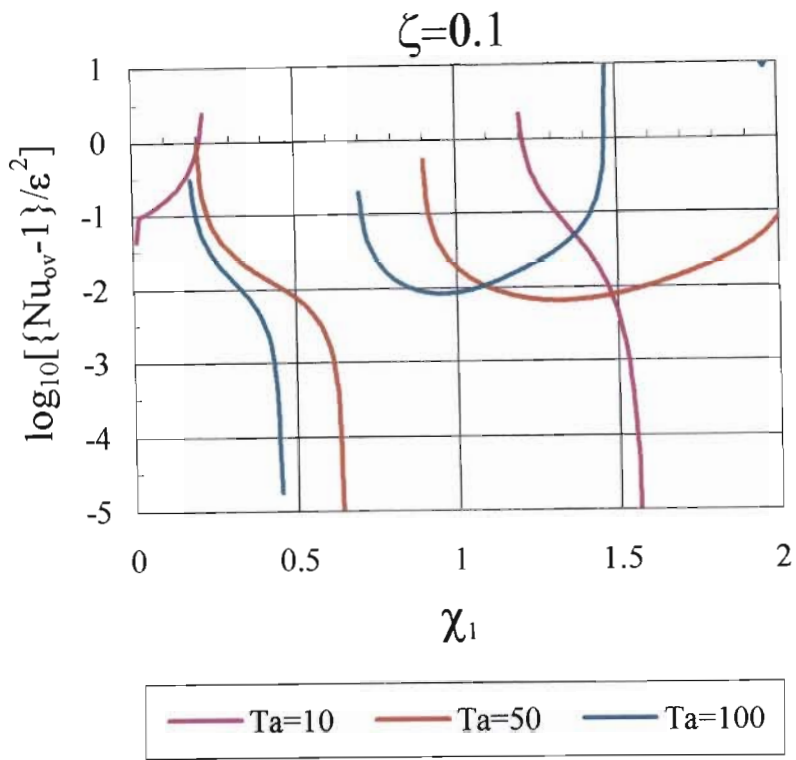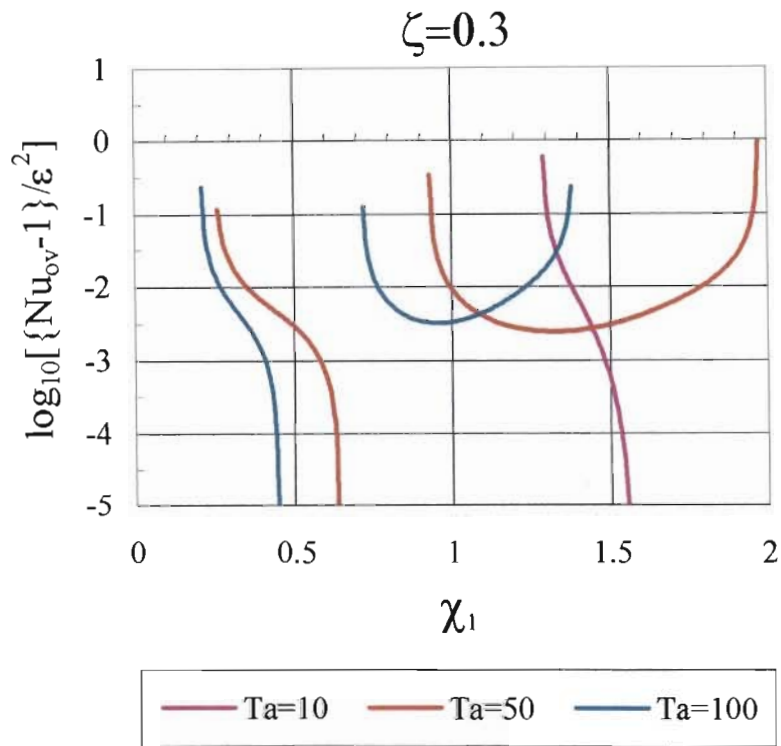
(b)

Figure 40 : Heat transfer results for overstable convection : Post -transient Nusselt number as a function of χ_1 for different values of Taylor number for (a) $\xi = 0.1$ and (b) $\xi = 0.3$.

$\zeta=0.7$

(c)

$\zeta=1.0$
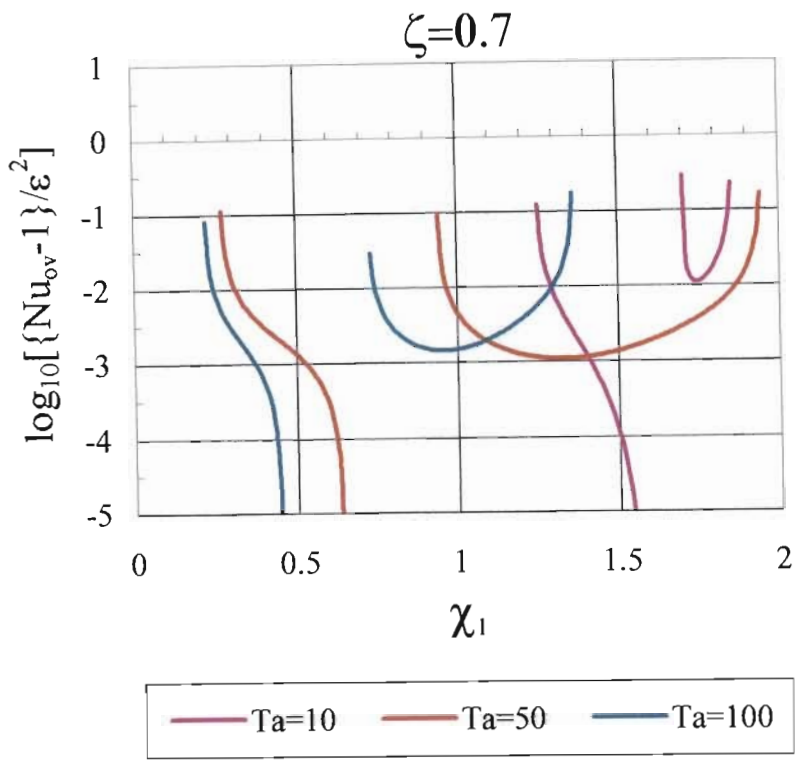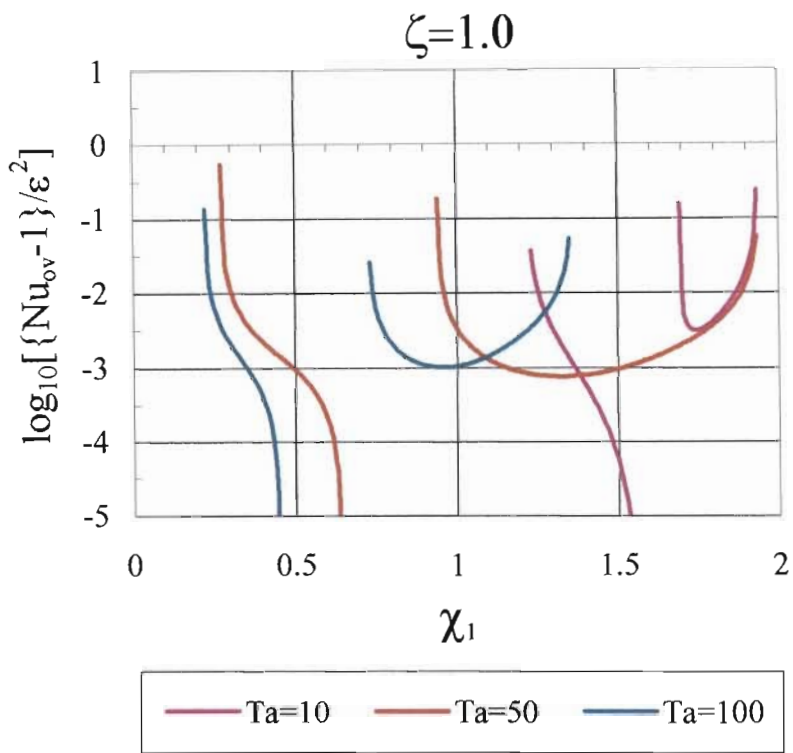
(d)

Figure 40 : Heat transfer results for overstable convection : Post -transient Nusselt number as a function of χ_1 for different values of Taylor number for (c) $\xi = 0.7$ and (d) $\xi = 1.0$.

6. Structure of the thermal, flow and solid fraction fields

To describe the flow and heat transfer we recall the eigenfunctions representing perturbations to the thermal, flow field and solid fraction developed in Section 2.4.2 for Anderson & Worster's (1996) scaling. Combining these perturbations with the basic state solution developed in Section 2.1 yields the following full solutions for the thermal, flow and solid fraction,

$$\theta = \theta_B - 2A \sin(\pi \bar{z}) \cos\left[s\bar{x} + \delta\sigma_{i1}\bar{t}\right] \tag{6.1}$$

$$\psi = 0 - 2A \frac{(\pi^2 + s^2)}{\Omega R_{00} s} \sin(\pi \bar{z}) \sin\left[s\bar{x} + \delta\sigma_{i1}\bar{t}\right] \tag{6.2}$$

$$\varphi = \varphi_B - 2A \frac{\pi(\pi^2 + s^2)}{\Omega c_S (\pi^2 - \sigma_{i1}^2)} \left\{ \left(\cos(\pi\bar{z}) + \cos\left[\sigma_{i1}(\bar{z} - 1)\right] \right) \cdot \cos\left[s\bar{x} + \delta\sigma_{i1}\bar{t}\right] - \right.$$

$$\left. \left(\sigma_{i1}/\pi \cdot \sin(\pi\bar{z}) + \sin\left[\sigma_{i1}(\bar{z} - 1)\right] \right) \cdot \sin\left[s\bar{x} + \delta\sigma_{i1}\bar{t}\right] \right\}. \tag{6.3}$$

Note that θ_B and φ_B have been previously evaluated and are given by Eqns.(2.15-2.16). Note that the amplitude A in the system (6.1-6.3) is defined as $A = \varepsilon A_{00}$. Note that ε is understood to be a small as required by weak non-linear theory. An amplitude value of A=0.01 is selected and is henceforth used in all of the graphical plots that follow.

The structure of the solutions presented in the system (6.1-6.3) varies quite dramatically with the values of frequency σ_{i1}, wavenumber s, Taylor number Ta, and the parameter $\chi = Pr\phi_0/Da$. The quantities just mentioned are related to important physical processes that occur within the mushy layer. The linear stability analysis presented in Section 2.2 for Anderson & Worster's (1996) scaling provided ample insight into the effect of these parameters on the flow physics within the mushy layer. Setting the frequency, $\sigma_{i1} = 0$

$\sigma_{il} = 0$ V $\uparrow$

(a)

$\chi = 2$ V $\uparrow$

(b)

$\chi = 50$ V $\uparrow$

(c)
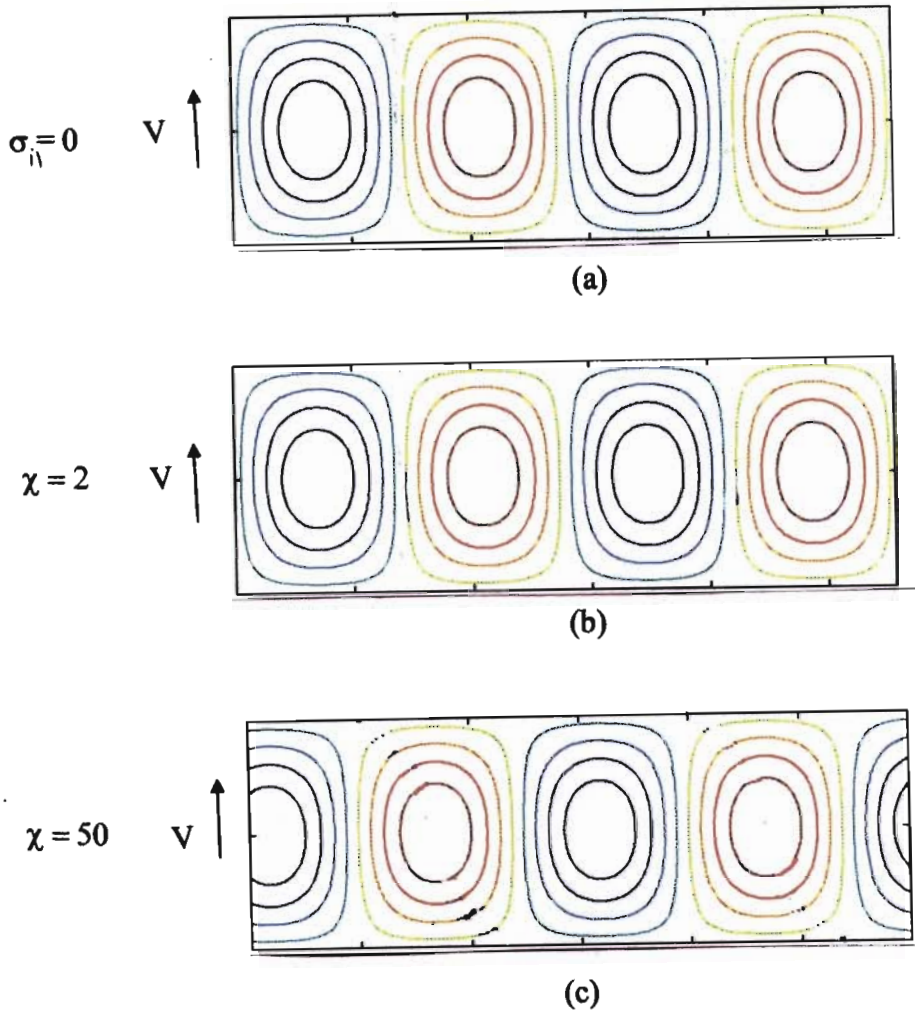
Figure 41 : Streamline plot for the case Ta=50, $\lambda = 1.0$

results in the onset of stationary convection, a case which is presented in Figure 41a (for the flowfield). Figure 41b represents a case when stationary convection is the most unstable mode thereby resulting $\sigma_{il} = 0$.

The case presented by $\sigma_{il} \neq 0$ corresponds to the case of oscillatory convection as presented in the system (6.1-6.3). These oscillations could manifest themselves as left or right travelling waves, or any combination thereof, including standing waves. The wave form that occurs within the mushy layer is highly system dependent. For example, the boundary condition at the axis of rotation viz. $\psi_{00} = 0$ at $\bar{x} = 0$ causes the solutions to the thermal, flow and solid fraction to assume the form of left travelling waves. For the

139

purposes of the current study we shall only focus on left travelling waves in order to illustrate the important flow characteristics within the mushy layer. Incidentally the system presented in the system (6.1–6.3) represents left travelling waves. The streamlines presented in Figure 41c represents left travelling convection cells. At any instant in time the form of these convection cells are identical to the stationary convection cells presented in Figure 41a. Eqns.(6.1-6.3) provides mathematical rationale for the horizontal translation, by a shift of the horizontal co-ordinate with increasing time. This implies that the thermal and flow fields are identical to the stationary case, as pointed out earlier. For this reason, only a single set of results are presented for the flow field.

The most profound effect of left translation can be observed for the solid fraction plots corresponding to the case of $\sigma_{i1} \neq 0$. Due to the left translation of the convection cells, the solid fingers/dendrites are no longer aligned vertically as, presented in the stationary case, but now tends to slope monotonically in the direction of translation as observed from Figures 42b,c,f and Figures 43b,c,f. The results presented in Figures 42e and 43e represent the case when $\gamma \to 0$ which results in the stationary mode manifesting itself as the most dangerous mode (note that $\gamma = \chi / \pi^2$). The point is that as $\gamma \to 0$ (or at high frequencies) the characteristic Rayleigh number approaches an asymptote which for all intents and purposes is taken as the convection threshold point for the onset of stationary convection. This was motivated mathematically in Section 2.3 and Section 2.4.

It can be observed from Figures 42 b-c and 43b-c that the increasing the parameter value for χ has very little effect of the slope of the solid finger/dendrite. It should be noted that the spaces between the streamlines for the solid fingers/dendrites represents the surrounding liquid melt in the pores/channels. It can be observed from Figure 42c,f that increasing the Taylor number from Ta=3 to Ta=50 for fluids that have high χ values prevents any channels from forming. Figure 42f captures the wavy nature of the solidified surface very well. The maximum points on the solid finger/dendrite plots were connected to illustrate the nature of the slopes of the solid fingers in the oscillatory case relative to the stationary case.
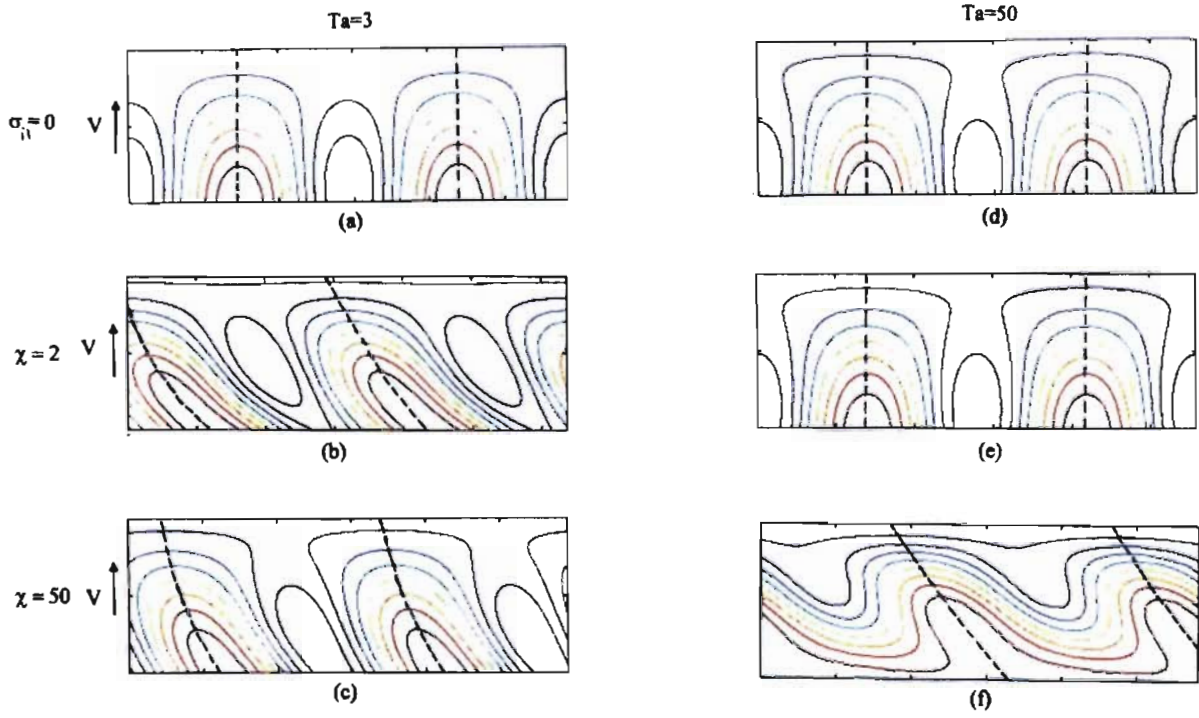
Figure 42 : Solid fraction plot showing solid finger slopes superimposed for the case $\lambda = 0.5$
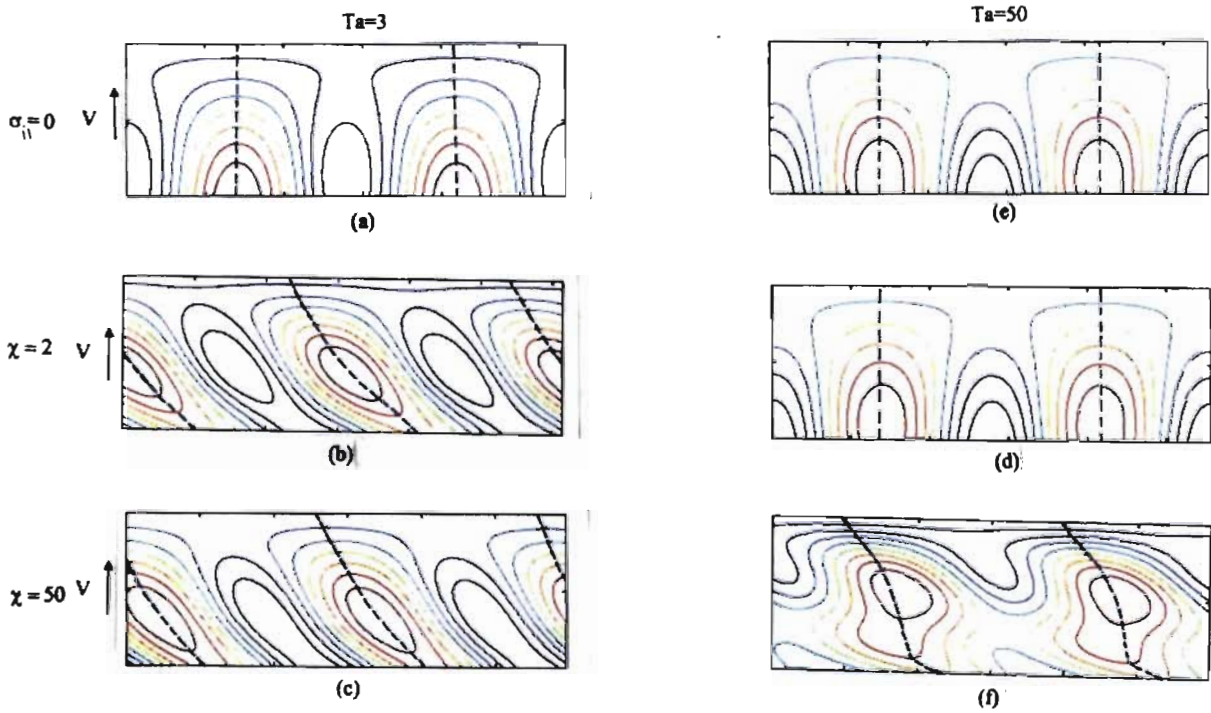
Figure 43 : Solid fraction plot showing solid finger slopes superimposed for the case $\lambda = 1.0$

Increasing the value of λ from $\lambda = 0.5$ to $\lambda = 1.0$ for Ta=3 causes the slope of the solid finger/dendrite to become steeper. Perhaps the most interesting feature is noted from Figures 43e,d (as was in Figure 42e,d) in that it can be observed that increasing the Taylor number for low values of the parameter χ actually forces the fingers/dendrites to become vertically aligned. This is important since the implications are that for select combinations of Taylor number and χ we have vertically orientated solid fingers/dendrites. At high Taylor numbers and χ values it can be seen that the slope of that solid fingers/dendrites changes from monotonic to non-monotonic. Increasing the value of λ to $\lambda = 1.0$ suppressed the formation of channels as can be observed when comparing Figures 42 b-f and Figures 43b-f. The most profound effect of increasing the value of λ can be observed from Figure 43f. It can be seen that virtually no channels appear in the whole domain considered.

The effect of the non-vertically orientated solid finger/dendrites is the horizontal translation of these fields. The fact that the thermal and flow fields does not differ from

the stationary case is as a result of the near-eutectic approximation upon which the solutions are based. The appearance of the convection rolls is similar to that of a porous medium of uniform permeability. This is attributed to the fact that the thermal and flow fields are decoupled from the solid fraction perturbation at the leading order. With this in mind the nature of the solid fraction fingers/dendrites forces the flow towards the left. It can be observed from Figures 42 and 43 that the left sloping channels forces the flow in that direction, or so it seems. The coupling between the flow field and the solid fraction occurs to higher orders in δ. The governing equations need to evaluated to higher orders to observe the interaction between the flow and solid fraction, but for the current study the linear stability results and the leading order perturbations are sufficient to infer flow patterns at higher orders.

The results presented in Figures 42 and 43 prove that increasing the Taylor number encourages a solid front with almost no channels, as observed from Figures 42f and 43f for high χ values. It can be clearly observed from Figure 42 and 43f that for higher λ values the solidification front has become flatter.

7. Summary and Conclusions

Analytical results were presented for convection in a solidifying binary alloy system at the near-eutectic point subject to Coriolis effects. The model is based on a simple model of the mushy layer given by Amberg & Homsey (1993) in which the dynamics of the mushy layer are decoupled from the dynamics of the overlying melt. The problem was investigated using the time scale proposed by Anderson & Worster (1996) and for a time scale proposed by the author. Linear stability analyses were performed for both the scalings above whilst a weak non linear analysis was performed for the Author's time scale only. In addition the heat transfer was inferred from the Nusselt number solutions that were developed for both stationary and overstable convection for the Author's scaling. The weak non-linear analysis utilized a permeability definition which was similar to that of Amberg & Homsey (1993) with the only difference being that the effects permeability was only introduced at the third order of the disturbance amplitude ε. In addition a new parameter $\zeta = K_c/\Omega^2 c_S^2$ was pointed out. This parameter served as a toggle switch between a mushy layer uniform or non-uniform permeability where $\zeta = 0$ represents the homogenous mushy layer and $\zeta \neq 0$ indicates a non-homogenous mushy layer. For the current study only $\zeta \neq 0$ was considered. The most interesting and salient features that were observed will be discussed separately for Anderson & Worster's (1996) scaling and the Author's time scale. The time scale used by Anderson & Wortser (1996) and the Author will henceforth be referred to as "Anderson & Worster's scaling" and "Govender's scaling" respectively.

Firstly for Anderson & Worster's scaling a full linear stability analysis was performed. It was found that the stationary mode became the most dangerous mode for increasing Taylor numbers and the parameter $\lambda = \overline{S}/\Omega^2 c_S^2$. The oscillatory mode still appeared to manifest itself but only at very high $\chi = \Pr \phi_0/Da$ values, whilst at the lower χ values the stationary mode was deemed to be the most dangerous. Figures 12-14 depicts this transition very clearly. Another interesting feature that was observed (and worthy of note) is that at low values of the parameter χ for increasing Taylor numbers, the characteristic curves tended to reach and asymptote as shown in Figures 15 and 19. As the value of χ

is increased to a very large value the curves resemble that presented by Anderson & Worster (1996). This feature is apparent from Figures 15-22. The most interesting feature though was observed at at low values of the parameter χ for increasing Taylor numbers. The curves for the different values of the parameter λ tended converge to an asymptotical wave number for the case $\gamma \to 0$ (or at high frequencies σ_{i1}). The characteristic equation for the asymptotical Rayleigh number was developed and is given in Eqn.(2.72). It must be borne in mind that this represents the asymptote at high frequencies and is distinctly different from the case of stationary convection where $\sigma_{i1} = 0$. However if the critical Rayleigh number corresponding to stationary convection is less than the asymptotical Rayleigh number mentioned above then only can we set $\sigma_{i1} = 0$. The results presented in Figures 24a,b and 26 a,b represents a case where the overstable asymptotical Rayleigh number was greater than the critical Rayleigh number associated with stationary convection over the entire λ domain. In this instance the stationary mode is the most dangerous and the frequency $\sigma_{i1} = 0$ applies. The results presented in Figure 26c shows a good illustration of a case of high frequency overstable convection the more dangerous mode in comparison to the stationary convection case. In this case the asymptotical Rayleigh number associated with overstable convection is less than the critical Rayleigh number for stationary convection over the entire λ domain, thereby implying that $\sigma_{i1} \neq 0$. Incidentally these results are in total agreement with that observed from the characteristic Rayleigh number plots in Figures 12-14. It was also demonstrated that the effect of rotation has a stabilising effect in comparison to a stationary mushy layer. Figure 27 shows that the critical values for the onset of convection for both stationary and overstable convection are greater than that of the non-rotating case, thereby implying that the non-rotating case is the most unstable.

The subsequent part of the linear stability analysis involved studying the stability of the system with regards to the various parameters as presented in Section 2.4.1. The stability results were presented as a function of the Stefan number St, the composition ratio ξ , the mushy layer depth $\delta \approx 1/T_\infty$ and the Taylor number Ta. It must be borne in mind that once a material is selected the values for St, $\chi = Pr\phi_0/Da$ and ξ are fixed. The remaining

control parameters are $\delta \approx 1/T_\infty$ (the farfield or furnace temperature) and the Taylor number.

It was found that increasing the Taylor number rendered the stationary mode most dangerous over the entire St domain. The oscillatory mode only manifested itself at low Taylor number values (Ta=3), but for $St > 1$, as observed from Figure 28. The effect of increasing the Taylor number as a function of the composition ratio rendered the stationary mode unstable. The oscillatory mode was most unstable at low Taylor numbers (Ta=3) but for $\xi \geq 6$ as observed from Figure 29. The variation of the Taylor number as a function the mushy layer height is provided in Figure 30. It was observed that the oscillatory mode was most unstable for small δ values or large far field temperatures T_∞. The effect of rotation however reduced this bandwidth of mushy layer heights over which the oscillatory mode is most unstable. The bandwidth of mushy layer heights over which the stationary mode is most unstable is increased with increasing rotation. Figure 31 shows the variation of the stability parameters as a function of the Taylor number. The results indicate that increasing the value of the parameter χ over the range of Taylor number values enhances the oscillatory mode. This feature agrees with the results observed from the characteristic curves presented in Figures 12-14.

The following part of the study involved analyzing the system of governing equations for the Govender's scaling and included both a linear stability analysis and a weak non linear analysis to establish the amplitude explicitly for the leading order solution. The linear results obtained for the case of stationary convection resembled Vadasz's (1998) solution. The linear stability results obtained for the overstable convection resembled Vadasz's (1998) overstable convection results for a certain parameter setting. Figure 32 suggested that the case of no rotation (Ta=0) is the most unstable in comparison to the case including rotational effects. It was observed that the oscillatory mode is independent of the Taylor number, thus no comment can be made with regards to the stability of the oscillatory mode with regards to the case of no rotation where Ta=0.

A weak non linear analysis was performed for both the stationary and overstable solutions. A new parameter viz. $\varsigma = K_c / \Omega^2 c_S^2$ was pointed out so as to distinguish between a mushy layer of uniform and non-uniform permeability. It is worth pointing out that if $K_c = c_S$ and if $\overline{S} = c_S$ so that $\Omega = 2$, we obtain an expression for the parameter ς which is of the form $\varsigma = 1/(4c_S) = \lambda$. This is deemed to be an important result as it relates the parameters ς and λ under the above mentioned circumstances. The most striking feature of the weak non linear results corresponding to stationary convection showed that increasing the parameter value for $\chi_1 = \delta \Pr \phi_0 \vartheta_0$ reduced the bandwidth of Taylor number values over which the relaxation time is positive. Similarly the linear amplitude coefficient assumed positive values over a larger range of Taylor number values for smaller ς values as compared to larger values.

No conclusion concerning the nature of the bifurcation (ie. if it is inverse or forward) could be made at weak non-linear level corresponding to the case of overstable convection as the results obtained at the linear stability level were insufficient. The presence of co-dimension 2 points (CTP) were also noted in the vicinity of the tricritical points, ie. the point where the bifurcation changes sign. It was noted that there existed multiple CTP points. The results for the modulus of the amplitude indicated that the effect of increasing the value for ς caused the amplitude of convection to get smaller. Physically this implies that as the permeability of the mush becomes more non-uniform, the strength of the oscillatory convection mode begins to damp out. It was found that increasing the parameter value for ς damped out the frequency correction, but very slightly.

The Nusselt number solutions were developed for both the stationary and overstable cases. For the stationary case is was observed that for a particular value of ς, increasing the Taylor number enhances the heat transfer. For a fixed Taylor number above Ta=3, it can be seen that increasing the value of the parameter ς enhances the heat transfer. This is in contrast to the results obtained less than Ta=3. The results produced by the

147

oscillatory case showed that increasing the parameter value for ζ reduces the heat transfer. For a fixed value for the parameter ζ, increasing the Taylor number retards the convective heat transfer for low χ_1 values, which is in contrast to the result at high χ_1 values.

Finally the graphical solutions presented for the flow and solid fraction indicated the form of the solid fingers/dendrites formed. It was also inferred that the solid fingers/dendrites with non-vertical channels caused the horizontal translation of the flowfield. The transformation of the slope of the channels from monotonic variation to a non-monotonic variation was also illustrated for a particular parameter combination.

It was also inferred from the leading order solutions of the perturbations to the flow and solid fraction that the presence of solid fingers/dendrites tends to confine the flow into steady patterns. From a practical point of view we thus require that oscillatory convection be confined to cases close to marginal conditions.

The most important result of the study was that the effect of rotation does indeed have a stabilising effect on convection in the mushy layer ie. the critical Rayleigh numbers for both stationary and overstable convection for the rotating mushy layer (for Anderson & Worster's (1996) scaling) were greater than the critical Rayleigh numbers for both stationary and overstable convection for the non rotating (Ta=0) mushy layer.

8. References

Amberg, G. & Homsey, G.M. 1993 Nonlinear analysis of buoyant convection in binary solidification to channel formation. *J. Fluid Mech.* **252**, 79-98.

Anderson, D.M & Worster, M.G. 1995 Weakly non-linear analysis of convection in mushy layers during the solidification of binary alloys. *J. Fluid Mech.* **302**, 307-331.

Anderson, D.M & Worster, M.G. 1996 A new oscillatory instability in a mushy layer during the solidification of binary alloys. *J. Fluid Mech.* **307**, 245-267.

Brattkus, K. & Davies, S.H. 1988 Cellular growth near absolute stability. *Phys. Rev.* **B38**, 11452-11460.

Chen, F. & Chen, F. 1991 Experimental study of directional solidification of aqueous ammonium chloride solution. *J. Fluid Mech.* **227**, 567-586.

Chen, F., Lu, J.W. & Yang, T.L. 1994 Convective instability in ammonium chloride solution directionally solidified from below. *J. Fluid Mech.* **276**, 163-187.

Chiarelli, A.O.P. & Worster, M.G. 1995 Flow focussing instability in a solidifying mushy layer. *J. Fluid Mech.* **297**, 293-308.

Copley, S.M., Giamei, A.F., Johnson, S.M. & Hornbecker, M.F. 1970 The origin of freckles in unidirectionally solidified castings. *Metall. Trans.* **1**, 2193-2205.

Drazin, P.G. & Reid, W.H 1981 Hydrodynamic Stability. *Cambride University Press.*

Fowler, A.C. 1985 The formation of freckles in binary alloys. *IMA J. App. Mathematics.* **35**, 159-174.

Hills, R.N., Loper, D.E. & Roberts, P.H. 1983 A thermodynamically consistent model of a mushy zone. *Q.J. Mech. Appl. Maths* **36**, 505-539.

Huppert, H.E. 1990 The fluid mechanics of solidification. *J. Fluid Mech.* **212**, 209-240.

Iooss, G. & Joseph, D.D. 1980 Elementary stability and bifurcation theory. *Springer.*

Newell, A.C. & Whitehead, J.C 1969 Finite bandwidth, finite amplitude convection. *J. Fluid Mech.* **38**, 297-303.

Palm, E., Weber, J.E. & Kvernvold, O. 1972 On steady convection in a porous medium *J. Fluid Mech.* **54**, 153-161.

Sample, A.K. & Hellawell, A. 1984 The mechanics of formation and prevention of channel segregation during alloy solidification. *Metall. Trans.* **15A**, 2163-2173.

Sarazin, J.R. & Hellawell, A. 1988 Channel formation in Pb-Sn, Pb-Sb and Pb-Sn-Sb alloy ingots and comparison with the system $NH_4Cl - H_2O$. *Metall. Trans.* **19A**, 1861-1870.

Segel, L.A. 1969 Distant side-walls cause slow amplitude modulation of cellular convection. *J. Fluid Mech.* **38**, 203-224.

Tait, S., Jahrling, K. & Jaupart, C. 1992 The planform compositional convection and chimney formation in a mushy layer. *Nature.* **359**, 406-408.

Tait, S. & Jaupart, C. 1992 Compositional convection in a reactive crystalline mush and melt differentiation. *J. Geophys.* **97(B5)**, 6735-6756.

Vadasz, P. 1998 Coriolis effect on gravity driven convection in a rotating porous layer heated from below. *J. Fluid. Mech.* **376**, 351-375.

Worster, M.G. 1991 Natural convection in a mushy layer. *J. Fluid. Mech.* **224**, 335-359.

Worster, M.G. 1992 Instabilities of the liquid and mushy regions during solidification of alloys. *J. Fluid. Mech.* **237**, 649-669.

Appendix A : Non-dimensionalistation of the governing system of equations

The non-dimensional analysis of the governing system of equations corresponding to flow and heat transfer in the rotating mushy layer will be performed using appropriate scaling parameters.

The dimensional continuity equation applicable to the problem may be represented as,

$$\frac{\partial\left(\rho^{*}\phi\right)}{\partial t^{*}} + \nabla^{*}\cdot\left[\rho^{*}\phi U_{f}^{*}\right] = 0, \tag{1}$$

where $(.)^{*}$ represents the dimensional quantities, ρ^{*} is the fluid phase density, ϕ is the porosity and U_{f}^{*} is the fluid average velocity. Letting $U^{*} = \phi U_{f}^{*}$, then Eqn.(1) may be written as

$$\frac{\partial\left(\rho^{*}\phi\right)}{\partial t^{*}} + \nabla^{*}\cdot\left[\rho^{*}U^{*}\right] = 0. \tag{2}$$

Expanding Eqn.(2) yields the following dimensional form of the continuity equation

$$\phi\frac{\partial\rho^{*}}{\partial t^{*}} + \rho^{*}\frac{\partial\phi}{\partial t^{*}} + \rho^{*}\nabla^{*}\cdot U^{*} + U^{*}\cdot\nabla^{*}\rho^{*} = 0. \tag{3}$$

Using κ^{*}/V^{*} for the length scale, κ^{*}/V^{*2} for the time scale and V^{*} for the velocity scale we may proceed to non-dimensionalise the continuity equation as follows,

$$\phi\frac{V^{*2}}{\kappa^{*}}\frac{\partial\rho^{*}}{\partial t} + \rho^{*}\frac{V^{*2}}{\kappa^{*}}\frac{\partial\phi}{\partial t} + \rho^{*}\frac{V^{*2}}{\kappa^{*}}\nabla\cdot U + \frac{V^{*2}}{\kappa^{*}}U\cdot\nabla\rho^{*} = 0 \tag{4}$$

Dividing Eqn.(4) by V^{*2}/κ^{*}, yields the following form of the continuity equation,

$$\phi \frac{\partial \rho^*}{\partial t} + \rho^* \frac{\partial \phi}{\partial t} + \rho^* \nabla \cdot \mathbf{U} + \mathbf{U} \cdot \nabla \rho^* = 0. \tag{5a}$$

Dividing Eqn.(5a) by a reference value of density ρ_0^* yields

$$\phi \frac{\partial \rho}{\partial t} + \rho \frac{\partial \phi}{\partial t} + \rho \nabla \cdot \mathbf{U} + \mathbf{U} \cdot \nabla \rho = 0, \tag{5b}$$

where $\rho = \rho^* / \rho_0^*$.

Noting that the definition for the fluid density is given as

$$\rho = \left[1 - \beta_T \theta + \beta_c c \right], \tag{6a}$$

where

$$\beta_T = \beta_T^* \left(T_L - T_E \right) \text{ and } \theta = \frac{T^* - T_L}{T_L - T_E}, \tag{6b}$$

and

$$\beta_c = \beta^* \left(c_0 - c_E \right) \text{ and } c = \frac{c^* - c_0}{c_0 - c_E}. \tag{6c}$$

Substituting Eqn.(6a) in Eqn.(5b) yields

$$\frac{\partial \phi}{\partial t} - \beta_T \theta \frac{\partial \phi}{\partial t} + \beta_T c \frac{\partial \phi}{\partial t} - \phi \beta_T \frac{\partial \theta}{\partial t} + \phi \beta_c \frac{\partial c}{\partial t} - \beta_T \mathbf{U} \cdot \nabla \theta + \beta_c \mathbf{U} \cdot \nabla c +$$

$$\left(1 - \beta_T \theta + \beta_c c \right) \nabla \cdot \mathbf{U} = 0. \tag{7}$$

153

Now, since $\beta_T \ll 1$ and $\beta_c \ll 1$ we apply the Boussinesq approximation and neglect density variations (in terms containing β_T or β_c as their coefficient) everywhere, except in body forces or buoyancy terms in the extended Darcy equation. Therefore Eqn.(7) becomes

$$\frac{\partial \phi}{\partial t} + \nabla \cdot \mathbf{U} = 0 .$$ (8)

Most of the publications thus far have assumed that $\phi = \phi_0$ thus implying that the continuity equation may be presented as

$$\nabla \cdot \mathbf{U} = 0 .$$ (9)

Eqn.(9) is identical to Eqn.(1.3).

The differential equation for the dimensional form of the energy equation is given as,

$$q_m \frac{\partial T^*}{\partial \hat{t}^*} + q_f \mathbf{U}^* \cdot \nabla^* T^* = \nabla^* \cdot \left(k_m \nabla^* T^* \right) + h_{fs} \frac{\partial \varphi}{\partial \hat{t}^*} ,$$ (10)

if we assume no contraction upon change of phase. The physical prameters in Eqn.(10) are the specific heat per unit volume q, the latent heat of solidification per unit volume, h_{fs}, and the thermal conductivity k. The subscripts 's', 'f', 'm' denote the properties of the solid, liquid and mushy phases respectively. The volume fraction of solid dendrites, of uniform composition c_S, is denoted by φ. The specific heat per unit volume of the mushy phase is given by,

$$q_m = \varphi q_s + (1 - \varphi) q_f .$$ (11)

The thermal conductivity of the mushy phase is given as,

$$k_m = \varphi k_s + (1 - \varphi) k_f . \tag{12}$$

If the specific heats and thermal conductivities are assumed to be to be equal then Eqn.(11-12) may be presented as,

$$q_m = \varphi q_s + (1 - \varphi) q_s = q_s , \tag{13}$$

$$k_m = \varphi k_s + (1 - \varphi) k_s = k_s . \tag{14}$$

Using the results in Eqns.(13-14), Eqn.(10) may be presented as,

$$q_s \frac{\partial T^*}{\partial \hat{t}^*} + q_s \mathbf{U}^* \cdot \nabla^* T^* = \nabla^* \cdot \left(k_m \nabla^* T^* \right) + h_{fs} \frac{\partial \varphi}{\partial \hat{t}^*} . \tag{15}$$

Dividing Eqn.(15) by q_s yields,

$$\frac{\partial T^*}{\partial \hat{t}^*} + \mathbf{U}^* \cdot \nabla^* T^* = \kappa^* \nabla^* \cdot \left(\nabla^* T^* \right) + \frac{h_{fs}}{q_s} \frac{\partial \varphi}{\partial \hat{t}^*} , \tag{16}$$

where κ^* is the thermal diffusivity. Rearranging Eqn.(16) as following,

$$\frac{\partial}{\partial \hat{t}^*} \left(T^* - \frac{h_{fs}}{q_s} \varphi \right) + \mathbf{U}^* \cdot \nabla^* T^* = \kappa^* \nabla^{*2} T^* . \tag{17}$$

Using the transformation,

$$\frac{\partial}{\partial \hat{t}^*} (\cdot) = \left[\frac{\partial}{\partial t^*} - V^* \frac{\partial}{\partial z^*} \right] (\cdot) , \tag{18}$$

to denote the solidifying translating front allows Eqn.(17) to be expressed follows,

$$
\left(\frac{\partial}{\partial t^{*}} - V^{*}\frac{\partial}{\partial z^{*}}\right)\left(T^{*} - \frac{h_{fs}}{q_{s}}\varphi\right) + \mathbf{U}^{*}\cdot\nabla^{*}T^{*} = \kappa^{*}\nabla^{*2}T^{*}. \tag{19}
$$

Using κ^{*}/V^{*} for the length scale and κ^{*}/V^{*2} for the time scale we may proceed to non-dimensionalise the energy equation (16) as follows,

$$
\frac{V^{*2}}{\kappa^{*}}\left(\frac{\partial}{\partial t} - \frac{\partial}{\partial z}\right)\left(T^{*} - \frac{h_{fs}}{q_{s}}\varphi\right) + \frac{V^{*2}}{\kappa^{*}}\mathbf{U}\cdot\nabla T^{*} = \frac{V^{*2}}{\kappa^{*}}\nabla^{2}T^{*}, \tag{20}
$$

which when divided through by V^{*2}/κ^{*} yields,

$$
\left(\frac{\partial}{\partial t} - \frac{\partial}{\partial z}\right)\left(T^{*} - \frac{h_{fs}}{q_{s}}\varphi\right) + \mathbf{U}\cdot\nabla T^{*} = \nabla^{2}T^{*}. \tag{21}
$$

Using the following definition for the dimensional temperture,

$$
T^{*} = \left(T_{L}(c_{o}) - T_{E}\right)\theta + T_{L}(c_{o}) = \Delta T\,\theta + T_{L}, \tag{22}
$$

allows Eqn.(21) to be written as,

$$
\left(\frac{\partial}{\partial t} - \frac{\partial}{\partial z}\right)\left(\Delta T\theta - \frac{h_{fs}}{q_{s}}\varphi\right) + \mathbf{U}\cdot\nabla(\Delta T\theta) = \nabla^{2}(\Delta T\theta). \tag{23}
$$

Dividing Eqn.(23) by ΔT yields,

$$
\left(\frac{\partial}{\partial t} - \frac{\partial}{\partial z}\right)\left(\theta - St\varphi\right) + \mathbf{U}\cdot\nabla\theta = \nabla^{2}\theta, \tag{24}
$$

where $St = h_{fs}/(q_{s}\Delta T)$. Incidentally Eqn.(24) is identical to Eqn.(1.4).

The dimensional form of the solute balance equation is given as,

$$(1-\varphi)\frac{\partial c^*}{\partial \hat{t}^*} + \mathbf{U}^* \cdot \nabla^* T^* = \nabla^* \cdot \left(D_m \nabla^* T^*\right) + \left(c^* - c_s\right)\frac{\partial \varphi}{\partial \hat{t}^*}, \tag{25}$$

where D_m represents the solutal diffusivity and is given as,

$$D_m = (1-\varphi)D_f. \tag{26}$$

Rearranging Eqn.(25) yields,

$$\frac{\partial}{\partial \hat{t}^*}\left[(1-\varphi)c^* + c'_s\varphi\right] + \mathbf{U}^* \cdot \nabla^* c^* = D_f \nabla^* \cdot \left((1-\varphi)\nabla^* c^*\right). \tag{27}$$

Applying Eqn.(18) to Eqn.(27) to accommodate the translational effect of the solidifying front yields,

$$\left(\frac{\partial}{\partial t^*} - V^* \frac{\partial}{\partial z^*}\right)\left[(1-\varphi)c^* + c'_s\varphi\right] + \mathbf{U}^* \cdot \nabla^* c^* = D_f \nabla^* \cdot \left((1-\varphi)\nabla^* c^*\right). \tag{28}$$

Using κ^*/V^* for the length scale and κ^*/V^{*2} for the time scale we may proceed to non-dimensionalise the continuity equation as follows,

$$\frac{V^{*2}}{\kappa^*}\left(\frac{\partial}{\partial t} - \frac{\partial}{\partial z}\right)\left[(1-\varphi)c^* + c'_s\varphi\right] + \frac{V^{*2}}{\kappa^*}\mathbf{U} \cdot \nabla c^* = \frac{V^{*2}}{\kappa^{*2}}D_f\nabla \cdot \left((1-\varphi)\nabla c^*\right). \tag{29}$$

which when divided through by V^{*2}/κ^* yields,

$$\left(\frac{\partial}{\partial t} - \frac{\partial}{\partial z}\right)\left[(1-\varphi)c^* + c'_s\varphi\right] + \mathbf{U} \cdot \nabla c^* = \frac{D_f}{\kappa^*}D_f\nabla \cdot \left((1-\varphi)\nabla c^*\right). \tag{30}$$

Using the following definition for the dimensional concentration,

$$c^* = \left(c_o - c_E\right)\theta + c_o = \Delta c\,\theta + c_o, \tag{31}$$

and applying to Eqn.(30) yields the following,

$$\Delta c\left(\frac{\partial}{\partial t} - \frac{\partial}{\partial z}\right)\left[(1 - \varphi)\theta + \frac{c'_s - c_o}{c_o - c_E}\varphi\right] + \Delta c\,\mathbf{U}\cdot\nabla\theta = \Delta c\frac{D_f}{\kappa^*}D_f\nabla\cdot\left((1 - \varphi)\nabla\theta\right). \tag{32}$$

Dividing Eqn.(32) by Δc yields,

$$\left(\frac{\partial}{\partial t} - \frac{\partial}{\partial z}\right)\left[(1 - \varphi)\theta + \xi\varphi\right] + \mathbf{U}\cdot\nabla\theta = \frac{1}{Le}D_f\nabla\cdot\left((1 - \varphi)\nabla\theta\right), \tag{33}$$

where Le represents the Lewis number defined as $Le = \kappa^*/D_f$ and ξ represents the concentration ratio defined as,

$$\xi = \frac{c'_s - c_o}{c_o - c_E}. \tag{34}$$

In the case of solidifying binary alloys the value of Lewis number is very high, thus implying that the effects of the term on the right hand side of Eqn.(33) are very small. Eqn.(33) may be approximated as follows for very high Lewis numbers,

$$\left(\frac{\partial}{\partial t} - \frac{\partial}{\partial z}\right)\left[(1 - \varphi)\theta + \xi\varphi\right] + \mathbf{U}\cdot\nabla\theta = 0. \tag{35}$$

Eqn.(35) is identical to Eqn.(1.5).

The dimensional form of the Darcy equation may be written as follows,

$$\frac{1}{\phi}\frac{\partial \mathbf{U}^*}{\partial \hat{t}^*} + \frac{\mu^*}{K^*}\frac{1}{\rho^*}\mathbf{U}^* = -\frac{1}{\rho^*}\nabla^*p^* + \rho^*g^*\hat{\mathbf{e}}_g - \frac{1}{\phi}2\omega^*\hat{\mathbf{e}}_\omega \times \mathbf{U}^*. \tag{36}$$

A basic approximation of fluid mechanics is the Boussinesq approximation, which consists of setting $\rho^* = \rho_0^*$ except in buoyancy terms emanating from body forces in the Darcy equation. Similarly we may also assume that the porosity is constant everywhere in the Darcy equation, ie. $\phi = \phi_0$ (as was assumed in the continuity equation above), except in those terms containing permeability variations. Multiplying Eqn.(36) by $\rho_0^* K^*/\mu^*$, noting that $\nu^* = \mu^*/\rho_0^*$, accounting for the translational effects by using Eqn.(18), and implementing the above definitions for the density and porosity yields the following form of the Darcy equation,

$$\frac{K^*}{\nu^*\phi_0}\left(\frac{\partial}{\partial t^*} - V^*\frac{\partial}{\partial z^*}\right)\mathbf{U}^* + \mathbf{U}^* = -\frac{K^*}{\mu^*}\nabla^*p^* + \frac{K^*}{\mu^*}\left(\rho_f^* - \rho_0^*\right)g^*\hat{\mathbf{e}}_g - \frac{K^*}{\phi_0\nu^*}2\omega^*\hat{\mathbf{e}}_\omega \times \mathbf{U}^*. \tag{37}$$

Note that $\hat{\mathbf{e}}_g$ and $\hat{\mathbf{e}}_\omega$ represents the unit vectors for gravity and rotation. We follow Anderson & Wortser (1996) and use V^*, κ^*/V^*, κ^*/V^{*2} to scale the velocity, length and time scales, and $\kappa^*\mu^*/k_0$ to scale the pressure term, where κ^* is the thermal diffusivity of the liquid, μ^* is the dynamic viscosity and k_0 is a characteristic value of permeability in the mushy layer. Implementing these scales in Eqn.(1) and dividing by V^* yields and equation of the form,

$$\frac{K^*V^{*2}}{\kappa^*\nu^*\phi_0}\left(\frac{\partial}{\partial t} - \frac{\partial}{\partial z}\right)\mathbf{U} + \mathbf{U} = -\frac{K^*}{k_0}\nabla p + \frac{K^*}{\mu^*V^*}\left(\rho_f^* - \rho_0^*\right)g^*\hat{\mathbf{e}}_g - \frac{K^*}{\phi_0\nu^*}2\omega^*\hat{\mathbf{e}}_\omega \times \mathbf{U}. \tag{38}$$

Recalling the linear liquidus relation as presented in Eqn.(1.2) in Section 1.2, and using a density relation of the form $\rho^* - \rho_0^* = \rho_0^*\beta^*\left(c^* - c_0\right)$ for the case when solutal buoyancy

effects dominate over thermal buoyancy effects. This also implies that density is largely a function of composition than it is of temperature. In addition the linear liquidus relation provides an additional relation between the temperature and the composition which is given as $c^* - c_0 = \Delta c \theta$. Applying these results to Eqn.(38) yields the following form of the Darcy equation,

$$\frac{K^* V^{*2}}{\kappa^* v^* \phi_0}\left(\frac{\partial}{\partial t} - \frac{\partial}{\partial z}\right)U + U = -\frac{K^*}{k_0}\nabla p + \frac{K^*}{\mu^* V^*}\rho_0^*\beta^*\Delta c g^*\theta\hat{e}_g - \frac{K^*}{\phi_0 v^*}2\omega^*\hat{e}_\omega \times U. \qquad (39)$$

Multiply Eqn.(39) by $\Pi(\varphi) = k_0/K^*$ to yield,

$$\frac{k_0 V^{*2}}{\kappa^* v^* \phi_0}\left(\frac{\partial}{\partial t} - \frac{\partial}{\partial z}\right)U + \Pi(\varphi)U = -\nabla p + \frac{k_0\beta^*\Delta c g^*}{v^* V^*}\theta\hat{e}_g - \frac{k_0}{\phi_0 v^*}2\omega^*\hat{e}_\omega \times U. \qquad (40)$$

The thermal diffusion length spacing may be defined as $l_{\kappa^*} = \kappa^*/V^*$, which may be rearranged to obtain a velocity definition of the form $V^* = \kappa^*/l_{\kappa^*}$. Substituting this form in Eqn.(40) yields,

$$\frac{k_0\kappa^*}{l_{\kappa^*}^2 v^* \phi_0}\left(\frac{\partial}{\partial t} - \frac{\partial}{\partial z}\right)U + \Pi(\varphi)U = -\nabla p + \frac{k_0\beta^*\Delta c g^* l_{\kappa^*}}{v^*\kappa^*}\theta\hat{e}_g - \frac{2\omega^* k_0}{\phi_0 v^*}\hat{e}_\omega \times U. \qquad (41)$$

Eqn.(41) may be written in terms of dimensionless groups as follows,

$$\frac{1}{\chi_0}\left(\frac{\partial}{\partial t} - \frac{\partial}{\partial z}\right)U + \Pi(\varphi)U = -\nabla p + Ra_m\theta\hat{e}_g - Ta^{1/2}\hat{e}_\omega \times U. \qquad (42)$$

With reference to Eqn.(42), $\chi_0 = \phi_0 Pr\vartheta_0$, where ϕ_0 is the porosity, Pr is the Prandtl number and $\vartheta_0 = l_{\kappa^*}^2/k_0$ is the mobility ratio which may thought of as the square of the thermal length scale (on which the depth of the mushy layer depends) to the average

spacing between the dendrites within the mushy layer. This is very similar to the porous media Darcy number. The other dimensionless group identified in Eqn.(42) is the mushy layer Rayleigh number which is defined as $Ra_m = \beta^* \Delta cg^* k_0 l_\kappa / v^* \kappa^*$ that describes the buoyancy effects due to compostion differences. Finally the Taylor number that appears in Eqn.(42) is defined as $Ta = \left(2\omega^* k_0 / \phi_0 v^* \right)^2$ and describes the effect of rotation on the mushy layer.

The parameter χ_0 in Eqn.(42) usually assumes values that are large, thus implying that the contribution from the first term in Eqn.(42) is very small. This provides the justification for neglecting the time and space derivative from the Darcy equation. In some instances linked to modern porous media applications the value of χ_0 can become a unit order of magnitude or even smaller, in which case the time and space derivative term should be retained. In the current study we retain only the time derivative in the Darcy equation in order to allow for the possibility of overstable convection and will observe how the value of χ_0 affects the frequency of overstable solutions. The following truncated form of the Darcy equation results,

$$\frac{1}{\chi_0} \frac{\partial \mathbf{U}}{\partial t} + \Pi(\varphi)\mathbf{U} = -\nabla p + Ra_m \theta \hat{e}_g - Ta^{1/2} \hat{e}_\omega \times \mathbf{U} , \qquad (43)$$

which is identical to Eqn.(1.6) in Section1.2.

Appendix B : Derivation of the governing system of equations for Anderson & Worster's (1996) scaling

The system of governing equations analysed by Anderson & Worster (1996) was scaled in space, and time in terms of the dimensionless mushy layer growth parameter δ. The Rayleigh number, velocity and pressure were also scaled in terms this parameter. The parameter δ is the ratio between the height of the mushy layer and the thermal length scale (defined in Appendix A) and is sometimes referred to as the growth Peclet number. Worster scaled space and time as follows,

$$x\hat{\mathbf{e}}_x + y\hat{\mathbf{e}}_y + z\hat{\mathbf{e}}_z = \delta(\overline{x}\hat{\mathbf{e}}_x + \overline{y}\hat{\mathbf{e}}_y + \overline{z}\hat{\mathbf{e}}_z), \qquad t = \delta^2\overline{t} \tag{1a-b}$$

whilst the Rayleigh number, velocity and pressure were scaed as,

$$R^2 = \delta Ra_m, \qquad \mathbf{U} = \frac{R}{\delta}\overline{\mathbf{U}}, \quad p = R\overline{p}. \tag{2a-c}$$

These scalings were then applied to the continuity equation (1.3) to yield,

$$\overline{\nabla}\cdot\overline{\mathbf{U}} = 0, \tag{2d}$$

which is identical to Eqn.(2.3).

Now considering applying the scalings defined in (1a-b and 2a-c) to the heat balance equation yields,

$$\left(\frac{1}{\delta^2}\frac{\partial}{\partial\overline{t}} - \frac{1}{\delta}\frac{\partial}{\partial\overline{z}}\right)\left(\theta - \frac{\overline{S}}{\delta}\varphi\right) + \frac{R}{\delta^2}\overline{\mathbf{U}}\cdot\overline{\nabla}\theta = \frac{1}{\delta^2}\overline{\nabla}^2\theta. \tag{3}$$

Multiplying this equation by δ^2 yields,

$$\left(\frac{\partial}{\partial \bar{t}} - \delta \frac{\partial}{\partial \bar{z}}\right)\left(\theta - \frac{\bar{S}}{\delta}\varphi\right) + R\bar{U} \cdot \bar{\nabla}\theta = \bar{\nabla}^2\theta \ , \tag{4}$$

which is identical to Eqn.(2.4).

Applying the scalings given in Eqn.(1a-b) and Eqn.(2a-c) to the solute balance equation (1.5) yields,

$$\left(\frac{1}{\delta^2}\frac{\partial}{\partial \bar{t}} - \frac{1}{\delta}\frac{\partial}{\partial \bar{z}}\right)\left[(1-\varphi)\theta + \frac{c_S}{\delta}\varphi\right] + \frac{R}{\delta^2}\bar{U} \cdot \bar{\nabla}\theta = 0 \ . \tag{5}$$

Multiplying Eqn.(5) by δ^2 gives,

$$\left(\frac{\partial}{\partial \bar{t}} - \delta \frac{\partial}{\partial \bar{z}}\right)\left[(1-\varphi)\theta + \frac{c_S}{\delta}\varphi\right] + R\bar{U} \cdot \bar{\nabla}\theta = 0 \ , \tag{6}$$

which is identical to Eqn.(2.5).

Finally apply the scalings given by Eqn.(1a-b) and Eqn.(2a-c) to the Darcy equation (1.6) to gives,

$$\frac{R}{\delta^3 \chi_0}\frac{\partial \bar{U}}{\partial \bar{t}} + \Pi(\varphi)\frac{R}{\delta}\bar{U} = -\frac{R}{\delta}\bar{\nabla}\bar{p} - Ra_m \theta \hat{e}_z - Ta^{1/2}\hat{e}_z \times \frac{R}{\delta}\bar{U} \tag{7}$$

where $\hat{e}_g = -\hat{e}_z$ and $\hat{e}_\omega = \hat{e}_z$ by virtue of the system of co-ordinates presented in Figure 2a. Multiplying Eqn.(7) by δ/R yields,

$$\frac{1}{\delta^2 \chi_0}\frac{\partial \bar{U}}{\partial \bar{t}} + \Pi(\varphi)\bar{U} = -\bar{\nabla}\bar{p} - \frac{\delta Ra_m}{R}\theta \hat{e}_z - Ta^{1/2}\hat{e}_z \times \bar{U} \ . \tag{8}$$

Substituting $R^2 = \delta Ra_m$ in Eqn.(8) reduces its to,

$$\frac{1}{\delta^2 \chi_0} \frac{\partial \overline{U}}{\partial \bar{t}} + \Pi(\varphi)\overline{U} = -\overline{\nabla}\bar{p} - R\theta\hat{e}_z - Ta^{1/2}\hat{e}_z \times \overline{U} . \qquad (9)$$

The coefficient of the time derivative $1/\delta^2 \chi_0$ may be simplified by using the definitions for δ and χ_0. Knowing that $\delta = H^*/l_{\kappa^*}$ and $\chi_0 = \phi_0 Pr \vartheta_0$ (where $\vartheta_0 = l_{\kappa^*}^2/k_0$) and introducing in the expression for $1/\delta^2 \chi_0$ yields,

$$\frac{1}{\delta^2 \chi_0} = \frac{l_{\kappa^*}^2}{H^{*2}} \frac{k_0}{\phi_0 Pr l_{\kappa^*}^2} = \frac{k_0}{H^{*2}\phi_0 Pr} = \frac{Da}{\phi_0 Pr} = \frac{1}{\chi} . \qquad (10)$$

where $\chi = Pr \phi_0/Da$. Substituting the result of Eqn.(10) in Eqn.(9) yields,

$$\frac{1}{\chi} \frac{\partial \overline{U}}{\partial \bar{t}} + \Pi(\varphi)\overline{U} = -\overline{\nabla}\bar{p} - R\theta\hat{e}_z - Ta^{1/2}\hat{e}_z \times \overline{U} , \qquad (11)$$

which is identical to Eqn.(2.6).

It should be noted that Vadasz(1998) was the first to point out the scaling $\chi = \phi_0 Pr/Da$. The parameter Da refers to the Darcy number, which is very similar to the mobility ratio the only difference being that it is the reciprocal of the mobility ratio with the thermal length scale being replaced by the mushy layer height.

Appendix C : Derivation of the Basic solution

The basic flow solution to the system represents flow corresponding to the conduction solution. At a later disturbances in the form of perturbations will be applied to the system and the stability thereof will be investigated. In order to establish the basic flow we need to analyse the equation set corresponding to the motionless state where the flow velocity is zero and the temperature and solid fraction is horizontally uniform. For this state, the governing system that needs to be solved may be presented as,

$$-\delta \frac{d}{d\bar{z}}\left[\theta_B - \frac{\bar{S}}{\delta}\varphi_B\right] = \frac{d^2\theta_B}{d\bar{z}^2} \tag{1}$$

$$-\delta \frac{d}{d\bar{z}}\left[(1-\varphi_B)\theta_B + \frac{c_S}{\delta}\varphi_B\right] = 0 \tag{2}$$

$$-\frac{d\bar{p}_B}{d\bar{z}} - R\theta_B = 0, \tag{3}$$

where the subscript "B" refers to the basic state. Eqns.(1-3) are subject to the boundary conditions $\theta_B(0) = 0$, $\theta_B(1) = -1$ and $\varphi_B(1) = 0$ at each order in δ. It can be observed that the equations system presented in Eqns.(1-2) represents a coupled non linear system. A solution in terms of the parameter δ is anticipated. This may be achieved by developing asymtotic expansions for the basic temperature and the solid fraction in terms of the small parameter δ where $\delta \ll 1$. The expansions for the basic temperature and solid fraction in terms of δ may be presented as,

$$\theta_B = \theta_{B0}(\bar{z}) + \delta\theta_{B1}(\bar{z}) + \delta^2\theta_{B2}(\bar{z}) + O(\delta^3) \tag{4}$$

$$\varphi_B = \varphi_{B0}(\bar{z}) + \delta\varphi_{B1}(\bar{z}) + \delta^2\varphi_{B2}(\bar{z}) + O(\delta^3). \tag{5}$$

The idea is to solve for the solid fraction and the temperature at each order in δ. The final solution is then presented as a function of the solutions evaluated at each order and δ.

To order $O(\delta^0)$ the governing system is given as,

$$-\overline{S}\frac{d\varphi_{B0}}{d\overline{z}} = \frac{d^2\theta_{B0}}{d\overline{z}^2} \tag{6}$$

$$-c_s\frac{d\varphi_{B0}}{d\overline{z}} = 0. \tag{7}$$

Substituting Eqn.(7) in Eqn.(6) yields,

$$\frac{d^2\theta_{B0}}{d\overline{z}^2} = 0, \tag{8}$$

which upon solving subject to the boundary conditions stated earlier yields the following solution for the basic temperature at $O(\delta^0)$,

$$\theta_{B0} = \overline{z} - 1. \tag{9}$$

Similarly the solution for the solid fraction at this order is given as,

$$\varphi_{B0} = 0. \tag{10}$$

We now proceed to solve the system of equations for the basic flow to the next order in δ. The governing equations to order $O(\delta)$ is given in terms of the lower order $O(\delta^0)$ solutions as follows,

$$\frac{d^2\theta_{B1}}{d\bar{z}^2} = \bar{S}\frac{d\varphi_{B1}}{d\bar{z}} - \frac{d\theta_{B0}}{d\bar{z}} \qquad (11)$$

$$\frac{d\varphi_{B1}}{d\bar{z}} = -\frac{1}{c_S}\frac{d\theta_{B0}}{d\bar{z}}. \qquad (12)$$

Substituting the $O(\delta^0)$ solutions in Eqns.(11-12) and decoupling the equation to obtain a single differential equation for the basic temperature as,

$$\frac{d^2\theta_{B1}}{d\bar{z}^2} = -\Omega. \qquad (13)$$

Solving Eqn.(13) subject to the stated boundary conditions yields,

$$\theta_{B1} = -\frac{\Omega}{2}(\bar{z}^2 - \bar{z}). \qquad (14)$$

Solving Eqn.(12) by similar methods yields the following solution for the solid fraction at this order,

$$\varphi_{B1} = -\frac{1}{c_S}(\bar{z} - 1). \qquad (15)$$

Now we present the governing system of equations for the temperature and solid fraction to order $O(\delta^2)$ in terms of the solutions evaluated at the lower orders,

$$\frac{d^2\theta_{B2}}{d\bar{z}^2} = \bar{S}\frac{d\varphi_{B2}}{d\bar{z}} - \frac{d\theta_{B1}}{d\bar{z}} \qquad (16)$$

$$-c_S\frac{d\varphi_{B2}}{d\bar{z}} = \frac{d\theta_{B1}}{d\bar{z}} - \varphi_{B1}\frac{d\theta_{B0}}{d\bar{z}} - \theta_{B0}\frac{d\varphi_{B1}}{d\bar{z}}. \qquad (17)$$

In this case we solve for the solid fraction first at order $O(\delta^2)$. Substituting the lower order solutions in Eqn.(17), then integrating with respect to z, and finally solving for the integration constant by applying the given boundary conditions yields the following solution for the solid fraction at this order,

$$\varphi_{B2} = \frac{1}{c_S}\left[-\frac{(\bar{z}-1)^2}{c_S} + \frac{\Omega}{2}(\bar{z}^2 - \bar{z}) \right].$$

(18)

Now we concentrate on evaluating the basic temperature at this order. Note that integrating Eqn.(16) once with respect to $\bar{z}$ yields,

$$\frac{d\theta_{B2}}{d\bar{z}} = \overline{S}\varphi_{B2} - \theta_{B1} + C_{\delta 2},$$

(19)

where $C_{\delta 2}$ is the integration constant at this order. Now by substituting Eqn.(18) and the temperature solution given by Eqn.(14) in Eqn.(19), integrating the result and applying the boundary conditions given earlier, yields,

$$\theta_{B2} = \frac{\Omega^2}{2}\left(\frac{1}{3}\bar{z}^3 - \frac{1}{2}\bar{z}^2 \right) - \frac{\overline{S}}{c_S^2}\left(\frac{1}{3}\bar{z}^3 - \bar{z}^2 \right) + \frac{1}{3}\left(2\frac{\overline{S}}{c_S^2} + \frac{1}{4} \right)\bar{z}.$$

(20)

The full solutions for both the basic temperature and the solid fraction is given by substituting the solutions evaluated for each order in δ in Eqns.(4-5) to yield,

$$\theta_B(\bar{z}) = (\bar{z}-1) + \delta\left[-\frac{\Omega}{2}(\bar{z}^2 - \bar{z}) \right] +$$

$$\delta^2\left[\frac{\Omega^2}{2}\left(\frac{1}{3}\bar{z}^3 - \frac{1}{2}\bar{z}^2 \right) - \frac{\overline{S}}{c_S^2}\left(\frac{1}{3}\bar{z}^3 - \bar{z}^2 \right) + \frac{1}{3}\left(2\frac{\overline{S}}{c_S^2} + \frac{1}{4}\Omega^2 \right)\bar{z} \right]$$

(21)

168

$$\varphi_B(\bar{z}) = -\delta \frac{(\bar{z}-1)}{c_S} + \delta^2 \left[-\frac{(\bar{z}-1)^2}{c_S^2} + \frac{\Omega}{2c_S}(\bar{z}^2 - \bar{z}) \right]. \tag{22}$$

Eqns.(21-22) are identical to the solution for the basic temperature and solid fraction as presented in Eqns.(2.15-2.16).

Appendix D : (a) Presentation of the Darcy equation in terms of the vertical component of velocity

(b) Derivation of the perturbed heat balance, solute balance and modified Darcy equation

(a) Presentation of the Darcy equation in terms of the vertical component of velocity

Before presenting a derivation of the perturbed system of equations, we need to modify the Darcy equation to a form that allows for ease of analysis. We proceed to develop this desired form of the Darcy equation by applying the curl operator ($\nabla \times$) Eqn.(2.6) in order to eliminate the pressure terms as follows,

$$\frac{1}{\chi}\frac{\partial(\nabla \times \overline{U})}{\partial \bar{t}} + \nabla \times \left(\Pi(\varphi)\overline{U}\right) = -R\left(\nabla \times \theta\hat{e}_z\right) - Ta^{1/2}\nabla \times \left(\hat{e}_z \times \overline{U}\right). \tag{1}$$

The theorem $\nabla \times (\nabla \bar{p}) = 0$ was used to eliminate the pressure terms in Eqn.(1). Noting that $\omega = \nabla \times \overline{U}$ and acknowledging that $\Pi(\varphi)$ is a function of $\bar{z}$ only, allows one to represent Eqn.(1) as,

$$\frac{1}{\chi}\frac{\partial\omega}{\partial\bar{t}} + \begin{vmatrix} \hat{e}_x & \hat{e}_y & \hat{e}_z \\ \partial/\partial\bar{x} & \partial/\partial\bar{y} & \partial/\partial\bar{z} \\ \Pi(\varphi)\bar{u} & \Pi(\varphi)\bar{v} & \Pi(\varphi)\bar{w} \end{vmatrix} = -R\begin{vmatrix} \hat{e}_x & \hat{e}_y & \hat{e}_z \\ \partial/\partial\bar{x} & \partial/\partial\bar{y} & \partial/\partial\bar{z} \\ 0 & 0 & \theta \end{vmatrix} - Ta^{1/2}\nabla \times \begin{vmatrix} \hat{e}_x & \hat{e}_y & \hat{e}_z \\ 0 & 0 & 1 \\ u & v & w \end{vmatrix}. \tag{2}$$

Performing the operations denoted in the matrices yields,

$$\frac{1}{\chi}\frac{\partial\omega}{\partial\bar{t}} + \Pi(\varphi)\left[\frac{\partial\bar{v}}{\partial\bar{x}} - \frac{\partial\bar{u}}{\partial\bar{y}}\right]\hat{e}_x - \Pi(\varphi)\left[\frac{\partial\bar{w}}{\partial\bar{x}} - \frac{\partial\bar{u}}{\partial\bar{z}}\right]\hat{e}_y + \Pi(\varphi)\left[\frac{\partial\bar{v}}{\partial\bar{x}} - \frac{\partial\bar{u}}{\partial\bar{y}}\right]\hat{e}_z -$$

$$\frac{d\Pi}{d\bar{z}}\bar{v}\hat{e}_x + \frac{d\Pi}{d\bar{z}}\bar{u}\hat{e}_y = -R\left[\frac{\partial\theta}{\partial\bar{y}}\hat{e}_x - \frac{\partial\theta}{\partial\bar{x}}\hat{e}_y\right] + Ta^{1/2}\frac{\partial\overline{U}}{\partial\bar{z}} \tag{3}$$

170

It can be seen that the three terms following the time derivative in Eqn.(3) is simply the vorticity definition in expanded notation. Eqn.(3) may simply be written as,

$$\frac{1}{\chi}\frac{\partial \omega}{\partial \bar{t}} + \Pi(\varphi)\omega + \frac{d\Pi}{d\bar{z}}\left[\bar{u}\hat{e}_y - \bar{v}\hat{e}_x\right] - Ta^{1/2}\frac{\partial \overline{U}}{\partial \bar{z}} = -R\left[\frac{\partial \theta}{\partial \bar{y}}\hat{e}_x - \frac{\partial \theta}{\partial \bar{x}}\hat{e}_y\right]. \tag{4}$$

Eqn.(4) is identical to the equation presented in Eqn.(2.17). It may be noticed from Eqn.(4) that the z-component is independent of temperature. This component is of importance and will be used later in another computation. Writing the z-component of Eqn.(4) as,

$$\left[\frac{1}{\chi}\frac{\partial}{\partial \bar{t}} + \Pi(\varphi)\right]\omega_z - Ta^{1/2}\frac{\partial \overline{w}}{\partial \bar{z}} = 0, \tag{5}$$

Rewriting Eqn.(5) for the vorticity as follows,

$$\left[\frac{1}{\chi}\frac{\partial}{\partial \bar{t}} + \Pi(\varphi)\right]\omega_z = Ta^{1/2}\,\partial\overline{w}/\partial\bar{z}, \tag{6}$$

which is identical to Eqn.(2.18). Note that, in Eqn.(6), ω_z represents the z-component of the vorticity vector.

Applying the curl operator once more, on Eqn.(4)

$$\frac{1}{\chi}\frac{\partial(\nabla \times \omega)}{\partial \bar{t}} + \nabla \times \left[\Pi(\varphi)\omega\right] + \nabla \times \left(\frac{d\Pi}{d\bar{z}}\left[\bar{u}\hat{e}_y - \bar{v}\hat{e}_x\right]\right) - Ta^{1/2}\frac{\partial(\nabla \times \overline{U})}{\partial \bar{z}} = -R\nabla \times \left[\frac{\partial \theta}{\partial \bar{y}}\hat{e}_x - \frac{\partial \theta}{\partial \bar{x}}\hat{e}_y\right]$$

$$\tag{7}$$

Eqn.(7) may be written in matrix notation as,

$$
\frac{1}{\chi}\frac{\partial}{\partial \bar{t}}
\begin{vmatrix}
\hat{e}_x & \hat{e}_y & \hat{e}_z \\
\partial/\partial\bar{x} & \partial/\partial\bar{y} & \partial/\partial\bar{z} \\
\omega_x & \omega_y & \omega_z
\end{vmatrix}
+
\begin{vmatrix}
\hat{e}_x & \hat{e}_y & \hat{e}_z \\
\partial/\partial\bar{x} & \partial/\partial\bar{y} & \partial/\partial\bar{z} \\
\Pi(\varphi)\omega_x & \Pi(\varphi)\omega_y & \Pi(\varphi)\omega_y
\end{vmatrix}
+
\begin{vmatrix}
\hat{e}_x & \hat{e}_y & \hat{e}_z \\
\partial/\partial\bar{x} & \partial/\partial\bar{y} & \partial/\partial\bar{z} \\
-\bar{v}\,d\Pi/d\bar{z} & \bar{u}\,d\Pi/d\bar{z} & 0
\end{vmatrix}
-
$$

$$
- Ta^{1/2}\frac{\partial\omega}{\partial\bar{z}} = R\frac{\partial^2\theta}{\partial\bar{x}\partial\bar{z}}\hat{e}_x - R\frac{\partial^2\theta}{\partial\bar{y}\partial\bar{z}}\hat{e}_y + R\left[\frac{\partial^2\theta}{\partial\bar{x}^2} + \frac{\partial^2\theta}{\partial\bar{y}^2}\right]\hat{e}_z. \tag{8}
$$

Evaluating the above matrices and considering only the z-component of the result yields,

$$
\left[\frac{1}{\chi}\frac{\partial}{\partial\bar{t}} + \Pi(\varphi)\right]\left(\frac{\partial\omega_y}{\partial\bar{x}} - \frac{\partial\omega_x}{\partial\bar{y}}\right) + \frac{d\Pi}{d\bar{z}}\left[\frac{\partial\bar{u}}{\partial\bar{x}} + \frac{\partial\bar{v}}{\partial\bar{y}}\right] - Ta^{1/2}\frac{\partial\omega_z}{\partial\bar{z}} = R\left[\frac{\partial^2\theta}{\partial\bar{x}^2} + \frac{\partial^2\theta}{\partial\bar{y}^2}\right]. \tag{9}
$$

Noting that $\omega_x = \partial\bar{w}/\partial\bar{y} - \partial\bar{v}/\partial\bar{z}$, $\omega_y = -\partial\bar{w}/\partial\bar{x} + \partial\bar{u}/\partial\bar{z}$ and recalling from the continuity equation that $\partial\bar{w}/\partial\bar{z} = -\partial\bar{u}/\partial\bar{x} - \partial\bar{v}/\partial\bar{y}$ yields upon substitution in Eqn.(9) the following equation,

$$
-\left[\frac{1}{\chi}\frac{\partial}{\partial\bar{t}} + \Pi(\varphi)\right]\left(\frac{\partial^2\bar{w}}{\partial\bar{x}^2} + \frac{\partial^2\bar{w}}{\partial\bar{y}^2} + \frac{\partial^2\bar{w}}{\partial\bar{z}^2}\right) - \frac{d\Pi}{d\bar{z}}\frac{\partial\bar{w}}{\partial\bar{x}} - Ta^{1/2}\frac{\partial\omega_z}{\partial\bar{z}} = R\left[\frac{\partial^2\theta}{\partial\bar{x}^2} + \frac{\partial^2\theta}{\partial\bar{y}^2}\right]. \tag{10}
$$

Using the definition of vertical component of the vorticity given by Eqn.(6) above and noting that $\nabla^2\bar{w} = \partial^2\bar{w}/\partial\bar{x}^2 + \partial^2\bar{w}/\partial\bar{y}^2 + \partial^2\bar{w}/\partial\bar{z}^2$ and $\nabla^2\theta_H = \partial^2/\partial\bar{x}^2 + \partial^2/\partial\bar{y}^2$ allows Eqn.(10) to be written in the form,

$$
\left[\frac{1}{\chi}\frac{\partial}{\partial\bar{t}} + \Pi(\varphi)\right]^2\nabla^2\bar{w} + \frac{d\Pi}{d\bar{z}}\frac{\partial\bar{w}}{\partial\bar{x}}\left[\frac{1}{\chi}\frac{\partial}{\partial\bar{t}} + \Pi(\varphi)\right] + Ta\frac{\partial^2\bar{w}}{\partial\bar{z}^2} + R\left[\frac{1}{\chi}\frac{\partial}{\partial\bar{t}} + \Pi(\varphi)\right]\nabla_H^2\theta = 0. \tag{11}
$$

172

Eqn.(11) resembles the final form of the modified form of the Darcy equation that will henceforth be used in the curreny study. We may now proceed to propose the perturbed system of governing equations.

(b) Derivation of the perturbed heat balance, solute balance and modified Darcy equation

For the derivation of the perturbation equations we adopt normal mode expansions for the temperature, solid fraction and velocity as,

$$\theta = \theta_B + \varepsilon\theta_1 = \theta_B + \varepsilon\hat{\theta}(\bar{z})e^{\sigma\bar{t}}e^{i(s_x\bar{x}+s_y\bar{y})} \tag{12}$$

$$\varphi = \varphi_B + \varepsilon\varphi_1 = \varphi_B + \varepsilon\hat{\varphi}(\bar{z})e^{\sigma\bar{t}}e^{i(s_x\bar{x}+s_y\bar{y})} \tag{13}$$

$$\overline{U} = 0 + \varepsilon\overline{U}_1 = 0 + \varepsilon\hat{\overline{U}}(\bar{z})e^{\sigma\bar{t}}e^{i(s_x\bar{x}+s_y\bar{y})} \ . \tag{14}$$

Applying the expansions given in (12-14) to the heat balance equation (2.4) yields the following perturbed to order ,

$$\left(\frac{\partial}{\partial\bar{t}} - \delta\frac{\partial}{\partial\bar{z}}\right)\mathbf{1}\left[\theta_B + \varepsilon\theta_1 - \frac{\overline{S}}{\delta}(\varphi_B + \varepsilon\varphi_1)\right] + \mathbf{Re}\overline{U}_1\nabla(\theta_B + \varepsilon\theta_1) = \nabla^2(\theta_B + \varepsilon\theta_1), \tag{15}$$

Neglecting the $O(\varepsilon^2)$ and presenting the heat balance equation to order $O(\varepsilon)$ yields,

$$\left(\frac{\partial}{\partial\bar{t}} - \delta\frac{\partial}{\partial\bar{z}}\right)\left[\theta_1 - \frac{\overline{S}}{\delta}\varphi_1\right] + \mathbf{R}\overline{w}_1 D\theta_B = \nabla^2\theta_1, \tag{16}$$

which after applying the definitions for the disturbed temperature, solid fraction and velocity as presented in Eqns.(12-14) at order $O(\varepsilon)$ yields the following form of the heat balance equation,

$$(\sigma - \delta D)\left[\hat{\theta} - \frac{\overline{S}}{\delta}\hat{\phi}\right] + R\hat{\overline{w}}D\theta_B = (D^2 - s^2)\hat{\theta}. \tag{17}$$

Incidentally, Eqn.(17) is identical to Eqn.(2.23).

Apply (12-14) to the solute balance equation (2.5) and using the sequence of steps outlined above yields,

$$(\sigma - \delta D)\left[(1 - \phi_B)\hat{\theta} - \theta_B\hat{\phi} + \frac{c_S}{\delta}\hat{\phi}\right] + R\hat{\overline{w}}D\theta_B = 0, \tag{18}$$

where the $O(\epsilon^2)$ terms have been neglected and the terms with the subscripts "B" refers to the basic solution. Eqn.(18) is identical to Eqn.(2.24).

Now apply the expansions (12-14) to the Darcy Equation given by Eqn.(11) and use exactly the same computation procedure as that outlined for the heat balance equation above to easily give the following disturbed form of the equation,

$$\left[\frac{\sigma}{\chi} + \Pi(\phi)\right]^2 (D^2 - s^2)\hat{\overline{w}} + \left[\frac{\sigma}{\chi} + \Pi(\phi)\right]\left[D\Pi\ D\hat{\overline{w}} - s^2R\hat{\theta}\right] + TaD^2\hat{\overline{w}} = 0. \tag{19}$$

Note that in Eqns.(15-19) that $D = d/d\overline{z}$ and $s^2 = s_x^2 + s_y^2$. Eqn.(19) is identical to Eqn.(2.25).

174

Appendix E : Derivation of the governing system of partial differential equations for the $O(\delta^0)$ case for Anderson & Worster's (1996) scaling

In order to derive the equations to order $O(\delta^0)$ we first propose an expansion of the perturbed quatities in terms of the parameter δ as follows,

$$\sigma = \sigma_{00} + \delta\sigma_{01} \tag{1}$$

$$R = R_{00} + \delta R_{01} \tag{2}$$

$$\hat{\theta} = \theta_{00} + \delta\theta_{01} \tag{3}$$

$$\hat{\varphi} = \varphi_{00} + \delta\varphi_{01} \tag{4}$$

$$\hat{\overline{w}} = w_{00} + \delta w_{01}, \tag{5}$$

where the parameter $\delta << 1$. Introducing the expansions (1-5) in the perturbed heat balance equation (2.23) yields,

$$\left(\sigma_{00} + \delta\sigma_{01} - \delta D\right)\left[\theta_{00} + \delta\theta_{01} - \frac{\overline{S}}{\delta}\left(\varphi_{00} + \delta\varphi_{01}\right)\right] + \left(R_{00} + \delta R_{01}\right)\left(w_{00} + \delta w_{01}\right)D\theta_B =$$

$$\left(D^2 - s^2\right)\left(\theta_{00} + \delta\theta_{01}\right) \tag{6}.$$

Firstly it is interesting to note that Eqn.(6) contains an $O(\delta^{-1})$ form which is of the form,

$$\sigma_{00}\overline{S}\varphi_{00} = 0 \tag{7}$$

175

The solution to Eqn.(7) is simply taken to assume the form $\sigma_{00} = \sigma_{r0} + i\sigma_{i0} = 0$. Using this solution and considering Eqn.(6) to $O(\delta^0)$ yields the following form of the heat balance equation,

$$\left(D^2 - s^2\right)\theta_{00} = \overline{S}\left(D - \sigma_{01}\right)\varphi_{00} + R_{00}w_{00}D\theta_{B0}, \tag{8}$$

where $\sigma_{01} = \sigma_{r1} + i\sigma_{i1}$. Adopting exactly the same sequence of steps used to compute the heat balance equation to order $O(\delta^0)$, we proceed to develop the solute balance equation from Eqn.(2.24) as,

$$c_S\left(\sigma_{01} - D\right)\varphi_{00} + R_{00}w_{00}D\theta_{B0} = 0. \tag{9}$$

For the Darcy equation we assume a definition for the permeability to be of the form, $\Pi(\varphi) = 1 + \delta\varphi_{B1}K_1$, where $\varphi_{B1} - (\overline{z} - 1)/c_S$ is the solid fraction at order $O(\delta)$ for the basic state solid fraction. To order $O(\delta^0)$ the permeability is uniform and $\Pi(\varphi) = 1$ is used in the the Darcy equation. Applying this permeability definition and adopting exactly the same approach as that used to evaluate the heat and solute balance equations to this order, yields the following form of the Darcy equation to order $O(\delta^0)$,

$$\left(D^2 - s^2\right)w_{00} - s^2R_{00}\theta_{00} + TaD^2w_{00} = 0. \tag{10}$$

We notice that Eqn.(8) and Eqn.(9) are coupled in terms temperature, solid fraction and the vertical component of the velocity. By writing Eqn.(9) as,

$$\left(D - \sigma_{01}\right)\varphi_{00} = \frac{R_{00}w_{00}D\theta_{B0}}{c_S}. \tag{11}$$

Substituting Eqn.(11) in Eqn.(8) yields an equation of the form,

$$\left(D^2 - s^2\right)\theta_{00} = \frac{\overline{S}}{c_S} R_{00} W_{00} D\theta_{B0} + R_{00} W_{00} D\theta_{B0}. \tag{12}$$

Refining Eqn.(12) further as follows,

$$\left(D^2 - s^2\right)\theta_{00} = \left(1 + \frac{\overline{S}}{c_S}\right) R_{00} W_{00} D\theta_{B0} = \Omega R_{00} W_{00} D\theta_{B0}, \tag{13}$$

where $\Omega = 1 + \overline{S}/c_S$. Noting that $D\theta_{B0} = 1$, the modified heat balance equation (13), the solute balance equation (9) and the Darcy equation (10) may be presented as,

$$\left(D^2 - s^2\right)\theta_{00} - \Omega R_{00} W_{00} = 0 \tag{14}$$

$$c_S\left(\sigma_{rl} + i\sigma_{il} - D\right)\varphi_{00} + R_{00} W_{00} = 0 \tag{15}$$

$$\left(D^2 - s^2\right)W_{00} - s^2 R_{00}\theta_{00} + TaD^2 W_{00} = 0, \tag{16}$$

which is identical to the system of equations presented in Eqns.(2.34-2.36).

Appendix F : Derivation of the temperature, solid fraction, and vertical component of velocity at $O(\delta^0)$ for Anderson & Worster's (1996) scaling

The solutions to the system of equations (2.34-2.36) is provided. This system of equations is given as,

$$\left(D^2 - s^2\right)\theta_{00} - \Omega R_{00} w_{00} = 0 \tag{1}$$

$$c_S\left(\sigma_{r1} + i\sigma_{i1} - D\right)\varphi_{00} + R_{00} w_{00} = 0 \tag{2}$$

$$\left(D^2 - s^2\right)w_{00} - s^2 R_{00}\theta_{00} + TaD^2 w_{00} = 0. \tag{3}$$

Following Anderson & Worster (1996), we conjecture a solution for the temperature which is of the form,

$$\theta_{00} = -A_{00}\sin(\pi\overline{z}), \tag{4}$$

and satisfies the imposed boundary conditions. Substituting Eqn.(4) in Eqn.(1) and performing the respective derivatives with respect to $\overline{z}$ yields the following expression for the vertical component of the velocity,

$$w_{00} = \frac{\left(\pi^2 + s^2\right)}{\Omega R_{00}} A_{00}\sin(\pi\overline{z}) = B_{00}\sin(\pi\overline{z}), \tag{5}$$

which is identical to Eqn.(2.39), where,

$$B_{00} = \frac{\left(\pi^2 + s^2\right)}{\Omega R_{00}} A_{00}. \tag{6}$$

It can be noted that coefficient relation given by Eqn.(6) is identical to Eqn.(2.42). We may now proceed to establish the solute balance solution at this order using the solutions evaluated for the temperature and the vertical component of velocity as given by Eqn.(4) and Eqn.(5).

From Eqn.(2), the solute balance equation, we have,

$$c_S\left(\sigma_{rl} + i\sigma_{il} - D\right)\varphi_{00} = -R_{00}w_{00},\tag{7}$$

which takes the following form after substituting for the vertical component of velocity as given by Eqn.(5),

$$c_S\left(D - \left(\sigma_{rl} + i\sigma_{il}\right)\right)\varphi_{00} = \frac{\left(\pi^2 + s^2\right)}{\Omega}A_{00}\sin(\pi\bar{z})\quad.\tag{8}$$

Eqn.(8) represents a non-homogenous ordinary differential equation for the solid fraction. We proceed by first solving the homogenous part,

$$\left(D - \left(\sigma_{rl} + i\sigma_{il}\right)\right)\varphi_{00,h} = 0,\tag{9}$$

which may be written as,

$$\frac{d\varphi_{00,h}}{\varphi_{00,h}} = \left(\sigma_{rl} + i\sigma_{il}\right)d\bar{z}.\tag{10}$$

The solution to this equation is simply given as,

$$\varphi_{00,h} = C_h e^{(\sigma_{rl} + i\sigma_{il})\bar{z}},\tag{12}$$

where C_h is simply an integration constant that will be solved for based on the full solution of the solid fraction in relation to the imposed boundary condition. We now move on to seek a solution for the non-homgenous part of Eqn.(8).

We proceed by proposing a probable particular solution solution to Eqn.(8). This is given as,

$$\varphi_{00,p} = A_{p0}\sin(\pi\bar{z}) + B_{p0}\cos(\pi\bar{z}). \tag{13}$$

The non-homgenous equation for the solid fraction is given as,

$$c_s\left(\frac{d}{d\bar{z}} - \left(\sigma_{rl} + i\sigma_{il}\right)\right)\varphi_{00,p} = \frac{\left(\pi^2 + s^2\right)}{\Omega}A_{00}\sin(\pi\bar{z}). \tag{14}$$

Substituting Eqn.(13) in Eqn.(14), performing the required derivatives and equating the like trigonometric terms, yields the following relationships for the coefficients,

$$A_{p0} = \frac{\sigma_{rl} + i\sigma_{il}}{\pi}B_{p0} \tag{15}$$

$$B_{p0} = -\frac{\pi\left(\pi^2 + s^2\right)}{\Omega c_s\left[\pi^2 + \left(\sigma_{rl} + i\sigma_{il}\right)^2\right]}A_{00}. \tag{16}$$

Noting that the full solution to the solid fraction is given by $\varphi_{00} = \varphi_{00,h} + \varphi_{00,p}$, and using the coefficients evaluated in Eqns.(15-16) together with the homogenous solution (12) and the particular solution (13) yield the following form of the solid fraction,

$$\varphi_{00} = C_h e^{(\sigma_{rl} + i\sigma_{il})\bar{z}} + \frac{\sigma_{rl} + i\sigma_{il}}{\pi}B_{0p}\sin(\pi\bar{z}) + B_{0p}\cos(\pi\bar{z}). \tag{17}$$

Applying the boundary condition $\varphi_{00}(1) = 0$ to Eqn.(17) yields the following relation between the coefficients in Eqn.(17),

$$C_h = B_{0p} e^{-(\sigma_{rl} + i\sigma_{il})}.$$ (18)

Substituting the relation given in Eqn.(18) in Eqn.(17) and using the coefficient relation given in Eqn.(16) gives the following full solution for the solid fraction,

$$\varphi_{00} = -C_{00}\left[e^{(\sigma_{rl} + i\sigma_{il})(\bar{z}-1)} + \cos(\pi\bar{z}) + \frac{\sigma_{rl} + i\sigma_{il}}{\pi} \sin(\pi\bar{z}) \right],$$ (19)

where

$$C_{00} = \frac{\pi(\pi^2 + s^2)}{\Omega c_s\left[\pi^2 + (\sigma_{rl} + i\sigma_{il})^2 \right]} A_{00}.$$ (20)

Eqn.(19) is identical to Eqn.(2.40) whilst Eqn.(20) is identical to Eqn.(2.43). Substituting the solutions given by Eqns.(5-6) in Eqn.(3) and using the amplitude relation given in Eqn.(6) yields the following relation for the Rayleigh number (after minor algebraic manipulation);

$$R_{00}^2 = \frac{(\pi^2 + s^2)(\pi^2 + s^2 + \pi^2 Ta)}{\Omega s^2}.$$ (21)

Eqn.(21) is identical to Eqn.(2.41)

Appendix G : Derivation of the governing system of partial differential equations for the $O(\delta^1)$ case for Anderson & Worster's (1996) scaling

In order to derive the equations to order $O(\delta^0)$ we first propose an expansion of the perturbed quatities in terms of the parameter δ as follows,

$$\sigma = \sigma_{00} + \delta\sigma_{01} \tag{1}$$

$$R = R_{00} + \delta R_{01} \tag{2}$$

$$\hat{\theta} = \theta_{00} + \delta\theta_{01} \tag{3}$$

$$\hat{\varphi} = \varphi_{00} + \delta\varphi_{01} \tag{4}$$

$$\hat{\overline{w}} = w_{00} + \delta w_{01}, \tag{5}$$

where the parameter $\delta \ll 1$. Introducing the expansions (1-5) in the perturbed heat balance equation (2.23) yields,

$$\left(\sigma_{00} + \delta\sigma_{01} - \delta D\right)\left[\theta_{00} + \delta\theta_{01} - \frac{\overline{S}}{\delta}\left(\varphi_{00} + \delta\varphi_{01}\right)\right] + \left(R_{00} + \delta R_{01}\right)\left(w_{00} + \delta w_{01}\right)D\theta_B =$$

$$\left(D^2 - s^2\right)\left(\theta_{00} + \delta\theta_{01}\right) \tag{6}.$$

Taking $\sigma_{00} = \sigma_{r0} + i\sigma_{i0} = 0$ and considering Eqn.(6) to $O(\delta^1)$ yields the following form of the heat balance equation after minor algebraic manipulation,

$$\left(D^2 - s^2\right)\theta_{01} + \overline{S}\left(\sigma_{01} - D\right)\varphi_{01} - R_{00}W_{01} = \left(\sigma_{01} - D\right)\theta_{00} + R_{00}W_{00}D\theta_{B1} + R_{01}W_{00}, \quad (7)$$

where $\sigma_{01} = \sigma_{r1} + i\sigma_{i1}$ and θ_{B1} is the basic temperature solution at order $O(\delta)$ and is simply inferred from Eqn.(2.15). Adopting exactly the same sequence of steps used to compute the heat balance equation to order $O(\delta)$, we simply present the solute balance equation from Eqn.(2.24) as,

$$c_S\left(\sigma_{01} - D\right)\varphi_{01} + R_{00}W_{01} = -\left(\sigma_{01} - D\right)\theta_{00} + \left(\sigma_{01} - D\right)\theta_{B0}\varphi_{00} - R_{00}W_{00}D\theta_{B1} - R_{01}W_{00} \quad (8)$$

It can be noted that the heat balance equation (7) and the solute balance equation (8) are coupled in temperature, solid fraction and vertical velocity. Ideally we prefer to have a modified heat balance equation which is composed of the temperature and vertical velocity. Using exactly the same technique as that outlined in *Appendix E* to decouple the heat and solute balance equations, we obtain the following modified heat balance equation,

$$\left(D^2 - s^2\right)\theta_{01} - \Omega R_{00}W_{01} = \left[(\sigma_{r1} + i\sigma_{i1}) - D\right]\left[\Omega\theta_{00} - \frac{\overline{S}}{c_S}\theta_{B0}\varphi_{00}\right] +$$

$$\Omega R_{00}W_{00}D\theta_{B1} + \Omega R_{01}W_{00}, \quad (9)$$

which is identical to Eqn.(2.44). For the Darcy equation we assume a definition for the permeability to be of the form, $\Pi(\varphi) = 1 + \delta\varphi_{B1}K_1$, where $\varphi_{B1} - (\overline{z} - 1)/c_S$ is the solid fraction at order $O(\delta)$ for the basic state solid fraction. Applying the permeability function definition together with the definitions given above for the dependant variables and parameters to Eqn.(2.25) gives,

$$\left[\frac{\delta\sigma_{01}}{\chi} + 1 + \delta K_1\varphi_{B1}\right]^2\left(D^2 - s^2\right)\left(w_{00} + \delta w_{01}\right) + \left[\frac{\delta\sigma_{01}}{\chi} + 1 + \delta K_1\varphi_{B1}\right]\left[D\left(1 + \delta K_1\varphi_{B1}\right).\right.$$

$$D\left(w_{00} + \delta w_{01}\right) - s^2\left(R_{00} + \delta R_{01}\right)\left(\theta_{00} + \delta\theta_{01}\right)\right] + Ta\, D\left(w_{00} + \delta w_{01}\right) = 0. \qquad (10)$$

We can now expand Eqn.(10) and collect those terms to order $O(\delta)$, the result of which contains known and unknown solutions for the temperature and vertical component of velocity. Separating the unknown solutions for the temperature and solid fraction from the known solutions evaluated at order $O(\delta^0)$, yields the following non-homogenous partial differential equation at order $O(\delta)$,

$$\left(D^2 - s^2\right)w_{01} - s^2 R_{00}\theta_{01} + TaD^2 w_{01} = -2\left[\frac{\sigma_{r1} + i\sigma_{i1}}{\chi} + K_1\varphi_{B1}\right]\left(D^2 - s^2\right)w_{00} -$$

$$K_1 D\varphi_{B1} Dw_{00} + s^2 R_{01}\theta_{00} + s^2 R_{00}\theta_{00}\left[\frac{\sigma_{r1} + i\sigma_{i1}}{\chi} + K_1\varphi_{B1}\right], \qquad (11)$$

which is identical to Eqn.(2.45).

Appendix H : Derivation of solvability condition at $O(\delta^1)$ for Anderson & Worster's (1996) scaling

In essence the solvability condition to an ordinary or partial differential equation is simply a parametric relation that renders the equation solvable. In our case the solvability condition would provide a relation between the Rayleigh number and frequency which are both a function of important parameters such as the Stefan number, composition, and permeability (to mention a few) that govern the flow patterns in the mushy layer. The various parameter settings found this way are defined in a manner that makes the system of equations solvable. The system of equations of which we are interested in finding a solvability condition for is given as,

$$\left(D^2 - s^2\right)\theta_{01} - \Omega R_{00}w_{01} = \left[\left(\sigma_{r1} + i\sigma_{i1}\right) - D\right]\left[\Omega\theta_{00} - \frac{\overline{S}}{c_S}\theta_{B0}\varphi_{00}\right] +$$

$$\Omega R_{00}w_{00}D\theta_{B1} + \Omega R_{01}w_{00} \qquad (1)$$

$$\left(D^2 - s^2\right)w_{01} - s^2 R_{00}\theta_{01} + TaD^2 w_{01} = -2\left[\frac{\sigma_{r1} + i\sigma_{i1}}{\chi} + K_1\varphi_{B1}\right]\left(D^2 - s^2\right)w_{00} -$$

$$K_1 D\varphi_{B1}Dw_{00} + s^2 R_{01}\theta_{00} + s^2 R_{00}\theta_{00}\left[\frac{\sigma_{r1} + i\sigma_{i1}}{\chi} + K_1\varphi_{B1}\right]. \qquad (2)$$

To ease the calculation of the solvability condition, we may adopt the following symbolic notation,

$$\left(D^2 - s^2\right)\theta_{01} - \Omega R_{00}w_{01} = RHS_{heat} \qquad (3)$$

$$\left(D^2 - s^2\right)w_{01} - s^2 R_{00}\theta_{01} + TaD^2 w_{01} = RHS_{Darcy}, \qquad (4)$$

185

where the right hand sides of Eqn.(3) and Eqn.(4) represent the respective function evaluated at the lower order and a full description of them is provided in Eqns.(1-2). Attention is also drawn to the scalar values P_1 and P_2 referred to below Eqn.(2.46) are defined with respect to Eqn.(4) as,

$$P_1 = \left(D^2 - s^2\right)w_{01}(0) - s^2 R_{00}\theta_{01}(0) + TaD^2 w_{01}(0) = RHS_{Darcy}(0) \tag{5}$$

$$P_2 = \left(D^2 - s^2\right)w_{01}(1) - s^2 R_{00}\theta_{01}(1) + TaD^2 w_{01}(1) = RHS_{Darcy}(1), \tag{6}$$

which represent the Darcy equation evaluated at $\bar{z} = 0$ and $\bar{z} = 1$ respectively. Noting that $w_{01}(\bar{x},0) = w_{01}(\bar{x},1) = \theta_{01}(\bar{x},0) = \theta_{01}(\bar{x},1) = 0$, reduces the system (5-6) to,

$$P_1 = D^2 w_{01}(0) = \frac{RHS_{Darcy}(0)}{(1+Ta)} \tag{7}$$

$$P_2 = D^2 w_{01}(1) = \frac{RHS_{Darcy}(1)}{(1+Ta)}. \tag{8}$$

Incidentally it was found that $P_1 + P_2 = 0$. The relations given in Eqn.(7-8) will prove useful later in the evaluation of the solvability condition. We decouple Eqns.(3-4) and obtain a single partial differntial equation for the vertical component of the velocity as follows,

$$\left(D^2 - s^2\right)^2 w_{01} - \Omega s^2 R_{00}^2 w_{01} + Ta\left(D^2 - s^2\right)D^2 w_{01} = s^2 R_{00}RHS_{heat} + \left(D^2 - s^2\right)RHS_{Darcy}, \tag{9}$$

where $D = d/d\bar{z}$. We multiply Eqn.(9) by the the eigenfunction $w_{00} = B_{00}\sin(\pi\bar{z})$ and integrate over the domain $\bar{z} \in [0,1]$, to give the following representation of Eqn.(9),

186

$$\int_0^1 \left(D^2 - s^2\right)^2 w_{01} \cdot w_{00} d\overline{z} - \int_0^1 \Omega s^2 R_{00}^2 w_{01} \cdot w_{00} d\overline{z} + \int_0^1 Ta\left(D^2 - s^2\right)D^2 w_{01} \cdot w_{00} d\overline{z} =$$

$$\int_0^1 s^2 R_{00} RHS_{heat} \cdot w_{00} d\overline{z} + \int_0^1 \left(D^2 - s^2\right)RHS_{Darcy} \cdot w_{00} d\overline{z}. \quad (10)$$

Noting that $w_{01}(\overline{x},0) = w_{01}(\overline{x},1) = 0$, allows the left hand side of Eqn.(10) to fall away, thereby allowing it to be presented as,

$$\int_0^1 s^2 R_{00} RHS_{heat} \cdot w_{00} d\overline{z} + \int_0^1 \left(D^2 - s^2\right)RHS_{Darcy} \cdot w_{00} d\overline{z} = 0. \quad (11)$$

Using *Mathematica* to evaluate the above integrals and remembering that $P_1 + P_2 = 0$, which is obtained from Eqns.(7-8), yields the following expression for the solvability condition,

$$\left(\frac{K_1}{4c_S} R_{00}s^2 + \frac{R_{01}}{2}s^2 + \frac{\sigma_{01}}{2\chi}R_{00}s^2\right)\left(\pi^2 + s^2\right) - \frac{\Omega\sigma_{01}}{2}R_{00}s^2\left(\frac{K_1}{2c_S} + \frac{\sigma_{01}}{\chi}\right)\frac{\left(\pi^2 + s^2\right)^3}{\Omega R_{00}} +$$

$$\frac{\left(\pi^2 + s^2\right)}{2}R_{01}s^2 - \frac{\overline{S}}{\Omega c_S^2}\left(\pi^2 + s^2\right)R_{00}s^2\left[\frac{1}{4} + \frac{\sigma_{01}}{2\left(\pi^2 + \sigma_{01}^2\right)} + \frac{\pi^2\left(1 + e^{-\sigma_{01}}\right)}{\left(\pi^2 + \sigma_{01}^2\right)^2}\right] = 0. \quad (12)$$

Multiplying Eqn.(12) by $-\left(\pi^2 + s^2\right)/s^2 R_{00}$ and using the fact that $\Omega s^2 R_{00} = \left(\pi^2 + s^2\right)\left(\pi^2 + s^2 + \pi^2 Ta\right)$, allows Eqn.(12) to be written in the following form after minor algebraic operation,

$$\frac{\left(\pi^2 + s^2\right)^2\left(\pi^2 + s^2 - \pi^2 Ta\right)}{\left(\pi^2 + s^2 + \pi^2 Ta\right)}\left[\frac{1}{4}\frac{K_1}{c_S} + \frac{\sigma_{01}}{2\chi}\right] - \left(\pi^2 + s^2\right)^2\frac{R_{01}}{R_{00}} + \left(\pi^2 + s^2\right)\frac{\Omega\sigma_{01}}{2} +$$

$$\frac{\overline{S}}{\Omega c_S^2}\left(\pi^2 + s^2\right)^2\left[\frac{1}{4} + \frac{\sigma_{01}}{2\left(\pi^2 + \sigma_{01}^2\right)} + \frac{\pi^2\left(1 + e^{-\sigma_{01}}\right)}{\left(\pi^2 + \sigma_{01}^2\right)^2}\right] = 0, \quad (13)$$

where $\sigma = \sigma_{r1} + i\sigma_{i1}$. Eqn.(13) is similar to the solvability condition presented in Eqn.(2.46).

Appendix I : Derivation of the characteristic Rayleigh number and asymtotical Rayleigh number, corresponding to Anderson & Worster's (1996) scaling

The Rayleigh number correction corresponding to the case of stationary convection is obtained by substituting $\sigma = \sigma_{r1} = \sigma_{i1} = 0$ in Eqn.(2.46). The result of this operation gives,

$$\frac{R_{01}}{R_{00}} = \frac{1}{4} \frac{K_1}{c_S} \frac{\left(\pi^2 + s^2 - \pi^2 Ta\right)}{\left(\pi^2 + s^2 + \pi^2 Ta\right)} + \frac{\overline{S}}{\Omega c_S^2}\left[\frac{1}{4} + \frac{2}{\pi^2}\right]. \tag{1}$$

Rescaling the wavenumber by setting $\alpha = s^2/\pi^2$ and defining a parameter of the form, $\lambda = \overline{S}/\Omega c_S^2$, allows Eqn.(1) to be written in the form,

$$\frac{R_{01}}{R_{00}} = \frac{(1+\alpha - Ta)}{(1+\alpha + Ta)} \frac{1}{4} \frac{K_1}{c_S} + \Omega\lambda\left[\frac{1}{4} + \frac{2}{\pi^2}\right], \tag{2}$$

which corresponds identically to Eqn.(2.48). Noting that the definition of the Rayleigh number my be presented as,

$$R = R_{00}\left[1 + \delta \frac{R_{01}}{R_{00}}\right]. \tag{3}$$

The Rayleigh number established at order $O(\delta^0)$ was found to be of the form,

$$R_{00}^2 = \frac{\pi^2}{\Omega} \frac{(\alpha + 1)(\alpha + 1 + Ta)}{\alpha}. \tag{4}$$

Substituting Eqn.(2) and Eqn.(4) in Eqn.(3) gives an expression of the form

$$R_{c,st} = \pi \sqrt{\frac{(\alpha + 1)(1 + \alpha + Ta)}{\Omega \alpha}} \left[1 + \delta \left(\frac{(1 + \alpha - Ta)}{(1 + \alpha + Ta)} \frac{1}{4} \frac{K_1}{c_S} + \Omega \lambda \left[\frac{1}{4} + \frac{2}{\pi^2} \right] \right) \right], \tag{5}$$

which is identical to Eqn.(2.50). It can be noted, as pointed out in the Section 2.3, that for the case of $Ta \to 0$, Eqn.(5) collapses to the Rayleigh number proposed by Anderson & Worster (1996), given as,

$$R_{c,st} = \pi(\alpha + 1)\sqrt{\frac{1}{\Omega \alpha}} \left[1 + \delta \left(\frac{1}{4} \frac{K_1}{c_S} + \Omega \lambda \left[\frac{1}{4} + \frac{2}{\pi^2} \right] \right) \right], \tag{6}$$

the only differnce being that Eqn.(6) is in the Author's current scaling.

It was noted from the characteristic curves presented in Figures 4 to 9 in Section 2.3 that as the Taylor number is increased, the Rayleigh number shows no appreciable changes with respect to the wavenumber. For the case of very high Taylor numbers we may obtain the minimum Rayleigh numbers from the limit, $\lim_{Ta \to \infty} R_{c,st}$. Before applying this limit, we write Eqn.(5) in the following form,

$$R_{c,st} = \pi \sqrt{\frac{(\alpha + 1)Ta(1/Ta + \alpha/Ta + 1)}{\Omega \alpha}} \left[1 + \delta \left(\frac{(1/Ta + \alpha/Ta - 1)}{(1/Ta + \alpha/Ta + 1)} \frac{1}{4} \frac{K_1}{c_S} + \Omega \lambda \left[\frac{1}{4} + \frac{2}{\pi^2} \right] \right) \right]. \tag{7}$$

Now applying the limit $\lim_{Ta \to \infty} R_{c,st}$ to Eqn.(7) negates terms that are of the order $O(1/Ta)$, thereby resulting in the following definition of the Rayleigh number at high values of Taylor number,

$$R_{c,st}^{(asym)} = \pi \sqrt{\frac{Ta}{\Omega}} \sqrt{1 + \frac{1}{\alpha}} \left[1 + \delta \left(-\frac{1}{4} \frac{K_1}{c_S} + \Omega \lambda \left[\frac{1}{4} + \frac{2}{\pi^2} \right] \right) \right]. \tag{8}$$

Eqn.(8) is exactly the same as Eqn.(2.52).With reference to Figures 4 to 9 it can be inferred that the minimum of the characteristic curve that forms the asymptote with the x-axis occurs at high wavenumbers. Applying the limit $\lim_{\alpha \to \infty} R_{c,st}$ to Eqn.(8) yields the critical value for high Taylor numbers and is expressed as,

$$R_{cr,st}^{(asym)} = \pi \sqrt{\frac{Ta}{\Omega}} \left[1 + \delta \left(-\frac{1}{4}\frac{K_1}{c_S} + \Omega\lambda \left[\frac{1}{4} + \frac{2}{\pi^2} \right] \right) \right].$$

(9)

Eqn.(9) is identical to Eqn.(2.53).

Appendix J : Derivation of the cubic equation for the critical wavenumber corresponding to Anderson & Worster's (1996) scaling

To find the convection threshold point for stationary convection, we actually seek the minimum points on the characteristic curves corresponding to the different parameter settings. These points are denoted by differentiating the characteristic Rayleigh number with respect to the wavenumber and solving for the resulting polynomial for the critical wavenumber as a function of the system parameters, ie. we solve $dR_{c,st}/d\alpha = 0$. Firstly the characteristic Rayleigh number for stationary convection was found to be of the form,

$$R_{c,st} = \pi\sqrt{\frac{(\alpha+1)(1+\alpha+Ta)}{\Omega\alpha}}\left[1+\delta\left(\frac{(1+\alpha-Ta)}{(1+\alpha+Ta)}\frac{1}{4}\frac{K_1}{c_S}+\Omega\lambda\left[\frac{1}{4}+\frac{2}{\pi^2}\right]\right)\right]. \qquad (1)$$

Applying the derivative $dR_{c,st}/d\alpha = 0$ to Eqn.(1) yields the following expression in symbolic form,

$$\frac{d}{d\alpha}\left\{\sqrt{\frac{(\alpha+1)(1+\alpha+Ta)}{\alpha}}\right\}\cdot\left[1+\delta\left(\frac{(1+\alpha-Ta)}{(1+\alpha+Ta)}\frac{1}{4}\frac{K_1}{c_S}+\Omega\lambda\left[\frac{1}{4}+\frac{2}{\pi^2}\right]\right)\right]+$$

$$\sqrt{\frac{(\alpha+1)(1+\alpha+Ta)}{\alpha}}\cdot\frac{d}{d\alpha}\left\{\left[1+\delta\left(\frac{(1+\alpha-Ta)}{(1+\alpha+Ta)}\frac{1}{4}\frac{K_1}{c_S}+\Omega\lambda\left[\frac{1}{4}+\frac{2}{\pi^2}\right]\right)\right]\right\} = 0 \qquad (2)$$

Setting $\eta_{stat} = 1+\delta\Omega\lambda\left[1/4+2/\pi^2\right]$, allows Eqn.(2) to be written in the form,

192

$$\frac{d}{d\alpha}\left\{\sqrt{\frac{(\alpha+1)(1+\alpha+Ta)}{\alpha}}\right\}\cdot\left[\eta_{stat}+\delta\left(\frac{(1+\alpha-Ta)}{(1+\alpha+Ta)}\frac{1}{4}\frac{K_1}{c_s}\right)\right]+$$

$$\sqrt{\frac{(\alpha+1)(1+\alpha+Ta)}{\alpha}}\cdot\frac{d}{d\alpha}\left\{\delta\left(\frac{(1+\alpha-Ta)}{(1+\alpha+Ta)}\frac{1}{4}\frac{K_1}{c_s}\right)\right\}=0 \qquad (3)$$

Using *Mathematica* to evaluate derivatives in Eqn.(3) and collecting the like coefficients for the critical wavenumber as follows,

$$\alpha^4 : 0 \qquad (4)$$

$$\alpha^3 : K_1\delta + 4c_s\eta_{stat} \qquad (5)$$

$$\alpha^2 : K_1\delta(1+3Ta)+4c_s\eta_{stat}(Ta+1) \qquad (6)$$

$$\alpha : -K_1\delta(1-3Ta)-4c_s\eta_{stat}(Ta+1) \qquad (7)$$

$$\alpha^0 : -K_1\delta + K_1Ta^2\delta - 4c_s\eta_{stat} - 8c_sTa\eta_{stat} - 4c_sTa^2\eta_{stat}. \qquad (8)$$

These terms may then be included in the third order polynomial, divided by c_s and substituting $\eta_{stat} = 1+\delta\Omega\lambda\left[1/4+2/\pi^2\right]$ to give,

$$\left[4+\delta\left(\frac{K_1}{c_s}+4\eta_s\right)\right]\alpha^3+\left[4(1+\mathrm{Ta})+\delta\left(\frac{K_1}{c_s}(1+3\mathrm{Ta})+4\eta_s(1+\mathrm{Ta})\right)\right]\alpha^2+$$

$$\left[-4(1+\mathrm{Ta})-\delta\left(\frac{K_1}{c_s}(1-3\mathrm{Ta})+4\eta_s(1+\mathrm{Ta})\right)\right]\alpha+$$

$$\left[-4(1+\mathrm{Ta})^2-\delta\left(\frac{K_1}{c_s}(1-\mathrm{Ta}^2)+4\eta_s(1+\mathrm{Ta})^2\right)\right]=0\,,\ (9)$$

which is identical to Eqn.(2.54a). Note that in Eqn.(9), $\eta_s=\Omega\lambda\left[1/4+2/\pi^2\right]$.

Appendix K : Derivation of the eigenfunctions for the temperature, stream function and solid fraction for the (a) oscillatory convection case, and (b) stationary convection case for Anderson & Worster's (1996) scaling

The expansion for the temperature in terms of the basic solution and the perturbation may be written as,

$$\theta = \theta_B + \varepsilon\theta_{00}(\overline{z})e^{\sigma i}e^{i(s_x\overline{x}+s_y\overline{y})} + c.c, \tag{1}$$

where the notation c.c stands to identify the complex conjugate of the first two terms in Eqn.(1).

(a) Eigenfunctions for Oscillatory Convection

The solution for θ_{00} was established earlier and is respresented as,

$$\theta_{00} = -A_{00}\sin(\pi\overline{z}). \tag{2}$$

In the current study we let $s_y = 0$ so that $s^2 = s_x^2$, thereby implying that there flowfield, though three-dimensional, is not a function of the co-ordinate y. Applying the above and noting that $\sigma = i\sigma_{i1}$ we may proceed to write Eqn.(1) in the following way,

$$\theta = \theta_B + \varepsilon\theta_{00}(\overline{z})e^{i(s_x\overline{x}+\sigma_{i1}\overline{t})} + c.c. \tag{3}$$

The exponential terms may now be written in terms of sines and cosines using the following general notation,

$$e^{iM} = \cos(M) + i\sin(M). \tag{4}$$

Applying the theorem illustrated in Eqn.(4) and the temperature solution provided in Eqn.(2) to Eqn.(3) yields the following form,

$$\theta = \theta_B - \left(\varepsilon A_{00}\right)\sin(\pi\overline{z})\left[\cos(s_x\overline{x} + \sigma_{i1}\overline{t}) + i\sin(s_x\overline{x} + \sigma_{i1}\overline{t})\right] + c.c., \tag{5}$$

which when added to the complex conjugate yields the following solution for temperature,

$$\theta = \theta_B - 2\left(\varepsilon A_{00}\right)\sin(\pi\overline{z})\cos(s_x\overline{x} + \sigma_{i1}\overline{t}), \tag{6}$$

which is identical to the solution presented in Eqn.(2.73). The solution for the vertical component of the velocity follows exactly the same lines as that used for the determination of the temperature above. The process will not be repeated, but the result thereof is,

$$\overline{w} = 0 + 2\left(\varepsilon A_{00}\right)\frac{\left(\pi^2 + s^2\right)}{\Omega R_{00}}\sin(\pi\overline{z})\cos(s_x\overline{x} + \sigma_{i1}\overline{t}). \tag{7}$$

Using the definition of the stream function viz, $\overline{w} = -\partial\psi/\partial\overline{x}$, we may integrate Eqn.(7) with respect to $\overline{x}$ to give the following definition for the stream function,

$$\psi = 0 - 2\left(\varepsilon A_{00}\right)\frac{\left(\pi^2 + s^2\right)}{\Omega R_{00}s}\sin(\pi\overline{z})\sin(s_x\overline{x} + \sigma_{i1}\overline{t}), \tag{8}$$

which is identical to Eqn.(2.74).

We now proceed to develop the eigenfunction for the solid fraction by first providing a definition in terms of the basic flow and the perturbation as follows,

$$\varphi = \varphi_B + \varepsilon\varphi_{00}(\overline{z})e^{i(s_x\overline{x} + \sigma_{i1}\overline{t})} + c.c. \tag{9}$$

196

In this case the solid fraction φ_{00} is given as,

$$\varphi_{00} = -C_{00}\left[e^{i\sigma_{i1}(\bar{z}-1)} + \cos(\pi\bar{z}) + \frac{i\sigma_{i1}}{\pi}\sin(\pi\bar{z})\right], \tag{10}$$

where

$$C_{00} = \frac{\pi(\pi^2 + s^2)}{\Omega c_S\left[\pi^2 - \sigma_{i1}^2\right]}A_{00}. \tag{11}$$

It can be noted that Eqn.(10) has both real and imaginary parts. Applying theorem (4) to Eqn.(10) yields,

$$\varphi_{00} = -C_{00}\left[\left\{\cos\left[\sigma_{i1}(\bar{z}-1)\right] + \cos(\pi\bar{z})\right\} + i\left\{\sin\left[\sigma_{i1}(\bar{z}-1)\right] + \sigma_{i1}/\pi\sin(\pi\bar{z})\right\}\right]. \tag{12}$$

Applying theorem (4) on Eqn.(9) yields the following form,

$$\varphi = \varphi_B - C_{00}\left[\left\{\cos\left[\sigma_{i1}(\bar{z}-1)\right] + \cos(\pi\bar{z})\right\} + i\left\{\sin\left[\sigma_{i1}(\bar{z}-1)\right] + \sigma_{i1}/\pi\sin(\pi\bar{z})\right\}\right] *$$

$$\left[\cos(s_x\bar{x} + \sigma_{i1}\bar{t}) + i\sin(s_x\bar{x} + \sigma_{i1}\bar{t})\right] + c.c. \tag{13}$$

Performing the algebra in Eqn.(13) above and adding the result to the complex conjugate yields,

$$\varphi = \varphi_B - 2(\varepsilon A_{00})\frac{\pi(\pi^2 + s^2)}{\Omega c_S(\pi^2 - \sigma_{i1}^2)}\left\{\left(\cos\left[\sigma_{i1}(\bar{z}-1)\right] + \cos(\pi\bar{z})\right).\cos\left[s\bar{x} + \delta\sigma_{i1}\bar{t}\right] - \right.$$

$$\left.\left(\sigma_{i1}/\pi.\sin(\pi\bar{z}) + \sin\left[\sigma_{i1}(\bar{z}-1)\right]\right)\right\}.\sin\left[s\bar{x} + \delta\sigma_{i1}\bar{t}\right], \tag{14}$$

which is identical to Eqn.(2.75).

(b) Eigenfunctions for Stationary Convection

The eigenfunctions for the the temperature, stream function and the solid fraction for the stationary case are obtained by substituting $\sigma_{i1} = 0$ in the solutions for the oscillatory case. This is fairly simple and the temperature, stream function and solid fraction are given as,

$$\theta = \theta_B - 2(\varepsilon A_{00}) \sin(\pi \overline{z}) \cos(s\overline{x}) \tag{15}$$

$$\psi = 0 - B_{00} \sin(\pi \overline{z}) \sin(s\overline{x}) \tag{16}$$

$$\varphi = \varphi_B - C_{00}(1 + \cos(\pi \overline{z})) \cos(s\overline{x}). \tag{17}$$

Eqns.(15-17) are identical to Eqns.(2.55-2.57). The coefficients in Eqns.(16-17) are defined as,

$$B_{00} = 2(\varepsilon A_{00}) \frac{(\pi^2 + s^2)}{\Omega R_{00} s} \tag{18}$$

and

$$C_{00} = 2(\varepsilon A_{00}) \frac{(\pi^2 + s^2)}{\Omega c_s \pi}. \tag{19}$$

Appendix L : Derivation of the equation for the characteristic Rayleigh number and oscillatory frequency for Anderson & Worster's (1996) scaling

Recall that the solvability condition was found to be of the form,

$$\frac{\left(\pi^2 + s^2\right)^2 \left(\pi^2 + s^2 - \pi^2 Ta\right)}{\left(\pi^2 + s^2 + \pi^2 Ta\right)} \left[\frac{1}{4}\frac{K_1}{c_S} + \frac{\sigma_{01}}{2\chi}\right] - \left(\pi^2 + s^2\right)^2 \frac{R_{01}}{R_{00}} + \left(\pi^2 + s^2\right)\frac{\Omega\sigma_{01}}{2} +$$

$$\frac{\overline{S}}{\Omega c_S^2}\left(\pi^2 + s^2\right)^2 \left[\frac{1}{4} + \frac{\sigma_{01}}{2\left(\pi^2 + \sigma_{01}^2\right)} + \frac{\pi^2\left(1 + e^{-\sigma_{01}}\right)}{\left(\pi^2 + \sigma_{01}^2\right)^2}\right] = 0, \qquad (1)$$

where $\sigma = \sigma_{r1} + i\sigma_{i1}$. The characteristic Rayleigh number and the corresponding oscillatory frequency equations for the case of oscillatory convection are obtained by substituting $\sigma = i\sigma_{i1}$ in Eqn.(1). Eqn.(1) then assumes the following form,

$$\frac{\left(\pi^2 + s^2\right)^2 \left(\pi^2 + s^2 - \pi^2 Ta\right)}{\left(\pi^2 + s^2 + \pi^2 Ta\right)} \left[\frac{1}{4}\frac{K_1}{c_S} + \frac{i\sigma_{i1}}{2\chi}\right] - \left(\pi^2 + s^2\right)^2 \frac{R_{01}}{R_{00}} + \left(\pi^2 + s^2\right)\frac{\Omega i\sigma_{i1}}{2} +$$

$$\frac{\overline{S}}{\Omega c_S^2}\left(\pi^2 + s^2\right)^2 \left[\frac{1}{4} + \frac{i\sigma_{i1}}{2\left(\pi^2 - \sigma_{i1}^2\right)} + \frac{\pi^2\left(1 + e^{-i\sigma_{i1}}\right)}{\left(\pi^2 - \sigma_{i1}^2\right)^2}\right] = 0. \qquad (2)$$

Eqn.(2) is of the form $Re + i\,Im = 0$, which case we require that Re=0 and Im=0 need to be satisfied. Using this fact and noting that $e^{-i\sigma_{i1}} = \cos(\sigma_{i1}) - i\sin(\sigma_{i1})$, Eqn.(2) provides two equations by equating the real and imaginary parts to zero. These equations are for the Rayleigh number correction for oscillatory convection,

$$\frac{R_{01,ov}}{R_{00}} = \frac{\left(\pi^2 + s^2 - \pi^2 Ta\right)}{\left(\pi^2 + s^2 + \pi^2 Ta\right)}\frac{1}{4}\frac{K_1}{c_S} + \frac{\overline{S}}{\Omega c_S^2}\left[\frac{1}{4} + \frac{\pi^2}{\left(\pi^2 - \sigma_{i1}^2\right)^2}\left(1 + \cos\sigma_{i1}\right)\right], \qquad (3)$$

and for the frequency,

$$\frac{\left(\pi^2+s^2\right)^2\left(\pi^2+s^2-\pi^2 Ta\right)}{\left(\pi^2+s^2+\pi^2 Ta\right)}\frac{\sigma_{i1}}{2\chi}+\frac{1}{2}\Omega\left(\pi^2+s^2\right)\sigma_{i1}+$$

$$\frac{\overline{S}}{\Omega c_S^2}\left(\pi^2+s^2\right)^2\left[\frac{\sigma_{i1}}{2\left(\pi^2-\sigma_{i1}^2\right)}-\frac{\pi^2}{\left(\pi^2-\sigma_{i1}^2\right)^2}\sin\sigma_{i1}\right]=0. \tag{4}$$

Applying the scaling $\alpha = s^2/\pi^2$, $\lambda = \overline{S}/\Omega^2 c_S^2$ and $\gamma = \chi/\pi^2$ to Eqns.(3-4) and dividing the frequency equation (4) by σ_{i1}, yields,

$$\frac{R_{01,ov}}{R_{00}}=\frac{\left(1+\alpha-Ta\right)}{\left(1+\alpha+Ta\right)}\frac{1}{4}\frac{K_1}{c_S}+\Omega\lambda\left[\frac{1}{4}+\frac{\pi^2}{\left(\pi^2-\sigma_{i1}^2\right)^2}\left(1+\cos\sigma_{i1}\right)\right] \tag{5}$$

$$\sigma_{i1}\left(\frac{1}{\Omega\gamma}\frac{\left(\alpha+1\right)\left(\alpha+1-Ta\right)}{\left(\alpha+1+Ta\right)}+1+\lambda\pi^2\left(1+\alpha\right)\left[\frac{1}{\left(\pi^2-\sigma_{i1}^2\right)}-\frac{2\pi^2}{\left(\pi^2-\sigma_{i1}^2\right)^2}\frac{\sin\sigma_{i1}}{\sigma_{i1}}\right]\right)=0. \tag{6}$$

Eqns.(5-6) are identical to Eqns.(2.60-2.61). If the limit $Ta\rightarrow 0$ and $\gamma\rightarrow\infty$, is applied to Eqn.(5) and Eqn.(6), we obtain,

$$\frac{R_{01,ov}}{R_{00}}=\frac{1}{4}\frac{K_1}{c_S}+\Omega\lambda\left[\frac{1}{4}+\frac{\pi^2}{\left(\pi^2-\sigma_{i1}^2\right)^2}\left(1+\cos\sigma_{i1}\right)\right] \tag{7}$$

$$\sigma_{i1}\left(1+\lambda\pi^2\left(1+\alpha\right)\left[\frac{1}{\left(\pi^2-\sigma_{i1}^2\right)}-\frac{2\pi^2}{\left(\pi^2-\sigma_{i1}^2\right)^2}\frac{\sin\sigma_{i1}}{\sigma_{i1}}\right]\right)=0, \tag{8}$$

which represents the exact form of the equations solved by Anderson & Worster (1996) for oscillatory convection, the only difference being that Eqns.(7-8) are presented in the author's scaling. Incidentally Eqns.(7-8) are identical to Eqns.(2.62-2.63).

Appendix M : Derivation of the characteristic equation for the wavenumber as a function of the frequency for Anderson and Worster's (1996) scaling

We observe from Eqn.(2.60) and (2.61) that the frequency appears implicitly, thus implying that the characteristic values for the wavenumber and the frequency need to be evaluated numerically in order to predict the Rayleigh number correction from Eqn.(2.61). It was decided that it would be easier to solve for the wavenumber as a function of the frequency and the system parameters. The frequency equation may be stated as,

$$\left(\frac{1}{\Omega\gamma} \frac{(\alpha+1)(\alpha+1-\text{Ta})}{(\alpha+1+\text{Ta})} + 1 + \lambda\pi^2(1+\alpha)\left[\frac{1}{\left(\pi^2 - \sigma_{i1}^2\right)} - \frac{2\pi^2}{\left(\pi^2 - \sigma_{i1}^2\right)^2} \frac{\sin\sigma_{i1}}{\sigma_{i1}} \right] \right) = 0. \quad (1)$$

Using the following variables to represent the parameters,

$$X_1 = \frac{1}{\Omega\gamma} \quad (2)$$

and

$$X_2 = \pi^2\lambda\left[\frac{1}{\left(\pi^2 - \sigma_{i1}^2\right)} - \frac{2\pi^2}{\left(\pi^2 - \sigma_{i1}^2\right)^2} \frac{\sin\sigma_{i1}}{\sigma_{i1}} \right]. \quad (3)$$

Substituting Eqns.(2-3) in Eqn.(1) yields the following form of Eqn.(1),

$$X_1 \frac{(\alpha+1)(\alpha+1-\text{Ta})}{(\alpha+1+\text{Ta})} + 1 + (1+\alpha)X_2 = 0. \quad (4)$$

Multiplying Eqn.(4) by $(\alpha+1+\text{Ta})$ to give,

$$X_1(\alpha + 1)(\alpha + 1 - Ta) + (\alpha + 1 + Ta) + X_2(1 + \alpha)(\alpha + 1 + Ta) = 0. \tag{5}$$

Expanding Eqn.(5) and grouping the like coefficients to yield an expression of the form,

$$\left(X_1 + X_2\right)\alpha^2 + \left[2\left(X_1 + X_2\right) + Ta\left(X_2 - X_1\right) + 1\right]\alpha + \left[\left(X_1 + X_2\right) + Ta\left(X_2 - X_1\right) + Ta + 1\right] = 0. \tag{6}$$

If,

$$a_1 = \left(X_1 + X_2\right) \tag{7}$$

$$a_2 = 2\left(X_1 + X_2\right) + Ta\left(X_2 - X_1\right) + 1 \tag{8}$$

$$a_3 = \left(X_1 + X_2\right) + Ta\left(X_2 - X_1\right) + Ta + 1, \tag{9}$$

then Eqn.(6) may be presented in terms of the quadratic formula as follows,

$$\alpha_{1,2} = \frac{-a_2 \pm \sqrt{a_2^2 - 4a_1a_3}}{2a_1}. \tag{10}$$

It can be noted that Eqn.(10) produces two roots for the wavenumber for a given frequency and a particular parameter setting. Obviously if only positive values of wavenumber are sought, and if one value is positive and the other is negative then only the positive root is considered. If both the roots are positive, then the root corresponding to the lower critical Rayleigh number is selected as it represents a lower convection threshold point. The definitions for X_1 and X_2 are substituted in Eqns.(7-9) and are rearranged as follows,

$$a_1 = \frac{1}{\Omega \gamma} + \pi^2 \lambda \left[\frac{1}{\left(\pi^2 - \sigma_{i1}^2\right)} - \frac{2\pi^2}{\left(\pi^2 - \sigma_{i1}^2\right)^2} \frac{\sin \sigma_{i1}}{\sigma_{i1}} \right] \tag{11}$$

$$a_2 = (2 - Ta)\frac{1}{\Omega \gamma} + \pi^2 \lambda (2 + Ta) \left[\frac{1}{\left(\pi^2 - \sigma_{i1}^2\right)} - \frac{2\pi^2}{\left(\pi^2 - \sigma_{i1}^2\right)^2} \frac{\sin \sigma_{i1}}{\sigma_{i1}} \right] + 1 \tag{12}$$

$$a_3 = (1 - Ta)\frac{1}{\Omega \gamma} + \left(\pi^2 \lambda \left[\frac{1}{\left(\pi^2 - \sigma_{i1}^2\right)} - \frac{2\pi^2}{\left(\pi^2 - \sigma_{i1}^2\right)^2} \frac{\sin \sigma_{i1}}{\sigma_{i1}} \right] + 1 \right) (1 + Ta). \tag{13}$$

Eqns.(10-13) are identical to Eqns.(2.64-2.67).

Appendix N : Derivation of the asymptotic wavenumber and Rayleigh number for Anderson & Worster's (1996) scaling

It was found that for low values of the parameter χ the curves of freqency versus the wavenumber reaches and asymptote, see Figures 15 and 19. This was found to occur at very high values of frequency. Considering the frequency equation,

$$X_1 \frac{(\alpha + 1)(\alpha + 1 - Ta)}{(\alpha + 1 + Ta)} + 1 + (1 + \alpha)X_2 = 0 , \tag{1}$$

where

$$X_1 = \frac{1}{\Omega \gamma} \tag{2}$$

and

$$X_2 = \pi^2 \lambda \left[\frac{1}{(\pi^2 - \sigma_{11}^2)} - \frac{2\pi^2}{(\pi^2 - \sigma_{11}^2)^2} \frac{\sin \sigma_{11}}{\sigma_{11}} \right] . \tag{3}$$

Multiply Eqn.(1) by γ to yield,

$$\frac{1}{\Omega} \frac{(\alpha + 1)(\alpha + 1 - Ta)}{(\alpha + 1 + Ta)} + \gamma + \gamma(1 + \alpha)X_2 = 0 . \tag{4}$$

Applying the limit $\lim_{\gamma \to 0}(\cdot)$ to Eqn.(4) for small values of γ gives

$$(\alpha + 1)(\alpha + 1 - Ta) = 0 . \tag{5}$$

Solving for the wavenumber yields,

$$\alpha = Ta - 1, \text{ (and } \alpha = -1 \text{ which is not of physical significance)} \tag{6}$$

which represents the wavenumber towards which the curves for the different values of λ converge. Eqn.(6) is identical to Eqn.(2.71).

The Rayleigh number corresponding to oscillatory convection is given as,

$$R_{c,ov} = R_{00}\left(1 + \delta\, R_{01,ov}/R_{00}\right). \tag{7}$$

The correction Rayleigh number is given by Eqn.(2.60) as,

$$\frac{R_{01,ov}}{R_{00}} = \frac{(1 + \alpha - Ta)}{(1 + \alpha + Ta)}\frac{1}{4}\frac{K_1}{c_S} + \Omega\lambda\left[\frac{1}{4} + \frac{\pi^2}{\left(\pi^2 - \sigma_{i1}^2\right)}\left(1 + \cos\sigma_{i1}\right)\right]. \tag{8}$$

Substituting Eqn.(8) in Eqn.(7) and using the definition of the Rayleigh number as given by Eqn.(2.49), yields the following characteristic Rayleigh number for oscillatory convection,

$$R_{c,ov} = \pi\sqrt{\frac{(\alpha + 1)(\alpha + 1 + Ta)}{\alpha\Omega}}\left[1 + \delta\left(\frac{(1 + \alpha - Ta)}{(1 + \alpha + Ta)}\frac{1}{4}\frac{K_1}{c_S} + \Omega\lambda\left[\frac{1}{4} + \frac{\pi^2}{\left(\pi^2 - \sigma_{i1}^2\right)}\left(1 + \cos\sigma_{i1}\right)\right]\right)\right] \tag{9}$$

which is identical to Eqn.(2.68). Substituting the limit $\sigma_{i1} \to \infty$ in Eqn.(9) yields,

$$R_{c,ov}^{(asym)} = \pi\sqrt{\frac{(\alpha + 1)(\alpha + 1 + Ta)}{\alpha\Omega}}\left[1 + \delta\left(\frac{(1 + \alpha - Ta)}{(1 + \alpha + Ta)}\frac{1}{4}\frac{K_1}{c_S} + \frac{\Omega\lambda}{4}\right)\right], \tag{10}$$

which is identical to Eqn.(2.72).

Appendix O : Derivation of the governing system of equations for the Author's scaling

The system of governing equations analysed by Anderson & Worster (1996) was scaled in space, and time in terms of the dimensionless mushy layer growth parameter δ. The Rayleigh number, velocity and pressure were also scaled in terms this parameter. The parameter δ is the ratio between the height of the mushy layer and the thermal length scale (defined in Appendix A) and is sometimes referred to as the growth Peclet number. The current scaling for space and time may be presented as,

$$x\hat{\mathbf{e}}_x + y\hat{\mathbf{e}}_y + z\hat{\mathbf{e}}_z = \delta(\overline{x}\hat{\mathbf{e}}_x + \overline{y}\hat{\mathbf{e}}_y + \overline{z}\hat{\mathbf{e}}_z), \qquad t = \delta\overline{t} \tag{1a-b}$$

whilst the Rayleigh number, velocity and pressure were scaed as,

$$R^2 = \delta Ra_m, \qquad \mathbf{U} = \frac{R}{\delta}\overline{\mathbf{U}}, \quad p = R\overline{p}. \tag{2a-c}$$

These scalings were then applied to the continuity equation (1.3) to yield,

$$\overline{\nabla}\cdot\overline{\mathbf{U}} = 0, \tag{2d}$$

which is identical to Eqn.(3.4).

Now considering applying the scalings defined in (1a-b and 2a-c) to the heat balance equation yields,

$$\left(\frac{1}{\delta}\frac{\partial}{\partial\overline{t}} - \frac{1}{\delta}\frac{\partial}{\partial\overline{z}}\right)\left(\theta - \frac{\overline{S}}{\delta}\varphi\right) + \frac{R}{\delta^2}\overline{\mathbf{U}}\cdot\overline{\nabla}\theta = \frac{1}{\delta^2}\overline{\nabla}^2\theta. \tag{3}$$

Multiplying this equation by δ^2 yields,

$$\delta\left(\frac{\partial}{\partial\bar{t}} - \frac{\partial}{\partial\bar{z}}\right)\left(\theta - \frac{\overline{S}}{\delta}\varphi\right) + R\overline{U}\cdot\overline{\nabla}\theta = \overline{\nabla}^2\theta. \tag{4}$$

Applying the scalings given in Eqn.(1a-b) and Eqn.(2a-c) to the solute balance equation (1.5) yields,

$$\left(\frac{1}{\delta}\frac{\partial}{\partial\bar{t}} - \frac{1}{\delta}\frac{\partial}{\partial\bar{z}}\right)\left[(1-\varphi)\theta + \frac{c_S}{\delta}\varphi\right] + \frac{R}{\delta^2}\overline{U}\cdot\overline{\nabla}\theta = 0. \tag{5}$$

Multiplying Eqn.(5) by δ^2 gives,

$$\delta\left(\frac{\partial}{\partial\bar{t}} - \frac{\partial}{\partial\bar{z}}\right)\left[(1-\varphi)\theta + \frac{c_S}{\delta}\varphi\right] + R\overline{U}\cdot\overline{\nabla}\theta = 0. \tag{6}$$

Finally apply the scalings given by Eqn.(1a-b) and Eqn.(2a-c) to the Darcy equation (1.6) to gives,

$$\frac{R}{\delta^2\chi_0}\frac{\partial\overline{U}}{\partial\bar{t}} + \Pi(\varphi)\frac{R}{\delta}\overline{U} = -\frac{R}{\delta}\overline{\nabla}\,\overline{p} - Ra_m\theta\hat{e}_z - Ta^{1/2}\hat{e}_z\times\frac{R}{\delta}\overline{U} \tag{7}$$

where $\hat{e}_g = -\hat{e}_z$ and $\hat{e}_\omega = \hat{e}_z$ by virtue of the system of co-ordinates presented in Figure 2a. Multiplying Eqn.(7) by δ/R yields,

$$\frac{1}{\delta\chi_0}\frac{\partial\overline{U}}{\partial\bar{t}} + \Pi(\varphi)\overline{U} = -\overline{\nabla}\,\overline{p} - \frac{\delta Ra_m}{R}\theta\hat{e}_z - Ta^{1/2}\hat{e}_z\times\overline{U}. \tag{8}$$

Substituting $R^2 = \delta Ra_m$ in Eqn.(8) reduces it to,

$$\frac{1}{\delta\chi_0}\frac{\partial\overline{U}}{\partial\bar{t}} + \Pi(\varphi)\overline{U} = -\overline{\nabla}\,\overline{p} - R\theta\hat{e}_z - Ta^{1/2}\hat{e}_z\times\overline{U}. \tag{9}$$

If we set $\chi_1 = \delta\chi_0$, where $\chi_0 = \mathrm{Pr}\,\phi_0\vartheta_0$. In addition, if we set $t' = \chi_1\bar{t}$, then we may write the heat balance, solute balance and Darcy equations given above as,

$$\overline{\nabla}\cdot\overline{\mathbf{U}} = 0 \tag{10}$$

$$\delta\left(\chi_1\frac{\partial}{\partial t'} - \frac{\partial}{\partial\overline{z}}\right)\left(\theta - \frac{\overline{S}}{\delta}\varphi\right) + R\overline{\mathbf{U}}\cdot\overline{\nabla}\theta = \overline{\nabla}^2\theta \tag{11}$$

$$\delta\left(\chi_1\frac{\partial}{\partial t'} - \frac{\partial}{\partial\overline{z}}\right)\left[(1-\varphi)\theta + \frac{c_s}{\delta}\varphi\right] + R\overline{\mathbf{U}}\cdot\overline{\nabla}\theta = 0 \tag{12}$$

$$\frac{\partial\overline{\mathbf{U}}}{\partial t'} + \Pi(\varphi)\overline{\mathbf{U}} = -\overline{\nabla}\overline{p} - R\theta\hat{\mathbf{e}}_z - \mathrm{Ta}^{1/2}\hat{\mathbf{e}}_z\times\overline{\mathbf{U}}. \tag{13}$$

Eqns.(10-13) are identical to the system presented in Eqns.(3.4-3.8).

Appendix P : Derivation of the perturbed heat balance, solute balance and modified Darcy equation for the Author's scaling

For the derivation of the perturbation equations we adopt normal mode expansions for the temperature, solid fraction and velocity as,

$$\theta = \theta_B + \varepsilon\theta_1 = \theta_B + \varepsilon\hat{\theta}(\bar{z})e^{\sigma t'}e^{i(s_x\bar{x}+s_y\bar{y})} \tag{1}$$

$$\varphi = \varphi_B + \varepsilon\varphi_1 = \varphi_B + \varepsilon\hat{\varphi}(\bar{z})e^{\sigma t'}e^{i(s_x\bar{x}+s_y\bar{y})} \tag{2}$$

$$\overline{U} = 0 + \varepsilon\overline{U}_1 = 0 + \varepsilon\hat{\overline{U}}(\bar{z})e^{\sigma t'}e^{i(s_x\bar{x}+s_y\bar{y})} \quad . \tag{3}$$

Applying the expansions given in (1-3) to the heat balance equation (3.5) yields the following perturbed to order ,

$$\delta\left(\chi_1\frac{\partial}{\partial t'} - \frac{\partial}{\partial\bar{z}}\right)1\left[\theta_B + \varepsilon\theta_1 - \frac{\overline{S}}{\delta}(\varphi_B + \varepsilon\varphi_1)\right] + R\varepsilon\overline{U}_1\nabla(\theta_B + \varepsilon\theta_1) = \nabla^2(\theta_B + \varepsilon\theta_1), \tag{4}$$

Neglecting the $O(\varepsilon^2)$ and presenting the heat balance equation to order $O(\varepsilon)$ yields,

$$\delta\left(\chi_1\frac{\partial}{\partial t'} - \frac{\partial}{\partial\bar{z}}\right)\left[\theta_1 - \frac{\overline{S}}{\delta}\varphi_1\right] + R\overline{w}_1 D\theta_B = \nabla^2\theta_1, \tag{5}$$

which after applying the definitions for the disturbed temperature, solid fraction and velocity as presented in Eqns.(1-3) at order $O(\varepsilon)$ yields the following form of the heat balance equation,

$$\delta(\chi_1\sigma - D)\left[\hat{\theta} - \frac{\overline{S}}{\delta}\hat{\varphi}\right] + R\hat{w}D\theta_B = (D^2 - s^2)\hat{\theta} . \tag{6}$$

Incidentally, Eqn.(6) is identical to Eqn.(3.20).

Apply (1-3) to the solute balance equation (3.6) and using the sequence of steps outlined above yields,

$$\delta\left(\chi_1\sigma - D\right)\left[(1-\varphi_B)\hat{\theta} - \theta_B\hat{\varphi} + \frac{c_s}{\delta}\hat{\varphi}\right] + R\bar{w}D\theta_B = 0, \tag{7}$$

where the $O(\varepsilon^2)$ terms have been neglected and the terms with the subscripts "B" refers to the basic solution. Eqn.(7) is identical to Eqn.(3.21).

Now apply the expansions (1-3) to the Darcy Equation given by Eqn.(3.7) and use exactly the same computation procedure as that outlined for the heat balance equation above to easily give the following disturbed form of the equation,

$$\left[\sigma + \Pi(\varphi)\right]^2\left(D^2 - s^2\right)\hat{w} + \left[\sigma + \Pi(\varphi)\right]\left[D\Pi\, D\hat{w} - s^2R\hat{\theta}\right] + TaD^2\hat{w} = 0. \tag{8}$$

Note that in Eqns.(5-8) that $D = d/d\bar{z}$ and $s^2 = s_x^2 + s_y^2$. Eqn.(8) is identical to Eqn.(3.22).

Appendix Q : Derivation of the permeability function used in Author's scaling

Amberg & Homsey (1993) and Anderson & Worster (1995) used a Taylor series expansion of the permeability function as a function of the solid fraction for $\varphi \ll 1$, given in their notation as,

$$\Pi(\varphi) = 1 + K_1\varphi + K_2\varphi^2 + + O(\varphi^3),\tag{1}$$

where K_1, K_2,...defines the permeability constants. The implications of Eqn.(1) is that the effects of permeability are introduced at each order of the computation. In the current study we follow Amberg & Homsey (1993) and Anderson & Worster (1995) with the only difference being that we introduce the effects of permeability from the third order of disturbance only. Our new formulation of the permeability function is given as,

$$\Pi(\varphi) = 1 + K_c\varphi^2,\tag{2}$$

where the constant $K_c > 0$, so that the permeability decreases with increasing solid fraction. Noting that the solid fraction may be written in terms of the basic state and soild fraction as follows,

$$\varphi = \varphi_B + \varepsilon\varphi_1,\tag{3}$$

where $\varphi_1 = \hat{\varphi}(\bar{z})e^{\sigma t'}e^{i(s_x\bar{x}+s_y\bar{y})}$ represents the solid fraction eigenfunction evaluated at the leading order. In the current study we only extend our expansions for the dependant variables to order $O(\delta^0)$. The basic solution solid fraction to order $O(\delta^0)$ was found to be $\varphi_{B0} = 0$. Substituting this result in Eqn.(3) yields the following definition for the solid fraction,

$$\varphi = \varepsilon\varphi_1.\tag{4}$$

Using the result presented in Eqn.(4), we may present the permeability function as

$$\Pi(\varepsilon\varphi_1) = 1 + K_c\varepsilon^2\varphi_1^2, \tag{5}$$

which is identical to Eqn.(3.26). As pointed out earlier, it can be noted from Eqn.(5) that the permeability effects are only introduced at the third order $O(\varepsilon^3)$.

.

Appendix R : Derivation of the system of governing equations at $O(\delta^0)$ for the Author's scaling

The perturbed system of governing equations found for the author's scaling may be summarised as,

$$\delta(\chi_1\sigma - D)\left[\hat{\theta} - \frac{\overline{S}}{\delta}\hat{\phi}\right] + R\hat{\overline{w}}D\theta_B = (D^2 - s^2)\hat{\theta} \tag{1}$$

$$\delta(\chi_1\sigma - D)\left[(1 - \phi_B)\hat{\theta} - \theta_B\hat{\phi} + \frac{c_S}{\delta}\hat{\phi}\right] + R\hat{\overline{w}}D\theta_B = 0 \tag{2}$$

$$[\sigma + \Pi(\phi)]^2(D^2 - s^2)\hat{\overline{w}} + [\sigma + \Pi(\phi)][D\Pi\ D\hat{\overline{w}} - s^2R\hat{\theta}] + TaD^2\hat{\overline{w}} = 0, \tag{3}$$

where $D = d/d\overline{z}$ and $s^2 = s_x^2 + s_y^2$. As pointed out earlier, we are only interested in the $O(\delta^0)$ problem, so we need a representation of this case by reconsidering the system (1-3). Expanding Eqn.(1) yields,

$$\delta(\chi_1\sigma - D)\hat{\theta} - \overline{S}(\chi_1\sigma - D)\hat{\phi} + R\hat{\overline{w}}D\theta_B = (D^2 - s^2)\hat{\theta}. \tag{4}$$

Although an expansion of the dependant variables in terms δ could be undertaken, we do not do this for clarity as the order $O(\delta)$ is not investigated here. We retain the dependant variable scaling here and present the $O(\epsilon\delta^0)$ system inferred from Eqn.(4) as,

$$-\overline{S}(\chi_1\sigma - D)\hat{\phi} + R\hat{\overline{w}}D\theta_{B0} = (D^2 - s^2)\hat{\theta}, \tag{5}$$

for the heat balance equation. By following the same steps as that above the soute balance equation may be presented as,

$$c_S\left(\chi_1\sigma - D\right)\hat{\varphi} + R\overline{\hat{w}}D\theta_{B0} = 0,\tag{6}$$

at order $O(\varepsilon\delta^0)$. For the Darcy equation we recall that $\Pi(\varepsilon\varphi_1) = 1 + K_c\varepsilon^2\varphi_1^2$, and present it as,

$$[\sigma + 1]^2\left(D^2 - s^2\right)\hat{\overline{w}} - [\sigma + 1]s^2R\hat{\theta} + TaD^2\hat{\overline{w}} = 0,\tag{7}$$

at order $O(\varepsilon\delta^0)$. Recalling that $D\theta_{B0} = 1$, and decoupling the heat and solute balance equation we may present the following system of governing equations for the modifed heat balance, solute balance and Darcy equations at order $O(\varepsilon\delta^0)$,

$$\left(D^2 - s^2\right)\hat{\theta} - \Omega R\hat{\overline{w}} = 0\tag{8}$$

$$c_S\left(\chi_1\sigma - D\right)\hat{\varphi} + R\hat{\overline{w}} = 0\tag{9}$$

$$[\sigma + 1]^2\left(D^2 - s^2\right)\hat{\overline{w}} - [\sigma + 1]s^2R\hat{\theta} + TaD^2\hat{\overline{w}} = 0.\tag{10}$$

Eqns.(8-10) are identical to the systems presented in Eqns.(3.27-3.29).

Appendix S : Derivation of the perturbed functions for the temperature, solid fraction and vertical velocity component for the Author's scaling

The system that needs to be solved may be represented as,

$$\left(D^2 - s^2\right)\hat{\theta} - \Omega R \hat{\overline{w}} = 0 \tag{1}$$

$$c_S\left(\chi_1 \sigma - D\right)\hat{\varphi} + R\hat{\overline{w}} = 0 \tag{2}$$

$$[\sigma + 1]^2\left(D^2 - s^2\right)\hat{\overline{w}} - [\sigma + 1]s^2 R\hat{\theta} + TaD^2\hat{\overline{w}} = 0. \tag{3}$$

As before we select an eigenfuncion for the temperature to be of the form, $\hat{\theta} = -B_1\sin(\pi\overline{z})$. Substituting this in Eqn.(1) yields a solution for the vertical component of the velocity to be of the form,

$$\hat{\overline{w}} = \frac{(\pi^2 + s^2)}{\Omega R}B_1\sin(\pi\overline{z}) = N_1\sin(\pi\overline{z}), \tag{4}$$

where

$$N_1 = \frac{(\pi^2 + s^2)}{\Omega R}B_1 = \frac{(1+\alpha)}{\Omega\overline{R}}B_1, \tag{5}$$

where the scaling $\alpha = s^2/\pi^2$ and $\overline{R} = R/\pi^2$. Note that Eqns.(4-5) are identical to Eqn.(3.31) and Eqn.(3.33). The solution for the solid fraction follows exactly the sames sequence of steps as outlined in *Appendix F*, the only difference being that the parameter χ_1 preceeds σ. The solution procedure won't be repeated here but the final solution is provided in the form,

$$\hat{\varphi} = -C_1\left[e^{\pi^2\gamma\sigma(\overline{z}-1)} + \sigma\pi\gamma\sin(\pi\overline{z}) + \cos(\pi\overline{z})\right], \tag{6}$$

where the coefficient,

$$C_1 = \frac{\pi(1+\alpha)}{\Omega c_S \left(1+\pi^2\gamma^2\sigma^2\right)} B_1,$$ (7)

and the scaling $\gamma = \chi_1/\pi^2$ has been used. Note that Eqns.(6-7) are identical to Eqn.(3.32) and Eqn.(3.34).

Substituting the solution for the temperature and vertical velocity given above in the Darcy Eqn,

$$[\sigma + 1]^2 \left(D^2 - s^2\right)\hat{\bar{w}} - [\sigma + 1]s^2 R\hat{\theta} + TaD^2\hat{\bar{w}} = 0,$$ (8)

gives,

$$R = \frac{N_1}{B_1} \frac{1}{[\sigma + 1]\alpha} \left([\sigma + 1]^2(1+\alpha) + Ta\right).$$ (9)

Using the relation between N_1 and B_1, given by Eqn.(5) as,

$$\frac{N_1}{B_1} = \frac{(1+\alpha)}{\Omega \bar{R}},$$ (10)

and upon substitution in Eqn.(9) yields,

$$R\bar{R} = \frac{(1+\alpha)}{[\sigma + 1]\Omega\alpha} \left([\sigma + 1]^2(1+\alpha) + Ta\right).$$ (11)

Using the scaling, $\bar{R} = R/\pi^2$, allows Eqn.(11) to be written as,

$$\overline{R}^2 = \frac{(1+\alpha)}{[\sigma + 1]\Omega\pi^2\alpha}\left([\sigma + 1]^2(1+\alpha) + Ta\right),$$ (12)

which is identical to Eqn.(3.35).

Appendix T : Derivation of the critical wavenumber and Rayleigh number for stationary convection for the Author's scaling

The expression for the Rayleigh number in terms of the oscillatory frequency is given as,

$$\overline{R}^2 = \frac{(1+\alpha)}{[\sigma+1]\Omega\pi^2\alpha}\left([\sigma+1]^2(1+\alpha)+Ta\right).$$ (1)

Substituting $\sigma = 0$ in Eqn.(1) to obtain the Rayleigh number for stationary convection yields the following expression,

$$\overline{R}^2 = \frac{(1+\alpha)}{\Omega\pi^2\alpha}(1+\alpha+Ta),$$ (2)

which may be written as,

$$\overline{R} = \sqrt{\frac{1}{\Omega\pi^2}}\cdot\sqrt{\frac{(1+\alpha)}{\alpha}(1+\alpha+Ta)}.$$ (3)

Minimising Eqn.(3) with respect to the wavenumber as follows,

$$\frac{d\overline{R}}{d\alpha} = \frac{d}{d\alpha}\sqrt{\frac{(1+\alpha)}{\alpha}(1+\alpha+Ta)} = 0,$$ (4)

and using trivial algebraic manipulation yields the following simple result for the critical wavenumber,

$$\alpha_{cr,st} = \sqrt{Ta+1},$$ (5)

which is identical to Eqn.(3.38). Substituting Eqn.(5) in the definition for the Rayleigh number yields the critical Rayleigh number defined as,

219

$$\overline{R}^2_{cr,st} = \frac{\left(1 + \sqrt{Ta + 1}\right)}{\Omega \pi^2 \sqrt{Ta + 1}} \left(Ta + 1 + \sqrt{Ta + 1}\right).$$

(6)

Eqn.(6) may be refined further by expanding the brackets and grouping as follows,

$$\overline{R}^2_{cr,st} = \frac{1}{\Omega \pi^2} \left((Ta + 1) + 2\sqrt{Ta + 1} + 1\right).$$

(7)

The terms within brackets may be factorised to yield,

$$\overline{R}^2_{cr,st} = \frac{1}{\Omega \pi^2} \left(1 + \sqrt{Ta + 1}\right)^2,$$

(8)

which may be written as,

$$\overline{R}_{cr,st} = \frac{1}{\pi \sqrt{\Omega}} \left(1 + \sqrt{Ta + 1}\right),$$

(9)

which represents the critical Rayleigh number for stationary convection and is identical to Eqn.(3.39).

Appendix U : Derivation of the critical composition difference for stationary convection for the Author's scaling

The critical wave number and Rayleigh number found for stationary convection at the linear stability level are,

$$\alpha_{cr,st} = \sqrt{Ta + 1} \tag{1}$$

$$\overline{R}_{cr,st} = \frac{1}{\pi\sqrt{\Omega}}\left(1 + \sqrt{Ta + 1}\right). \tag{2}$$

These equations may be represented in the following form,

$$\alpha_{cr,st} = \sqrt{Ta}\sqrt{1 + 1/Ta} \tag{3}$$

$$\overline{R}_{cr,st} = \frac{1}{\pi\sqrt{\Omega}}\left(1 + \sqrt{Ta}\sqrt{1 + 1/Ta}\right). \tag{4}$$

For the case of high Taylor numbers, $Ta \to \infty$, Eqns.(3-4) reduces to,

$$\alpha_{cr,st} = \sqrt{Ta} \tag{5}$$

$$\overline{R}_{cr,st} = \frac{1}{\pi\sqrt{\Omega}}\left(1 + \sqrt{Ta}\right), \tag{6}$$

and are identical to the expressions presented in Eqn.(3.40). From Eqn.(6) it can be concluded that as $Ta \to \infty$ then $\sqrt{Ta} \gg 1$. Hence Eqn.(6) can be expressed as,

$$\overline{R}_{cr,st} \cong \frac{\sqrt{Ta}}{\pi\sqrt{\Omega}}. \tag{7}$$

Using the definition of the Rayleigh number given as

$$\mathrm{Ra}_{m} = \frac{\beta^* \Delta c g^* k_0 \kappa^*/V^*}{\nu^* \kappa^*}.$$
(8)

Recall that the Rayleigh number was scaled in the form,

$$R^2 = \delta \mathrm{Ra}_m,$$
(9)

and in the stationary case a further scaling on the Rayleigh number of the form,

$$R = \pi^2 \overline{R},$$
(10)

was undertaken. Substituting Eqn.(10) in Eqn.(9) yields,

$$\pi^4 \overline{R}^2 = \delta \mathrm{Ra}_m.$$
(11)

Substituting Eqn.(11) in Eqn(8) yields the following expression,

$$\overline{R}^2_{cr,st} = \frac{\delta \beta^* \Delta c g^* k_0 \kappa^*/V^*}{\nu^* \kappa^* \pi^4}.$$
(12)

Recalling that $\delta = H^*/(\kappa^*/V^*)$ and rearranging Eqn.(12) for the viscosity $\beta^* \Delta c$ yields,

$$\beta^* \Delta c = \frac{\overline{R}^2_{cr,st} \nu^* \kappa^* \pi^4}{g^* k_0 H^*}.$$
(13)

Using the critical Rayleigh number defined in Eqn.(7), and substituting in Eqn.(13) to yield,

$$\beta^* \Delta c = \frac{Tav^* \kappa^* \pi^2}{g^* k_0 H^* \Omega},$$

(14)

where the Taylor number is defined as,

$$Ta = \left[\frac{2\omega^* k_0}{v^* \phi_0} \right]^2.$$

(15)

Introducing definition of the Taylor number given by Eqn.(15) in Eqn.(14) yields,

$$\beta^* \Delta c = \frac{4\pi^2 \omega^{*2} k_0 \kappa^*}{g^* H^* \Omega v^* \phi_0^2}.$$

(16)

Recalling that $\Omega = 1 + St/\xi$ and letting $\overline{\beta} = \beta^* \Delta c$, allows Eqn.(16) to be presented as,

$$\overline{\beta}_{cr,st} = \frac{4\pi^2 \omega^{*2} k_0 \kappa^*}{g^* H^* \phi_0^2 \Omega (1 + St/\xi)} \frac{1}{v^*},$$

(17)

which represents the critical compositional difference at high Taylor numbers and is identical to Eqn.(3.41).

Now for the case when $Ta \to 0$, the critcal wavenumber and Rayleigh number may be given as,

$$\alpha_{cr,st} = 1$$

(18)

$$\overline{R}_{cr,st} = \frac{2}{\pi \sqrt{\Omega}}.$$

(19)

Substituting these values for the critical composition difference in the following expression,

$$\overline{\beta}_{cr,st} = \frac{4\kappa^*\pi^2}{g^*H^*(1+St/\xi)k_0}v^*,$$

(20)

which represents the critical composition difference in the case of no rotation, and is identical to Eqn.(3.42).

Appendix V : Derivation of the leading order temperature, solid fraction, and velocity solutions together with the definition of the wavenumber on the oblique plane containing the streamlines for the case of stationary convection for the Author's scaling

For the case of stationary convection, the eigenfunctions for the temperature, solid fraction and vertical component of velocity may be presented as

$$\theta_1 = \hat{\theta}(\bar{z})e^{i(s_x\bar{x}+s_y\bar{y})} + c.c \tag{1}$$

$$\varphi_1 = \hat{\varphi}(\bar{z})e^{i(s_x\bar{x}+s_y\bar{y})} + c.c \tag{2}$$

$$\overline{w}_1 = \hat{\overline{w}}e^{i(s_x\bar{x}+s_y\bar{y})} + c.c. \tag{3}$$

where c.c stands for the complex conjugate and,

$$\hat{\theta} = -B_1 \sin(\pi\bar{z}) \tag{4}$$

$$\hat{\overline{w}} = N_1 \sin(\pi\bar{z}) \tag{5}$$

$$\hat{\varphi} = -C_1\left[1 + \cos(\pi\bar{z})\right], \tag{6}$$

where

$$N_1 = \frac{(1+\alpha)}{\Omega\overline{R}}B_1 \tag{7}$$

$$C_1 = \frac{\pi(1+\alpha)}{\Omega c_S}B_1. \tag{8}$$

The scaling $\alpha = s^2/\pi^2$, $\overline{R} = R/\pi^2$ and $\gamma = \chi_1/\pi^2$ has been used in the above equations. In the current study we assume that $s_y = 0$ so that $s^2 = s_x^2$, thereby enabling the solution for the temperature equation (1) to be of the form,

$$\theta_1 = -2B_1 \cos(s\overline{x})\sin(\pi\overline{z}) . \tag{9}$$

Similarly, the solid fraction is given as,

$$\varphi_1 = -2C_1\left[1 + \cos(\pi\overline{z})\right]\cos(s\overline{x}), \tag{10}$$

and the vertical component of the velocity as,

$$\overline{w}_1 = 2N_1 \cos(s\overline{x})\sin(\pi\overline{z}) . \tag{11}$$

The method used to compute Eqns.(9-11) is identical to that employed earlier in *Appendix K*. Eqns.(9-11) are identical to Eqns.(3.43-3.45).

Noting that although the y-co-ordinate does not appear in the eigenfunctions (9-11), the flow is still three dimensional. The three flow vectors are just not a function of $\overline{y}$. We anticipate a stream function to describe the resulting flow. The plane containing the streamlines is somewhat oblique in nature due to the presence of a flow in the y-direction that is independent of the $\overline{y}$ co-ordinate. To find the wavenumber on this oblique plane we need to first evluate the the y-component of the velocity.

Recall from Eqn.(2.18) that the vertical component of the vorticity is given by

$$\omega_z = \left[\frac{\partial \overline{v}_1}{\partial \overline{x}} - \frac{\partial \overline{u}_1}{\partial \overline{y}}\right] = Ta^{1/2}\frac{\partial \overline{w}_1}{\partial \overline{z}} . \tag{12}$$

Noting that there are no variations in the y-directions and using Eqn.(11) yields,

$$\overline{v}_1 = 2Ta^{1/2} \frac{N_1}{\alpha^{1/2}} \sin(s\overline{x})\cos(\pi\overline{z}).$$ (13)

Eqn.(13) is identical to Eqn.(3.47). Now using the continuity equation $\partial\overline{u}/\partial\overline{x} = -\partial\overline{w}/\partial\overline{z}$ and Eqn.(11) to evaluate the horizontal component of the velocity yields,

$$\overline{u}_1 = -2\frac{N_1}{\alpha^{1/2}} \sin(s\overline{x})\cos(\pi\overline{z}),$$ (14)

which is identical to Eqn.(3.49). The solutions presented by Eqns.(13-14) represents the convection cells that are tilted in the y-direction and form and angle $\tan^{-1}(\overline{v}_1/\overline{u}_1)$ relative to the x-axis. Incidentally there is no velocity component normal to this plane, and is therefore deemed to be the plane that contains the streamlines. The ratio between the y-component and the x-component of the velocities is simply inferred from Eqns.(13-14) and may be presented as,

$$\frac{\overline{v}_1}{\overline{u}_1} = -Ta^{1/2},$$ (15)

which is identical to Eqn.(3.50). The wavenumber on the oblique plane containing the streamlines is given as

$$s_{cr,st}^{(oblique)} = s_{cr,st}\cos(\tan^{-1}(\overline{v}_1/\overline{u}_1)).$$ (16)

The critical wavenumber for stationary convection is given as $\alpha_{cr,st} = s_{cr,st}^2/\pi^2 = \sqrt{Ta+1}$, thereby allowing the original wavenumber to be written as, $s_{cr,st} = \pi(Ta+1)^{1/4}$.

The oblique plane angle relative to the x-axis may be defined as, $\upsilon_{ob.} = \tan^{-1}(\overline{v}_1/\overline{u}_1)$. This could be rewritten as, $\tan(\upsilon_{ob.}) = (\overline{v}_1/\overline{u}_1) = -Ta^{1/2}$. Now using a trigonometric identity of the form,

$$\tan^2(\upsilon_{ob.}) + 1 = \frac{1}{\cos^2(\upsilon_{ob.})} \,. \tag{17}$$

Using the fact that $\tan(\upsilon_{ob.}) = -Ta^{1/2}$, we may rewrite Eqn.(17) to yield the following result,

$$Ta + 1 = \frac{1}{\cos^2(\upsilon_{ob.})} \,, \tag{18}$$

which may be rearranged to give,

$$\cos(\upsilon_{ob.}) = \frac{1}{(Ta+1)^{1/2}} \,. \tag{19}$$

Substituting Eqn.(19) in Eqn.(16) and using the fact that $s_{cr,st} = \pi(Ta+1)^{1/4}$ gives,

$$s_{cr,st}^{(oblique)} = s_{cr,st}\cos(\upsilon_0) = \frac{\pi(Ta+1)^{1/4}}{(Ta+1)^{1/2}} = \frac{\pi}{(Ta+1)^{1/4}} \,, \tag{20}$$

which is identical to Eqn.(3.51).

Appendix W : Derivation of the characteristic Rayleigh number and the frequency of the oscillations for the case of oscillatory convection for the Author's scaling

The general definition for the Rayleigh number is given as,

$$\overline{R}^2 = \frac{(1+\alpha)}{[\sigma+1]\Omega\pi^2\alpha}\left([\sigma+1]^2(1+\alpha)+Ta\right).$$ (1)

For the case of ocillatory convection, we set $\sigma = i\sigma_i$ in the expression for the general definition for the Rayleigh number, Eqn.(1), which yields,

$$\overline{R}^2 = \frac{(1+\alpha)}{[i\sigma_i+1]\Omega\pi^2\alpha}\left([i\sigma_i+1]^2(1+\alpha)+Ta\right).$$ (2)

Eqn.(2) may be expanded to give the following expression,

$$[i\sigma_i+1]\Omega\pi^2\alpha\overline{R}^2 = (1+\alpha)\left([-\sigma_i^2+i2\sigma_i+1](1+\alpha)+Ta\right),$$ (3)

which after equating real and imaginary parts yields the two equations of the form,

$$\Omega\pi^2\alpha\overline{R}^2_{c,ov} = (1+\alpha)\left([1-\sigma_i^2](1+\alpha)+Ta\right),$$ (4)

and

$$\sigma_i\Omega\pi^2\alpha\overline{R}^2_{cr,ov} = (1+\alpha)\left(2\sigma_i(1+\alpha)\right).$$ (5)

From Eqn.(5) we get the definition of the Rayleigh number presented as,

$$\overline{R}^2_{cr,ov} = \frac{2}{\pi^2\alpha\Omega}(1+\alpha)^2,$$ (6)

which is identical to Eqn.(3.52). Now substituting Eqn.(6) in Eqn.(4) yields the following expression

$$2(1+\alpha)^2 = (1+\alpha)\left(\left[1-\sigma_i^2\right](1+\alpha)+Ta\right).$$

(7)

Refining Eqn.(7) and solving for σ_i yields the following expression for the frequency,

$$\sigma_i^2 = \frac{Ta}{(\alpha+1)} - 1,$$

(8)

which is identical to Eqn.(3.53).

Appendix X : Derivation of the critical wavenumber, Rayleigh number and frequency for the case of oscillatory convection for the Author's scaling

The characteristic wavenumber for oscillatory convection is given as

$$\overline{R}_{cr,ov} = \frac{1}{\pi}\sqrt{\frac{2}{\Omega}} \cdot \frac{(1+\alpha)}{\sqrt{\alpha}}.$$

(1)

Minimising the Rayleigh number given by Eqn.(1) yields the following critical wavenumber relation,

$$\frac{d\overline{R}_{cr,ov}}{d\alpha} = \frac{1}{2}(\alpha + 1) + \alpha = 0,$$

(2)

which after solving for α, yields the following critical wavenumber,

$$\alpha_{cr,ov} = 1.$$

(3)

which is identical to Eqn.(3.54). Substituting this result in,

$$\overline{R}_{cr,ov} = \frac{1}{\pi}\sqrt{\frac{2}{\Omega}} \cdot \frac{(1+\alpha)}{\sqrt{\alpha}},$$

(4)

yields,

$$\overline{R}_{cr,ov} = \frac{2}{\pi}\sqrt{\frac{2}{\Omega}},$$

(5)

which is identical to Eqn.(3.55). Once more substituting Eqn.(3) in,

$$\sigma_i^2 = \frac{Ta}{(\alpha + 1)} - 1, \tag{6}$$

yields,

$$\sigma_i^2 = \frac{Ta}{2} - 1, \tag{7}$$

which is identical to Eqn.(3.56).

Appendix Y : Weak non-linear analysis : A stream function representation of the governing equations for the Author's scaling

For the weak non-linear analysis it is convenient to use the definition of the stream function in the form, $\bar{u} = \partial \psi / \partial \bar{z}$, $\bar{w} = -\partial \psi / \partial \bar{x}$. Recall that the heat balance equation corresponding to the author's scaling may be presented as,

$$\delta \left(\chi_1 \frac{\partial}{\partial t'} - \frac{\partial}{\partial \bar{z}} \right) \left(\theta - \frac{\bar{S}}{\delta} \varphi \right) + R\bar{u} \frac{\partial \theta}{\partial \bar{x}} + R\bar{w} \frac{\partial \theta}{\partial \bar{z}} = \bar{\nabla}^2 \theta . \tag{1}$$

Applying the stream function definition given in the opening paragraph allows Eqn.(1) to be written as,

$$\delta \left(\chi_1 \frac{\partial}{\partial t'} - \frac{\partial}{\partial \bar{z}} \right) \left(\theta - \frac{\bar{S}}{\delta} \varphi \right) + R \frac{\partial \psi}{\partial \bar{z}} \frac{\partial \theta}{\partial \bar{x}} - R \frac{\partial \psi}{\partial \bar{x}} \frac{\partial \theta}{\partial \bar{z}} = \bar{\nabla}^2 \theta , \tag{2}$$

which is identical to Eqn.(4.1). Similary one may present the solute balance equation in exactly the same manner as follows,

$$\delta \left(\chi_1 \frac{\partial}{\partial t'} - \frac{\partial}{\partial \bar{z}} \right) \left[(1 - \varphi)\theta + \frac{c_s}{\delta} \varphi \right] + R \frac{\partial \psi}{\partial \bar{z}} \frac{\partial \theta}{\partial \bar{x}} - R \frac{\partial \psi}{\partial \bar{x}} \frac{\partial \theta}{\partial \bar{z}} = 0, \tag{3}$$

which is identical to Eqn.(4.2). Note that $\chi_1 = \delta \chi_0$ (where $\chi_0 = Pr \phi_0 \vartheta_0$) and $t' = \chi_1 \bar{t}$.

Recall that the Darcy equation was found to be of the form,

$$\frac{\partial \bar{U}}{\partial t'} + \Pi (\varphi) \bar{U} = -\bar{\nabla} \bar{p} - R\theta \hat{e}_z - Ta^{1/2} \hat{e}_z \times \bar{U} . \tag{4}$$

In order to get the Darcy equation represented in terms of stream functions we need to first write the Eqn.(4) in component form as follows,

$$\frac{\partial \overline{u}}{\partial t'} + \Pi(\varphi)\overline{u} = -\frac{\partial \overline{p}}{\partial \overline{x}} + Ta^{1/2}\overline{v} \tag{5}$$

$$\frac{\partial \overline{v}}{\partial t'} + \Pi(\varphi)\overline{v} = -\frac{\partial \overline{p}}{\partial \overline{y}} - Ta^{1/2}\overline{u} \tag{6}$$

$$\frac{\partial \overline{w}}{\partial t'} + \Pi(\varphi)\overline{w} = -\frac{\partial \overline{p}}{\partial \overline{z}} - R\theta \ . \tag{7}$$

First differentiate Eqn.(5) with respect $\overline{z}$ to give,

$$\frac{\partial^2 \overline{u}}{\partial \overline{z}\partial t'} + \Pi(\varphi)\frac{\partial \overline{u}}{\partial \overline{z}} + \overline{u}\frac{\partial \Pi(\varphi)}{\partial \overline{z}} = -\frac{\partial^2 \overline{p}}{\partial \overline{z}\partial \overline{x}} + Ta^{1/2}\frac{\partial \overline{v}}{\partial \overline{z}} \ . \tag{8}$$

Now differentiate Eqn.(7) with respect to $\overline{x}$ as follows,

$$\frac{\partial^2 \overline{w}}{\partial \overline{x}\partial t'} + \Pi(\varphi)\frac{\partial \overline{w}}{\partial \overline{x}} = -\frac{\partial^2 \overline{p}}{\partial \overline{x}\partial \overline{z}} - R\frac{\partial \theta}{\partial \overline{x}} \ . \tag{9}$$

Subract Eqn.(9) from Eqn.(8) to give,

$$\left[\frac{\partial}{\partial t'} + \Pi(\varphi)\right]\left(\frac{\partial \overline{u}}{\partial \overline{z}} - \frac{\partial \overline{w}}{\partial \overline{x}}\right) + \overline{u}\frac{\partial \Pi(\varphi)}{\partial \overline{z}} = Ta^{1/2}\frac{\partial \overline{v}}{\partial \overline{z}} + R\frac{\partial \theta}{\partial \overline{x}} \ . \tag{10}$$

Now differentiate Eqn.(6) with respect to $\overline{z}$ to give,

$$\frac{\partial^2 \overline{v}}{\partial \overline{z}\partial t'} + \Pi(\varphi)\frac{\partial \overline{v}}{\partial \overline{z}} + \overline{v}\frac{\partial \Pi(\varphi)}{\partial \overline{z}} = -\frac{\partial^2 \overline{p}}{\partial \overline{z}\partial \overline{y}} - Ta^{1/2}\frac{\partial \overline{u}}{\partial \overline{z}} \ . \tag{11}$$

Now differentiate Eqn.(7) with respect to $\overline{y}$ to give,

$$\frac{\partial^2 \overline{w}}{\partial \overline{y} \partial t'} + \Pi(\varphi) \frac{\partial \overline{w}}{\partial \overline{y}} = -\frac{\partial^2 \overline{p}}{\partial \overline{y} \partial \overline{z}} - R\frac{\partial \theta}{\partial \overline{y}} . \tag{12}$$

Now subtract Eqn.(12) from Eqn.(11) to give,

$$\left[\frac{\partial}{\partial t'} + \Pi(\varphi)\right]\left(\frac{\partial \overline{v}}{\partial \overline{z}} - \frac{\partial \overline{w}}{\partial \overline{y}}\right) + \overline{v}\frac{\partial \Pi(\varphi)}{\partial \overline{z}} = -Ta^{1/2}\frac{\partial \overline{u}}{\partial \overline{z}} + R\frac{\partial \theta}{\partial \overline{y}} . \tag{13}$$

From Eqn.(13) we get,

$$\left[\frac{\partial}{\partial t'} + \Pi(\varphi)\right]\frac{\partial \overline{v}}{\partial \overline{z}} = -Ta^{1/2}\frac{\partial \overline{u}}{\partial \overline{z}} + R\frac{\partial \theta}{\partial \overline{y}} - \overline{v}\frac{\partial \Pi(\varphi)}{\partial \overline{z}} + \left[\frac{\partial}{\partial t'} + \Pi(\varphi)\right]\frac{\partial \overline{w}}{\partial \overline{y}} . \tag{14}$$

Substituting Eqn.(14) in Eqn.(10) yields,

$$\left[\frac{\partial}{\partial t'} + \Pi(\varphi)\right]^2\left(\frac{\partial \overline{u}}{\partial \overline{z}} - \frac{\partial \overline{w}}{\partial \overline{x}}\right) + \left[\frac{\partial}{\partial t'} + \Pi(\varphi)\right]\overline{u}\frac{\partial \Pi(\varphi)}{\partial \overline{z}} = R\left[\frac{\partial}{\partial t'} + \Pi(\varphi)\right]\frac{\partial \theta}{\partial \overline{x}} +$$

$$- Ta\frac{\partial \overline{u}}{\partial \overline{z}} + RTa^{1/2}\frac{\partial \theta}{\partial \overline{y}} - \overline{v}Ta^{1/2}\frac{\partial \Pi(\varphi)}{\partial \overline{z}} + Ta^{1/2}\left[\frac{\partial}{\partial t'} + \Pi(\varphi)\right]\frac{\partial \overline{w}}{\partial \overline{y}} \quad .\tag{15}$$

Introducing the stream function definition in Eqn.(15) and neglecting effects in the y-direction yields,

$$\left[\frac{\partial}{\partial t'} + \Pi(\varphi)\right]^2 \nabla^2 \psi + \left[\frac{\partial}{\partial t'} + \Pi(\varphi)\right]\left(\frac{\partial \psi}{\partial \overline{z}}\frac{\partial \Pi(\varphi)}{\partial \overline{z}} - R\frac{\partial \theta}{\partial \overline{x}}\right) + Ta\frac{\partial^2 \psi}{\partial \overline{z}^2} + Ta^{1/2}\overline{v}\frac{\partial \Pi(\varphi)}{\partial \overline{z}} = 0,$$

$$\tag{16}$$

which is identical to Eqn.(4.3).

Appendix Z : Weak non-linear analysis – Stationary convection : Derivation of the governing equations for each order of the disturbance amplitude ε

The governing equations to each order of the disturbance amplitude is derived for the stationary case by considering each of the energy balance, solute balance and Darcy equations separately. To further clarify the process each term in each of the governing equations are then considered separately so as to ensure that the correct equation set to each order is obtained.

For the case of stationary convection we allow variations only at the slow time scale $\tau = \varepsilon^2 t'$ in order to prevent exponential growth and reaching finite values for the amplitude at steady state. Slow spaces scale are also adopted in the form $X = \varepsilon \overline{x}$ so as to include a continuous finite band of horizontal modes. Bearing these scalings in mind we may propose the following form of the energy equation,

$$-\overline{S}\left(\varepsilon^2\chi_1\frac{\partial}{\partial\tau} - \frac{\partial}{\partial\overline{z}}\right)\varphi + R\frac{\partial\psi}{\partial\overline{z}}\frac{\partial\theta}{\partial\overline{x}} + R\varepsilon\frac{\partial\psi}{\partial\overline{z}}\frac{\partial\theta}{\partial X} - R\frac{\partial\psi}{\partial\overline{x}}\frac{\partial\theta}{\partial\overline{z}} - R\varepsilon\frac{\partial\psi}{\partial X}\frac{\partial\theta}{\partial\overline{z}} =$$

$$\nabla^2\theta + 2\varepsilon\frac{\partial^2\theta}{\partial\overline{x}\partial X} + \varepsilon^2\frac{\partial^2\theta}{\partial X^2} = 0 \quad . \quad (1)$$

In addition we expand the dependant variables in terms of the disturbance amplitude as follows,

$$[\psi,\theta,\varphi] = [\psi_B,\theta_B,\varphi_B] + \varepsilon[\psi_1,\theta_1,\varphi_1] + \varepsilon^2[\psi_2,\theta_2,\varphi_2] + \varepsilon^3[\psi_3,\theta_3,\varphi_3]. \quad (2)$$

In addition the expansion for the permeability function and the Rayleigh number is given as,

$$\Pi(\varphi) = 1 + \varepsilon^2 K_c\varphi_1^2, \quad R = R_{cr}(1+\varepsilon^2). \quad (3)$$

The basic solution depicted by subscript "B" in Eqn.(2) is given as,

$$[\psi_B, \theta_B, \varphi_B] = [0, (\bar{z} - 1), 0].$$

(4)

Using these expansions (where necessary) we consider each term in Eqn.(1) separately and adopt the following naming convention, where the subscript "E" refers to the energy equation.

$$t_{1E} = -\overline{S}\left(\varepsilon^2 \chi_1 \frac{\partial}{\partial \tau} - \frac{\partial}{\partial \bar{z}}\right)\varphi,$$

(5)

which to the different orders in the disturbance amplitude is presented as,

$$t_{1E}(\varepsilon^1) = \overline{S}\frac{\partial \varphi_1}{\partial \bar{z}}$$

(5a)

$$t_{1E}(\varepsilon^2) = \overline{S}\frac{\partial \varphi_2}{\partial \bar{z}}$$

(5b)

$$t_{1E}(\varepsilon^3) = -\overline{S}\left(\frac{\partial \varphi_1}{\partial \tau} - \frac{\partial \varphi_3}{\partial \bar{z}}\right).$$

(5c)

Next consider the second term,

$$t_{2E} = R\frac{\partial \psi}{\partial \bar{z}}\frac{\partial \theta}{\partial \bar{x}},$$

(6)

which to the different orders of the disturbance amplitude yields,

$$t_{2E}(\varepsilon^1) = 0$$

(6a)

$$t_{2E}\left(\varepsilon^2\right) = R_{cr} \frac{\partial\psi_1}{\partial\overline{z}} \frac{\partial\theta_1}{\partial\overline{x}} \tag{6b}$$

$$t_{2E}\left(\varepsilon^3\right) = R_{cr}\left[\frac{\partial\psi_1}{\partial\overline{z}} \frac{\partial\theta_2}{\partial\overline{x}} - \frac{\partial\psi_2}{\partial\overline{z}} \frac{\partial\theta_1}{\partial\overline{x}}\right]. \tag{6c}$$

We now consider the third term

$$t_{3E} = R\varepsilon \frac{\partial\psi}{\partial\overline{z}} \frac{\partial\theta}{\partial X}, \tag{7}$$

which to different orders of the disturbance amplitude produces,

$$t_{3E}\left(\varepsilon^1\right) = 0 \tag{7a}$$

$$t_{3E}\left(\varepsilon^2\right) = 0 \tag{7b}$$

$$t_{3E}\left(\varepsilon^3\right) = R_{cr} \frac{\partial\psi_1}{\partial\overline{z}} \frac{\partial\theta_1}{\partial X}. \tag{7c}$$

Now consider the fourth term

$$t_{4E} = -R \frac{\partial\psi}{\partial\overline{x}} \frac{\partial\theta}{\partial\overline{z}}, \tag{8}$$

which to different orders of the disturbance amplitude yields,

$$t_{4E}\left(\varepsilon^1\right) = -R_{cr} \frac{\partial\psi_1}{\partial\overline{x}} \tag{8a}$$

238

$$t_{4E}\left(\varepsilon^2\right) = -R_{cr}\left[\frac{\partial\psi_2}{\partial\overline{x}} + \frac{\partial\psi_1}{\partial\overline{x}}\frac{\partial\theta_1}{\partial\overline{z}}\right] \tag{8b}$$

$$t_{4E}\left(\varepsilon^3\right) = -R_{cr}\left[\frac{\partial\psi_3}{\partial\overline{x}} + \frac{\partial\psi_1}{\partial\overline{x}} + \frac{\partial\psi_1}{\partial\overline{x}}\frac{\partial\theta_2}{\partial\overline{z}} + \frac{\partial\psi_2}{\partial\overline{x}}\frac{\partial\theta_1}{\partial\overline{z}}\right]. \tag{8c}$$

Considering the fifth term,

$$t_{5E} = -R\varepsilon\frac{\partial\psi}{\partial X}\frac{\partial\theta}{\partial\overline{z}}, \tag{9}$$

to the different orders of the disturbance amplitude yields,

$$t_{5E}\left(\varepsilon^1\right) = 0 \tag{9a}$$

$$t_{5E}\left(\varepsilon^2\right) = -R_{cr}\frac{\partial\psi_1}{\partial X} \tag{9b}$$

$$t_{5E}\left(\varepsilon^3\right) = -R_{cr}\left[\frac{\partial\psi_2}{\partial X} + \frac{\partial\psi_1}{\partial X}\frac{\partial\theta_1}{\partial\overline{z}}\right]. \tag{9c}$$

Considering the sixth term,

$$t_{6E} = \nabla^2\theta, \tag{10}$$

which simply yields

$$t_{6E}\left(\varepsilon^1\right) = \nabla^2\theta_1 \tag{10a}$$

$$t_{6E}\left(\varepsilon^2\right) = \nabla^2\theta_2 \tag{10b}$$

$$t_{6E}\left(\varepsilon^{3}\right) = \nabla^{2}\theta_{3}, \tag{10c}$$

to the different orders of the disturbance amplitude.

Considering the seventh term,

$$t_{7E} = 2\varepsilon\frac{\partial^{2}\theta}{\partial\bar{x}\partial X}, \tag{11}$$

and considering to the different orders of the disturbance amplitude yields,

$$t_{7E}\left(\varepsilon^{1}\right) = 0 \tag{11a}$$

$$t_{7E}\left(\varepsilon^{2}\right) = 2\frac{\partial^{2}\theta_{1}}{\partial\bar{x}\partial X} \tag{11b}$$

$$t_{7E}\left(\varepsilon^{3}\right) = 2\frac{\partial^{2}\theta_{2}}{\partial\bar{x}\partial X}. \tag{11c}$$

Finally considering the eighth term,

$$t_{8E} = \varepsilon^{2}\frac{\partial^{2}\theta}{\partial X^{2}}, \tag{12}$$

to the different orders of the disturbance amplitude yields,

$$t_{8E}\left(\varepsilon^{1}\right) = 0 \tag{12a}$$

$$t_{8E}\left(\varepsilon^{2}\right) = 0 \tag{12b}$$

$$t_{8E}\left(\varepsilon^3\right) = \frac{\partial^2 \theta_1}{\partial X^2}.$$ (12c)

It can be observed that the energy balance and solute blance equations are very similar, the only difference being that the solute balance equations omits the Laplacian operator. For this reason, the process adopted above won't be repeated for the solute balance equation set. We now proceed to develop the Darcy equation to different orders of the disturbance amplitude. The Darcy equation containing the slow time and space scales may be presented as,

$$\left[\varepsilon^2 \frac{\partial}{\partial \tau} + \Pi(\varphi)\right]^2 \nabla^2 \psi + 2\varepsilon \left[\varepsilon^2 \frac{\partial}{\partial \tau} + \Pi(\varphi)\right]^2 \frac{\partial^2 \psi}{\partial \bar{x} \partial X} + \varepsilon^2 \left[\varepsilon^2 \frac{\partial}{\partial \tau} + \Pi(\varphi)\right]^2 \frac{\partial^2 \psi}{\partial X^2} +$$

$$\left[\varepsilon^2 \frac{\partial}{\partial \tau} + \Pi(\varphi)\right] \frac{\partial \psi}{\partial \bar{z}} \frac{\partial \Pi(\varphi)}{\partial \bar{z}} - R\left[\varepsilon^2 \frac{\partial}{\partial \tau} + \Pi(\varphi)\right] \frac{\partial \theta}{\partial \bar{x}} - R\varepsilon \left[\varepsilon^2 \frac{\partial}{\partial \tau} + \Pi(\varphi)\right] \frac{\partial \theta}{\partial X} +$$

$$Ta \frac{\partial^2 \psi}{\partial \bar{z}^2} + Ta^{1/2} v_1 \frac{\partial \Pi(\varphi)}{\partial \bar{z}} = 0.$$ (13)

It should be pointed out that the effects of permeability are only felt at order $O(\varepsilon^3)$. With this in mind it can be seen that the last term in Eqn.(13) falls away at the first two orders of the disturbance amplitude. Using the proposed expansions for the permeability function and the Rayleigh number we may consider each term in Eqn.(13) separately for clarity, noting that the variables with the subscript "D" refers to the Darcy equation.

Referring to the first term in Eqn.(13),

$$t_{1D} = \left[\varepsilon^2 \frac{\partial}{\partial \tau} + \Pi(\varphi)\right]^2 \nabla^2 \psi,$$ (14)

and considering to each order of the disturbance amplitude yields,

$$t_{1D}(\varepsilon^1) = \nabla^2 \psi_1 \tag{14a}$$

$$t_{1D}(\varepsilon^2) = \nabla^2 \psi_2 \tag{14b}$$

$$t_{1D}(\varepsilon^3) = \nabla^2 \psi_3 + 2K_c \varphi_1^2 \nabla^2 \psi_1 + 2\frac{\partial}{\partial \tau} \nabla^2 \psi_1. \tag{14c}$$

Considering the second term in Eqn.(13),

$$t_{2D} = 2\varepsilon \left[\varepsilon^2 \frac{\partial}{\partial \tau} + \Pi(\varphi) \right]^2 \frac{\partial^2 \psi}{\partial \overline{x} \partial X}, \tag{15}$$

and developing to the different orders of the disturbance amplitude yields,

$$t_{2D}(\varepsilon^1) = 0 \tag{15a}$$

$$t_{2D}(\varepsilon^2) = 2\frac{\partial^2 \psi_1}{\partial \overline{x} \partial X} \tag{15b}$$

$$t_{2D}(\varepsilon^2) = 2\frac{\partial^2 \psi_2}{\partial \overline{x} \partial X}. \tag{15c}$$

Analysing the third term in Eqn.(13),

$$t_{3D} = \varepsilon^2 \left[\varepsilon^2 \frac{\partial}{\partial \tau} + \Pi(\varphi) \right]^2 \frac{\partial^2 \psi}{\partial X^2}, \tag{16}$$

and considering to the different orders of the disturbance amplitude yields,

$$t_{3D}(\varepsilon^1) = 0 \tag{16a}$$

$$t_{3D}(\varepsilon^2) = 0 \tag{16b}$$

$$t_{3D}(\varepsilon^3) = \frac{\partial^2 \psi_1}{\partial X^2}. \tag{16c}$$

Recalling the fourth term in Eqn.(13),

$$t_{4D} = \left[\varepsilon^2 \frac{\partial}{\partial \tau} + \Pi(\varphi) \right] \frac{\partial \psi}{\partial \bar{z}} \frac{\partial \Pi(\varphi)}{\partial \bar{z}}, \tag{17}$$

and considering to each order of the disturbance amplitude yields,

$$t_{4D}(\varepsilon^1) = 0 \tag{17a}$$

$$t_{4D}(\varepsilon^2) = 0 \tag{17b}$$

$$t_{4D}(\varepsilon^3) = K_c \frac{\partial \psi_1}{\partial \bar{z}} \frac{\partial \varphi_1^2}{\partial \bar{z}}. \tag{17c}$$

Recalling the fifth term in Eqn.(13),

$$t_{5D} = -R \left[\varepsilon^2 \frac{\partial}{\partial \tau} + \Pi(\varphi) \right] \frac{\partial \theta}{\partial \bar{x}}, \tag{18}$$

and considering to each order of the disturbance amplitude yields,

$$t_{5D}\left(\varepsilon^1\right) = -R_{cr}\frac{\partial\theta_1}{\partial\overline{x}}$$
(18a)

$$t_{5D}\left(\varepsilon^2\right) = -R_{cr}\frac{\partial\theta_2}{\partial\overline{x}}$$
(18b)

$$t_{5D}\left(\varepsilon^3\right) = -R_{cr}\frac{\partial\theta_3}{\partial\overline{x}} - R_{cr}\left(\frac{\partial\theta_1}{\partial\overline{x}} + K_c\varphi_1^2\frac{\partial\theta_1}{\partial\overline{x}} + \frac{\partial}{\partial\tau}\frac{\partial\theta_1}{\partial\overline{x}}\right).$$
(18c)

Recalling the sixth term in Eqn.(13),

$$t_{6D} = -R\varepsilon\left[\varepsilon^2\frac{\partial}{\partial\tau} + \Pi(\varphi)\right]\frac{\partial\theta}{\partial X},$$
(19)

and considering to each order of the disturbance amplitude yields,

$$t_{6D}\left(\varepsilon^1\right) = 0$$
(19a)

$$t_{6D}\left(\varepsilon^2\right) = -R_{cr}\frac{\partial\theta_1}{\partial X}$$
(19b)

$$t_{6D}\left(\varepsilon^3\right) = -R_{cr}\frac{\partial\theta_2}{\partial X}.$$
(19c)

Recalling the seventh term in Eqn.(13),

$$t_{7D} = Ta\frac{\partial^2\psi}{\partial\overline{z}^2},$$
(20)

and considering to the different orders of the disturbance amplitude yields,

$$t_{7D}(\varepsilon^1) = Ta\frac{\partial^2\psi_1}{\partial\overline{z}^2} \tag{20a}$$

$$t_{7D}(\varepsilon^2) = Ta\frac{\partial^2\psi_2}{\partial\overline{z}^2} \tag{20b}$$

$$t_{7D}(\varepsilon^3) = Ta\frac{\partial^2\psi_3}{\partial\overline{z}^2} \; . \tag{20c}$$

Finally recalling the eighth term in Eqn.(13),

$$t_{8D} = Ta^{1/2}v_1\frac{\partial\Pi(\varphi)}{\partial\overline{z}} \; , \tag{21}$$

and considering to the different orders of the disturbance amplitude yields,

$$t_{8D}(\varepsilon^1) = 0 \tag{21a}$$

$$t_{8D}(\varepsilon^2) = 0 \tag{21b}$$

$$t_{8D}(\varepsilon^3) = K_c Ta^{1/2}v_1\frac{\partial\varphi_1^2}{\partial\overline{z}} \; . \tag{21c}$$

We may now proceed to build the governing system of equations to each order by taking into account the terms developed to each order of the disturbance amplitude for the energy, solute and Darcy equations. This process is simply achieved by collecting the respective terms for each of the energy, solute balance and Darcy equations from Eqns.(5-21) above.

245

The governing system to order $O(\varepsilon^1)$ is given as,

$$\overline{S}\frac{\partial \varphi_1}{\partial \overline{z}} - R_{cr}\frac{\partial \psi_1}{\partial \overline{x}} - \nabla^2\theta_1 = 0 \tag{22a}$$

$$-c_s\frac{\partial \varphi_1}{\partial \overline{z}} - R_{cr}\frac{\partial \psi_1}{\partial \overline{x}_1} = 0 \tag{22b}$$

$$\nabla^2\psi_1 - R_{cr}\frac{\partial \theta_1}{\partial \overline{x}} + Ta\frac{\partial^2\psi_1}{\partial \overline{z}^2} = 0, \tag{22c}$$

which is identical to the system presented in Eqns.(4.11-4.13).

Next we propose the goiverning system to order $O(\varepsilon^2)$ which is given as,

$$\overline{S}\frac{\partial \varphi_2}{\partial \overline{z}} - R_{cr}\frac{\partial \psi_2}{\partial \overline{x}} - \nabla^2\theta_2 = R_{cr}\frac{\partial \psi_1}{\partial X} + 2\frac{\partial^2\theta_1}{\partial \overline{x}\partial X} - R_{cr}\left[\frac{\partial \psi_1}{\partial \overline{z}}\frac{\partial \theta_1}{\partial \overline{x}} - \frac{\partial \psi_1}{\partial \overline{x}}\frac{\partial \theta_1}{\partial \overline{z}}\right] \tag{23a}$$

$$-c_s\frac{\partial \varphi_2}{\partial \overline{z}} - R_{cr}\frac{\partial \psi_2}{\partial \overline{x}_2} = R_{cr}\frac{\partial \psi_1}{\partial X} - R_{cr}\left[\frac{\partial \psi_1}{\partial \overline{z}}\frac{\partial \theta_1}{\partial \overline{x}} - \frac{\partial \psi_1}{\partial \overline{x}}\frac{\partial \theta_1}{\partial \overline{z}}\right] \tag{23b}$$

$$\nabla^2\psi_2 - R_{cr}\frac{\partial \theta_2}{\partial \overline{x}} + Ta\frac{\partial^2\psi_2}{\partial \overline{z}^2} = R_{cr}\frac{\partial \theta_1}{\partial X} - 2\frac{\partial^2\psi_1}{\partial \overline{x}\partial X}, \tag{23c}$$

which is identical to Eqns.(4.19-4.21).

Finally by carefully collecting the terms pertinent to order $O(\varepsilon^3)$ and using the fact that $v_1 = -Ta^{1/2}\,\partial\psi_1/\partial\bar{z}$, we may present the governing system to order $O(\varepsilon^3)$ as follows,

$$\bar{S}\frac{\partial\varphi_3}{\partial\bar{z}} - R_{cr}\frac{\partial\psi_3}{\partial\bar{x}} - \nabla^2\theta_3 = \bar{S}\frac{\partial\varphi_1}{\partial\tau} + R_{cr}\frac{\partial\psi_1}{\partial\bar{x}} + R_{cr}\frac{\partial\psi_2}{\partial X} + 2\frac{\partial^2\theta_2}{\partial\bar{x}\partial\bar{z}} -$$

$$R_{cr}\left[\left\{\frac{\partial\psi_1}{\partial\bar{z}}\frac{\partial\theta_2}{\partial\bar{x}} - \frac{\partial\psi_1}{\partial\bar{x}}\frac{\partial\theta_2}{\partial\bar{z}}\right\} + \left\{\frac{\partial\psi_2}{\partial\bar{z}}\frac{\partial\theta_1}{\partial\bar{x}} - \frac{\partial\psi_2}{\partial\bar{x}}\frac{\partial\theta_1}{\partial\bar{z}}\right\} + \left\{\frac{\partial\psi_1}{\partial\bar{z}}\frac{\partial\theta_1}{\partial X} - \frac{\partial\psi_1}{\partial X}\frac{\partial\theta_1}{\partial\bar{z}}\right\} + \frac{\partial^2\theta_1}{\partial X^2}\right]$$

$$(24a)$$

$$-c_S\frac{\partial\varphi_3}{\partial\bar{z}} - R_{cr}\frac{\partial\psi_3}{\partial\bar{x}} = -c_S\frac{\partial\varphi_1}{\partial\tau} + R_{cr}\frac{\partial\psi_1}{\partial\bar{x}} + R_{cr}\frac{\partial\psi_2}{\partial X} -$$

$$R_{cr}\left[\left\{\frac{\partial\psi_1}{\partial\bar{z}}\frac{\partial\theta_2}{\partial\bar{x}} - \frac{\partial\psi_1}{\partial\bar{x}}\frac{\partial\theta_2}{\partial\bar{z}}\right\} + \left\{\frac{\partial\psi_2}{\partial\bar{z}}\frac{\partial\theta_1}{\partial\bar{x}} - \frac{\partial\psi_2}{\partial\bar{x}}\frac{\partial\theta_1}{\partial\bar{z}}\right\} + \left\{\frac{\partial\psi_1}{\partial\bar{z}}\frac{\partial\theta_1}{\partial X} - \frac{\partial\psi_1}{\partial X}\frac{\partial\theta_1}{\partial\bar{z}}\right\}\right] \qquad (24b)$$

$$\nabla^2\psi_3 - R_{cr}\frac{\partial\theta_3}{\partial\bar{x}} + Ta\frac{\partial^2\psi_3}{\partial\bar{z}^2} = -2K_c\varphi_1^2\nabla^2\psi_1 - 2\frac{\partial}{\partial\tau}\nabla^2\psi_1 - 2\frac{\partial^2\psi_2}{\partial\bar{x}\partial X} + K_cTa\frac{\partial\varphi_1^2}{\partial\bar{z}}\frac{\partial^2\psi_1}{\partial\bar{z}} -$$

$$K_c\frac{\partial\varphi_1^2}{\partial\bar{z}}\frac{\partial\psi_1}{\partial\bar{z}} + R_{cr}\frac{\partial\theta_1}{\partial\bar{x}} + K_c\varphi_1^2R_{cr}\frac{\partial\theta_1}{\partial\bar{x}} + R_{cr}\frac{\partial}{\partial\bar{x}}\frac{\partial\theta_1}{\partial\tau} + R_{cr}\frac{\partial\theta_2}{\partial X} - \frac{\partial^2\psi_1}{\partial X^2}, \qquad (24c)$$

which is identical to Eqns.(4.25-4.27).

Appendix AA : Weak non-linear Analysis – Stationary convection : Derivation of the eigenfunctions to the leading order $O(\varepsilon)$

The eigenfunctions to the leading order system

$$\overline{S}\frac{\partial \varphi_1}{\partial \overline{z}} - R_{cr}\frac{\partial \psi_1}{\partial \overline{x}} - \nabla^2\theta_1 = 0 \tag{1}$$

$$-c_S\frac{\partial \varphi_1}{\partial \overline{z}} - R_{cr}\frac{\partial \psi_1}{\partial \overline{x}}_1 = 0 \tag{2}$$

$$\nabla^2\psi_1 - R_{cr}\frac{\partial \theta_1}{\partial \overline{x}} + Ta\frac{\partial^2\psi_1}{\partial \overline{z}^2} = 0, \tag{3}$$

is sought. The solutions to the stream function and temperature is given as,

$$\psi_1 = \left[A_1 e^{is\overline{x}} + A_1^* e^{-is\overline{x}}\right]\sin(\pi\overline{z}) \tag{4}$$

$$\theta_1 = \left[B_1 e^{is\overline{x}} + B_1^* e^{-is\overline{x}}\right]\sin(\pi\overline{z}). \tag{5}$$

Substituting Eqn.(4) in Eqn.(2) yields the following differential equation,

$$\frac{\partial \varphi_1}{\partial \overline{z}} = -\frac{i\pi\alpha^{1/2}R_{cr}}{c_S}\left[A_1 e^{is\overline{x}} - A_1^* e^{-is\overline{x}}\right]\sin(\pi\overline{z}), \tag{6}$$

which upon integration with respect to $\overline{z}$ yields,

$$\varphi_1 = \frac{i\alpha^{1/2}R_{cr}}{c_S}\left[A_1 e^{is\overline{x}} - A_1^* e^{-is\overline{x}}\right]\cos(\pi\overline{z}) + C_\varepsilon, \tag{7}$$

where C_ε represents the integration constant. Applying the boundary condition $\varphi_1(1) = 0$ to Eqn.(7) in order to solve for the integration constant, yields the following final solution for the solid fraction at the leading order,

$$\varphi_1 = \left[C_1 e^{is\bar{x}} + C_1^* e^{-is\bar{x}}\right]\left[1 + \cos(\pi\bar{z})\right], \tag{8}$$

which is identical to Eqn.(4.16). Note that

$$C_1 = \frac{i\alpha^{1/2} R_{cr}}{c_S} A_1 \quad \text{and} \quad C_1^* = -\frac{i\alpha^{1/2} R_{cr}}{c_S} A_1^* \tag{9}$$

which is identical to Eqn.(4.18)

We now set out to evaluate the relationship between the coefficients A_1 and B_1. From the solute balance equation (2) we have,

$$\frac{\partial\varphi_1}{\partial\bar{z}} = -\frac{R_{cr}}{c_S}\frac{\partial\psi_1}{\partial\bar{x}_1}, \tag{10}$$

which upon substitution in the energy equation (1) yields

$$-\frac{\bar{S}}{c_S} R_{cr} \frac{\partial\psi_1}{\partial\bar{x}} - R_{cr}\frac{\partial\psi_1}{\partial\bar{x}} - \nabla^2\theta_1 = 0. \tag{11}$$

Setting $\Omega = 1 + \bar{S}/c_S$ we may present Eqn.(11) as,

$$\nabla^2\theta_1 + \Omega R_{cr}\frac{\partial\psi_1}{\partial\bar{x}} = 0, \tag{12}$$

which for all intents and purposes represents the modified heat balance equation. Using the definition for the stream function and temperature given in Eqns.(4-5) above and substituting in Eqn.(12) above gives,

$$-\pi^2(1+\alpha)\left[B_1 e^{is\bar{x}} + B_1^* e^{-is\bar{x}}\right]\sin(\pi\bar{z}) + \Omega R_{cr} i\pi\alpha^{1/2}\left[A_1 e^{is\bar{x}} - A_1^* e^{-is\bar{x}}\right]\sin(\pi\bar{z}) = 0 . \qquad (13)$$

Equating the like exponential indices gives the following relation between the amplitiudes,

$$B_1 = i\frac{\Omega R_{cr}\alpha^{1/2}}{\pi(1+\alpha)}A_1 \quad \text{and} \quad B_1^* = -i\frac{\Omega R_{cr}\alpha^{1/2}}{\pi(1+\alpha)}A_1^* , \qquad (14)$$

which is identical to Eqn.(4.17).

Appendix AB : Weak non-linear Analysis – Stationary convection : Derivation of the eigenfunctions to order $O(\varepsilon^2)$

At order $O(\varepsilon^2)$ of the disturbance amplitude the modified heat balance and Darcy equation is given as,

$$\nabla^2\theta_2 + \Omega R_{cr}\frac{\partial\psi_2}{\partial\overline{x}} = RHS_A \tag{1}$$

$$\nabla^2\psi_2 - R_{cr}\frac{\partial\theta_2}{\partial\overline{x}} + Ta\frac{\partial^2\psi_2}{\partial\overline{z}^2} = RHS_B, \tag{2}$$

where RHS_A and RHS_B are evaluated from known solutions at order $O(\varepsilon)$ and is given as,

$$RHS_A = -\frac{2\pi\alpha\Omega^2 R_{cr}^2}{(1+\alpha)}A_1 A_1^* \sin(2\pi\overline{z}) - \Omega R_{cr}\left[\frac{\partial A_1}{\partial X}e^{is\overline{x}} + \frac{\partial A_1^*}{\partial X}e^{-is\overline{x}}\right]\sin(\pi\overline{z}) -$$

$$2i\pi\alpha^{1/2}\left[\frac{\partial B_1}{\partial X}e^{is\overline{x}} - \frac{\partial B_1^*}{\partial X}e^{-is\overline{x}}\right]\sin(\pi\overline{z}) \tag{3}$$

and,

$$RHS_B = R_{cr}\left[\frac{\partial B_1}{\partial X}e^{is\overline{x}} + \frac{\partial B_1^*}{\partial X}e^{-is\overline{x}}\right]\sin(\pi\overline{z}) - 2i\pi\alpha^{1/2}\left[\frac{\partial A_1}{\partial X}e^{is\overline{x}} - \frac{\partial A_1^*}{\partial X}e^{-is\overline{x}}\right]\sin(\pi\overline{z}). \tag{4}$$

Decoupling Eqns.(1-2) by multiplying Eqn.(1) by $R_{cr}\partial/\partial\overline{x}(.)$ and Eqn.(2) by $\nabla^2(.)$ and adding the result to yield a single equation for the stream function, given as,

$$\nabla^4\psi_2 + \Omega R_{cr}^2\frac{\partial^2\psi_2}{\partial\overline{x}^2} + Ta\frac{\partial^2}{\partial\overline{z}^2}\nabla^2\psi_2 = \nabla^2 RHS_B + R_{cr}\frac{\partial}{\partial\overline{x}}RHS_A. \tag{5}$$

We may express the right hand side of Eqn.(5) symbolically as,

$$RHS_5 = \nabla^2 RHS_B + R_{cr} \frac{\partial}{\partial \overline{x}} RHS_A \,.$$

(6)

We may further evaluate Eqn.(6), taking into account the relationship between the coefficients A_1 and B_1 and that between the critical Rayleigh number and wavenumber, yields

$$RHS_5 = \frac{2i\pi^3}{\alpha^{1/2}} \left[\alpha^2 - (Ta+1) \right] \frac{\partial A_1}{\partial X} e^{is\overline{x}} \sin(\pi \overline{z}) + \frac{2i\pi^3}{\alpha^{1/2}} \left[(Ta+1) - \alpha^2 \right] \frac{\partial A_1^*}{\partial X} e^{-is\overline{x}} \sin(\pi \overline{z})$$

(7)

Using the result of the critical wave number for the case of stationary convection given as

$$\alpha = \alpha_{cr} = \sqrt{Ta+1} \,,$$

(8)

results in the right hand side of Eqn.(7) collapsing to zero, ie. $RHS_5 = 0$. Note that the subscripts referring to the critical values have been omitted for clarity. The implications of the result $RHS_5 = 0$ is that the particular solution for the stream function at this order vanishes thus resulting in the homogenous solution being the only solution. The solutiuon to the stream function at this order resembles the form of the homogenous solution for the stream function found at the leading order and is given as,

$$\psi_2 = \left[A_2 e^{is\overline{x}} + A_2^* e^{-is\overline{x}} \right] \sin(\pi \overline{z}) \,,$$

(9)

which is identical to Eqn.(4.22).

We now proceed to decouple the energy and Darcy equation at this order in order to obtain a single equation for the temperature at this order. This is achieved by multiplying

252

the energy equation (1) by $\left[\nabla^2 + Ta\,\partial^2/\partial\bar{z}^2\right](.)$ and the Darcy equation (2) by $\Omega R_{cr}\,\partial/\partial\bar{x}(.)$. The resulting Darcy equation is then subtracted from the energy equation to give,

$$\left[\nabla^2 + Ta\,\partial^2/\partial\bar{z}^2\right]\nabla^2\theta_2 + \Omega R_{cr}^2\frac{\partial^2\theta_2}{\partial\bar{x}^2} = \left[\nabla^2 + Ta\,\partial^2/\partial\bar{z}^2\right]RHS_A - \Omega R_{cr}\frac{\partial}{\partial\bar{x}}RHS_B. \qquad (10)$$

Adopting exactly the same method as outlined above for the evaluation of the streamline solution, we attack Eqn.(10) to result in the following net result,

$$\left[\nabla^2 + Ta\,\partial^2/\partial\bar{z}^2\right]\nabla^2\theta_2 + \Omega R_{cr}^2\frac{\partial^2\theta_2}{\partial\bar{x}^2} = \frac{8\pi^3\alpha\Omega R_{cr}^2}{(\alpha+1)}(Ta+1)A_1A_1^*\sin(2\pi\bar{z}). \qquad (11)$$

As before the terms containing the slow spaces scales cancelled out as a result of algebraic manipilulations. The homogenous solution to Eqn.(11) is known and was found at the leading order. At this point we concern ourselves with establishing the correct particular solution. We select a trial function of the form,

$$\theta_{2,p} = B_p\sin(2\pi\bar{z}) + C_p\cos(2\pi\bar{z}), \qquad (12)$$

which upon substitution in Eqn.(11) yields the following results for the coefficients of the trial functions selected in Eqn.(12),

$$B_p = \frac{\alpha\Omega R_{cr}^2}{2\pi(\alpha+1)}A_1A_1^* \quad \text{and} \quad C_p = 0. \qquad (13)$$

The resulting solution for the temperature at this order is simply the sum of the homogenous and particular solutions respectively which is given as,

$$\theta_2 = \left[B_2e^{is\bar{x}} + B_2^*e^{-is\bar{x}}\right]\sin(\pi\bar{z}) + \frac{\alpha\Omega^2 R_{cr}^2}{2\pi(\alpha+1)}A_1A_1^*\sin(2\pi\bar{z}), \qquad (14)$$

253

which is identical to Eqn.(4.23).

Now we need only find the solution to the solid fraction at this order. Recalling the solute balance equation to this order,

$$c_S \frac{\partial \varphi_2}{\partial \overline{z}} = -R_{cr} \frac{\partial \psi_2}{\partial \overline{x}} + R_{cr} \left[\frac{\partial \psi_1}{\partial \overline{z}} \frac{\partial \theta_1}{\partial \overline{x}} - \frac{\partial \psi_1}{\partial \overline{x}} \frac{\partial \theta_1}{\partial \overline{z}} \right] - R_{cr} \frac{\partial \psi_1}{\partial X} \tag{15}$$

and substituting the known solutions on the right hand side yields the following form of the solid fraction to be solved,

$$\frac{\partial \varphi_2}{\partial \overline{z}} = \frac{1}{c_S} \left[-\frac{2\pi \alpha \Omega R_{cr}^2}{(1+\alpha)} A_1 A_1^* \sin(2\pi \overline{z}) - i\pi \alpha^{1/2} R_{cr} \left\{ A_2 e^{is\overline{x}} - A_2^* e^{-is\overline{x}} \right\} \sin(\pi \overline{z}) - \right.$$

$$\left. R_{cr} \left\{ \frac{\partial A_1}{\partial X} e^{is\overline{x}} + \frac{\partial A_1^*}{\partial X} e^{-is\overline{x}} \right\} \sin(\pi \overline{z}) \right]. \tag{16}$$

Integrating Eqn.(16) with respect to $\overline{z}$,

$$\varphi_2 = \frac{1}{c_S} \left[\frac{\alpha \Omega R_{cr}^2}{(1+\alpha)} A_1 A_1^* \cos(2\pi \overline{z}) + i\alpha^{1/2} R_{cr} \left\{ A_2 e^{is\overline{x}} - A_2^* e^{-is\overline{x}} \right\} \cos(\pi \overline{z}) + \right.$$

$$\left. \frac{R_{cr}}{\pi} \left\{ \frac{\partial A_1}{\partial X} e^{is\overline{x}} + \frac{\partial A_1^*}{\partial X} e^{-is\overline{x}} \right\} \cos(\pi \overline{z}) \right] + C_{\varepsilon^2}, \tag{17}$$

where C_{ε^2} represents the integration constant. Using the boundary condition $\varphi_2(1) = 0$, we may evaluate the integration constant and thereby present the full solution to the solid fraction at this order as,

$$\varphi_2 = \frac{1}{c_S}\left[\frac{\alpha\Omega R_{cr}^2}{(1+\alpha)}A_1 A_1^*\left(\cos(2\pi\bar{z})-1\right) + i\alpha^{1/2}R_{cr}\left\{A_2 e^{is\bar{x}} - A_2^* e^{-is\bar{x}}\right\}\left(\cos(\pi\bar{z})+1\right)+\right.$$

$$\left. \frac{R_{cr}}{\pi}\left\{\frac{\partial A_1}{\partial X}e^{is\bar{x}} + \frac{\partial A_1^*}{\partial X}e^{-is\bar{x}}\right\}\left(\cos(\pi\bar{z})+1\right)\right], \qquad (18)$$

which may be rearranged as,

$$\varphi_2 = \left\{C_2 e^{is\bar{x}} + C_2^* e^{-is\bar{x}}\right\}\left(\cos(\pi\bar{z})+1\right) + \frac{\alpha\Omega R_{cr}^2}{c_S(1+\alpha)}A_1 A_1^*\left(\cos(2\pi\bar{z})-1\right)+$$

$$\frac{R_{cr}}{c_S\pi}\left\{\frac{\partial A_1}{\partial X}e^{is\bar{x}} + \frac{\partial A_1^*}{\partial X}e^{-is\bar{x}}\right\}\left(\cos(\pi\bar{z})+1\right), \qquad (19)$$

which is identical to Eqn.(4.24).

Appendix AC : Weak non-linear Analysis – Stationary convection : Derivation of the leading order amplitude differential equation at order $O(\varepsilon^3)$

The decoupled Darcy equation in terms of the stream function only may be presented as,

$$
\nabla^2(\nabla^2\psi_3) + \Omega R_{cr}^2 \frac{\partial^2\psi_3}{\partial\overline{x}^2} + Ta\frac{\partial^2}{\partial\overline{z}^2}\nabla^2\psi_3 = \nabla^2 RHS_D + R_{cr}\frac{\partial}{\partial\overline{x}}RHS_E \qquad (1)
$$

where RHS_D represents the right hand side of the Darcy equation at this order and is given as

$$
RHS_D = -2K_c\varphi_1^2\nabla^2\psi_1 - 2\frac{\partial}{\partial\tau}\nabla^2\psi_1 - 2\frac{\partial^2\psi_2}{\partial\overline{x}\partial X} + KcTa\frac{\partial\varphi_1^2}{\partial\overline{z}}\frac{\partial^2\psi_1}{\partial\overline{z}} -
$$

$$
K_c\frac{\partial\varphi_1^2}{\partial\overline{z}}\frac{\partial\psi_1}{\partial\overline{z}} + R_{cr}\frac{\partial\theta_1}{\partial\overline{x}} + K_c\varphi_1^2 R_{cr}\frac{\partial\theta_1}{\partial\overline{x}} + R_{cr}\frac{\partial}{\partial\overline{x}}\frac{\partial\theta_1}{\partial\tau} + R_{cr}\frac{\partial\theta_2}{\partial X} - \frac{\partial^2\psi_1}{\partial X^2} . \qquad (2)
$$

$$
RHS_E = \Omega R_{cr}\left[\left\{\frac{\partial\psi_1}{\partial\overline{z}}\frac{\partial\theta_2}{\partial\overline{x}} - \frac{\partial\psi_1}{\partial\overline{x}}\frac{\partial\theta_2}{\partial\overline{z}}\right\} + \left\{\frac{\partial\psi_2}{\partial\overline{z}}\frac{\partial\theta_1}{\partial\overline{x}} - \frac{\partial\psi_2}{\partial\overline{x}}\frac{\partial\theta_1}{\partial\overline{z}}\right\} + \left\{\frac{\partial\psi_1}{\partial\overline{z}}\frac{\partial\theta_1}{\partial X} - \frac{\partial\psi_1}{\partial X}\frac{\partial\theta_1}{\partial\overline{z}}\right\}\right] -
$$

$$
\Omega R_{cr}\frac{\partial\psi_1}{\partial\overline{x}} - \Omega R_{cr}\frac{\partial\psi_2}{\partial X} - 2\frac{\partial^2\theta_2}{\partial\overline{x}\partial X} - \frac{\partial^2\theta_1}{\partial X^2} \qquad (3)
$$

Now we multiply Eqn.(1) by the complex conjugate of the leading order solution ψ_1 and note that the stream function ψ_3 is zero at the boundaries of the mushy layer, $\overline{x}\in[0,L]$ and $\overline{z}\in[0,1]$. The above operation enables the left hand side of Eqn.(1) to cancel off, leaving behind the right hand side solution which represents the solvability condition. The evaluation of the left hand side is complex from a algebraic point of view hence this process will be broken down into several sub-steps in order to maintain clarity

$$RHS_{E1}^{''} = \int_0^1 \int_0^L RHS_{E1}^{'} \cdot \psi_1 d\overline{x}d\overline{z} \; , \qquad (7)$$

yields,

$$RHS_{E1}^{''} = \int_0^1 \int_0^L \frac{\pi^2\alpha^2\Omega^3R_{cr}^4}{(\alpha+1)} A_1 A_1^* \left[A_1 A_1^* + A_1^* A_1^* e^{-2is\overline{x}} \right] \sin^2(\pi\overline{z})\cos(2\pi\overline{z}) \, d\overline{x}d\overline{z} \qquad (8)$$

which after integration produces,

$$RHS_{E1}^{''} = -\frac{\pi^2\alpha^2\Omega^3R_{cr}^4L}{4(\alpha+1)} \left(A_1 A_1^* \right)^2 . \qquad (9)$$

Following this procedure yields the following final result for the solvability condition contributed by the terms from the energy equation,

$$RHS_E^{''} = -\frac{\pi^2\alpha^2\Omega^3R_{cr}^4L}{4(\alpha+1)} \left(A_1 A_1^* \right)^2 - \frac{i\pi\alpha^{1/2}R_{cr}L}{2} A_1^* \frac{\partial^2 B_1}{\partial X^2} + \frac{\pi^2\alpha\Omega R_{cr}^2L}{2} A_1 A_1^* -$$

$$\frac{i\pi\alpha^{1/2}\Omega R_{cr}^2L}{2} A_1^* \frac{\partial A_2}{\partial X} + \pi^2\alpha R_{cr}LA_1^* \frac{\partial B_2}{\partial X} . \quad (10)$$

We now proceed to evaluate the solvability condition contributed by the terms in the Darcy equation. Again we will evaluate one term and list the rest.

Recalling the first term from Eqn.(2),

$$RHS_{D1} = -2K_c\varphi_1^2\nabla^2\psi_1 \qquad (11)$$

Using the lower order solutions for the stream functions and the solid fraction that are pertinent to the case of stationary convection yields the following form of Eqn.(11),

258

$$RHS_{D1} = -2\pi^2\alpha(\alpha+1)R_{cr}^2 \frac{K_c}{c_s^2}\left[A_1^3 e^{3is\bar{x}} - A_1^2 A_1^* e^{is\bar{x}} - A_1 A_1^{*2} e^{-is\bar{x}} + A_1^{*3} e^{-3is\bar{x}}\right]\sin(\pi\bar{z}).$$

$$\left(1+\cos(\pi\bar{z})\right)^2. \qquad (12)$$

Applying the Laplacian operator on Eqn.(12) (as illustrated in Eqn.(1)) yields the following expression,

$$RHS_{D1}' = 2\pi^4\alpha^2(\alpha+1)R_{cr}^2 \frac{K_c}{c_s^2}\left[9A_1^3 e^{3is\bar{x}} - A_1^2 A_1^* e^{is\bar{x}} - A_1 A_1^{*2} e^{-is\bar{x}} + 9A_1^{*3} e^{-3is\bar{x}}\right]\sin(\pi\bar{z}).$$

$$\left(1+\cos(\pi\bar{z})\right)^2 +$$

$$-2\pi^2\alpha(\alpha+1)R_{cr}^2 \frac{K_c}{c_s^2}\left[A_1^3 e^{3is\bar{x}} - A_1^2 A_1^* e^{is\bar{x}} - A_1 A_1^{*2} e^{-is\bar{x}} + A_1^{*3} e^{-3is\bar{x}}\right]D_z^2\left[\sin(\pi\bar{z}).\right.$$

$$\left.\left(1+\cos(\pi\bar{z})\right)^2\right]. \qquad (13)$$

Multiplying this equation by $\psi_1 = A_1^* e^{-s\bar{x}}\sin(\pi\bar{z})$ and integrating over $\bar{x}\in[0,L]$ and $\bar{z}\in[0,1]$ as follows,

$$RHS_{D1}'' = \int_0^1\int_0^L RHS_{D1}' \cdot \psi_1\, d\bar{x}d\bar{z}, \qquad (14)$$

yields,

$$RHS_{D1}'' = \int_0^1\int_0^L 2\pi^4\alpha^2(\alpha+1)R_{cr}^2 \frac{K_c}{c_s^2} A_1^*\left[9A_1^3 e^{2is\bar{x}} - A_1^2 A_1^* - A_1 A_1^{*2} e^{-2is\bar{x}} + 9A_1^{*3} e^{-4is\bar{x}}\right]\sin^2(\pi\bar{z})$$

$$\left(1+\cos(\pi\bar{z})\right)^2 d\bar{x}d\bar{z} +$$

$$-\int_0^1\int_0^L 2\pi^2\alpha(\alpha+1)R_{cr}^2 \frac{K_c}{c_s^2} A_1^*\left[A_1^3 e^{2is\bar{x}} - A_1^2 A_1^* - A_1 A_1^{*2} e^{-2is\bar{x}} + A_1^{*3} e^{-4is\bar{x}}\right]D_z^2\left[\sin(\pi\bar{z}).\right.$$

$$\left(1 + \cos(\pi \overline{z})\right)^2 \Big] \sin(\pi \overline{z}) d\overline{x} d\overline{z}, \quad (15)$$

which after integration provides,

$$RHS_{DI}{}'' = \frac{-10}{8} \frac{K_c}{c_S^2} \pi^4 \alpha (\alpha + 1)^2 R_{cr}^2 L \left(A_1 A_1^*\right)^2. \quad (16)$$

Following exactly the same procedure as this for the remaining terms, we evaluate the solvability condition contributed by the Darcy terms,

$$RHS_D{}'' = \left\{ \frac{-10}{8} \frac{K_c}{c_S^2} \pi^4 \alpha (\alpha + 1)^2 R_{cr}^2 L + (Ta - 1) \frac{1}{4} \frac{K_c}{c_S^2} \pi^4 \alpha (\alpha + 1) R_{cr}^2 L + \right.$$

$$\left. \frac{5}{8} \frac{K_c}{c_S^2} \pi^2 \alpha^2 \Omega R_{cr}^4 L \right\} \left(A_1 A_1^*\right)^2 + \frac{1}{2}(\alpha + 1)\pi^4 [Ta - (\alpha + 1)] L A_1^* \frac{\partial A_1}{\partial \tau} +$$

$$\left\{ 2\pi^2(\alpha + 1) - \Omega R_{cr}^2 \right\} \frac{\pi \alpha^{1/2} L}{2} i A_1^* \frac{\partial A_2}{\partial X} + \frac{1}{2}\pi^2(\alpha + 1) L A_1^* \frac{\partial^2 A_1}{\partial X^2} +$$

$$\frac{\pi^2 \alpha \Omega R_{cr}^2 L}{2} A_1 A_1^*. \quad (17)$$

Now we may combine the results of Eqn.(10) and Eqn.(17) by simply adding them to give the following result,

$$f_i A_1^2 A_1^* + s_e \frac{\partial A_1}{\partial \tau} + t_h A_1 + f_o \frac{\partial^2 A_1}{\partial X^2} = 0, \quad (18)$$

where

260

$$f_i = \frac{\pi^6 \Omega}{4}(\alpha + 1)(\alpha + 1 + Ta)\left[\frac{K_c}{2\Omega^2 c_S^2}(\alpha + 1)(-5\alpha - 7 + 7Ta) - (\alpha + 1 + Ta)\right] \quad (19)$$

$$s_e = \frac{1}{2}(\alpha + 1)\pi^4(Ta - (\alpha + 1)) \quad (20)$$

$$t_h = \pi^4(\alpha + 1)(\alpha + 1 + Ta) \quad (21)$$

$$f_o = \frac{\pi^2}{2}(2\alpha + 2 + Ta). \quad (22)$$

Reintroducing the original timescale $\tau = \varepsilon^2 \chi_1 \bar{t}$, slow space scales, $X = \varepsilon \bar{x}$ and rearranging Eqn.(18) as follows,

$$\left(\frac{s_e}{\chi_1 f_i}\right)\frac{\partial A}{\partial \bar{t}} + \left(\frac{f_o}{f_i}\right)\frac{\partial^2 A}{\partial \bar{x}^2} = \left(-\frac{t_h}{f_i}\right)\varepsilon^2 A - A^2 A^*, \quad (23)$$

which may further be written as

$$\eta_0 \frac{\partial A}{\partial \bar{t}} + \eta_1 \frac{\partial^2 A}{\partial \bar{x}^2} = \left[\xi_{st}^0 - AA^*\right]A, \quad (24)$$

where $A = \varepsilon A_1$ and $A^* = \varepsilon A_1^*$, whilst $\varepsilon^2 = \left[R/R_{cr,st} - 1\right]$. Eqn.(24) is identical to Eqn.(4.30). The coefficients in Eqn.(24) are very simply evaluated from the definition of the terms in Eqns.(19-22) and are simply listed as,

$$\eta_0 = \frac{2\left[Ta - (\alpha + 1)\right]}{\pi^4 \Omega \gamma(\alpha + 1 + Ta)\left[\frac{K_c}{2\Omega^2 c_S^2}(\alpha + 1)\{7Ta - (5\alpha + 7)\} - (\alpha + 1 + Ta)\right]} \quad (25)$$

$$\eta_1 = \frac{2\big[Ta + 2(\alpha + 1)\big]}{\pi^4 \Omega (\alpha + 1)(\alpha + 1 + Ta)\left[\dfrac{K_c}{2\Omega^2 c_S^2}(\alpha + 1)\{7Ta - (5\alpha + 7)\} - (\alpha + 1 + Ta)\right]} \qquad (26)$$

$$\xi_{st}^0 = \frac{4}{\pi^2 \Omega \left[\dfrac{K_c}{2\Omega^2 c_S^2}(\alpha + 1)\{5\alpha + 7 - 7Ta\} + (\alpha + 1 + Ta)\right]} \left[\frac{R}{R_{cr,st}} - 1\right]. \qquad (27)$$

Eqns.(25-27) are identical to Eqns.(4.31-4.33).

Appendix AD : Weak non linear analysis – Overstable convection : Derivation of the governing equations for each order of the disturbance amplitude ε

The governing equations to each order of the disturbance amplitude is derived for the case of overstable convection by considering each of the energy balance, solute balance and Darcy equations separately. To further clarify the process each term in each of the governing equations are then considered separately so as to ensure that the correct equation set to each order is obtained.

For the case of overstable convection we allow variations at the slow time scales $\tau = \varepsilon^2 t'$ and $\tau_0 = \varepsilon^1 t'$ and allow the short time scale t' to be present in order to represent the amplitude fluctuations. We rescale the short time scale in the form, $\tilde{t} = \sigma_0 t'$, where $\sigma_0 = \sigma_{i,cr}$. Slow spaces scale are also adopted in the form $X = \varepsilon \bar{x}$ so as to include a continuous finite band of horizontal modes. Bearing these scalings in mind we may propose the following form of the energy equation,

$$-\bar{S}\left(\varepsilon^2 \chi_1 \frac{\partial}{\partial \tau} - \frac{\partial}{\partial \bar{z}}\right)\varphi + R\frac{\partial \psi}{\partial \bar{z}}\frac{\partial \theta}{\partial \bar{x}} + R\varepsilon\frac{\partial \psi}{\partial \bar{z}}\frac{\partial \theta}{\partial X} - R\frac{\partial \psi}{\partial \bar{x}}\frac{\partial \theta}{\partial \bar{z}} - R\varepsilon\frac{\partial \psi}{\partial X}\frac{\partial \theta}{\partial \bar{z}} =$$

$$\nabla^2\theta + 2\varepsilon\frac{\partial^2\theta}{\partial \bar{x}\partial X} + \varepsilon^2\frac{\partial^2\theta}{\partial X^2} = 0 \quad .$$

(1)

In addition we expand the dependant variables in terms of the disturbance amplitude as follows,

$$\left[\psi,\theta,\varphi\right] = \left[\psi_B,\theta_B,\varphi_B\right] + \varepsilon\left[\psi_1,\theta_1,\varphi_1\right] + \varepsilon^2\left[\psi_2,\theta_2,\varphi_2\right] + \varepsilon^3\left[\psi_3,\theta_3,\varphi_3\right].$$

(2)

In addition the expansion for the permeability function and the Rayleigh number is given as,

$$\Pi(\varphi) = 1 + \varepsilon^2 K_c \varphi_1^2, \qquad R = R_{cr}\left(1 + \varepsilon^2\right). \tag{3}$$

The basic solution depicted by subscript "B" in Eqn.(2) is given as,

$$\left[\psi_B, \theta_B, \varphi_B\right] = \left[0, (\overline{z} - 1), 0\right]. \tag{4}$$

Using these expansions (where necessary) we consider each term in Eqn.(1) separately and adopt the following naming convention, where the subscript "E" refers to the energy equation. Note that all the terms in the energy and solute balance equations in the case of overstable convection are identical to the stationary case except for the time derivatives that use a different scaling. For these two equations, this is trivial and only the first term in the energy and solute blance equations are affected. The rest of the terms remain unchanged. The first term of the energy equation is given as,

$$t_{1E} = -\overline{S}\left(\sigma_0 \chi_1 \frac{\partial}{\partial \tilde{t}} + \varepsilon \chi_1 \frac{\partial}{\partial \tau_0} + \varepsilon^2 \chi_1 \frac{\partial}{\partial \tau} - \frac{\partial}{\partial \overline{z}}\right)\varphi. \tag{5}$$

Using the expansion for the solid fraction given above and considering Eqn.(5) to the different orders of the disturbance amplitudes yields,

$$t_{1E}\left(\varepsilon^1\right) = -\overline{S}\left(\sigma_0 \chi_1 \frac{\partial}{\partial \tilde{t}} - \frac{\partial}{\partial \overline{z}}\right)\varphi_1 \tag{5a}$$

$$t_{1E}\left(\varepsilon^2\right) = -\overline{S}\left(\sigma_0 \chi_1 \frac{\partial}{\partial \tilde{t}} - \frac{\partial}{\partial \overline{z}}\right)\varphi_2 - \overline{S}\chi_1 \frac{\partial \varphi_1}{\partial \tau_0} \tag{5b}$$

$$t_{1E}\left(\varepsilon^3\right) = -\overline{S}\left(\sigma_0 \chi_1 \frac{\partial}{\partial \tilde{t}} - \frac{\partial}{\partial \overline{z}}\right)\varphi_3 - \overline{S}\chi_1 \frac{\partial \varphi_2}{\partial \tau_0} - \overline{S}\chi_1 \frac{\partial \varphi_1}{\partial \tau_0}. \tag{5c}$$

The other terms in the energy and solute balance equations are exactly the same as that evaluated for the stationary case.

Representing the term containing the time derivative and the permeability function may be represented as,

$$T_{Dt} = \left[\sigma_0 \frac{\partial}{\partial \tilde{t}} + \varepsilon^1 \frac{\partial}{\partial \tau_0} + \varepsilon^2 \frac{\partial}{\partial \tau} + 1 + \varepsilon^2 K_c \varphi_1^2 \right],$$ (6)

thereby enabling the Darcy equation containing the slow time and space scales may be presented as,

$$T_{Dt}^2 \nabla^2 \psi + 2\varepsilon T_{Dt}^2 \frac{\partial^2 \psi}{\partial \bar{x} \partial X} + \varepsilon^2 T_{Dt}^2 \frac{\partial^2 \psi}{\partial X^2} +$$

$$T_{Dt} \frac{\partial \psi}{\partial \bar{z}} \frac{\partial K(\varphi)}{\partial \bar{z}} - RT_{Dt} \frac{\partial \theta}{\partial \bar{x}} - R\varepsilon T_{Dt} \frac{\partial \theta}{\partial X} +$$

$$Ta \frac{\partial^2 \psi}{\partial \bar{z}^2} + Ta^{1/2} \bar{v} \frac{\partial \Pi(\varphi)}{\partial \bar{z}} = 0.$$ (7)

It should be pointed out that the effects of permeability are only felt at order $O(\varepsilon^3)$. With this in mind it can be seen that the last term in Eqn.(7) falls away at the first two orders of the disturbance amplitude. For these two orders Eqn.(7) is simply divided by T_{Dt}, thereby simplifying the task of evaluating the Darcy equation to the different orders. Using the proposed expansions for the permeability function and the Rayleigh number we may consider each term in Eqn.(7) separately for clarity, noting that the variables with the subscript "D" refers to the Darcy equation.

Referring to the first term in Eqn.(7),

$$t_{1D} = T_{Dt}^2 \nabla^2 \psi,$$ (8)

and considering to each order of the disturbance amplitude yields,

$$t_{1D}(\varepsilon^1) = \left(\sigma_0 \frac{\partial}{\partial \tilde{t}} + 1\right)^2 \nabla^2 \psi_1 \tag{8a}$$

$$t_{1D}(\varepsilon^2) = \left(\sigma_0 \frac{\partial}{\partial \tilde{t}} + 1\right)^2 \nabla^2 \psi_2 + 2\frac{\partial}{\partial \tau_0}\left(\sigma_0 \frac{\partial}{\partial \tilde{t}} + 1\right)\nabla^2 \psi_1 \tag{8b}$$

$$t_{1D}(\varepsilon^3) = \left(\sigma_0 \frac{\partial}{\partial \tilde{t}} + 1\right)^2 \nabla^2 \psi_3 + 2\left(\sigma_0 \frac{\partial}{\partial \tilde{t}} + 1\right)\left(K_c \varphi_1^2 + \frac{\partial}{\partial \tau}\right)\nabla^2 \psi_1 +$$

$$2\frac{\partial}{\partial \tau_0}\left(\sigma_0 \frac{\partial}{\partial \tilde{t}} + 1\right)\nabla^2 \psi_2 + \frac{\partial^2}{\partial \tau_0^2}\nabla^2 \psi_1 \tag{8c}$$

Considering the second term in Eqn.(7),

$$t_{2D} = 2\varepsilon T_{Dt}^2 \frac{\partial^2 \psi}{\partial \overline{x}\partial X}, \tag{9}$$

and developing to the different orders of the disturbance amplitude yields,

$$t_{2D}(\varepsilon^1) = 0 \tag{9a}$$

$$t_{2D}(\varepsilon^2) = 2\left(\sigma_0 \frac{\partial}{\partial \tilde{t}} + 1\right)^2 \frac{\partial^2 \psi_1}{\partial \overline{x}\partial X} \tag{9b}$$

$$t_{2D}(\varepsilon^3) = 2\left(\sigma_0 \frac{\partial}{\partial \tilde{t}} + 1\right)^2 \frac{\partial^2 \psi_2}{\partial \overline{x}\partial X} + 4\frac{\partial}{\partial \tau_0}\left(\sigma_0 \frac{\partial}{\partial \tilde{t}} + 1\right)\frac{\partial^2 \psi_1}{\partial \overline{x}\partial X}. \tag{9c}$$

Analysing the third term in Eqn.(7),

266

$$t_{3D} = \varepsilon^2 T_{Dt}{}^2 \frac{\partial^2 \psi}{\partial X^2},$$ (10)

and considering to the different orders of the disturbance amplitude yields,

$$t_{3D}\left(\varepsilon^1\right) = 0$$ (10a)

$$t_{3D}\left(\varepsilon^2\right) = 0$$ (10b)

$$t_{3D}\left(\varepsilon^3\right) = \left(\sigma_0 \frac{\partial}{\partial \tilde{t}} + 1\right)^2 \frac{\partial^2 \psi_1}{\partial X^2}.$$ (10c)

Recalling the fourth term in Eqn.(11),

$$t_{4D} = T_{Dt} \frac{\partial \psi}{\partial \bar{z}} \frac{\partial \Pi(\varphi)}{\partial \bar{z}},$$ (11)

and considering to each order of the disturbance amplitude yields,

$$t_{4D}\left(\varepsilon^1\right) = 0$$ (11a)

$$t_{4D}\left(\varepsilon^2\right) = 0$$ (11b)

$$t_{4D}\left(\varepsilon^3\right) = K_c \left(\sigma_0 \frac{\partial}{\partial \tilde{t}} + 1\right) \frac{\partial \psi_1}{\partial \bar{z}} \frac{\partial \varphi_1^2}{\partial \bar{z}}.$$ (11c)

Recalling the fifth term in Eqn.(7),

$$t_{5D} = -RT_{Dt}\frac{\partial\theta}{\partial\overline{x}},$$ (12)

and considering to each order of the disturbance amplitude yields,

$$t_{5D}(\varepsilon^{1}) = -R_{cr}\left(\sigma_0\frac{\partial}{\partial\widetilde{t}}+1\right)\frac{\partial\theta_1}{\partial\overline{x}}$$ (12a)

$$t_{5D}(\varepsilon^{2}) = -R_{cr}\frac{\partial}{\partial\tau_0}\left(\sigma_0\frac{\partial}{\partial\widetilde{t}}+1\right)\frac{\partial\theta_1}{\partial\overline{x}} - R_{cr}\left(\sigma_0\frac{\partial}{\partial\widetilde{t}}+1\right)^2\frac{\partial\theta_2}{\partial\overline{x}}$$ (12b)

$$t_{5D}(\varepsilon^{3}) = -R_{cr}\left(\sigma_0\frac{\partial}{\partial\widetilde{t}}+1\right)\frac{\partial\theta_3}{\partial\overline{x}} - R_{cr}\left(\sigma_0\frac{\partial}{\partial\widetilde{t}}+1\right)\frac{\partial\theta_1}{\partial\overline{x}} - R_{cr}\left(\frac{\partial}{\partial\tau_0}\frac{\partial\theta_2}{\partial\overline{x}}+K_c\varphi_1^2\frac{\partial\theta_1}{\partial\overline{x}}+\frac{\partial}{\partial\tau}\frac{\partial\theta_1}{\partial\overline{x}}\right)$$ (12c)

Recalling the sixth term in Eqn.(7),

$$t_{6D} = -R\varepsilon T_{Dt}\frac{\partial\theta}{\partial X},$$ (13)

and considering to each order of the disturbance amplitude yields,

$$t_{6D}(\varepsilon^{1}) = 0$$ (13a)

$$t_{6D}(\varepsilon^{2}) = -R_{cr}\left(\sigma_0\frac{\partial}{\partial\widetilde{t}}+1\right)\frac{\partial\theta_1}{\partial X}$$ (13b)

$$t_{6D}(\varepsilon^{3}) = -R_{cr}\left(\sigma_0\frac{\partial}{\partial\widetilde{t}}+1\right)\frac{\partial\theta_2}{\partial X} - R_{cr}\frac{\partial}{\partial\tau_0}\frac{\partial\theta_1}{\partial X}.$$ (13c)

Recalling the seventh term in Eqn.(7),

268

$$t_{7D} = Ta \frac{\partial^2 \psi}{\partial \bar{z}^2},$$ (14)

and considering to the different orders of the disturbance amplitude yields,

$$t_{7D}\left(\varepsilon^1\right) = Ta \frac{\partial^2 \psi_1}{\partial \bar{z}^2}$$ (14a)

$$t_{7D}\left(\varepsilon^2\right) = Ta \frac{\partial^2 \psi_2}{\partial \bar{z}^2}$$ (14b)

$$t_{7D}\left(\varepsilon^3\right) = Ta \frac{\partial^2 \psi_3}{\partial \bar{z}^2}$$ (14c)

Finally recalling the eighth term in Eqn.(7),

$$t_{8D} = Ta^{1/2} \bar{v} \frac{\partial \Pi(\varphi)}{\partial \bar{z}},$$ (15)

and considering to the different orders of the disturbance amplitude yields,

$$t_{8D}\left(\varepsilon^1\right) = 0$$ (15a)

$$t_{8D}\left(\varepsilon^2\right) = 0$$ (15b)

$$t_{8D}\left(\varepsilon^3\right) = K_c Ta^{1/2} v_1 \frac{\partial \varphi_1^2}{\partial \bar{z}}.$$ (15c)

We may now proceed to build the governing system of equations to each order by taking into account the terms developed to each order of the disturbance amplitude for the energy, solute and Darcy equations. This process is simply achieved by collecting the respective terms for each of the energy, solute balance and Darcy equations from Eqns.(5-15) above.

The governing equations to the leading order are given as,

$$\overline{S}\left(\chi_1\sigma_0\frac{\partial}{\partial\widetilde{t}} - \frac{\partial}{\partial\overline{z}}\right)\varphi_1 + R_{cr}\frac{\partial\psi_1}{\partial\overline{x}} + \nabla^2\theta_1 = 0 \tag{16a}$$

$$c_S\left(\chi_1\sigma_0\frac{\partial}{\partial\widetilde{t}} - \frac{\partial}{\partial\overline{z}}\right)\varphi_1 - R_{cr}\frac{\partial\psi_1}{\partial\overline{x}} = 0 \tag{16b}$$

$$\left(\sigma_0\frac{\partial}{\partial\widetilde{t}} + 1\right)^2\nabla^2\psi_1 - R_{cr}\left(\sigma_0\frac{\partial}{\partial\widetilde{t}} + 1\right)\frac{\partial\theta_1}{\partial\overline{x}} + Ta\frac{\partial^2\psi_1}{\partial\overline{z}^2} = 0, \tag{16c}$$

which is identical to eqns.(4.37-4.39).

The system of governing equations to order ε^2,

$$\overline{S}\left(\chi_1\sigma_0\frac{\partial}{\partial\widetilde{t}} - \frac{\partial}{\partial\overline{z}}\right)\varphi_2 + R_{cr}\frac{\partial\psi_2}{\partial\overline{x}} + \nabla^2\theta_2 = -\overline{S}\chi_1\frac{\partial\varphi_1}{\partial\tau_0} + R_{cr}\left[\frac{\partial\psi_1}{\partial\overline{z}}\frac{\partial\theta_1}{\partial\overline{x}} - \frac{\partial\psi_1}{\partial\overline{x}}\frac{\partial\psi_1}{\partial\overline{z}}\right] \tag{17a}$$

$$c_S\left(\chi_1\sigma_0\frac{\partial}{\partial\widetilde{t}} - \frac{\partial}{\partial\overline{z}}\right)\varphi_2 - R_{cr}\frac{\partial\psi_2}{\partial\overline{x}} = -\chi_1 c_S\frac{\partial\varphi_1}{\partial\tau_0} - R_{cr}\left[\frac{\partial\psi_1}{\partial\overline{z}}\frac{\partial\theta_1}{\partial\overline{x}} - \frac{\partial\psi_1}{\partial\overline{x}}\frac{\partial\theta_1}{\partial\overline{z}}\right] \tag{17b}$$

$$\left(\sigma_0\frac{\partial}{\partial\widetilde{t}} + 1\right)^2\nabla^2\psi_2 - R_{cr}\left(\sigma_0\frac{\partial}{\partial\widetilde{t}} + 1\right)\frac{\partial\theta_2}{\partial\overline{x}} + Ta\frac{\partial^2\psi_2}{\partial\overline{z}^2} = -2\frac{\partial}{\partial\tau_0}\left(\sigma_0\frac{\partial}{\partial\widetilde{t}} + 1\right)\nabla^2\psi_1 + R_{cr}\frac{\partial}{\partial\tau_0}\frac{\partial\theta_1}{\partial\overline{x}} \tag{17c}$$

which is identical to Eqns.(4.47-4.49).

Finally the governing equations to order ε^3 were decoupled to provide a single equation for the stream function since this form is required to obtain the solvability condition. The decoupled equation to order ε^3 is exclusive of the slow space scales and is given as,

$$\left(\sigma_0 \frac{\partial}{\partial \tilde{t}} + 1\right)^2 \nabla^4 \psi_3 + \Omega R_{cr}^2 \left(\sigma_0 \frac{\partial}{\partial \tilde{t}} + 1\right) \frac{\partial^2 \psi_3}{\partial \overline{x}^2} + Ta \frac{\partial^2}{\partial \overline{z}^2} \nabla^2 \psi_3 =$$

$$R_{cr} \left(\sigma_0 \frac{\partial}{\partial \tilde{t}} + 1\right) \frac{\partial}{\partial \overline{x}} RHS1 + \nabla^2 RHS2, \qquad (18)$$

where RHS1 and RHS2 are the non-homogenous terms defined as,

$$RHS1 = \Omega R_{cr} \left\{ \left[\frac{\partial \psi_1}{\partial \overline{z}} \frac{\partial \theta_2}{\partial \overline{x}} - \frac{\partial \psi_1}{\partial \overline{x}} \frac{\partial \psi_2}{\partial \overline{z}} \right] + \left[\frac{\partial \psi_2}{\partial \overline{z}} \frac{\partial \theta_1}{\partial \overline{x}} - \frac{\partial \psi_2}{\partial \overline{x}} \frac{\partial \psi_1}{\partial \overline{z}} \right] - \frac{\partial \psi_1}{\partial \overline{x}} \right\} \qquad (19)$$

$$RHS2 = -2 \left(\sigma_0 \frac{\partial}{\partial \tilde{t}} + 1\right) \left(K_c \varphi_1^2 + \frac{\partial}{\partial \tau_1} \right) \nabla^2 \psi_1 - 2 \frac{\partial}{\partial \tau_0} \left(\sigma_0 \frac{\partial}{\partial \tilde{t}} + 1\right) \nabla^2 \psi_2 -$$

$$K_c \left(\sigma_0 \frac{\partial}{\partial \tilde{t}} + 1\right) \frac{\partial \varphi_1^2}{\partial \overline{z}} \frac{\partial \psi_1}{\partial \overline{z}} + R_{cr} \left(\sigma_0 \frac{\partial}{\partial \tilde{t}} + 1\right) \frac{\partial \theta_1}{\partial \overline{z}} - K_c Ta^{1/2} v_1 \frac{\partial \varphi_1^2}{\partial \overline{z}} +$$

$$R_{cr} K_c \varphi_1^2 \frac{\partial \theta_1}{\partial \overline{x}} + R_{cr} \frac{\partial}{\partial \tau} \frac{\partial \theta_1}{\partial \overline{x}} + R_{cr} \frac{\partial}{\partial \tau_0} \frac{\partial \theta_1}{\partial \overline{x}}, \qquad (20)$$

which is identical to Eqns.(4.60-4.62)

Appendix AE : Weak non-linear Analysis – Overstable convection : Derivation of the eigenfunctions to the leading order $O(\varepsilon)$

The special case of standing waves is analysed by applying the boundary conditions applicable to the stream function adjacent the axis of rotation. This results in the following form of the stream function and temperature to the leading order,

$$\psi_1 = 2i\left[A_1 e^{is\tilde{t}} + A_1^* e^{-is\tilde{t}}\right]\sin(s\overline{x})\sin(\pi\overline{z}) \tag{1}$$

$$\theta_1 = 2\left[C_1 e^{is\tilde{t}} + C_1^* e^{-is\tilde{t}}\right]\cos(s\overline{x})\sin(\pi\overline{z}). \tag{2}$$

We now proceed to develop the solution for the solid fraction by stating the solute balance equation to the leading order as follows,

$$c_S\left(\chi_1\sigma_0\frac{\partial}{\partial\tilde{t}} - \frac{\partial}{\partial\overline{z}}\right)\varphi_1 - R_{cr}\frac{\partial\psi_1}{\partial\overline{x}} = 0. \tag{3}$$

Eqn.(3) may be rearranged as,

$$\left(\chi_1\sigma_0\frac{\partial}{\partial\tilde{t}} - \frac{\partial}{\partial\overline{z}}\right)\varphi_1 = \frac{R_{cr}}{c_S}\frac{\partial\psi_1}{\partial\overline{x}}. \tag{4}$$

Using the solution for the stream function stated in Eqn.(1) , Eqn.(4) may then be written as,

$$\left(\chi_1\sigma_0\frac{\partial}{\partial\tilde{t}} - \frac{\partial}{\partial\overline{z}}\right)\varphi_1 = 2i\pi\alpha^{1/2}\frac{R_{cr}}{c_S}\left[A_1 e^{i\tilde{t}} + A_1^* e^{-i\tilde{t}}\right]\cos(s\overline{x})\sin(\pi\overline{z}). \tag{5}$$

The solution to for the solid fraction assumes a solution of the form,

$$\varphi_1 = \left[\overline{\varphi}_1(\overline{z}) M_1 e^{i\overline{\tau}} + \overline{\varphi}_1^*(\overline{z}) M_1^* e^{-i\overline{\tau}} \right] \cos(s\overline{x}) . \tag{6}$$

Substituting Eqn.(6) in Eqn.(5) and collecting like indices of the exponential terms which are a function of time, yields two differential equations that need to be solved,

$$\text{coeff}\left(e^{i\overline{\tau}}\right) \quad : \quad \pi^2 \gamma \sigma_0 i M_1 \overline{\varphi}_1 - M_1 \frac{d\overline{\varphi}_1}{d\overline{z}} = \frac{2i\pi\alpha^{1/2}R_{cr}}{c_S} A_1 \sin(\pi\overline{z}) \tag{7}$$

$$\text{coeff}\left(e^{-i\overline{\tau}}\right) \quad : \quad -\pi^2 \gamma \sigma_0 i M_1^* \overline{\varphi}_1^* - M_1^* \frac{d\overline{\varphi}_1^*}{d\overline{z}} = \frac{2i\pi\alpha^{1/2}R_{cr}}{c_S} A_1^* \sin(\pi\overline{z}) . \tag{8}$$

First we start by solving Eqn.(7),

$$\pi^2 \gamma \sigma_0 i M_1 \overline{\varphi}_1 - M_1 \frac{d\overline{\varphi}_1}{d\overline{z}} = \frac{2i\pi\alpha^{1/2}R_{cr}}{c_S} A_1 \sin(\pi\overline{z}) . \tag{9}$$

We first solve the homogenous part of Eqn.(9),

$$\frac{d\overline{\varphi}_1}{d\overline{z}} - \pi^2 \gamma \sigma_0 i \overline{\varphi}_1 = 0 , \tag{10}$$

the solution to which is given as,

$$\overline{\varphi}_1 = C_\varepsilon e^{i\pi^2 \gamma \sigma_0 \overline{z}} . \tag{11}$$

Solving the full non-homogenous equation (9),

$$\frac{d\overline{\varphi}_1}{d\overline{z}} - \pi^2 \gamma \sigma_0 i \overline{\varphi}_1 = - \frac{2i\pi\alpha^{1/2}R_{cr}}{c_S} \frac{A_1}{M_1} \sin(\pi\overline{z}) , \tag{12}$$

by assuming a particular solution of the form,

$$\overline{\varphi}_{1,p} = P_1 \sin(\pi \overline{z}) + P_2 \cos(\pi \overline{z}). \tag{13}$$

Substituting Eqn.(13) in Eqn.(12) and equating like coefficients of like trigonometric terms as follows,

$$\text{coeff} : \sin(\pi \overline{z}) \quad : \quad \pi P_2 + \pi^2 \gamma \sigma_0 i P_1 = \frac{2 i \pi \alpha^{1/2} R_{cr}}{c_S} \frac{A_1}{M_1} \tag{14}$$

$$\text{coeff} : \cos(\pi \overline{z}) \quad : \quad \pi P_1 - \pi^2 \gamma \sigma_0 i P_2 = 0. \tag{15}$$

Resolving these coefficients allows the particular solution to be written as,

$$\overline{\varphi}_{1,p} = P_2 \big[i \pi \gamma \sigma_0 \sin(\pi \overline{z}) + \cos(\pi \overline{z}) \big], \tag{16}$$

where the definition for P_2 is given as,

$$P_2 = \frac{2 i \pi \alpha^{1/2} R_{cr}}{c_S} \frac{1}{\pi \left(1 - \pi^2 \gamma^2 \sigma_0^2\right)} \frac{A_1}{M_1}. \tag{17}$$

The solution to the solid fraction is given as,

$$\overline{\varphi}_1 = C_\varepsilon e^{i\pi^2 \gamma \sigma_0 \overline{z}} + P_2 \big[i \pi \gamma \sigma_0 \sin(\pi \overline{z}) + \cos(\pi \overline{z}) \big]. \tag{18}$$

Applying the boundary condition $\overline{\varphi}_1(1) = 0$ allows one to solve for the integration constant C_ε, thus enabling the solution to be written as,

$$\overline{\varphi}_1 = P_2 \big[e^{i\pi^2 \gamma \sigma_0 (\overline{z} - 1)} + i \pi \gamma \sigma_0 \sin(\pi \overline{z}) + \cos(\pi \overline{z}) \big]. \tag{19}$$

Using exactly the same procedure as that outlined above, the solution for the solid fraction corresponding to the contribution from the complex conjugate yields,

$$\overline{\varphi}_1^* = P_2^* \left[e^{-i\pi^2 \gamma \sigma_0 (\overline{z}-1)} - i\pi\gamma\sigma_0 \sin(\pi\overline{z}) + \cos(\pi\overline{z}) \right], \tag{20}$$

where the definition for P_2^* is given as,

$$P_2^* = \frac{2i\pi\alpha^{1/2} R_{cr}}{c_S} \frac{1}{\pi \left(1 - \pi^2 \gamma^2 \sigma_0^2\right)} \frac{A_1^*}{M_1^*}. \tag{21}$$

The full solution to the solid fraction may then be presented by substituting the solutions in Eqns.(19-20) in Eqn.(6) to give,

$$\varphi_1 = \left\{ D_1 \left[e^{i\pi^2 \gamma \sigma_0 (\overline{z}-1)} + i\pi\gamma\sigma_0 \sin(\pi\overline{z}) + \cos(\pi\overline{z}) \right] e^{i\tilde{\tau}} + \right.$$

$$\left. D_1^* \left[e^{-i\pi^2 \gamma \sigma_0 (\overline{z}-1)} - i\pi\gamma\sigma_0 \sin(\pi\overline{z}) + \cos(\pi\overline{z}) \right] e^{-i\tilde{\tau}} \right\} \cos(s\overline{x}), \tag{22}$$

where,

$$D_1 = i \frac{2\alpha^{1/2} R_{cr}}{c_S \left(1 - \pi^2 \gamma^2 \sigma_0^2\right)} A_1, \qquad\qquad D_1^* = i \frac{2\alpha^{1/2} R_{cr}}{c_S \left(1 - \pi^2 \gamma^2 \sigma_0^2\right)} A_1^*. \tag{23}$$

Note that Eqn.(22) is identical to Eqn.(4.44) and Eqn(23) is identical to Eqn.(4.46).

We now proceed to develop the relationship between the coefficients A_1 and C_1. Using the modified heat balance equation at the leading order,

$$\nabla^2 \theta_1 + \Omega R_{cr} \frac{\partial \psi_1}{\partial \overline{x}} = 0, \tag{24}$$

and substituting the leading order stream function and temperature solutions yields the following form of Eqn.(24),

$$-2\pi^2(\alpha + 1)\left[C_1 e^{i\tilde{\tau}} + C_1^* e^{-i\tilde{\tau}}\right]\cos(s\overline{x})\sin(\pi\overline{z}) +$$

$$2\pi i\alpha^{1/2}\Omega R_{cr}\left[A_1 e^{i\tilde{\tau}} + A_1^* e^{-i\tilde{\tau}}\right]\cos(s\overline{x})\sin(\pi\overline{z}) = 0, \tag{25}$$

Equating coefficients of like exponential terms yields,

$$\text{coeff}\left(e^{i\tilde{\tau}}\right) \quad : \quad C_1 = \frac{i\alpha^{1/2}\Omega R_{cr}}{\pi(\alpha + 1)} A_1 \tag{26}$$

$$\text{coeff}\left(e^{-i\tilde{\tau}}\right) \quad : \quad C_1^* = \frac{i\alpha^{1/2}\Omega R_{cr}}{\pi(\alpha + 1)} A_1^*. \tag{27}$$

Eqns.(26-27) compare identically with Eqn.(4.45).

Appendix AF : Weak non-linear Analysis – Overstable convection : Derivation of the eigenfunctions to order $O(\varepsilon^2)$

The governing equations to order $O(\varepsilon^2)$ is given as,

$$\overline{S}\left(\chi_1\sigma_0\frac{\partial}{\partial\tilde{t}} - \frac{\partial}{\partial\overline{z}}\right)\varphi_2 + R_{cr}\frac{\partial\psi_2}{\partial\overline{x}} + \nabla^2\theta_2 = -\overline{S}\chi_1\frac{\partial\varphi_1}{\partial\tau_0} + R_{cr}\left[\frac{\partial\psi_1}{\partial\overline{z}}\frac{\partial\theta_1}{\partial\overline{x}} - \frac{\partial\psi_1}{\partial\overline{x}}\frac{\partial\psi_1}{\partial\overline{z}}\right] \quad (1)$$

$$c_s\left(\chi_1\sigma_0\frac{\partial}{\partial\tilde{t}} - \frac{\partial}{\partial\overline{z}}\right)\varphi_2 - R_{cr}\frac{\partial\psi_2}{\partial\overline{x}} = -\chi_1 c_s\frac{\partial\varphi_1}{\partial\tau_0} - R_{cr}\left[\frac{\partial\psi_1}{\partial\overline{z}}\frac{\partial\theta_1}{\partial\overline{x}} - \frac{\partial\psi_1}{\partial\overline{x}}\frac{\partial\theta_1}{\partial\overline{z}}\right] \quad (2)$$

$$\left(\sigma_0\frac{\partial}{\partial\tilde{t}}+1\right)^2\nabla^2\psi_2 - R_{cr}\left(\sigma_0\frac{\partial}{\partial\tilde{t}}+1\right)\frac{\partial\theta_2}{\partial\overline{x}} + Ta\frac{\partial^2\psi_2}{\partial\overline{z}^2} = -2\frac{\partial}{\partial\tau_0}\left(\sigma_0\frac{\partial}{\partial\tilde{t}}+1\right)\nabla^2\psi_1 + R_{cr}\frac{\partial}{\partial\tau_0}\frac{\partial\theta_1}{\partial\overline{x}}$$

$$(3)$$

Decoupling Eqns.(1-2) yields the modified heat balance equation,

$$\nabla^2\theta_2 + \Omega R_{cr}\frac{\partial\psi_2}{\partial\overline{x}} = -\Omega R_{cr}\left[\frac{\partial\psi_1}{\partial\overline{z}}\frac{\partial\theta_1}{\partial\overline{x}} - \frac{\partial\psi_1}{\partial\overline{x}}\frac{\partial\psi_1}{\partial\overline{z}}\right], \quad (4)$$

which is solved together with the Darcy equation (3),

$$\left(\sigma_0\frac{\partial}{\partial\tilde{t}}+1\right)^2\nabla^2\psi_2 - R_{cr}\left(\sigma_0\frac{\partial}{\partial\tilde{t}}+1\right)\frac{\partial\theta_2}{\partial\overline{x}} + Ta\frac{\partial^2\psi_2}{\partial\overline{z}^2} = -2\frac{\partial}{\partial\tau_0}\left(\sigma_0\frac{\partial}{\partial\tilde{t}}+1\right)\nabla^2\psi_1 + R_{cr}\frac{\partial}{\partial\tau_0}\frac{\partial\theta_1}{\partial\overline{x}}$$

$$(5)$$

To omit terms that produce resonance at this order, we obtain particular solutions by setting, $\partial A_1/\partial\tau_0 = 0$. Eqns.(4-5) may now be written as,

$$\nabla^2\theta_2 + \Omega R_{cr}\frac{\partial\psi_2}{\partial\overline{x}} = -\Omega R_{cr}\left[\frac{\partial\psi_1}{\partial\overline{z}}\frac{\partial\theta_1}{\partial\overline{x}} - \frac{\partial\psi_1}{\partial\overline{x}}\frac{\partial\psi_1}{\partial\overline{z}}\right] \quad (6)$$

$$\left(\sigma_0\frac{\partial}{\partial\tilde{t}}+1\right)^2\nabla^2\psi_2-R_{cr}\left(\sigma_0\frac{\partial}{\partial\tilde{t}}+1\right)\frac{\partial\theta_2}{\partial\overline{x}}+Ta\frac{\partial^2\psi_2}{\partial\overline{z}^2}=0. \tag{7}$$

The homogeneous solution to these equation are exactly of the same form as the lower order solutions, except for the coefficients, and may be written as,

$$\psi_{2,h}=2i\left[A_2e^{i\tilde{t}}+A_2^*e^{-i\tilde{t}}\right]\sin(s\overline{x})\sin(\pi\overline{z}) \tag{8}$$

$$\theta_{2,h}=2\left[C_2e^{i\tilde{t}}+C_2^*e^{-i\tilde{t}}\right]\cos(s\overline{x})\sin(\pi\overline{z}). \tag{9}$$

The relationship between the coefficients are identical to that presented at the lower order. It can be very clearly seen that the particular solution to Eqn.(7) is zero, thus implying that to this order the full solution for the stream function is simply given as,

$$\psi_2=2i\left[A_2e^{i\tilde{t}}+A_2^*e^{-i\tilde{t}}\right]\sin(s\overline{x})\sin(\pi\overline{z}), \tag{10}$$

which is identical to Eqn.(4.50). We now proceed to solve for the particular solution for the temperature at this order. As before we evaluate the right hand side of Eqn.(6) using the leading order solutions in the process and present the following form of the equation to be solved,

$$\nabla^2\theta_2+\Omega R_{cr}\frac{\partial\psi_2}{\partial\overline{x}}=RHS_A, \tag{11}$$

where

$$RHS_A=-\frac{2\pi\alpha\Omega^2R_{cr}^2}{(\alpha+1)}\left[A_1^2e^{2i\tilde{t}}+2A_1A_1^*+A_1^{*2}e^{-2i\tilde{t}}\right]\sin(2\pi\overline{z}). \tag{12}$$

Decoupling the modified heat balance and Darcy equations by applying the Laplacian operator $\nabla^2(.)$ on the Darcy equation (7) and the operator $R_{cr}\,\partial/\partial\bar{x}(.)$ on the modified heat balance equation (11), the result of which is added to provide a single partial differential equation for the temperature at this order,

$$\left(\sigma_0\frac{\partial}{\partial\tilde{t}}+1\right)^2\nabla^2\theta_2+\Omega R_{cr}^2\left(\sigma_0\frac{\partial}{\partial\tilde{t}}+1\right)\frac{\partial^2\theta_2}{\partial\bar{x}^2}+Ta\frac{\partial^2}{\partial\bar{z}^2}\nabla^2\theta_2=RHS_B,\tag{13}$$

where

$$RHS_B=\left(\sigma_0\frac{\partial}{\partial\tilde{t}}+1\right)\nabla^2RHS_A+Ta\frac{\partial^2}{\partial\bar{z}^2}RHS_A.\tag{14}$$

The result of the operations on RHS_A as depicted in Eqn.(14) is carried out and presented as,

$$RHS_B=-\frac{32\pi^3\alpha\Omega^2R_{cr}^2}{(\alpha+1)}\sigma_0^2\left[A_1^2e^{2i\tilde{t}}+A_1^{*2}e^{-2i\tilde{t}}\right]\sin(2\pi\bar{z})+$$

$$\frac{32\pi^3\alpha\Omega^2R_{cr}^2}{(\alpha+1)}i\sigma_0\left[A_1^2e^{2i\tilde{t}}-A_1^{*2}e^{-2i\tilde{t}}\right]\sin(2\pi\bar{z})+$$

$$\frac{8\pi^3\alpha\Omega^2R_{cr}^2}{(\alpha+1)}(Ta+1)\left[A_1^2e^{2i\tilde{t}}+2A_1A_1^*+A_1^{*2}e^{-2i\tilde{t}}\right]\sin(2\pi\bar{z}).\tag{15}$$

We select a particular solution of the form,

$$\theta_{2,p}=\left[b_2+b_1e^{2i\tilde{t}}+b_1^*e^{-2i\tilde{t}}\right]\sin(2\pi\bar{z}).\tag{16}$$

Substituting Eqn.(16) in Eqn.(13) and collecting coefficients of like terms yields the following solutions for the coefficients of the particular solution presented in eqn.(16),

$$b_1 = \frac{\alpha \Omega^2 R_{cr}^2}{2\pi(\alpha + 1)} A_1^2 \tag{17}$$

$$b_1^* = \frac{\alpha \Omega^2 R_{cr}^2}{2\pi(\alpha + 1)} A_1^{*2} \tag{18}$$

$$b_2 = \frac{\alpha \Omega^2 R_{cr}^2}{\pi(\alpha + 1)} A_1 A_1^*. \tag{19}$$

Eqns.(17-19) are identical to Eqns.(4.53-4.55). The full solution to the temperature at this order is given as,

$$\theta_2 = \left[b_2 + b_1 e^{2i\bar{t}} + b_1^* e^{-2i\bar{t}} \right] \sin(2\pi\bar{z}), \tag{20}$$

where the coefficients are defined in Eqns.(17-19). Eqn.(20), incidentally is identical to the solution presented by Eqn.(4.52).

We now proceed to develop the solution for the solid fraction at this order. Although it is not used in any computations henceforth, it will nonetheless be provided very briefly.

The solid fraction equation that needs to be solved at this order may be presented as,

$$\left(\chi_1 \sigma_0 \frac{\partial}{\partial \bar{t}} - \frac{\partial}{\partial \bar{z}} \right) \varphi_2 = 2i\pi\alpha^{1/2} \frac{R_{cr}}{c_s} \left[A_2 e^{i\bar{t}} + A_2^* e^{-i\bar{t}} \right] \cos(s\bar{x}) \sin(\pi\bar{z}) -$$

$$- \frac{2\pi\alpha\Omega R_{cr}^2}{(\alpha + 1)} \left[A_1^2 e^{2i\bar{t}} + 2A_1 A_1^* + A_1^{*2} e^{-2i\bar{t}} \right] \sin(2\pi\bar{z}). \tag{21}$$

A particular solution of the form,

$$\varphi_{2,p} = \left[D_2 \overline{\varphi}_2 e^{i\tilde{\tau}} + D_2^* \overline{\varphi}_2^* e^{-i\tilde{\tau}} \right] \cos(s\overline{x}) + \left[F_2 \overline{\varphi}_{20} e^{2i\tilde{\tau}} + F_2^* \overline{\varphi}_{20}^* e^{-2i\tilde{\tau}} + G\varphi_{21} \right] \sin(2\pi\overline{z}) \qquad (22)$$

Substituting Eqn.(22) in Eqn.(21), performing the derivatives and equating the coefficients of the like indices of the exponential time terms, allows the terms which are a function of z in Eqn.(22) to be solved for. The full solution to Eqn.(22) is complicated and great care must be exercised in the algebraic process. The full solution for the solid fraction at this order is given as,

$$\varphi_2 = \left[D_2 \left\{ e^{i\pi^2\gamma\sigma_0(\overline{z}-1)} + i\pi\gamma\sigma_0 \sin(\pi\overline{z}) + \cos(\pi\overline{z}) \right\} e^{i\tilde{\tau}} + \right.$$

$$D_2^* \left\{ e^{-i\pi^2\gamma\sigma_0(\overline{z}-1)} - i\pi\gamma\sigma_0 \sin(\pi\overline{z}) + \cos(\pi\overline{z}) \right\} e^{-i\tilde{\tau}} \Big] \cos(s\overline{x}) -$$

$$\left[F_2 \left\{ -e^{2i\pi^2\gamma\sigma_0(\overline{z}-1)} + i\pi\gamma\sigma_0 \sin(2\pi\overline{z}) + \cos(2\pi\overline{z}) \right\} e^{2i\tilde{\tau}} + \right.$$

$$F_2^* \left\{ -e^{-2i\pi^2\gamma\sigma_0(\overline{z}-1)} - i\pi\gamma\sigma_0 \sin(2\pi\overline{z}) + \cos(2\pi\overline{z}) \right\} e^{-2i\tilde{\tau}} \Big] \cos(s\overline{x}) +$$

$$G \left[\cos(2\pi\overline{z}) - 1 \right],$$

$$(23)$$

where the amplitude relations for D_2 and D_2^* are exactly the same as that presented in Eqn.(4.46). The amplitude relations for F_2, F_2^* and G are given as,

$$F_2 = \frac{\alpha\Omega R_{cr}^2}{(\alpha+1)(1-\pi^2\sigma_0^2\gamma^2)} A_1^2 \qquad (24)$$

$$F_2^* = \frac{\alpha\Omega R_{cr}^2}{(\alpha+1)(1-\pi^2\sigma_0^2\gamma^2)} A_1^{*2} \qquad (25)$$

$$G = \frac{2\alpha\Omega R_{cr}^2}{(\alpha + 1)} A_1 A_1^*. \tag{26}$$

Eqns.(23-26) are identical to Eqns.(4.56-4.59). It is very interesting to note that the first term in Eqn.(23) resembles the solution to the leading order solid fraction. The two terms that follow the mentioned term simply implies the particular solution as a result of the nonlinear terms present on the right hand side of the solute balance equation (2).

Appendix AG : Weak non-linear Analysis – Overstable convection : Derivation of the leading order amplitude differential equation at order $O(\varepsilon^3)$

The governing equations to order ε^3 was decoupled to provide a single equation for the stream function in the form,

$$\left(\sigma_0 \frac{\partial}{\partial \tilde{t}} + 1\right)^2 \nabla^4 \psi_3 + \Omega R_{cr}^2 \left(\sigma_0 \frac{\partial}{\partial \tilde{t}} + 1\right) \frac{\partial^2 \psi_3}{\partial \bar{x}^2} + Ta \frac{\partial^2}{\partial \bar{z}^2} \nabla^2 \psi_3 =$$

$$R_{cr}\left(\sigma_0 \frac{\partial}{\partial \tilde{t}} + 1\right) \frac{\partial}{\partial \bar{x}} RHS1 + \nabla^2 RHS2, \qquad (1)$$

where RHS1 and RHS2 are the non-homogenous terms defined in Eqns.(4.61-4.62).

Now we multiply Eqn.(1) by the complex conjugate of the leading order solution ψ_1 and note that the stream function ψ_3 is zero at the boundaries of the mushy layer, $\bar{x} \in [0,L]$ and $\bar{z} \in [0,1]$. The above operation enables the left hand side of Eqn.(1) to cancel off, leaving behind the right hand side solution which represents the solvability condition given as,

$$\int_0^1 \int_0^L \int_0^{2\pi} \left\{ R_{cr}\left(\sigma_0 \frac{\partial}{\partial \tilde{t}} + 1\right) \frac{\partial}{\partial \bar{x}} RHS1 \right\} \cdot \psi_1 d\tilde{t} d\bar{x} d\bar{z} + \int_0^1 \int_0^L \int_0^{2\pi} \nabla^2 RHS2 \cdot \psi_1 d\tilde{t} d\bar{x} d\bar{z} = 0, \qquad (1a)$$

Noting that,

$$\left[\frac{\partial}{\partial \tilde{t}} + 1\right] v_1 = -Ta^{1/2} \frac{\partial \psi_1}{\partial \bar{z}}, \qquad (1b)$$

we multiply Eqn.(1a) by the operator $\left[\partial/\partial \tilde{t} + 1\right]$, thus enabling Eqn.(1a) to be expressed as,

$$\int_0^1 \int_0^L \int_0^{2\pi} \left\{ R_{cr}\left(\sigma_0 \frac{\partial}{\partial \tilde{t}} + 1 \right)^2 \frac{\partial}{\partial \overline{x}} RHS1 \right\} \cdot \psi_1 \, d\tilde{t} \, d\overline{x} \, d\overline{z} + \int_0^1 \int_0^L \int_0^{2\pi} \nabla^2 RHS2_m \cdot \psi_1 \, d\tilde{t} \, d\overline{x} \, d\overline{z} = 0, \qquad (1c)$$

where,

$$RHS1 = \Omega R_{cr} \left\{ \left[\frac{\partial \psi_1}{\partial \overline{z}} \frac{\partial \theta_2}{\partial \overline{x}} - \frac{\partial \psi_1}{\partial \overline{x}} \frac{\partial \psi_2}{\partial \overline{z}} \right] + \left[\frac{\partial \psi_2}{\partial \overline{z}} \frac{\partial \theta_1}{\partial \overline{x}} - \frac{\partial \psi_2}{\partial \overline{x}} \frac{\partial \psi_1}{\partial \overline{z}} \right] - \frac{\partial \psi_1}{\partial \overline{x}} \right\} \qquad (2)$$

$$RHS2_m = -2\left(\sigma_0 \frac{\partial}{\partial \tilde{t}} + 1 \right)^2 \left(K_c \varphi_1^2 + \frac{\partial}{\partial \tau} \right) \nabla^2 \psi_1 - 2\frac{\partial}{\partial \tau_0}\left(\sigma_0 \frac{\partial}{\partial \tilde{t}} + 1 \right)^2 \nabla^2 \psi_2 -$$

$$K_c \left(\sigma_0 \frac{\partial}{\partial \tilde{t}} + 1 \right)^2 \frac{\partial \varphi_1^2}{\partial \overline{z}} \frac{\partial \psi_1}{\partial \overline{z}} + R_{cr}\left(\sigma_0 \frac{\partial}{\partial \tilde{t}} + 1 \right)^2 \frac{\partial \theta_1}{\partial \overline{z}} + KcTa \frac{\partial \varphi_1^2}{\partial \overline{z}} \frac{\partial \psi_1}{\partial \overline{z}} +$$

$$R_{cr} K_c \left(\sigma_0 \frac{\partial}{\partial \tilde{t}} + 1 \right)\left[\varphi_1^2 \frac{\partial \theta_1}{\partial \overline{x}} \right] + R_{cr}\left(\sigma_0 \frac{\partial}{\partial \tilde{t}} + 1 \right)\frac{\partial}{\partial \tau} \frac{\partial \theta_1}{\partial \overline{x}} + R_{cr}\left(\sigma_0 \frac{\partial}{\partial \tilde{t}} + 1 \right)\frac{\partial}{\partial \tau_0} \frac{\partial \theta_1}{\partial \overline{x}},$$

$$(3)$$

In Eqn.(3), RHS1 and $RHS2_m$ stands to identify the right hand side terms which have been evaluated from previously known solutions at orders ε and ε^2. The evaluation of the left hand side is complex from a algebraic point of view hence this process will be broken down into several sub-steps in order to maintain clarity throughout. In addition we shall refer to $RHS2_m$ as RHS2 for clarity. A detailed solution of the first term in Eqn.(3) will be provided whilst the final result of the remaining terms will be listed.

Recalling the first term from Eqn.(3),

$$RHS_{A1} = \Omega R_{cr} \left\{ \frac{\partial \psi_1}{\partial \overline{z}} \frac{\partial \theta_2}{\partial \overline{x}} - \frac{\partial \psi_1}{\partial \overline{x}} \frac{\partial \theta_2}{\partial \overline{z}} \right\} \qquad (4)$$

Using the lower order solutions for the temperature and the stream functions we may evaluate Eqn.(4) to be,

$$\mathrm{RHS}_{A1} = -\Omega R_{cr}\left\{2i\pi^2\alpha^{1/2}\left[A_1 e^{i\tilde{t}} + A_1^* e^{-i\tilde{t}}\right]\left[C_1 e^{i\tilde{t}} + C_1^* e^{-i\tilde{t}}\right]\sin(2\pi\bar{z})\right\} -$$

$$\Omega R_{cr}\left\{4i\pi^2\alpha^{1/2}\left[A_1 e^{i\tilde{t}} + A_1^* e^{-i\tilde{t}}\right]\left[b_2 + b_1 e^{i\tilde{t}} + b_1^* e^{-i\tilde{t}}\right]\cos(s\bar{x})\sin(\pi\bar{z})\cos(2\pi\bar{z})\right\} \quad (5)$$

Applying the operator shown in Eqn.(1) on Eqn.(5) as follows,

$$\mathrm{RHS}_{A1}' = R_{cr}\left(\sigma_0\frac{\partial}{\partial\tilde{t}} + 1\right)^2\frac{\partial}{\partial\bar{x}}\mathrm{RHS}_{A1},$$

yields the following result,

$$\mathrm{RHS}_{A1}' = -4i\pi^3\alpha\Omega R_{cr}^2\sigma_0^2\left[\left(A_1 b_2 + A_1^* b_1\right)e^{i\tilde{t}} + 9A_1 b_1 e^{3i\tilde{t}} + 9A_1^* b_1^* e^{-3i\tilde{t}} + \left(A_1^* b_2 + A_1 b_1^*\right)e^{-i\tilde{t}}\right].$$

$$\sin(s\bar{x})\sin(\pi\bar{z})\cos(2\pi\bar{z}) +$$

$$8i^2\pi^3\alpha\Omega R_{cr}^2\sigma_0\left[\left(A_1 b_2 + A_1^* b_1\right)e^{i\tilde{t}} + 3A_1 b_1 e^{3i\tilde{t}} - 3A_1^* b_1^* e^{-3i\tilde{t}} + \left(A_1^* b_2 + A_1 b_1^*\right)e^{-i\tilde{t}}\right].$$

$$\sin(s\bar{x})\sin(\pi\bar{z})\cos(2\pi\bar{z}) +$$

$$4i\pi^3\alpha\Omega R_{cr}^2\left[\left(A_1 b_2 + A_1^* b_1\right)e^{i\tilde{t}} + A_1 b_1 e^{3i\tilde{t}} + A_1^* b_1^* e^{-3i\tilde{t}} + \left(A_1^* b_2 + A_1 b_1^*\right)e^{-i\tilde{t}}\right].$$

$$\sin(s\bar{x})\sin(\pi\bar{z})\cos(2\pi\bar{z}).$$

$$(6)$$

Multiplying this equation by $\psi_1 = 2iA_1^* e^{-i\tilde{t}} \sin(s\overline{x})\sin(\pi\overline{z})$ and integrating over the domain $\overline{x} \in [0, L]$ and $\overline{z} \in [0,1]$ and over time $\tilde{t} \in [0, 2\pi]$ as follows,

$$\text{RHS}_{A1}'' = \int_0^1 \int_0^L \int_0^{2\pi} \text{RHS}_{A1}' \cdot \psi_1 \, d\tilde{t} \, d\overline{x} \, d\overline{z} \,, \tag{7}$$

which after integration produces,

$$\text{RHS}_{A1}'' = 2\pi^4 \alpha \Omega R_{cr}^2 L \left(1 + i\sigma_0\right)^2 \left[A_1^* A_1 b_2 + A_1^{*2} b_1\right]. \tag{8}$$

The exact procedure is followed for the remaining terms for RHS_A and the final form of the solution to RHS_A is given as,

$$\text{RHS}_A \big|_{\text{final}} = 2\pi^4 \alpha \Omega R_{cr}^2 L \left(1 + i\sigma_0\right)^2 \left[A_1^* A_1 b_2 + A_1^{*2} b_1\right] -$$

$$2\pi^3 \alpha \Omega R_{cr}^2 L \left(1 + i\sigma_0\right)^2 A_1^* A_1 . \tag{9}$$

We now proceed to evaluate the solvability condition contributed by the terms in the Darcy equation. Again we will evaluate one term and list the rest.

Recalling the first term from Eqn.(3),

$$\text{RHS}_{D1} = -2\left(\sigma_0 \frac{\partial}{\partial \tilde{t}} + 1\right)^2 \left(K_c \phi_1^2 + \frac{\partial}{\partial \tau}\right) \nabla^2 \psi_1 \tag{10}$$

Using the lower order solutions for the stream functions and the solid fraction that are pertinent to the case of overstable convection and solving the first part of Eqn.(10),

286

$$RHS_{D1}{}' = \left(K_c\varphi_1^2 + \frac{\partial}{\partial\tau}\right)\nabla^2\psi_1 , \qquad (11)$$

yields the following form of Eqn.(11),

$$RHS_{D1}{}' = -2i\pi^2(\alpha + 1)K_cK_0^2\left[A_1f_ze^{i\tilde{\tau}} + A_1^*f_z^*e^{-i\tilde{\tau}}\right]^2\left[A_1e^{i\tilde{\tau}} + A_1^*e^{-i\tilde{\tau}}\right]\cos^2(s\overline{x})\sin(s\overline{x})\sin(\pi\overline{z}) -$$

$$2i\pi^2(\alpha + 1)\left[\frac{\partial A_1}{\partial\tau}e^{i\tilde{\tau}} + \frac{\partial A_1^*}{\partial\tau}e^{-i\tilde{\tau}}\right]\sin(s\overline{x})\sin(\pi\overline{z}) , \qquad (12)$$

where f_z and f_z^* are functions of $\overline{z}$ given as,

$$f_z = e^{i\pi^2\gamma\sigma_0.(\overline{z}-1)} + i\pi\gamma\sigma_0\sin(\pi\overline{z}) + \cos(\pi\overline{z}) \qquad (13)$$

$$f_z^* = e^{-i\pi^2\gamma\sigma_0(\overline{z}-1)} - i\pi\gamma\sigma_0\sin(\pi\overline{z}) + \cos(\pi\overline{z}) , \qquad (14)$$

whilst the coefficient K_0 is simply,

$$K_0 = i\frac{2\alpha^{1/2}R_{cr}}{c_S\left(1 - \pi^2\gamma^2\sigma_0^2\right)} . \qquad (15)$$

Now applying the following operator,

$$RHS_{D1}{}'' = -2\left(\sigma_0\frac{\partial}{\partial\tilde{t}} + 1\right)^2 RHS_{D1}{}' , \qquad (16)$$

on Eqn.(12) and noting that all exponential terms for time that are of the order $\int_0^{2\pi}e^{\pm i2n\tilde{\tau}}d\tilde{t}$

produces a result of zero enables Eqn.(12) to be written in the following truncated form,

$$RHS_{D1}^{''} = 4i\pi^2(\alpha+1)K_cK_0^2A_1^2A_1^*\left(1+i\sigma_0\right)^2\left(f_z^2+2f_zf_z^*\right)e^{i\tilde{t}}\cos^2(s\overline{x})\sin(s\overline{x})\sin(\pi\overline{z})+$$

$$4i\pi^2(\alpha+1)\left(1+i\sigma_0\right)^2\frac{\partial A_1}{\partial\tau}e^{i\tilde{t}}\sin(s\overline{x})\sin(\pi\overline{z}). \qquad (17)$$

Multiplying this equation by $\psi_1 = 2iA_1^*e^{-i\tilde{t}}\sin(s\overline{x})\sin(\pi\overline{z})$ and integrating over $\overline{x} \in [0,L]$ and $\overline{z} \in [0,1]$ and in time over $\tilde{t} \in [0,2\pi]$ as follows,

$$RHS_{D1}^{'''} = \int_0^1\int_0^L RHS_{D1}^{''}.\psi_1 d\overline{x}d\overline{z}, \qquad (18)$$

which after integration provides,

$$RHS_{D1}^{'''} = -16\pi^3(\alpha+1)\left(1+i\sigma_0\right)^2 K_cK_0^2\kappa_0\left(A_1A_1^*\right)^2 + 4\pi^5(\alpha+1)^2\left(1+i\sigma_0\right)^2 LA_1^*\frac{\partial A_1}{\partial\tau},$$

$$(19)$$

where ,

$$\kappa_0 = \int_0^1\int_0^L\left\{\nabla^2\left[\left(f_z^2+2f_zf_z^*\right)\cos^2(s\overline{x})\sin(s\overline{x})\sin(\pi\overline{z})\right]\right\}.\sin(s\overline{x})\sin(\pi\overline{z})d\overline{x}d\overline{z}. \qquad (20)$$

Following exactly the same procedure as this for the remaining terms, we evaluate the solvability condition contributed by the Darcy terms, to give an expression of the form,

$$RHS_D\big|_{final} = -16\pi^3(\alpha+1)\left(1+i\sigma_0\right)^2 K_cK_0^2\kappa_0\left(A_1A_1^*\right)^2 + 4\pi^5(\alpha+1)^2\left(1+i\sigma_0\right)^2 LA_1^*\frac{\partial A_1}{\partial\tau}+$$

$$8\pi^2K_cK_0^2\left(1+i\sigma_0\right)^2\kappa_1A_1^2A_1^{*2} + \frac{8\pi\alpha\Omega R_{cr}^2K_cK_0^2}{(\alpha+1)}\left(1+i\sigma_0\right)\kappa_0A_1^2A_1^{*2} -$$

$$8\pi^2K_cK_0^2Ta\kappa_1A_1^2A_1^{*2} - 2\pi^3\alpha\Omega R_{cr}^2\left(1+i\sigma_0\right)^2 LA_1A_1^* - 2\pi^3\alpha\Omega R_{cr}^2\left(1+i\sigma_0\right)LA_1^*\frac{\partial A_1}{\partial\tau}, \text{(21)}$$

288

where

$$\kappa_1 = \int_0^1 \int_0^L \left\{ \nabla^2 \left[D_z \left(f_z^2 + 2f_z f_z^* \right) \cos^2(s\overline{x}) \sin(s\overline{x}) \sin(\pi\overline{z}) \right] \right\} . \sin(s\overline{x}) \sin(\pi\overline{z}) d\overline{x} d\overline{z} , \tag{22}$$

where $D_z = d/d\overline{z}$. Now the solvability condition is simply be found by adding Eqn.(9) and Eqn.(21) and presenting as,

$$t_a A_1^* \frac{\partial A_1}{\partial \tau} + t_b A_1 A_1^* + t_c \left(A_1 A_1^* \right)^2 = 0 , \tag{23}$$

where

$$t_a = 4\pi^5 (\alpha + 1)^5 \sigma_0 \left(i - \sigma_0 \right) L \tag{24}$$

$$t_b = -8\pi^5 (\alpha + 1)^2 \sigma_0 \left(1 + i\sigma_0 \right)^2 L \tag{25}$$

$$t_c = 4\pi^7 (\alpha + 1)^3 (2 + \Omega) \left(1 + i\sigma_0 \right)^2 + 16\pi^3 (\alpha + 1) K_c K_0^2 \kappa_0 \sigma_0 \left(\sigma_0 - i \right) +$$

$$8\pi^2 K_c K_0^2 \kappa_1 \left[\left(1 + i\sigma_0 \right)^2 - Ta \right] . \tag{26}$$

Reintroducing the original unscaled time as $\tau = \varepsilon^2 \chi_1 \tilde{t}$ and setting $A = \varepsilon A_1$ and $A^* = \varepsilon A_1^*$, whilst performing some minor algebra on Eqn.(23), allows the following form of the amplitude equation,

$$\frac{dA}{d\tilde{t}} = \left(-\pi^2 \gamma \frac{t_b}{t_a} \right) \left[\xi_{ov} - \left(-\frac{t_c}{t_b} \right) A A^* \right] A , \tag{27}$$

which may be further presented as,

289

$$\frac{dA}{d\bar{t}} = h_{21}\left[\xi_{ov} - h_{32}AA^*\right]A, \tag{28}$$

where

$$h_{21} = \left(-\pi^2\gamma\,\frac{t_b}{t_a}\right) \text{ and } h_{32} = \left(-\frac{t_c}{t_b}\right). \tag{29}$$

Incidentally Eqn.(28) is identical to Eqn.(4.64). In addition we note that

$$\xi_{ov} = \varepsilon^2 = \left[\frac{R}{R_{cr,ov}} - 1\right], \tag{30}$$

and the coefficients given in Eqn.(29) contain real and imaginary parts which may then be represented in the following manner,

$$h_{21} = h_{21}^0 + im_{21} \text{ and } h_{32} = h_{32}^0 + im_{32}. \tag{31}$$

Eqns.(30-31) are identical to the set presented in Eqn.(4.65).

The next step involves solving for the individual components of the terms in Eqn.(31).

Firstly we evaluate the term,

$$h_{21} = \left(-\pi^2\gamma\,\frac{t_b}{t_a}\right), \tag{32}$$

which results in the following form,

$$h_{21} = \frac{2\pi^2\gamma\left(1 + i\sigma_0\right)^2}{(\alpha + 1)^3\sigma_0\left(i - \sigma_0\right)}. \tag{33}$$

$$\overline{\mathrm{Nu}}_{\mathrm{ov0}} = \frac{1}{2\pi L} \int_0^{2\pi} \int_0^L d\theta_B / d\overline{z}\Big|_{\overline{z}=0} \, d\overline{x} d\widetilde{t} = 1. \tag{13}$$

The second term in Eqn.(12) is given as,

$$\overline{\mathrm{Nu}}_{\mathrm{ov1}} = \frac{1}{2\pi L} \int_0^{2\pi} \int_0^L -2\pi \left[C_1 e^{i\widetilde{t}} + C_1^* e^{-i\widetilde{t}} \right] \cos(s\overline{x}) \, d\overline{x} d\widetilde{t} = 0. \tag{14}$$

Finally the third term is given as,

$$\overline{\mathrm{Nu}}_{\mathrm{ov2}} = \frac{1}{2\pi L} \int_0^{2\pi} \int_0^L \left\{ -2\pi \left[C_2 e^{i\widetilde{t}} + C_2^* e^{-i\widetilde{t}} \right] \cos(s\overline{x}) + \right.$$

$$\left. 2\pi \left[b_2 + b_1 e^{2i\widetilde{t}} + b_1^* e^{-2i\widetilde{t}} \right] \right\} d\overline{x} d\widetilde{t}. \tag{15}$$

Performing the integration yields the following result,

$$\overline{\mathrm{Nu}}_{\mathrm{ov2}} = 2\pi b_2, \tag{16}$$

where

$$b_2 = \frac{\alpha \Omega^2 R_{cr}^2}{\pi(\alpha+1)} A_1 A_1^*. \tag{17}$$

Using the fact that $\pi^2 \alpha \Omega R_{cr}^2 = 2(\alpha+1)^2$, and using the definition for b_2 as provided by Eqn.(17), yields the following result,

$$\overline{\mathrm{Nu}}_{\mathrm{ov2}} = \frac{4(\alpha+1)\Omega}{\pi^2} A_1 A_1^*. \tag{18}$$

The solution for the Nusslet number is given as,

$$\overline{Nu}_{ov} = 1 + \frac{4(\alpha + 1)\Omega}{\pi^2}\varepsilon^2 A_1 A_1^* .$$ (19)

Noting that $A = \varepsilon A_1$ and $A^* = \varepsilon A_1^*$ and $AA^* = r^2$, allows Eqn.(19) to be written as,

$$\overline{Nu}_{ov} = 1 + \frac{4(\alpha + 1)\Omega}{\pi^2} r^2 .$$ (20)

Recall that the modulus of the amplitude was found to be of the form $r^2 = h_{24}^0 \xi_{ov}$, where $\xi_{ov} = \varepsilon^2 = \left[R/R_{cr,ov} - 1 \right]$. Applying this to Eqn.(20) allows the Nusselt number at the post transient state for order ε^2 to be given as

$$\overline{Nu}_{ov} = 1 + \frac{4(\alpha + 1)\Omega h_{24}^0}{\pi^2}\left[R/R_{cr,st} - 1 \right] + O(\varepsilon^3) \qquad \forall\; R \geq R_{cr,ov} .$$ (21)

Note that $h_{24}^0 = 1/h_{42}^0$ and h_{42}^0 is defined in Eqn.(4.75). Eqn.(21) is identical to Eqn.(5.6).

302